

SYNTHESIS, CHARACTERIZATION AND BIOLOGICAL  
PROPERTIES OF METAL(II) POLYPYRIDYL  
COMPLEXES WITH OO', ONO', OR NO-CHELATING  
COLIGANDS

CHIN LEE FANG

MASTER OF SCIENCE

FACULTY OF SCIENCE  
UNIVERSITI TUNKU ABDUL RAHMAN  
JUNE 2013

**SYNTHESIS, CHARACTERIZATION AND BIOLOGICAL  
PROPERTIES OF METAL(II) POLYPYRIDYL COMPLEXES WITH  
*OO'*-, *ONO'*-, OR *NO*-CHELATING COLIGANDS**

By

**CHIN LEE FANG**

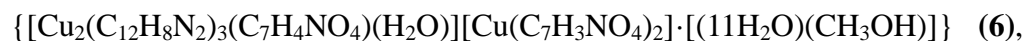
A thesis submitted to the Department of Chemical Science,  
Faculty of Science,  
Universiti Tunku Abdul Rahman,  
in partial fulfillment of the requirements for the degree of  
Master of Science  
JUNE 2013

## ABSTRACT

### SYNTHESIS, CHARACTERIZATION AND BIOLOGICAL PROPERTIES OF METAL(II) POLYPYRIDYL COMPLEXES WITH *OO'*-, *ONO'*-, OR *NO*-CHELATING COLIGANDS

Chin Lee Fang

Exploring the combination of ligands and metal(II) ion to form ternary metal complexes is an attempt to gain insight into rational design of metal complexes for specific application, such as anticancer drug. 1,10-phenanthroline (phen) has been chosen as the main ligand and as an intercalator. This kind of ternary metal(II) complexes allows intercalation of phen ligand between the DNA nucleobase pairs and orientation of the coligand(s) to interact with nucleobases in their vicinity. Maltol, dipicolinic acid and threonine have been chosen as coligands partly because their non-toxicity may result in lower toxicity of metal(II) complexes. The coordinated maltolate has H-acceptor site, dipicolinate has two H-acceptor sites whereas threonine has both H-acceptor and H-donor sites. This study compares the effect of three coligands, the number of chelated coligand and the types of metal(II) ion on the physical and biological properties of resultant ternary metal(II) complexes. The complexes were characterized by elemental analysis, FTIR, UV-Vis and FL spectroscopy, X-ray diffraction, molar conductivity, ESI-MS, TGA and CD spectroscopy. Based on the elemental analysis, molecular formulae of the synthesised metal(II) complexes are  $[\text{Co}(\text{C}_{12}\text{H}_8\text{N}_2)(\text{C}_6\text{H}_5\text{O}_3)\text{Cl}] \cdot 4\text{H}_2\text{O}$  (1),  $[\text{Cu}(\text{C}_{12}\text{H}_8\text{N}_2)(\text{C}_6\text{H}_5\text{O}_3)\text{Cl}] \cdot \frac{1}{2}\text{H}_2\text{O}$  (2),



[phen =  $\text{C}_{12}\text{H}_8\text{N}_2$ ; maltolate =  $\text{C}_6\text{H}_5\text{O}_3$ ;  $\mu$ -dipicolinate =  $\text{C}_7\text{H}_4\text{NO}_4$ ; dipicolinate =  $\text{C}_7\text{H}_3\text{NO}_4$ ; threoninate =  $\text{C}_4\text{H}_8\text{NO}_3$ ].

X-ray structure analyses show that complexes **4 - 5** and **7 - 11** have octahedral geometry about the central metal(II) ion. Complex **6** is a trinuclear complex with a bridging dipicolinate ligand. A change in the type of metal(II) ion, coligand and the number of coordinated ligands influence the FL emission intensities but not the  $\lambda_{\text{max}}$  and the shape of the bands. Most of the studied compounds are 1:1 electrolyte except for complexes **4, 5** and **7** which are non-electrolytes in water-methanol (1:1 v/v) solution. Based on the molar conductance and ESI-MS obtained, metal(II) complexes studied were found to be stable within the duration of the measurement up to 24 hours except for the neutral  $[\text{Co}(\text{phen})(\text{maltolate})_2]$ . The lability of the metal complexes studied appears to depend on the type of metal, nature of the coordinated ligand and the number of the coordinated ligand. The complexes **8 - 11** are optically active and they are grouped into two pairs of enantiomers based on their CD spectra. However, there are no significant differences observed for each enantiomer pair of complexes in FTIR, CHN, UV-Vis, FL, molar conductivity, ESI-MS and TGA. Meanwhile, two groups of metal(II) complexes *viz.* Co(II) complexes (**1** and **4**) and Zn(II) complexes (**7** and **10**) were selected to

investigate the effect of changing the coligand on their biological properties. It is believed that the type of coordinated ligand is a crucial factor in bestowing the binding site specificity and selectivity of a given metal complex. Moreover, not many Co(II) and Zn(II) complexes have been studied for their anticancer properties. Hence, it will be interesting to find out the biological properties of Co(II) complexes (**1** and **4**) and Zn(II) complexes (**7** and **10**). Indeed, a change of coligand and the number of chelated ligands of Co(II) and Zn(II) complexes seem to influence their DNA recognition, topoisomerase I inhibition and antiproliferative properties. Both Zn(II) complexes (**7** and **10**) can inhibit topoisomerase I, and have better anticancer activity than cisplatin against nasopharyngeal cancer cell lines, HK1 and HONE-1, with IC<sub>50</sub> values in low  $\mu\text{M}$  range.  $[\text{Zn}(\text{phen})(\text{L-threoninate})(\text{H}_2\text{O})\text{Cl}]\cdot 2\text{H}_2\text{O}$  (**10**) has the highest therapeutic index for HK1 (3.9). Both Zn(II) complexes (**7** and **10**) can induce cell death by apoptosis. Changing the coligand in the Zn(II) complexes (**7** and **10**) affects the biological properties of the complexes such as the binding affinity for some DNA sequences, nucleobase sequence-selective binding, the phase at which cell cycle progression was arrested for treated cancer cells and their therapeutic index.

## ACKNOWLEDGEMENTS

Foremost, I offer my sincerest gratitude to my main supervisor, Dr. Ng Chew Hee and co-supervisor, Dr. Neo Kian Eang for the continuous support of my master study and research, for their patience, motivation, enthusiasm, and immense knowledge.

This thesis would not have been completed or written without the guidance and the help of several individuals who in one way or another contributed and extended their valuable assistance in the preparation and completion of this study.

I wish to acknowledge the efforts of the staff from Chemical, Molecular and Materials Analysis Centre (CMMAC), National University of Singapore (NUS), for helping me carrying out the Electrospray Ionisation Mass Spectrometry (ESI-MS). My sincere thanks also goes to Prof. Leong Weng Kee from Nanyang Technological University (NTU), Dr. Koh Lip Lin, Ms. Tan Geok Kheng and Ms. Hong Yimian from NUS and Prof. Ng Seik Weng from University Malaya for helping with the X-ray crystallographic studies. The Director General of Health Malaysia is acknowledged for part of the anticancer work done in the Institute for Medical Research. Siew Ming, Hoi Ling, Yee Lian and James Chong are acknowledged for being great help in conducting part of the biological studies. Special thanks go to colleagues in the Department of Chemistry: Wai San, Kok Leei, Teck Leong, Nicholas, Jason and to those who have helped me during my stay in Universiti Tunku Abdul Rahman (UTAR).

I would like to thank UTARRF for an internal grant (UTARF6200/N03) and the Malaysian Government and MOSTI for the eScience grant 02-02-11-SF0033. I would also like to thank Ministry of Higher Education Malaysia (MOHE) for their scholarship to allow me to pursue master degree in UTAR.

Last but not the least, my family members for supporting me spiritually throughout my life and Mr. Chu Chee Kiat, who was always there to cheer me up and stood by me through the good times and bad.

## APPROVAL SHEET

This dissertation/thesis entitled “**SYNTHESIS, CHARACTERIZATION AND BIOLOGICAL PROPERTIES OF METAL(II) POLYPYRIDYL COMPLEXES WITH *OO'*-, *ONO'*-, OR *NO*-CHELATING COLIGANDS**” was prepared by CHIN LEE FANG and submitted as partial fulfillment of the requirements for the degree of Master of Science at Universiti Tunku Abdul Rahman.

Approved by:

---

(Assoc. Prof. Dr. Ng Chew Hee)

Date:.....  
Supervisor  
Department of Chemical Science  
Faculty of Science  
Universiti Tunku Abdul Rahman

---

(Asst. Prof. Dr. Neo Kian Eang)

Date:.....  
Co-supervisor  
Department of Chemical Science  
Faculty of Science  
Universiti Tunku Abdul Rahman

**FACULTY OF SCIENCE**  
**UNIVERSITI TUNKU ABDUL RAHMAN**

Date: \_\_\_\_\_

**SUBMISSION OF THESIS**

It is hereby certified that **CHIN LEE FANG** (ID No: **09ADM09166**) has completed this thesis entitled "**SYNTHESIS, CHARACTERIZATION AND BIOLOGICAL PROPERTIES OF METAL(II) POLYPYRIDYL COMPLEXES WITH OO'-, ONO'-, OR NO-CHELATING COLIGANDS**" under the supervision of Associates Prof. Dr. Ng Chew Hee (Supervisor) from the Department of Chemical Science, Faculty of Science, and Assistance Prof. Dr. Neo Kian Eang (Co-Supervisor) from the Department of Chemical Science, Faculty of Science.

I understand that University will upload softcopy of my thesis in pdf format into UTAR Institutional Repository, which may be made accessible to UTAR community and public.

Yours truly,

\_\_\_\_\_  
(CHIN LEE FANG)

## DECLARATION

I hereby declare that the dissertation is based on my original work except for quotations and citations which have been duly acknowledged. I also declare that it has not been previously or concurrently submitted for any other degree at UTAR or other institutions.

Name : \_\_\_\_\_

Date : \_\_\_\_\_

## TABLE OF CONTENTS

	<b>Page</b>
<b>ABSTRACT</b>	<b>ii</b>
<b>ACKNOWLEDGEMENTS</b>	<b>v</b>
<b>APPROVAL SHEET</b>	<b>vii</b>
<b>SUBMISSION SHEET</b>	<b>viii</b>
<b>DECLARATION</b>	<b>ix</b>
<b>LIST OF TABLES</b>	<b>xiii</b>
<b>LIST OF FIGURES</b>	<b>xv</b>
<b>LIST OF ABBREVIATIONS</b>	<b>xviii</b>
<b>CHAPTER</b>	
<b>1.0 INTRODUCTION</b>	
1.1 General	2
1.2 Objectives	10
<b>2.0 LITERATURE REVIEW</b>	
2.1 1,10-phenanthroline complexes	15
2.2 Maltolato complexes	19
2.3 Dipicolinato complexes	25
2.4 Threoninato complexes	32
2.5 Comparative review of biological studies of cobalt(II), copper(II) and zinc(II) complexes	39
2.6 Summary	44
<b>3.0 SYNTHESIS AND CHARACTERIZATION OF METAL(II) 1,10-PHENANTHROLINE COMPLEXES WITH <i>O,O'</i>- MALTOL, [M(phen)(ma)Cl]·xH<sub>2</sub>O (M(II) = Co, Cu, Zn) and [Co(phen)(ma)<sub>2</sub>]·5H<sub>2</sub>O</b>	
3.1 Introduction	48
3.2 Experimental	
3.2.1 Materials and reagents	49
3.2.2 Preparation of [M(phen)(ma)Cl]·xH <sub>2</sub> O (M = Co, Cu or Zn) <b>1-3</b> and [Co(phen)(ma) <sub>2</sub> ]·5H <sub>2</sub> O <b>4</b>	49
3.2.3 Characterization of solids complexes	51
3.2.4 Determination of crystal structure of <b>4</b>	51
3.2.5 Characterization of aqueous solutions of complexes	52
3.3 Results and discussion	
3.3.1 Characterization of solids complexes	54
3.3.2 Analysis of crystal structure of <b>4</b>	61
3.3.3 Characterization of aqueous solutions of complexes	65
3.4 Conclusion	72

<b>4.0</b>	<b>SYNTHESIS AND CHARACTERIZATION OF METAL(II) 1,10-PHENANTHROLINE COMPLEXES WITH <i>O,N,O'</i>-DIPICOLINIC ACID</b>	
4.1	Introduction	75
4.2	Experimental	76
4.2.1	Materials and reagents	76
4.2.2	Preparation of [M(phen)(dipico)(H <sub>2</sub> O)]·xH <sub>2</sub> O (M = Co or Zn; x = 1 or 2) ( <b>5</b> and <b>7</b> ) and [Cu <sub>2</sub> (phen) <sub>3</sub> (dipico)(H <sub>2</sub> O)][Cu(dipico) <sub>2</sub> ]·[(11H <sub>2</sub> O)(CH <sub>3</sub> OH)] <b>6</b>	76
4.2.3	Characterization of solids complexes	77
4.2.4	Determination of crystal structures	77
4.2.5	Characterization of aqueous solutions of complexes	79
4.3	Results and discussion	
4.3.1	Characterization of solids complexes	80
4.3.2	Analysis of crystal structures	83
4.3.3	Characterization of aqueous solutions of complexes	93
4.4	Conclusion	99
<b>5.0</b>	<b>SYNTHESIS AND CHARACTERIZATION OF METAL(II) 1,10-PHENANTHROLINE COMPLEXES WITH <i>N,O</i>-THREONINE, [M(phen)(AA)(H<sub>2</sub>O)Cl]·2H<sub>2</sub>O (M(II) = Cu, Zn; AA = L-thr, D-thr)</b>	
5.1	Introduction	102
5.2	Experimental	103
5.2.1	Materials and reagents	103
5.2.2	Preparation of [M(phen)(AA)(H <sub>2</sub> O)Cl]·2H <sub>2</sub> O (M(II) = Cu, Zn; AA = L-thr, D-thr) <b>8 -11</b>	103
5.2.3	Characterization of solids complexes	104
5.2.4	Determination of crystal structures	105
5.2.5	Characterization of aqueous solutions of complexes	106
5.3	Results and discussion	
5.3.1	Characterization of solids complexes	108
5.3.2	Analysis of crystal structures	113
5.3.3	Characterization of aqueous solutions of complexes	119
5.4	Conclusion	127
<b>6.0</b>	<b>BIOLOGICAL STUDIES OF COBALT(II) 1,10-PHENANTHROLINE COMPLEXES WITH <i>O,O'</i>-MALTOL, [Co(phen)(ma)Cl]·4H<sub>2</sub>O and [Co(phen)(ma)<sub>2</sub>]·5H<sub>2</sub>O</b>	
6.1	Introduction	130
6.2	Experimental	133
6.2.1	Materials and reagents	133
6.2.2	DNA binding studies	134
6.2.3	Restriction enzyme inhibition assay and human	135

	topoisomerase I inhibition assay	
6.2.4	Anticancer study	135
6.3	Results and discussion	136
6.3.1	DNA binding studies	136
6.3.2	Restriction enzyme (RE) inhibition	139
6.3.3	Human topoisomerase I inhibition	141
6.3.4	Anticancer study	144
6.4	Conclusion	145
<b>7.0</b>	<b>BIOLOGICAL STUDIES OF ZINC(II) 1,10-PHENANTHROLINE COMPLEXES WITH <i>O,N,O'</i>-DIPICOLINIC ACID OR <i>N,O</i>-L-THREONINE, [Zn(phen)(dipico)(H<sub>2</sub>O)]·H<sub>2</sub>O and [Zn(phen)(L-thr)(H<sub>2</sub>O)Cl]·2H<sub>2</sub>O</b>	
7.1	Introduction	148
7.2	Experimental	150
7.2.1	Materials and reagents	150
7.2.2	DNA binding studies	150
7.2.3	Restriction enzyme inhibition assay and human topoisomerase I inhibition assay	151
7.2.4	Anticancer studies	151
7.3	Results and discussion	154
7.3.1	DNA binding studies	154
7.3.2	Restriction enzyme (RE) inhibition	155
7.3.3	Human topoisomerase I inhibition	157
7.3.4	Anticancer studies	158
7.4	Conclusion	165
<b>8.0</b>	<b>GENERAL CONCLUSION</b>	166
	<b>REFERENCES</b>	176
	<b>APPENDICES</b>	220
	<b>LIST OF PUBLICATIONS / CONFERENCE PRESENTATIONS</b>	

## LIST OF TABLES

<b>Table</b>		<b>Page</b>
<b>1.1</b>	List of analytical methods	12
<b>2.1</b>	List of ternary metal(II) complexes with 1,10-phenanthroline as main ligand and various co-ligand	46
<b>3.1</b>	Crystal data and structure refinement for [Co(phen)(ma) <sub>2</sub> ].5H <sub>2</sub> O <b>4</b>	52
<b>3.2</b>	Physical and chemical data of metal(II) complexes, <b>1 - 4</b>	55
<b>3.3</b>	Characteristic Infrared band assignments of metal(II) complexes, <b>1 - 4</b>	58
<b>3.4</b>	TGA data of metal(II) complexes, <b>1 - 4</b>	61
<b>3.5</b>	Selected bond lengths (Å) and angles (°) for complex <b>4</b>	63
<b>3.6</b>	ESI-MS data for metal(II) complexes, <b>1 - 4</b>	66
<b>3.7</b>	Absorption spectral data for metal(II) complexes, <b>1 - 4</b>	69
<b>4.1</b>	Crystal data and structure refinement for metal(II) complexes, <b>5 - 7</b>	78
<b>4.2</b>	Physical and chemical data of metal(II) complexes, <b>5 - 7</b>	80
<b>4.3</b>	Characteristic Infrared band assignments of metal(II) complexes, <b>5 - 7</b>	83
<b>4.4</b>	Selected bond lengths (Å) for metal(II) complexes, <b>5 - 7</b>	91
<b>4.5</b>	Selected bond angles (°) for metal(II) complexes, <b>5 - 7</b>	92
<b>4.6</b>	Absorption spectral data of metal(II) complexes, <b>5 - 7</b>	97
<b>5.1</b>	Crystal data and structure refinement for metal(II) complexes, <b>7 - 10</b>	107

<b>5.2</b>	Physical and chemical data of metal(II) complexes, <b>8 - 11</b>	108
<b>5.3</b>	Characteristic Infrared band assignments of metal(II) complexes, <b>8 - 11</b>	110
<b>5.4</b>	TGA data for metal(II) complexes, <b>8 - 11</b> .	113
<b>5.5</b>	Selected bond lengths, (Å) and bond angles (°) for metal(II) complexes, <b>8 - 11</b> .	118
<b>5.6</b>	ESI-MS data for metal(II) complexes, <b>8 - 11</b>	121
<b>5.7</b>	Electronic absorption and emission data for metal(II) complexes, <b>8 - 11</b> .	123
<b>6.1</b>	Binding constant of Co(II) complexes for various DNA	139
<b>6.2</b>	Restriction enzyme inhibition for Co(II) complexes, <b>1</b> and <b>4</b>	141
<b>6.3</b>	IC <sub>50</sub> values of complexes <b>1</b> and <b>4</b> for the MDA-MB-231, MCF7 and MCF10A cell lines	145
<b>7.1</b>	Binding constants for various duplexes and G-4 (with standard deviations < ±0.1)	155
<b>7.2</b>	Restriction enzyme inhibition for Zn(II) complexes	157
<b>7.3</b>	IC <sub>50</sub> values of incubating cancer and non cancer nasopharyngeal cells with compounds for 72 hours	162

## LIST OF FIGURES

Figures	Page	
1.1	Chemical structure of platinum drugs	3
1.2	Structure of 1,10-phenanthroline (phen)	5
1.3	Structure of maltol	7
1.4	Structure of dipicolinic acid	8
1.5	Structure of (a) L-threonine (L-thr); (b) D-threonine (D-thr)	9
1.6	Modular system in this research study	11
2.1	Structure of (a) L-threonine (L-thr); (b) D-threonine (D-thr)	33
3.1	ORTEP structure of $[\text{Co}(\text{phen})(\text{ma})_2] \cdot 5\text{H}_2\text{O}$ <b>4</b> with ellipsoids at 50%.	62
3.2	Packing diagram of <b>4</b> viewing along $a^*$ axis (light blue dotted lines are H-bonds).	64
3.3	Molar conductivity ( $\Omega^{-1} \text{ cm}^2 \text{ mol}^{-1}$ ) for maltolate complexes, <b>1 - 4</b> .	67
3.4	Fluorescence spectra of <b>3</b> (I), phen (II), <b>1</b> (III), <b>4</b> (IV), <b>2</b> (V), maltol (VI) and water-methanol mixture (1:1 v/v) (VII) at 1 $\mu\text{M}$ .	71
4.1	An ORTEP structure of $[\text{Co}(\text{phen})(\text{dipico})(\text{H}_2\text{O})] \cdot 2\text{H}_2\text{O}$ , <b>5</b> with ellipsoid at 50%.	86
4.2	An ORTEP structure of $[\text{Zn}(\text{phen})(\text{dipico})(\text{H}_2\text{O})] \cdot \text{H}_2\text{O}$ , <b>7</b> with ellipsoids at 50%.	86
4.3	ORTEP structure of $[\text{Cu}_2(\text{phen})_3(\text{dipico})(\text{H}_2\text{O})][\text{Cu}(\text{dipico})_2] \cdot [(11\text{H}_2\text{O})(\text{CH}_3\text{OH})]$ , with ellipsoid at 50 %	90
4.4	Packing diagram of <b>6</b> viewing along b axis	91
4.5	Molar conductivity of 1 mM of <b>5 - 7</b> , metal(II) chloride, phen and dipicolinate ligand in deionised water-methanol (1:1 v/v) at 25 $^\circ\text{C}$ .	95

<b>4.6</b>	Fluorescence spectra of <b>7</b> (I), phen (II), <b>5</b> (III), <b>6</b> (IV), dipico (V) and solvent mixture (VI) at 0.1 $\mu$ M.	98
<b>5.1</b>	Crystal structure of (a) [Cu(phen)(L-thr)(H <sub>2</sub> O)Cl]·2H <sub>2</sub> O <b>8</b> ; (b) [Cu(phen)(D-thr)(H <sub>2</sub> O)Cl]·2H <sub>2</sub> O <b>9</b>	114
<b>5.2</b>	Crystal structure of (a) [Zn(phen)(L-thr)(H <sub>2</sub> O)Cl]·2H <sub>2</sub> O <b>10</b> ; (b) [Zn(phen)(D-thr)(H <sub>2</sub> O)Cl]·2H <sub>2</sub> O <b>11</b>	114
<b>5.3</b>	The molecular packing with hydrogen-bonding of <b>8</b> (left) and its enantiomer, <b>9</b> (right) on the direction of <i>a</i> -axis. The mirror is drawn as a dash line.	116
<b>5.4</b>	The molecular structure with hydrogen-bonding of <b>10</b> (left) and its enantiomer, <b>11</b> (right) on the direction of <i>a</i> -axis. The mirror is drawn as a dash line.	117
<b>5.5</b>	Molar conductivity of 1 mM of <b>8</b> - <b>11</b> and other compounds in deionised water-methanol (1:1 v/v) at 25 °C.	122
<b>5.6</b>	Fluorescence spectra of <b>9</b> (I), <b>10</b> (II), phen (III), <b>7</b> (IV), <b>8</b> (V), L-thr (VI) and D-thr (VII) at 0.5 $\mu$ M.	125
<b>5.7</b>	CD spectra of (a) Cu(II) complexes, <b>8</b> - <b>9</b> and (b) Zn(II) complexes, <b>10</b> - <b>11</b>	126
<b>6.1</b>	DNA double helix structure cited from U.S. National Library of Medicine	131
<b>6.2</b>	The three binding modes of metal complexes with DNA: (a) groove binding, (b) intercalation, and (c) insertion.	131
<b>6.3</b>	CD spectra of CT-DNA alone (a) and in the presence of the <b>1</b> (b) and <b>4</b> (c).	137
<b>6.4</b>	Human topoisomerase I inhibition assay by gel electrophoresis. Electrophoresis results of incubating human topoisomerase I (1 unit/21 $\mu$ L) with pBR322 (0.25 $\mu$ g) in the absence or presence of 5-40 $\mu$ M of complex <b>1</b> : Lane 1 & 5, gene ruler 1 Kb DNA ladder; Lane 2, DNA alone; Lane 3, DNA + 40 $\mu$ M complex <b>1</b> (control); Lane 4, DNA + 1 unit Human Topoisomerase I (control). Lanes 6-9, DNA + 1 unit Human Topoisomerase I + varying concentration of complex <b>1</b> : Lane 6, 5 $\mu$ M complex <b>1</b> ; Lane 7, 10 $\mu$ M complex <b>1</b> ; Lane 8, 20 $\mu$ M complex <b>1</b> ; Lane 9, 40 $\mu$ M complex <b>1</b> .	142

<b>6.5</b>	Human topoisomerase I inhibition assay by gel electrophoresis. Electrophoresis results of incubating human topoisomerase I (1 unit/21 $\mu$ L) with pBR322 (0.25 $\mu$ g) in the absence or presence of 10-200 $\mu$ M of complex <b>4</b> : Lanes 1 & 12, gene ruler 1 Kb DNA ladder; Lane 2, DNA alone; Lane 3, DNA + 200 $\mu$ M complex <b>4</b> (control); Lane 4, empty; Lane 5, DNA + 1 unit Human Topoisomerase I (control); Lane 6, empty. Lanes 7-11, DNA + 1 unit Human Topoisomerase I + varying concentration of complex <b>4</b> : Lane 7, 10 $\mu$ M complex <b>4</b> ; Lane 8, 20 $\mu$ M complex <b>4</b> ; Lane 9, 50 $\mu$ M; Lane 10, 100 $\mu$ M complex <b>4</b> ; Lane 11, 200 $\mu$ M complex <b>4</b> .	143
<b>7.1</b>	Anatomy of the pharynx	160
<b>7.2</b>	Apoptosis analysis of HONE-1 cells untreated (A) or treated for 72 hours with IC <sub>50</sub> concentration of cisplatin (B), phen (C), [Zn(phen)Cl <sub>2</sub> ] (D), <b>7</b> (E) and <b>10</b> (F).	163
<b>7.3</b>	% viable cells, necrotic cells and apoptotic cells for HONE-1 treated with test compounds.	163
<b>7.4</b>	Cell cycle analysis of HONE-1 cells untreated and treated with <b>7</b> and <b>10</b> for 24 hours.	164

## LIST OF ABBREVIATION

$\Delta$	Delta
$\Lambda$	Lamda
<i>ca.</i>	Approximately
Calc.	Calculated
$\text{Co}^{\text{II}}$	Cobalt(II) ion
$\text{Cu}^{\text{II}}$	Copper(II) ion
$\text{C}^{\alpha}\text{-C}^{\beta}$ bonds	Alpha-carbon-beta-carbon bond
dipico	Dipicolinate
D-thr	D-threonine
<i>e.g.</i>	For example
<i>etc</i>	Et cetera
$\text{H}_2\text{dipico}$	Dipicolinic acid
Hma	Maltol
hrs	Hours
Hthr	Threonine
<i>i.e.</i>	That is
L-thr	L-threonine
<i>m/z</i>	Mass-to-charge
ma	Maltolate
mins	Minutes
mL	Milliliters
mmol	Millimole
MTT assay	3-(4,5-dimethylthiazol-2-yl)-2,5-diphenyltetrazolium bromide assay
phen	1,10-phenanthroline
Ppt.	Precipitate
Topo I	Topoisomerase I
v/v	Volume per volume
<i>viz.</i>	Namely
$\text{Zn}^{\text{II}}$	Zinc(II) ion

**CHAPTER 1**  
**INTRODUCTION**

**SYNTHESIS, CHARACTERIZATION AND BIOLOGICAL  
PROPERTIES OF METAL(II) POLYPYRIDYL COMPLEXES WITH  
*oo'*-, *ono'*- OR *no*-CHELATING COLIGANDS**

## CHAPTER 1

### INTRODUCTION

#### 1.1 GENERAL

According to Werner (1893), a metal complex is a compound formed from a Lewis acid (electron-pair acceptor) and a Lewis base (electron-pair donor). Metal ions can act as Lewis acids, accepting electron pairs from their ligands (Lewis base) because metal ions have one or more empty orbitals. A ternary metal complex is formed when two different ligands are coordinated to the metal centre. Metal complexes have many medicinal, industrial and pharmaceutical applications (Erkilla et al., 1999; Chris, 2002; Bhattacharya, 2005; Sakurai, 2010; Warra, 2011). The discovery of cisplatin as anticancer agent is a milestone in the development of metal complexes as medicine (Rosenberg et al., 1969; Kostova, 2006; Florea and Büsselberg, 2011). Besides cisplatin, carboplatin, oxaliplatin, nedaplatin and lobaplatin (**Figure 1.1**) have been approved for clinical use in Europe, Japan, China and the United States for cancer treatment (Kostova, 2006; Bharti and Singh, 2009). The cytotoxicity of platinum drugs is attributed to their ability to bind DNA and induce apoptosis (Griffith et al., 2007). However, therapy with platinum anticancer drugs is accompanied by severe side effects, such as nephrotoxicity, neurotoxicity, ototoxicity, and emetogenicity, which limit their widespread use (Bharti and Singh, 2009; Eastman, 1999; Gonzalez et al., 2001; Piulats et al.,

2009; Rafique et al., 2010).

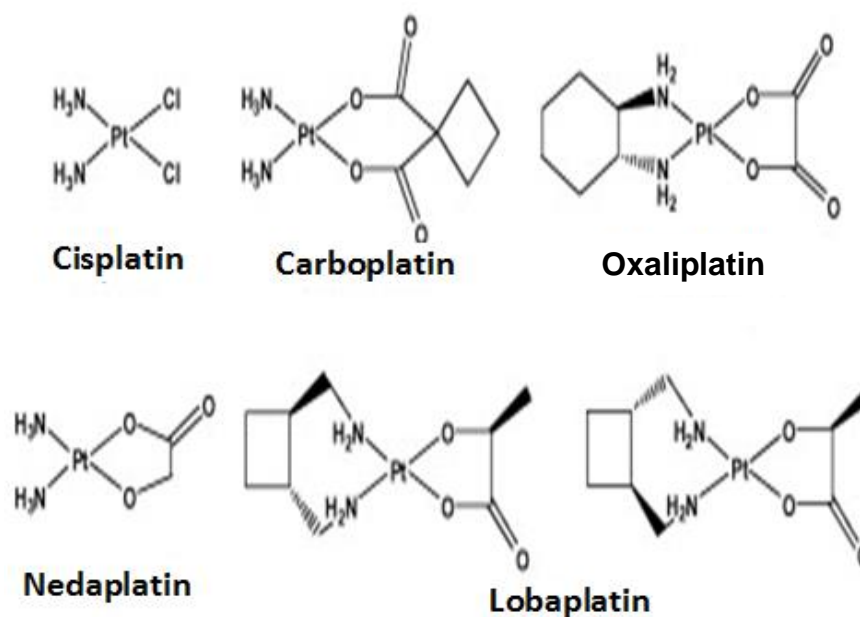


**Figure 1.1:** Chemical structure of platinum drugs (Kostova, 2006; Bharti and Singh, 2009).

Thus, researchers have extended their search for other anticancer-active inorganic complexes, attempt to improve their pharmacological properties. In recent years, the research on complexes of essential metals have received much attention based on the assumption that endogenous metals may be less toxic than non essential metals (Becco et al., 2012). Hence, there are more and more studies on complexes of essential metals such as cobalt, copper and zinc. A previous theoretical study conducted by Huang and coworkers (2005), using clustering analysis and self-organising maps, of more than 1000 metal containing compounds with potential anticancer properties, concluded that their cytotoxicity is determined by the identity of the metal and the organic ligand, and the target-specificity can be accomplished by the right

metal-ligand combination (Huang et al., 2005). Among the vast variety of possible designs, one interesting series involving simple mixed-ligand metal complexes with intercalating ligand may have both DNA binding and molecular recognition capabilities (Seng et al., 2010; Zeglis et al., 2007). Intercalation occurs when ligands of an appropriate size and chemical nature fit themselves in between base pairs of DNA. Most of these intercalating ligands are polycyclic, aromatic or planar compounds (Bencini and Lippolis, 2010).

Among all the polypyridyl ligands, 1,10-phenanthroline (phen) (**Figure 1.2**) has been chosen as the main ligand and as an intercalator in this project owing to the biological or pharmacological properties (antiproliferative, antifungal, antimycoplasma and antiviral) of some of its metal complexes (Farrell, 2003; García-Raso et al., 2003; Rao et al., 2007; Jia et al., 2010; Rao et al., 2008). The phen is a bidentate, heterocyclic diamine which is widely used as a chelating agent for transition metal ions, and the resultant complexes have played an important role in the development of coordination chemistry. Also, it is a versatile starting material to design more luminescent organic ligands, and metal complexes with phen-based ligands have many diagnostic and therapeutic applications (Bencini and Lippolis, 2010; Accorsi et al., 2009; Chen et al., 2008; Balzani et al., 2008).

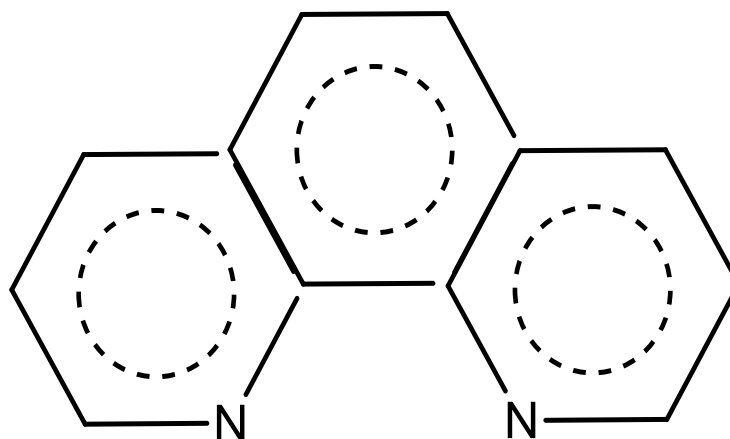


**Figure 1.2:** Structure of 1,10-phenanthroline (phen).

Phen is a rigid planar, hydrophobic, electron-poor heteroaromatic compound (Summers, 1978; Sammes and Yahsioglu, 1994; Luman and Castellano, 2004; Bencini and Lippolis, 2010). It has two nitrogen donor atoms at 1- and 10-position (Lever, 2003; Brahma et al., 2008; Bencini and Lippolis, 2010). The lone pairs of electrons on the nitrogen atoms, combined with the rigidity of the aromatic ring system, makes phen a good chelating ligand for forming metal complexes. The poorer  $\sigma$ -donor ability of the heteroaromatic nitrogen atoms is compensated by the ability of phen to behave as excellent  $\pi$ -acceptors (Anderegg, 1963; Bencini and Lippolis, 2010; Monzon, 2010). Ternary metal(II) complexes with phen as main ligand can allow intercalation of phen ligand between the DNA nucleobase pairs and orientation of the subsidiary ligand(s) to interact with nucleobases in their vicinity (Sammes and Yahsioglu, 1994; Erkkila and Odom, 1999; Sigman et al., 1996).

In the design of ternary metal complexes, selection of coligand can be a crucial factor in determining their DNA binding property and their affinity for specific DNA binding site(s), if any. Maltol (Hma), dipicolinic acid (H<sub>2</sub>dipico) and threonine (Hthr) have been chosen as coligands in the design of the ternary metal complexes in the present thesis. Maltol (**Figure 1.3**) is a naturally occurring and non-toxic compound. It is an approved food additive in many countries due to its flavour and antioxidant properties (Kato, 2003; Yanagimoto et al., 2004; LeBlanc and Akers, 1989; Schenck et al., 1945; Thompson et al., 2004). Maltol is a planar compound with hydroxypyrrone structure and it can act as a monoanionic, bidentate *OO'*-ligand (Marwaha et al., 1994; Yasumoto et al., 2004; Zborowski et al., 2007). Many biologically important metals form stable complexes with maltol due to the relative easiness to deprotonate the hydroxyl group of maltol at the 3<sup>rd</sup> position (Hsieh et al., 2006; Lamboy et al., 2007; Maurya et al., 2011). The coordinated maltolate has H-acceptor sites (three oxygen atoms in chelated maltolate). From the literature search, various metal complexes of maltol (e.g. *bis*(maltolato)oxovanadium(IV) and *bis*(maltolato)cobalt(II)) have been reported to have various catalytic and biochemical properties (Li et al., 2008; Caravan et al., 1995; Sun et al., 1996; Hanson et al., 1996; McNeil et al., 1992). Thus, the study of metal complexes with maltolate has been a topic of considerable interest.

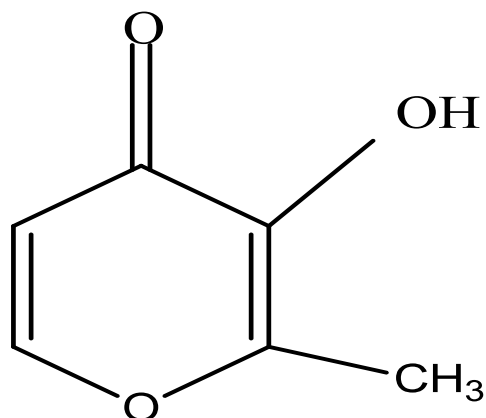


**Figure 1.3:** Structure of maltol

Meanwhile, dipicolinic acid (**Figure 1.4**) is also used as a coligand in this project. Dipicolinic acid is another essential compound use by living organism, including human (Vargová et al., 2004). It is a flexible and versatile ONO'-ligand and has diverse coordination modes (Erikson et al., 1987; Ducommun et al., 1989; Lubes et al., 2010). It can act as a bidentate, tridentate (Chatterjee et al., 1998; Trivedi et al., 2010), meridian or bridging ligand in various metal complexes (Andreev et al., 2010). Dipicolinic acid is a rigid and planar molecule with hydrogen bond acceptor sites (carboxylate group). Pyridinecarboxylate compounds are particularly interesting owing to their photophysical properties (Qin et al., 2005; Lamture et al., 1995; Mesquita et al., 2002). In addition, metal complexes with dipicolinate-based ligand ( $[\text{Co}(\text{dipico})_2]^{2-}$ ,  $[\text{Na}_3\text{Y}(\text{dipico})_3] \cdot 12\text{H}_2\text{O}$ ,  $[\text{Y}_2(\text{dipico})(\text{OH})_4] \cdot 3\text{H}_2\text{O}$ ,  $\{[\text{Ni}(\text{phen})_3[\text{Ni}(\text{dipico})_2]\}_2 \cdot 17\text{H}_2\text{O}$  where dipico = dipicolinate; phen = 1,10-phenanthroline, Y = Yttrium(III)) were reported by a number of researchers to exhibit various biological functions, *viz.* insulin mimetic, antibacterial and anticancer (Yang et al., 2002; Cai et al., 2010; Çolak et al., 2010).

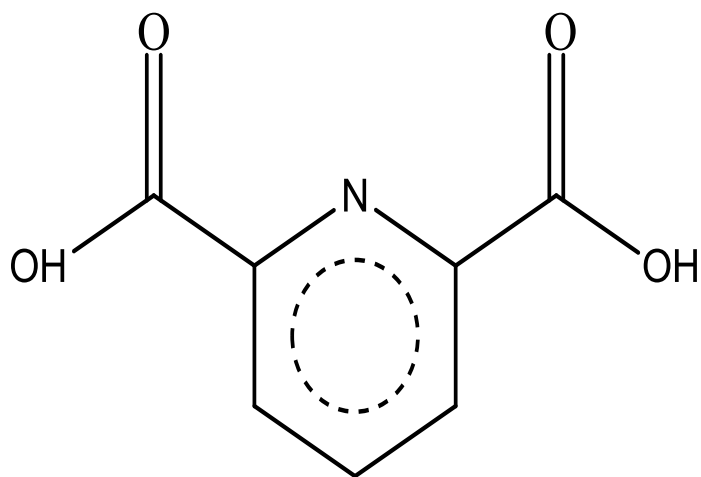


**Figure 1.4:** Structure of dipicolinic acid

Stereochemistry is of utmost importance in the construction of metal complexes as site-specific recognition agents. Many transition metal complexes are optically active. Enantiomers of chiral metal complexes have attracted considerable attention as potential structural probes of DNA conformation. Norden and Tjerneld (1976) first reported the preference of the  $\Delta$  enantiomer of *tris*(dipyridyl)iron(II) for right-handed B-form DNA. The Barton group of researchers subsequently developed elaborate series of chiral metal complexes, some of which were reported to be able to recognize specific DNA conformational features (A-DNA, B-DNA and Z-DNA) (Barton, 1986; Chow and Barton, 1992). In the year 1984, Barton and co-workers found that  $\Lambda$ -*tris*(4,7-diphenyl-1,10-phenanthroline)ruthenium(II) does not bind B-DNA owing to steric constraint, however it binds avidly to Z-DNA. Later, Barton and Raphael (1985) have reported the chiral complex  $\Lambda$ -*tris*(4,7-diphenyl-1,10-phenanthroline)cobalt(III) binds to and cleaves left-handed DNA helices and thereby may be used as molecular probe for DNA conformation.

Extensive researches have been done on delta ( $\Delta$ ) and lambda ( $\Lambda$ ) chiral octahedral complexes but less research have been done on L- and D-chiral metal complexes. Therefore, a pair of optically active essential amino acid, L-threonine and D-threonine (**Figure 1.5**) were chosen as one of the coligand to synthesize chiral L- and D-metal(II) complexes. The coordinated L-threoninate and D-threoninate have both H-acceptor (carboxylate group) and H-donor sites (amine group).

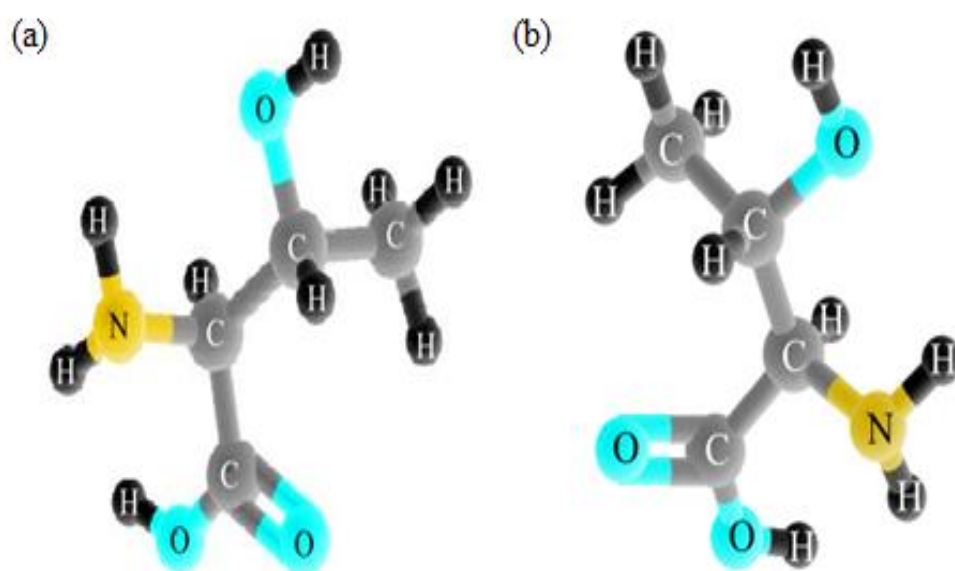


**Figure 1.5:** Structures of (a) L-threonine (L-thr); (b) D-threonine (D-thr)

For the series of metal(II) complexes,  $[M(\text{phen})(L)X]$ ,  $[M(\text{phen})(L)(\text{H}_2\text{O})]$  and  $[M(\text{phen})(L)_2]$  ( $L$  = monoanionic or dianionic ligand) in this project, it is expected that these metal(II) complexes can have two important properties *viz.* DNA binding specificity (molecular recognition) and anticancer property with less harmful side-effect(s). Design of the above

ternary complexes involves “modular assembly” of a main ligand and a coligand with the chosen metal cation. The metal centre acts as an anchor that can hold a rigid, three-dimensional scaffold of ligands in place and can also bear the desired ligand(s) as DNA recognition element(s). If these complexes use the phenanthroline to intercalate into the base pairs of DNA, the geometry of the complexes will have profound effect on the orientation of the coligand. The coordinated coligand(s) and the geometry of the complexes should contribute to the desired DNA recognition of nucleobases.

## 1.2 OBJECTIVES

There are three main aims for this study *viz.* (i) to synthesize three series of ternary metal(II) polypyridyl complexes with the chosen *OO'*-, *ONO'*- and *NO*-coligands; (ii) to characterize metal(II) complexes in solid and solution state; (iii) to conduct biological studies on selected Co(II) and Zn(II) complexes. Further description on each aim is elaborated in this section. The modular system comprises of three sets of ternary metal(II) complexes. Each set of ternary metal(II) complexes contain phen as the main ligand (polypyridyl) and the three sets are constructed by varying the coligand (*OO'*-, *ONO'*- or *NO*-) and metal ion (Co(II), Cu(II) or Zn(II)). This modular system is systematically assembled to study the effect of varying coligand and metal(II) ion on its solid and solution properties.

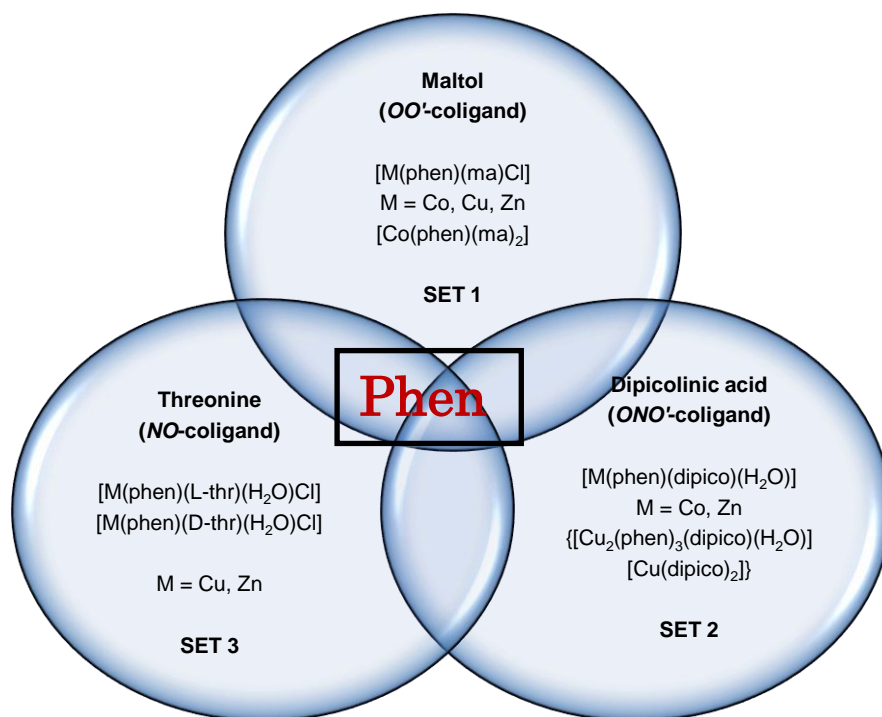


**Figure 1.6:** Modular system in this research study.

The series of ternary metal(II) complexes, summarized in **Figure 1.6**, are characterized by using analytical methods shown in **Table 1.1**. There are mainly two types of characterization *viz.* characterization of solid complexes and characterization of aqueous solution of these complexes. Different methods were used for studies of complexes in the solid state and complexes in the solution state as listed in **Table 1.1**. The solid state studies of these metal(II) complexes synthesized are to find out their molecular formulae and structural geometries. The purpose of solution state studies of these metal(II) complexes synthesized was to characterize the species in their respective solutions when these complexes dissolved in water-methanol (1:1 v/v). This is important for the last part of my study, *i.e.* selecting some of these complexes for biological studies.

**Table 1.1:** List of analytical methods

Characterization		
<p><b>SET 1</b> [M(phen)(ma)Cl] M = Co, Cu, Zn [Co(phen)(ma)<sub>2</sub>]</p>	<p><b>SET 2</b> [M(phen)(dipico)(H<sub>2</sub>O)] M = Co or Zn {[Cu<sub>2</sub>(phen)<sub>3</sub>(dipico)(H<sub>2</sub>O)] [Cu(dipico)<sub>2</sub>]}</p>	<p><b>SET 3</b> [M(phen)(L-thr)(H<sub>2</sub>O)Cl] [M(phen)(D-thr)(H<sub>2</sub>O)Cl] M = Cu, Zn</p>
<p><b>Solid characterization</b> * FTIR spectroscopy * CHN analysis * Thermogravimetric analysis (TGA) * X-ray crystallography</p>	<p><b>Solid characterization</b> * FTIR spectroscopy * CHN analysis * X-ray crystallography</p>	<p><b>Solid characterization</b> * FTIR spectroscopy * CHN analysis * Thermogravimetric analysis (TGA) * X-ray crystallography</p>
<p><b>Aqueous solutions characterization</b> * Electrospray Ionization Mass spectrometry (ESI-MS) * Molar conductivity measurement * UV-Visible spectrophotometry * Fluorescence spectroscopy</p>	<p><b>Aqueous solutions characterization</b> * Molar conductivity measurement * UV-Visible spectrophotometry * Fluorescence spectroscopy</p>	<p><b>Aqueous solutions characterization</b> * Electrospray Ionization Mass spectrometry (ESI-MS) * Molar conductivity measurement * UV-Visible spectrophotometry * Fluorescence spectroscopy * Circular Dichroism (CD)</p>

Numerous clinical, anticancer drugs are topoisomerase (Topo) I inhibitors (Kikuta et al., 2000; Chuang et al., 1996; Sunami et al., 2009; Pommier, 2006; Beretta et al., 2008; Rothenberg, 1997). However, none of these clinical drugs are zinc complexes. In fact, not many zinc complexes have been studied for their anticancer properties. From literature search, only a few cobalt(II) and zinc(II) complexes are known to inhibit Topo I. For this reason, two sets of ternary metal(II) complexes were chosen *viz.* Co(II) complexes ([Co(phen)(ma)Cl]·4H<sub>2</sub>O and [Co(phen)(ma)<sub>2</sub>]·5H<sub>2</sub>O) and Zn(II) complexes ([Zn(phen)(dipico)(H<sub>2</sub>O)]·H<sub>2</sub>O and [Zn(phen)(L-thr)(H<sub>2</sub>O)·2H<sub>2</sub>O]), to investigate their interaction with Topo I and DNA besides studying their anticancer property. Two Co(II) complexes as mentioned above were selected

to investigate the effect of number of chelated maltolate ligand on their biological properties. Both Zn(II) complexes were chosen to investigate the effect of changing coligands from *ONO'*-dipicolinate to *NO'*-L-threoninate on biological properties.

**CHAPTER 2**

**LITERATURE REVIEW**

**SYNTHESIS, CHARACTERIZATION AND BIOLOGICAL  
PROPERTIES OF METAL(II) POLYPYRIDYL COMPLEXES WITH  
*oo'*-, *ono'*- OR *no*-CHELATING COLIGANDS**

## CHAPTER 2

### LITERATURE REVIEW

In the past decade, many metal(II) complexes have been synthesized. These metal(II) complexes have attracted considerable attention in various fields of research, *viz.* catalysis, crystal engineering, medicine and DNA interaction (Adachi and Sakurai, 2004; Peng et al., 2007; Sharma et al., 2012). In this chapter, the background of the chosen main ligand (1,10-phenanthroline), coligands (maltolate, dipicolinate, L-threoninate and D-threoninate) and their related metal(II) complexes will be reviewed. This review mainly focuses on the chemical (*e.g.* structural geometry, thermal studies, photophysical, photochemical, catalysis and *etc.*) and biological (*e.g.* DNA interaction, insulin-mimetic, anti-hyperglycemic, anti-cancer, antimicrobial and *etc.*) studies. In the last section of this chapter, a focus review of cobalt, copper and zinc complexes on their biological activity is included.

#### 2.1 1,10-PHENANTHROLINE COMPLEXES

From the list of polypyridyl ligands, such as 2,2'-bipyridine, 1,10-phenanthroline, dipyrdo[3,2-a:2',3'c]phenanzine, 1,10-phenantroline-5,6-dione, dipyrdo[3,2:2',3'-f]quinoxaline and *etc.*, 1,10-phenanthroline has been

chosen as the main ligand to make a few series of ternary metal(II) complexes in this project. Phen is a versatile starting material due to its rigidity, planarity, aromaticity, basicity and chelating capability (Bencini and Lippolis, 2010). After Brandt et al. (1954) reviewed the metal complexes of 1,10-phenanthroline, extensive research was carried out on the coordination chemistry of phen. It played an important role in the development of coordination chemistry (Sammes and Yohioglu, 1994; Luman and Castellano, 2004). As phen could coordinate to many metal ions in the Periodic Table, phen-based complexes have been actively studied for their catalytic, redox, photochemical and photophysical (luminescence) properties (Armaroli, 2001; Scaltrito et al., 2000; Luman and Castellano, 2004; Bossert and Daniel, 2008; Lavie-Cambot et al., 2008).

Aboul-Gheit et al. (2011) prepared a platinum complex,  $[\text{Pt}(\text{phen})]\text{Cl}_2$  and used it as a photosensitizer in water to photodegrade 4-chlorophenol under three irradiation wavelengths, viz. 254, 364 and 400 - 800 nm (visible). The rate of photodegradation by  $[\text{Pt}(\text{phen})]\text{Cl}_2$  was found to be in the order: 400 - 800 nm (visible) > 364 nm > 254 nm. Besides photodegradation (photosensitizer) properties, antibacterial and antifungal properties of phen-based complexes were reported. A series of ternary phen-based complexes were synthesized by Shebl et al. (2010) and their antibacterial and antifungal properties were investigated. These metal complexes, viz.  $[\text{Co}(\text{phen})(\text{H}_3\text{L})]\text{Cl}\cdot 4\text{H}_2\text{O}$ ,  $[\text{Ce}(\text{NO}_3)(\text{H}_2\text{O})(\text{phen})(\text{H}_3\text{L})]\cdot 5\text{H}_2\text{O}$  and  $[\text{UO}_2(\text{H}_3\text{L})(\text{phen})]\cdot 2\text{H}_2\text{O}$  ( $\text{H}_3\text{L}$ = thiocarbohydrazone), showed antibacterial

activity towards *Staphylococcus aureus* (Gram-positive bacteria) and *Escherichia coli* bacteria (Gram-negative bacteria). The [Co(phen)(H<sub>3</sub>L)]Cl·4H<sub>2</sub>O complex showed higher antifungal activity towards *Candida albicans* and *Aspergillus flavus* than Amphotricine B which was used as a control antifungal agent. Other phen-containing complexes, viz. [Cu(bpy)(phen)]Cl<sub>2</sub>·2H<sub>2</sub>O, [Co(bpy)(phen)<sub>2</sub>](NO<sub>3</sub>)<sub>2</sub>·2H<sub>2</sub>O (Agwara et al., 2010), [Mn(4-MPipzcdt)<sub>2</sub>(phen)], [Co(4-MPipzcdt)(phen)<sub>2</sub>]Cl (Kalia et al., 2009), [Cu(SAla)(phen)]·H<sub>2</sub>O (Chandrakeka et al., 2011), [CuL(phen)<sub>2</sub>]Cl<sub>2</sub>, [ZnL(phen)<sub>2</sub>]Cl<sub>2</sub> (Raman and Sobha, 2010), [M(L)(phen)Cl] (Raman et al., 2010) (bpy = 2,2'-bipyridine; 4-MPipzcdt = 4-methylpiperazine-1-carbodithioate; SAla = Salicylaldehyde-alanine; L = isatin-based schiff base; M = Cu, Co, Ni or Zn), were also found to have antibacterial and/or antifungal properties.

In the past decades, many researchers reported various cationic phen-based complexes having anticancer property. These include iridium complex, [Ir(η<sup>5</sup>-cp)(phen)Cl]<sup>+</sup> (Liu et al., 2011), ruthenium porphyrin complex, [(Py-3')TPP-Ru(phen)<sub>2</sub>Cl]<sup>+</sup> (Liu et al., 2010), ruthenium-selenium complex, [Ru(phen)<sub>2</sub>(phenSe)]<sup>2+</sup> (Li et al., 2012), lanthanide complex, Ln[(phen)<sub>2</sub>(5-Fu)<sub>3</sub>(NO<sub>3</sub>)]<sup>2+</sup> (Zhong et al., 2005) (where η<sup>5</sup>-cp = pentamethylcyclopentadienyl; (py-3')TPP = 5-(3'-pyridyl-10,15,20-triphenylporphyrin; phenSe = 1,10-phenanthrolineselenazole; Ln = yttrium, lanthanum, cerium, samarium, gadolinium, dysprosium, erbium; 5-Fu = fluorouracil). Neutral phen-based complexes such as [M(phen)(edda)] (where

M = Co, Cu, or Zn; edda = ethylenediaminediacetic acid) (Ng et al., 2007) and [Cu(phen)<sub>2</sub>(ma)] (ma = maltol) (Coyle et al., 2004) were reported to have anticancer property. Both [Cu(phen)(edda)] and [Cu(phen)<sub>2</sub>(ma)] could induce cell death mainly *via* apoptosis. On the other hand, Ng and coworkers (2008) revealed that an octahedral [Zn(phen)(edda)] could induce cell cycle arrest. Heffeter et al. (2006) showed that the [tris(1,10-phenanthroline)lanthanum(III)] trithiocyanate exerts anticancer activity *via* potent induction of cell cycle arrest and/or apoptosis and has promising *in vivo* anticancer activity against a human colon cancer xenograft.

The potential use of phen-based complexes as DNA intercalating agents has been a hot topic of study by many inorganic chemists. Apart from the DNA intercalating property, these complexes have been studied for their potential use as artificial nucleases. Cu(I)-phen is a well known DNA nuclease that could cleave DNA *via* an oxygen-dependent reaction (Sigman et al., 1979; Thederahn et al., 1989; Chen et al., 1993). The chemical nuclease Cu(I)-phen cleaved DNA by oxidative attack on the deoxyribose moiety yielding 3'- and 5'-phosphomonoesters, free purine and pyrimidine, and 5-methylenefuranone as stable products (Zelenko et al., 1998). In addition, studies of García-Raso et al. (2003) showed that the Cu(II)-phen-peptide complexes with L-Val-gly and gly-L-trp cleaved pBR322 plasmid DNA without the presence of an external reducing agent. However, a recent research report by Rao and coworkers (2007) revealed that [Cu(L-pro)(phen)(H<sub>2</sub>O)](NO<sub>3</sub>) showed chemical nuclease activity under physiological reaction condition *via* a mechanistic pathway

involving formation of hydroxyl radicals in presence of the 3-mercaptopropionic acid (reducing agent).

## 2.2 MALTOLATO COMPLEXES

Maltol has been known since the late 1800's but its coordination chemistry has only developed in the 1900's. Maltol has a hydroxypyrrone structure and it deprotonates its hydroxyl group in basic media to form the monoanionic maltolate (ma; an *OO'*-bidentate chelator) (Yasumoto et al., 2004). Maltol was found to induce apoptosis of HL60 cells in the presence of iron, but maltol or iron alone did not affect the cells. Basically, apoptosis of HL60 cells can be explained by the prooxidant properties of maltol/iron compound (Murakami et al., 2006). Nonetheless, maltol enhancement of aluminium and gallium toxicity has been well studied (Katsetos et al., 1990; Savory et al., 1995; Farrar et al., 1988). Farrar et al. (1988) showed that the presence of maltol in fasted (16 hours) animals enhanced gallium uptake into liver, kidney, spleen, heart and brain. Farrar and coworkers (1988) suggested that the enhancement of gallium uptake indicates that gallium-maltol is soluble and carries a neutral charge thereby facilitating its movement across the membrane of the intestinal epithelial cell.

Owing to its high affinity towards metal ion, more and more maltolato complexes have been synthesized and screened for their biological properties.

Parajón-Costa and Baran (2011) have compared the spectra of *bis(maltolato)oxovanadium(IV)*,  $[\text{VO}(\text{ma})_2]$  (where  $\text{V}^{\text{IV}}\text{O} = \text{Oxovanadium(IV)}$ ,  $\text{ma} = \text{maltolate}$ ) with uncoordinated maltol and with some related species. Zborowski et al. (2007) have presented FT-IR and FT-Raman spectra of maltol (anion and cation form). Quantum chemical calculations were used to interpret vibrational data of FT-IR and FT-Raman spectra and described the changes upon protonation or deprotonation (Zborowski et al., 2007). The insulin-mimetic property of *bis(maltolato)oxovanadium(IV)* have been investigated by many researchers (McNeil et al., 1992; Thompson et al., 2003; Peters et al., 2003; Thompson et al., 2004; Sakurai et al., 2003). When *bis(maltolato)oxovanadium(IV)* is absorbed, it may meet many other potential  $\text{V}^{\text{IV}}\text{O}$ -binding molecules (such as nucleotides, inorganic and organic phosphate, lactate, *etc.*) present in extracellular or intracellular biological fluids. Hence, a study was carried out by Kiss and colleagues (1998) to assess the solution state of  $\text{V}^{\text{IV}}\text{O}$  in organism by mixing  $[\text{VO}(\text{ma})_2]$  with various bioligands (potential metal ion binders of biofluids and tissues). It was found that  $[\text{VO}(\text{ma})_2]$  underwent transformation into mixed ligand complexes by interacting with bioligands. Meanwhile, the interaction of vanadyl sulfate and  $[\text{VO}(\text{ma})_2]$  with human serum apo-transferrin were investigated by Bordbar et al. (2009). A series of binary maltolato complexes,  $[\text{M}(\text{ma})_n]$  (M is Co(II), Cu(II), Cr(III) and Zn(II); n is 2 or 3) and  $[\text{MoO}_2(\text{ma})_2]$  were prepared by Thompson's group (2004) to compare their anti-hyperglycemic effect. Amongst all the tested compound, only  $[\text{MoO}_2(\text{ma})_2]$  and  $[\text{Co}(\text{ma})_2]$  showed hypoglycemic activity at  $\text{ED}_{50}$  dose for  $[\text{VO}(\text{ma})_2]$ ,  $0.6 \text{ mmol kg}^{-1}$  by oral gavage in streptozotocin (STZ)-diabetic rats within 72 hours of administration

of compound.

Other than  $[\text{VO}(\text{ma})_2]$ , a neutral *bis*(maltolato)zinc(II),  $[\text{Zn}(\text{ma})_2]$  complex was also reported to have insulin-mimetic property (Sakurai et al., 2002; Yoshikawa et al., 2001; Fugono et al., 2002; Adachi and Sakurai, 2004). In 2001, a group of Japanese researchers tested  $[\text{Zn}(\text{ma})_2]$  in KK-A(y) mice with Type 2 diabetes mellitus. It was found that the blood glucose level was reduced to within normal range during administration of the  $[\text{Zn}(\text{ma})_2]$  for two weeks (Yoshikawa et al., 2001). In order to understand the insulinomimetic activity of  $[\text{Zn}(\text{ma})_2]$ , Fugono et al. (2002) carried out a metallokinetic study of zinc in the blood of GK rats treated with  $[\text{Zn}(\text{ma})_2]$ . The result was compared with zinc chloride. These studies revealed that oral administration of  $[\text{Zn}(\text{ma})_2]$  lowered the blood glucose levels in GK rats with Type 2 diabetes mellitus.

Besides, a comparative study of insulin-mimetic activity of  $[\text{Zn}(\text{ma})_2]$  and  $[\text{VO}(\text{ma})_2]$  complexes was carried out by Adachi and Sakurai (2004). It was reported that  $[\text{VO}(\text{ma})_2]$  lowered the high blood glucose levels in both Type 1 and Type 2 diabetes mellitus mice, while  $[\text{Zn}(\text{ma})_2]$  was found to lower the blood glucose levels only in Type 2 diabetes mellitus mice. Enyedy and co-workers (2006) carried out an *in vitro* study of the interaction between insulin-mimetic zinc(II) complexes and selected plasma components (such as cysteine, histidine and citric acid). Their results showed that binary zinc(II)

complexes formed various ternary zinc(II) complexes with plasma components, especially cysteine.

Besides the above insulin-mimetic property, some maltolato complexes have been reported to have anticancer property. For example, *tris*(maltolato)ruthenium(III) has been prepared by Kennedy and coworkers (2005) and it was tested for anti-proliferative activity against the human breast cancer cell line MDA-MB-435S (a spindle shaped variant of the parental MDA-MB-435 strain) and gave IC<sub>50</sub> value of 140 μM. Later, Kennedy and coworkers extended their work from binary ruthenium(III) complexes to ternary ruthenium(III) complexes. The ternary Ru(III) metronidazole-maltolato complex, *trans*-[Ru(ma)<sub>2</sub>(metro)<sub>2</sub>]CF<sub>3</sub>SO<sub>3</sub> (where ma = maltolate; metro = metronidazole) was prepared and examined for anti-tumor activity against human breast cancer cell line MDA-MB-435S using 3-(4,5-dimethylthiazol-2-yl)-2,5-diphenyltetrazolium bromide (MTT) assay in phosphate-buffered saline (Kennedy et al., 2006). Surprisingly, the ternary ruthenium(III) complex had a lower IC<sub>50</sub> value than the binary ruthenium(III) complex, *tris*(maltolato)ruthenium(III).

Although many ruthenium complexes with anticancer property were reported, a titanium complex was the first non-platinum complex to be tested against solid tumor (Clarke et al., 1999; Keppler et al., 1991; Schilling et al., 1996). Lamboy et al. (2007) determined the crystal structure of

$[\text{Ti}_4(\text{maltolato})_8(\mu\text{-O})_4]$  and found that it was a tetranuclear complex with two bridging oxides and two bidentate maltolate ligands per titanium in a pseudo-octahedral coordination environment. Subsequently, the anticancer property of this complex was tested on colon cancer HT-29 cells (Hernández et al., 2008) and caco-2 (human colon adenocarcinoma) cell line (Hernández et al., 2010). It had greater cytotoxic activity than various titanocene complexes ( $[\text{Cp}_2\text{TiCl}_2]$  and  $[\text{Cp}_2\text{Ti}(\text{aa})_2]\text{Cl}_2$  where Cp = cyclopentadienyl; Ti = titanium; aa = L-cysteine, L-methionine, and D-penicillamine) that were investigated together.

More binary metal-maltolato complexes had been synthesized. A neutral *mer-tris*(maltolato)iron(III),  $[\text{Fe}(\text{ma})_3]$ , was found to be a potential candidate to treat iron deficiency anemia (Ahmet et al., 1988). Later, its crystal structure was determined by using X-ray diffraction method. This complex possessed a distorted octahedral geometry with the three maltolato ligands bonded through the hydroxy and ketone oxygen atoms to give the *mer* configuration (Ahmet et al., 1988). Another neutral complex, *tris*(maltolato)aluminium(III),  $[\text{Al}(\text{ma})_3]$ , has found applications in the Alzheimer's disease (Finnegan et al., 1986; Nelson et al., 1988; Yu et al., 2002; Obulesu et al., 2009). Recently, *tris*(maltolato)gallium(III),  $[\text{Ga}(\text{ma})_3]$ , is undergoing clinical and preclinical testing as a potential therapeutic agent for cancer, infectious disease and inflammatory disease (Bernstein, 2012; Chua et al., 2006; Chitambar et al., 2007; Bernstein et al., 2000).

Many researchers had synthesized and studied the antimicrobial property of complexes of maltolate with various heavy transition metals. For instance, *tris(maltolato)gallium(III)*,  $[\text{Ga}(\text{ma})_3]$ , significantly reduced the colonization of *Staphylococcus aureus* and *Acinetobacter baumannii* in the wound of thermally injured mice (DeLeon et al., 2009). It also prevented the growth of *Pseudomonas aeruginosa* bacteria in the wound. Two other heavy transition metal complexes containing maltolate, viz. oxoperoxomolybdenum(VI) compound,  $[\text{MoO}(\text{O}_2)(\text{ma})(\text{acac})]\cdot\text{H}_2\text{O}$ , and  $[\text{MoO}(\text{O}_2)(\text{ma})(\text{macac})]\cdot\text{H}_2\text{O}$  (ma = maltolate; acac = acetylacetonate; macac = methylacetonate), were reported to have antimicrobial property towards *Escherichia coli* and *Vibrio cholera* (Maurya et al., 2011).

Maltolato complexes not only have potential to be therapeutic agents but they have been used as catalysts in transesterification and esterification reactions. A series of maltolato complexes,  $[\text{M}(\text{ma})_2(\text{H}_2\text{O})_2]$  (M =  $\text{Sn}^{2+}$ ,  $\text{Zn}^{2+}$ ,  $\text{Pb}^{2+}$  and  $\text{Hg}^{2+}$ ) were found to be able to catalyse transesterification of soybean oil with methanol. The results showed that the tin complex,  $[\text{Sn}(\text{ma})_2(\text{H}_2\text{O})_2]$  was a better catalyst than the traditional sodium hydroxide and sulfuric acid catalyst under the same conditions (Abreu et al., 2003). Brito et al. (2008) prepared two other series of similar complexes with the general formula  $\text{M}(\text{n-butoxide})_{4-x}(\text{ma})_x$ , where M = Ti or Zr and x = 0-4. Both series of complexes were screened for their catalytic activity. Among these complexes, the zirconium complexes containing at least one maltolate ligand were very efficient esterification catalysts for preparing fatty acid methyl esters.

### 2.3 DIPICOLINATO COMPLEXES

Pyridine-2,6-dicarboxylic acid or also called dipicolinic acid ( $\text{H}_2\text{dipico}$ ) is an oxygen and nitrogen donor ligand that can exhibit diverse coordination modes such as bidentate, tridentate and bridging (Sileo et al., 1997; Ma et al., 2003; Ranjbar et al., 2002; Devereux et al., 2002; Koman et al., 2000; Mao et al., 2004). During the past few years, its diverse coordination modes have attracted considerable attention from inorganic and bioinorganic chemists, and numerous metal complexes containing the dipicolinate ligand were synthesized and studied (Sileo et al., 1997; Vargová et al., 2004; Kirillova et al., 2007). Others had reported the crystal structures of different  $3d$  and lanthanide metal dipicolinate complexes (Teoh et al., 2008; Gonzalez-Baró et al., 2005; Yang et al., 2002; Hakansson et al., 1993; Hadadzadeh et al., 2010; Uçar et al., 2007; Fernandes et al., 2001; Çolak et al., 2010).

Besides the above monometallic complexes, two series of homodimetallic aqua complexes,  $[\text{M}(\text{H}_2\text{O})_5\text{M}(\text{dipico})_2]\cdot 2\text{H}_2\text{O}$  and  $[\text{M}(\text{H}_2\text{O})_6][\text{M}(\text{dipico})_2]\cdot 2\text{H}_2\text{O}$ , ( $\text{M} = \text{Fe}$  (Laine et al., 1995),  $\text{Co}$  (Shiu et al., 2004; Xie et al., 2004; Qi et al., 2004; Wang et al., 2004a),  $\text{Ni}$  (Wen et al., 2002),  $\text{Cu}$  (Wang et al., 2004b) or  $\text{Zn}$  (Hakansson et al., 1993)) were reported. Later, several heterometallic complexes with dipicolinate ligand were prepared by self-assembly synthesis in aqueous solution at room temperature. These examples of heteronuclear dipicolinate complexes with  $3d$  metals sharing the same general formula  $[\text{M}(\text{H}_2\text{O})_5\text{M}'(\text{dipico})_2]\cdot m\text{H}_2\text{O}$  ( $\text{M}/\text{M}' = \text{Cu}^{\text{II}}/\text{Co}^{\text{II}}$ ,

$\text{Cu}^{\text{II}}/\text{Ni}^{\text{II}}$ ,  $\text{Cu}^{\text{II}}/\text{Zn}^{\text{II}}$ ,  $\text{Zn}^{\text{II}}/\text{Co}^{\text{II}}$ ,  $\text{Ni}^{\text{II}}/\text{Co}^{\text{II}}$ ,  $m = 2-3$ ; dipico = dipicolinate) were reported by Kirillova et al. (2007). Extensive H-bonded networks between the dipicolinate ligands and coordinated and/or uncoordinated water molecules were observed in most of the crystal packing structures of dipicolinato complexes (Hakansson et al., 1993; Sileo et al., 1997; Uçar et al., 2007; Kirillova et al., 2007; Hadadzadeh et al., 2010).

Also, thermal studies of dipicolinato complexes were studied by several researchers (Sileo et al., 1997; Vargová et al., 2004; Çolak et al., 2010). Sileo and coworkers (1997) carried out a kinetic study of the isothermal dehydration of the monoclinic and triclinic polymorphs of  $[\text{Cu}(\text{dipico})]\cdot 2\text{H}_2\text{O}$  (where dipico = dipicolinate). It was reported that both the rate law and the morphology of dehydration were well accounted for by the packing characteristics of the structures. This included both the pathways for water elimination and the ease of the process (with temperatures of dehydration at measurable rates). Later, Vargová and colleague (2004) correlated with the thermal (TG/DTG, DTA) and spectral (infrared spectroscopy) properties of  $[\text{Zn}(\text{dipicoH})_2]\cdot 3\text{H}_2\text{O}$  (where dipicoH = hydrogendipicolinate) with its structure. Çolak et al. (2010) has synthesized and characterized  $\{[\text{Ni}(\text{phen})_3][\text{Ni}(\text{dipic})_2]\}_2\cdot 17\text{H}_2\text{O}$  (where phen = 1,10-phenanthroline; dipic = dipicolinate) by spectroscopic and thermal analysis. The complex has also been investigated for its biological activity and it showed high activity against *S. aureus* from Gram positive bacteria and *C. albicans* from yeast.

Other than crystal structure and thermal studies, other researchers have extended the work to electron paramagnetic resonance (EPR) and electrochemical studies of dipicolinato complexes. For instance, the (2,2'-dipyridylamine)(pyridine-2,6-dicarboxylato)copper(II) trihydrate complex was synthesized and characterized by spectroscopic (IR, UV-vis, EPR), X-ray diffraction technique and electrochemical methods by Uçar et al. (2007). Based on EPR and optical absorption studies, Uçar et al. (2007) determined the spin-Hamiltonian and bonding parameters. The  $g$ -values obtained indicated the presence of the unpaired electron in the  $d_{x^2-y^2}$  orbital. The evaluated metal-ligand bonding parameters showed strong in-plane  $\sigma$ - and  $\pi$ -bonding. Furthermore, the cyclic voltammogram of the (2,2'-dipyridylamine)(pyridine-2,6-dicarboxylato)copper(II) trihydrate complex in dimethylformamide (DMF) solution exhibited only metal centered electroactivity in the potential range  $\pm 1.25$  V versus Ag/AgCl reference electrode (Uçar et al., 2007).

Recently, ternary complex species formed by vanadium(III) cation with the picolinato and dipicolinato ligands in aqueous solutions were studied potentiometrically and by spectrophotometric measurements (Lubes et al., 2010). The stability constants of these ternary complexes, viz.  $[\text{V}(\text{dipico})(\text{pico})]$ ,  $[\text{V}(\text{dipico})(\text{pico})\text{OH}]^-$  and  $[\text{V}(\text{dipico})(\text{pico})_2]^-$ , were determined by potentiometric measurements. In order to obtain a qualitative characterization of the complexes formed in aqueous solution, the spectrophotometric studies were carried out by Lubes and coworkers (2010).

In addition, dipicolinate ligand was well known for its ability to enhance the lanthanide luminescence by a ligand to metal energy transfer mechanism. For example, it was found that the  $\text{Eu}^{3+}$  and  $\text{Tb}^{3+}$  *tris*-dipicolinato complexes were strong emitters in solution (Latva et al., 1997). Later, luminescence properties of *bis*-dipicolinato lanthanide complexes,  $[\text{Eu}(\text{Hdipico})(\text{dipico})]$  with dipico = 2,6-pyridinedicarboxylate were examined by Fernandes et al. (2001). Fernandes and colleagues reported that the  $^5\text{D}_0$  emission lifetime of  $[\text{Eu}(\text{Hdipico})(\text{dipico})]$  was only slightly shorter than that of  $[\text{Eu}(\text{dipico})_3]^{3-}$  in solution (Latva et al., 1997). It was later found that the ligand to metal energy transfer was found to be much less efficient (Fernandes et al., 2001).

A short chain di-ureasil hybrid, designated as d-U(600), was doped with a Eu(III) complex containing dipicolinate ligands,  $\text{Na}_3[\text{Eu}(\text{dipico})_3] \cdot x\text{H}_2\text{O}$ . As a result, the addition of the Eu(III) complex to d-U(600) resulted in an enhancement of the absolute emission quantum yield value, whose maximum value (0.66; excited at 280 nm) is the highest value reported for organic-inorganic hybrids modified by lanthanide complexes (Mesquita et al., 2009). Moreover, the use of terbium-sensitized luminescence for the detection of *Bacillus* spores, such as anthrax, has attracted much attention in recent years due to its applications in biodefense (Hindle and Hall, 1999; Cable et al., 2009) and microbial diagnostics (Gültekin et al., 2010; Kort et al., 2005). Accordingly, Barnes et al. (2011) have measured the effects of terbium chelation upon the parameters associated with dipicolinate ligation and *Bacillus* spore detection. The study revealed that the thermodynamic and

emission stabilities of the [Tb(chelate)(dipicolinate)] (where chelate = 2,2',2''-nitrilotriacetic acid; 2,2-bis(hydroxymethyl)-2,2',2''-nitrilotriethanol; ethylene glycol-bis(2-aminoethyl ether)-*N,N,N',N'*-tetraacetic acid; ethylenediamine-*N,N,N',N'*-tetraacetic acid; 1,2-bis(2-aminophenoxy)ethane-*N,N,N',N'*-tetraacetic acid; 1,4,7,10-tetraazacyclododecane-1,7-diacetic acid; diethylenetriamine-*N,N,N',N'',N''*-pentaacetic acid; 1,4,7,10-tetraazacyclododecane-1,4,7-triacetic acid; and 1,4,7,10-tetraazacyclododecane-1,4,7,10-tetraacetic acid) complexes were directly related to chelate rigidity.

Two novel complexes of rare earth yttrium(III) with 2,6-pyridinedicarboxylate, namely  $[\text{Na}_3\text{Y}(\text{dipico})_3] \cdot 12\text{H}_2\text{O}$  and  $[\text{Y}_2(\text{dipico})(\text{OH})_4] \cdot 3\text{H}_2\text{O}$  (dipico = 2,6-pyridinedicarboxylate) have been prepared by Cai et al. (2010). Minimum inhibitory concentration (MIC) of these two yttrium(III) complexes against *Bacillus coli* and *Staphylococcus aureus* were determined. Antibacterial data indicated two yttrium(III) complexes showed antagonistic effect in their antibacterial activities against *B. coli* and *S. aureus*. In another report, *in vitro* antimicrobial activity of  $\{[\text{Ni}(\text{phen})_3[\text{Ni}(\text{dipico})_2]]_2 \cdot 17\text{H}_2\text{O}$  (dipico = pyridine-2,6-dicarboxylic acid, phen = 1,10-phenanthroline) was investigated by agar well diffusion method (Çolak et al., 2010). This complex exhibited higher activity towards gram positive bacteria (*Staphylococcus aureus*) than *Candida albicans* from yeast. Another dipicolinato complex that was screened for antimicrobial activity was a bridged binuclear Cu(II) complex with mixed ligands, di- $\mu$ -(2-

aminopyridine(*N,N'*)-bis[(2,6-pyridinedicarboxylate)aquacopper(II)] tetrahydrate (Yenikaya et al., 2009).

The study of Murakami and co-workers showed that dipicolinic acid acted as an antioxidant: dipicolinic acid inhibited lipid peroxidation (Murakami et al., 1998) and protected glutathione reductase from the inactivation by copper (Murakami and Yoshino, 1999). Later in 2003, the same research group examined the protective effect of dipicolinic acid on LDL oxidation in relation to copper reduction. Here, the dipicolinic acid showed an antioxidant effect by forming a chelation complex with copper. The formation of the complex has a better antioxidant property due to the effect of chelation at two carboxylate anion (2 and 6 position) (Murakami et al., 2003). Besides, dipicolinato complexes were used as electron carriers in some model biological system, as specific molecular tools in DNA cleavage (Groves and Kady, 1993) and as NO scavengers (Cameron et al., 2003).

A cobalt(II)-dipicolinate complex,  $[\text{Co}(\text{dipico})_2]^{2-}$  was found to be effective in reducing the hyperlipidemia of diabetes in rats with STZ-induced diabetes using oral administration in drinking water (Yang et al., 2002). A series of vanadium (III, IV, V)-dipicolinate complexes with different redox properties were selected by Zhang's research group to investigate the structure-property relationship of insulin-mimetic vanadium complexes for membrane permeability and gastrointestinal (GI) stress-related toxicity using

the Caco-2 cell monolayer model. The cytotoxicity of the vanadium complexes on Caco-2 cells was measured by the decrease of cell viability using the MTT assay. The order of vanadium complexes to induce reactive oxygen and nitrogen species RONS was found to be V(V)-dipico > V(III)-dipico > V(IV)-dipico. The order of redox potential was found to be V(V)-dipico > V(IV)-dipico > V(III)-dipico, respectively (Zhang et al., 2006).

Recently, Willsky and friends (2011) reviewed the anti-diabetic effects of a series of vanadium dipicolinate complexes in rats with streptozotocin-induced diabetes. It was demonstrated that changes in coordination geometry caused the greatest improvement in the insulin-enhancing properties of these complexes. Willsky and coworkers (2011) proposed that the stability of the complexes and the ability to interact with cellular redox substrates were important for the insulin-enhancing activity exerted by vanadium complexes. Redox properties of vanadium complexes can be tuned from favouring one-electron transfer reactions to two-electron transfer reactions, potentially decreasing the toxicity of these complexes (Willsky et al., 2011). Dipicolinato complexes not only have biological properties, they also show catalytic activity (Devereux et al., 2002; Trivedi et al., 2010). All the manganese complexes synthesized by Devereux research group exhibited catalytic activity towards the disproportionation of hydrogen peroxide in the presence of imidazole (Devereux et al., 2002). Recently, a dinuclear  $\mu$ -bis(oxido)bis{oxidovanadium(V)}dipicolinato complex exhibited efficient catalytic activity toward selective epoxidation of *cis*-cyclooctene by using *tert*-

butylhydroperoxide as an oxidant (Trivedi et al., 2010).

## 2.4 THREONINATO COMPLEXES

Amino acids are the building blocks of proteins. Threonine is a chiral  $\alpha$ -amino acid bearing an alcohol group. This essential amino acid is classified as a polar uncharged amino acid. Threonine has two chiral centers. Threonine can exist in four possible stereoisomers with the following configuration: (2*S*, 3*R*), (2*R*,3*S*), (2*S*, 3*S*) and (2*R*, 3*R*). The name L-threonine is used for (2*S*, 3*R*)-2-amino-3-hydroxybutanoic acid; D-threonine is used for (2*R*,3*S*)-2-amino-3-hydroxybutanoic acid. Such pair of chiral molecules (called enantiomers, **Figure 2.1**) can be differentiated by their optical rotation. Optical rotation is the turning of the plane of linearly polarized light about the direction of motion as the light travels through certain materials (Carey, 2000; Wikipedia®, 2012). It occurs in solutions of chiral molecules. Each enantiomer will rotate the light in a different direction, clockwise ((+)-form) or counter clockwise ((-)-form). The optical rotation of L-threonine and D-threonine in water are -28 and +29 (5 mg/mL), respectively (Chem Spider 6051, 2010; Chem Spider 62643, 2010).

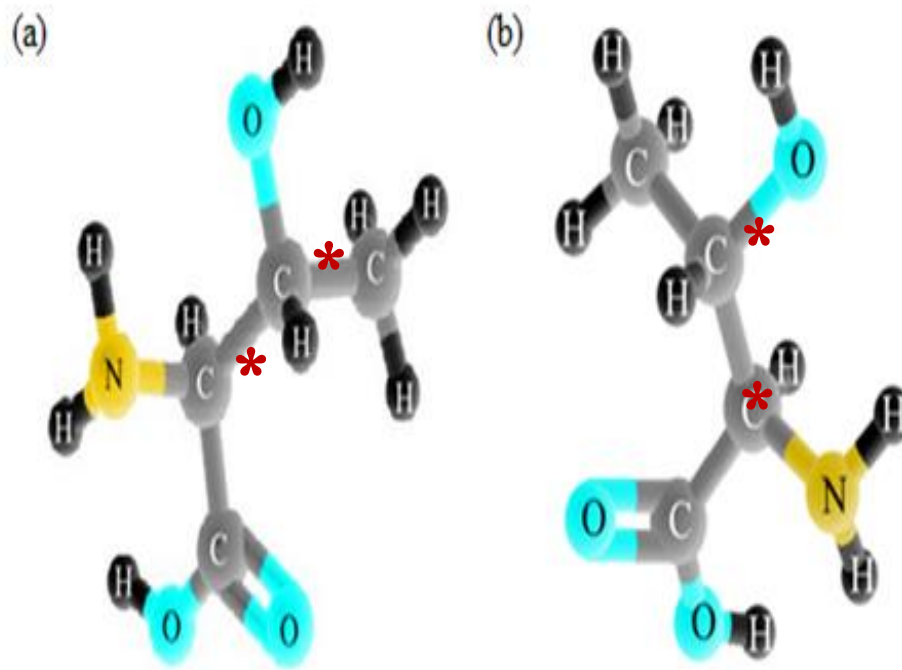


**Figure 2.1:** Structure of (a) L-threonine (L-thr); (b) D-threonine (D-thr) with their chiral centres marked with asterisks.

Enantiomers of chiral metal complexes were discovered to be able to function as structural probes of DNA (Qu et al., 2000). Hence, enantiomers of chiral metal complexes, especially chiral amino acid complexes, have attracted considerable attention from researchers (Nakabayashi et al., 2004; Chetana et al., 2009; Zhang et al., 2009; Jin and Ranford, 2000; Rao et al., 2007). Zhang et al. (2004) synthesized a ternary copper(II) complex,  $[\text{Cu}(\text{phen})(\text{L-thr})(\text{H}_2\text{O})](\text{ClO}_4)$  and determined its crystal structure. The crystal structure of  $[\text{Cu}(\text{phen})(\text{L-thr})(\text{H}_2\text{O})](\text{ClO}_4)$  shows that the  $[\text{Cu}(\text{phen})(\text{L-thr})(\text{H}_2\text{O})]^+$  cation has a distorted square-pyramidal geometry. This copper(II) complex was reported to exhibit potent cytotoxic effects against human leukemia cell line HL-60 and human stomach cancer cell line SGC-7901 with inhibition rates of over 90% ( $1.0 \times 10^{-6}$  M) (Zhang et al., 2004). The structure of the D-

enantiomer and its biological activity has not been reported.

Rizzi and colleagues (2000) reported the structure and single crystal EPR studies of a binary copper(II) complex, *bis*(L-threoninato)copper(II) monohydrate,  $[\text{Cu}(\text{L-thr})_2] \cdot \text{H}_2\text{O}$ . The  $[\text{Cu}(\text{L-thr})_2] \cdot \text{H}_2\text{O}$  exists as an octahedral complex. The copper ion is in an elongated octahedral coordination. *Trans* coordination by two threonine molecules produces square planar environment. The axial ligands are carboxylate oxygen atoms of a pair of symmetry related molecules obtained through  $\pm b$  translations (Cu-O<sub>ax</sub> distances of 2.478(8) and 2.972(3) Å, respectively). The O<sub>eq</sub>-Cu-O<sub>ax</sub> interaction of adjacent  $\text{Cu}(\text{L-thr})_2$  molecules in a chain provides the main path for the transmission of the super-exchange coupling between copper unpaired electrons. The EPR data for  $[\text{Cu}(\text{L-thr})_2] \cdot \text{H}_2\text{O}$  indicated that this complex had carboxylate-bridged copper ion chains, which are linked through complex chemical paths involving the amino acid side chain and hydrogen bonds (Rizzi et al., 2000). A series of zinc(II) complexes of L- and D-amino acids,  $[\text{Zn}(\text{aa})_2]$  and their derivatives,  $[\text{ZnL}]$  (where aa = L-asparagine, D-asparagine, L-proline, D-proline, L-threonine, D-threonine, L-valine, D-valine, glycine, L-alanine, D-alanine, L-histidine and D-histidine; L = *N,N'*-ethylene-bis-glycine, *N,N'*-ethylene-bis-sarcosine, *N,N'*-ethylene-bis-L-methionine, *N,N'*-ethylene-bis- $\beta$ -alanine, *N,N'*-trimethylene-bis-glycine and *N,N'*-trimethylene-bis-L-valine) were prepared to study their insulin-mimetic activity (Yoshikawa et al., 2001). Zinc(II) complexes with a  $\text{Zn}(\text{N}_2\text{O}_2)$  coordination mode were found to have *in vitro* insulin-mimetic activity. Using isolated rat adipocytes treated with epinephrine,

the insulin-mimetic activity of the complexes was evaluated in terms of inhibition of free fatty acid release. Furthermore, it was reported that the insulin-mimetic activity of zinc(II) complexes with overall stability constants ( $\log \beta$ ) less than 10.5 was higher than that of  $\text{ZnSO}_4$  and  $\text{VOSO}_4$ . It was revealed that daily injections of *cis*- $[\text{Zn}(\text{L-thr})_2(\text{H}_2\text{O})_2]$  for 14 days successfully lowered down the high blood glucose level of KK- $\text{A}^y$  mice with Type 2 diabetes mellitus (Yoshikawa et al., 2001).

A series of metal(II) complexes with threonine as ligand,  $[\text{M}(\text{Thr})_2] \cdot n\text{H}_2\text{O}$  (where M = Cobalt(II), Copper(II) and Zinc(II); Thr = threonine;  $n = 1-2$ ), was synthesized and characterized by Marcu et al. (2008). Their main aim was to elucidate the structure of the synthesized threonine complexes by using several spectroscopy methods such as atomic absorption, elemental analysis, FTIR, UV-Vis and EPR spectroscopy. It was revealed that the amino acids are coordinated to the metal centre with its carbonyl oxygen and the nitrogen atom of amino group with the metal-ligand in the ratio of 1:2. Then, the EPR spectra were used to confirm the pseudotetrahedral local symmetry for copper ion and octahedral symmetry for cobalt ion respectively (Marcu et al., 2008). Both the structure and the stability constant of these complexes play an important role in their biological functions. In Na'aliya's (2010) report, the stability constants of nickel complexes with non-polar amino acids,  $[\text{Ni}(\text{aa})_3]^-$  (where aa = proline, threonine, asparagine) was reported. It was reported that the high stability of the complexes could be associated to the nature of the chelation taking place in the complexes. All the

complexes form rings in their structure which resulted from coordination of the Ni(II) ion with bidentate amino acids, and this resulted in the complexes being more stable. The high stability of the complexes is one of the factors that enhance the functioning of the complexes in the relevant biological processes taking place in the body.

Shi and coworkers (2007) carried out a mechanistic study of oxidation of L-serine and L-threonine by *bis*(hydrogen periodato)argentate(III) complex anion,  $[\text{Ag}(\text{HIO}_6)_2]^{5-}$ . The oxidation reaction took place in alkaline medium and each silver complex selectively broke down the  $\text{C}^\alpha\text{-C}^\beta$  bonds, leading to the formation of its aldehyde (formaldehyde for serine and acetaldehyde for threonine). This suggests that the silver complex might be useful as a reagent for modification of peptides and proteins in alkaline medium (Shi et al., 2007). In 2000, Jin and Ranford synthesized nine ternary platinum(II) complexes with phen and amino acids (where amino acids are glycine (Gly), L-histidine (His), L-cysteine (Cys), L-isoleucine (Ile), L-alanine (Ala), L-proline (Pro), L-serine (Ser), L-aspartic acid (Asp), L-glutamic acid (glu)) as well as two ternary palladium(II) complexes with phen and amino acids (where amino acids are L-aspartic acid (Asp), L-glutamic acid (Glu)). All eleven metal(II) complexes were tested for cytotoxicity on Molt-4, a human leukaemia cell line, and it was found that  $[\text{Pt}(\text{phen})(\text{Pro})]\text{Cl}\cdot 2\text{H}_2\text{O}$  and  $[\text{Pd}(\text{phen})(\text{Asp})]\text{Cl}\cdot 1\frac{1}{2}\text{H}_2\text{O}$  showed cytotoxicity comparable to cisplatin (Jin and Ranford, 2000). No D-amino acids were used to make these complexes. DNA recognition (DNA binding and DNA recognition) of palladium(II) and platinum(II) complexes

were not investigated by Jin and Ranford (2000).

Besides anticancer property, some amino acids complexes were reported to exhibit nucleolytic property (Rao et al., 2007; Chetana et al., 2009; Yodoshi et al., 2007; Ng et al., 2006). In 2007, two ternary copper(II) complexes,  $[\text{Cu}(\text{L-pro})(\text{L})(\text{H}_2\text{O})](\text{NO}_3)$  (where L-pro = L-proline; L = 2,2'-bipyridine or phen) were synthesized and investigated for their nucleolytic property. Significant chemical nuclease activity was observed for the  $[\text{Cu}(\text{L-pro})(\text{phen})(\text{H}_2\text{O})](\text{NO}_3)$  under physiological reaction conditions and the cleavage mechanism involved formation of hydroxyl radicals in the presence of the 3-mercaptopropionic. It was reported that the binding ability of the complexes was important to achieve efficient DNA cleavage activity. At the same time,  $[\text{Cu}(\text{Gly})(\text{bpy})\text{Cl}]$  complex synthesized by Yodoshi and coworkers (2007) showed effective DNA binding and cleavage. This complex showed a propensity to bind to CT DNA and to cleave SC DNA in the presence of  $\text{H}_2\text{O}_2$  and ascorbic acid. The complex also degraded CT DNA in the presence of  $\text{H}_2\text{O}_2$  and ascorbic acid. Recently, ternary copper(II) complexes with polypyridyl bases (2,2'-bipyridyl (bpy), 1,10-phenanthroline (phen), 1,10-phenanthroline-5,6-dione (phendione), dipyrido[3,2:2',3'-f]quinoxaline (dpq)) and L-alanine were synthesized and tested for DNA cleavage activity (Chetana et al., 2009). Both phen and dpq complexes showed chemical nuclease activity in the presence of 3-mercaptopropionic as a reducing agent. Hydroxyl radicals were found to be the DNA cleavage active species.

Zhang et al. (2009) investigated the enantioselective binding of L- and D-phenylalanine to calf thymus DNA by circular dichroism, fluorescence quenching, viscosity, salt effect and fluorescence experiments. Although both L- and D-phenylalanines bound to CT-DNA with groove binding, only L-phenylalanine bound preferentially to CT-DNA. A more simple method was proposed by Zhang et al. (2007) to separate DL-tyrosine and DL-tryptophan. L-enantiomers preferentially bind to CT-DNA and remained in the dialysis tubing, while D-enantiomers easily escaped from the CT-DNA and permeated through dialysis tubing. CT-DNA could discriminate and separate L-enantiomer from D-enantiomer. Thus, the chiral separation of CT-DNA can be widely used for the separation of other amino acid enantiomers in industrial production. Arjmand et al. (2010) have also done a comparative study of enantiomeric pairs of L, D and DL-tryptophan of late transition metals,  $[\text{Co}(\text{tryp})(\text{dab})(\text{H}_2\text{O})_2]\text{Cl}$  and  $[\text{M}(\text{tryp})(\text{dab})]\text{Cl}$  (where M = Cu or Zn; tryp = L-tryptophan, D-tryptophan or DL-tryptophan; dab = 1,2-diaminobenzene). The *in vitro* DNA binding studies demonstrated that the  $[\text{Co}(\text{L-tryp})(\text{dab})(\text{H}_2\text{O})_2]\text{Cl}$  and  $[\text{M}(\text{L-tryp})(\text{dab})]\text{Cl}$  (where M = Cu or Zn; L-tryp = L-tryptophan; dab = 1,2-diaminobenzene) exhibited highest propensity for binding DNA. The DNA binding mode was essentially non-covalent *viz.* electrostatic *via* phosphate backbone of DNA double helix. The copper(II) complex,  $[\text{Cu}(\text{L-tryp})(\text{dab})]\text{Cl}$  bound DNA more avidly than the Co(II) and Zn(II) analogues. The  $[\text{Cu}(\text{L-tryp})(\text{dab})]\text{Cl}$  exhibited significant antitumor activity against MCF-7 cell line. Even though quite a number of studies were done on amino acid complexes, there are very few studies on DNA binding and biological properties of ternary metal(II) complexes with an enantiomeric

pairs of amino acid.

## **2.5 COMPARATIVE REVIEW OF BIOLOGICAL STUDIES OF COBALT(II), COPPER(II) and ZINC(II) COMPLEXES**

Cobalt is an essential trace element in humans, exhibiting many useful biological functions. Numerous compounds, naturally occurring and man-made, contain cobalt at two common oxidation states Co(II) and Co(III). There is growing interest in investigating cobalt and other transition metal complexes for their interaction with DNA (Richards and Rodger, 2007; Terrón et al., 2007; Keene et al., 2009; Zeglis et al., 2007; Boerner and Zaleski, 2005). This may be partly influenced by the results of extensive investigation into two areas of research, *viz.* (i) the binding specificity of small organic molecules for their possible modulation and inhibition of DNA replication, transcription and recombination, and (ii) anticancer, antiviral and antibacterial drugs (Du et al., 2010). The DNA specific interactions of organic molecules include abasic, mismatch or bulge site recognition, secondary structure recognition and specific sequence recognition. Although there are numerous investigations into the DNA binding and nucleolytic property of cobalt complexes, there seems less attention on their ability for binding recognition of DNA base, DNA secondary structures or base sequences (Jiao et al., 2005; Kong and Xie, 2000; Efthimiadou et al., 2008; Chen et al., 2010; Gust et al., 2004; Cheng et al., 1999). Thus far, the DNA recognition ability of metal complexes is still not well understood. However, it is believed that the type of coordinated ligand and the geometrical orientation of the ligands are crucial

factors in bestowing the binding site specificity and selectivity of a given metal complex. Recently, Ng et al. (2008) and Seng et al. (2008) have reported the preferential binding of (ethylenediamine-*N,N'*-diacetato)(1,10-phenanthroline)metal(II), [M(phen)(edda)], for ds(AT)<sub>6</sub> over ds(CG)<sub>6</sub> and its anticancer property.

Besides DNA binding studies, cobalt complexes have been investigated for their anticancer properties (Nagababu et al., 2008; Klanicová et al., 2006). Cobalt(III) complexes have also been tested as hypoxia-activated anticancer prodrugs which upon reduction in the reducing environment of cancer tissues can release toxic ligands to kill the cancer cells (Failes and Hambley, 2006). In more recent approaches to anticancer drug development, inhibition of proteasome and topoisomerase with metal complexes have been studied (Chen et al., 2009; Milacic et al., 2008; Lo et al., 2009; Jayaraju et al., 1999). Apoptosis induced by cobalt(II) chloride seemed to involve inhibition of proteasome (Araya et al., 2002). From the literature search, only a few anticancer cobalt(II) complexes are known to inhibit proteasome or topoisomerase I. Among the [M(phen)(edda)] complexes mentioned above, [Co(phen)(edda)] was the least antiproliferative against MCF7 breast cancer cell line with an IC<sub>50</sub> value of 11.4 μM at 72 hours incubation (Ng et al., 2008).

Other than cobalt complexes, there is growing interest in investigating copper and zinc complexes for their interaction with DNA. Copper is an

essential trace element present in many species especially protein (*e.g.* cytochrome *c* oxidase, copper/zinc superoxide dismutase, tyrosinase, hemocyanin and laccase) (Fenton, 1995; Ettinger, 1984; Karlin and Zubieta, 1996). Owing to the biological role of copper(II) and its synergetic activity with the drug, copper(II) complexes have been extensively studied (Kato and Muto, 1988; Weder et al., 2002; Sorenson, 1989). A large number of copper(II) complexes have been reported to be able to induce DNA cleavage with or without oxidizing and reducing agents (such as hydrogen peroxide and ascorbic acid). Lamour and coworkers (1999) reported that copper(II) complexes of polyhydroxysalens(hydroxysalicylidene)ethylenediamine can act as self-activated chemical nucleases. Earlier investigations on the chemical nuclease activity of the *bis*(1,10-phenanthroline)copper(I) complex,  $[\text{Cu}(\text{o-phen})_2]^+$ , in presence of  $\text{H}_2\text{O}_2$ , indicated that this complex induced oxidative strand scission mediated by free radicals (Sigman et al., 1993a; Sigman et al., 1993b). According to Sitlani et al. (1992), the active oxo-species formed attacked the deoxyribose sugar proton of the nucleotide which was in the vicinity of the metal complex in the minor groove, initiating a series of oxidative reactions mediated by free radicals that lead to DNA strand scission.

Copper complexes are able to promote the generation of reactive oxygen species (ROS) in the presence of mild reducing agents, which has been exploited to oxidatively break the DNA strands and to further inhibit the proliferation of tumour cells (Zhang et al., 2004; Maheswari et al., 2008; Loganathan et al., 2012). A variety of copper complexes have been designed

for these reasons (Silva et al., 2011; O'Connor et al., 2012). For example, ternary copper(II) complex of 1,10-phenanthroline with L-threonine, [Cu(phen)(L-thr)(H<sub>2</sub>O)](ClO<sub>4</sub>) can inhibit HL-60 and SGC-7901 tumour cell lines (Zhang et al., 2004). It was found that the copper(II) complex cleaved pBR322 DNA via intercalation of the DNA. The DNA cleavage occurred in the presence of ascorbate involved the hydroxyl radical species. Other than that, several copper(II)-terpyridine complexes such as [Cu(Itpy)<sub>2</sub>](ClO<sub>4</sub>)<sub>2</sub>, [Cu(tpy)Cl]Cl, [Cu(itpy)Cl]Cl and [Cu(Itpy)(phen)(ClO<sub>4</sub>)](ClO<sub>4</sub>)·(H<sub>2</sub>O) (Itpy = imidazole terpyridine; tpy = tolylterpyridine) have shown considerable nuclease property and antitumor activity in physiologically relevant conditions (Uma et al., 2005; Uma et al., 2007; Manikandamathavan et al., 2011).

Besides DNA binding studies, copper complexes have been investigated for their catalytic oxidation properties. Copper is incorporated in metalloenzymes that are involved mainly in oxygen transport, electron transfer, and catalytic oxidation processes (Karlin and Tyeklar, 1993; Reinhammer, 1984; Solomon et al., 1996; Magnus et al., 1994; Linder, 1991; Adman, 1991). For example, blue copper electron transfer proteins use copper as a one electron relay, shuttling between the cuprous and cupric oxidation states (Solomon and Hadt, 2011). The tuning Cu<sup>II</sup>/Cu<sup>I</sup> redox couple play important role in electron transfer in blue copper proteins and also in catalysis (Roy et al., 2009; Yang and Du, 2011). Synthetic coordination complexes employing copper(II) have proven effective functional models for several classes of metalloenzymes including oxidases (catechol oxidase) (Zhang et al., 2007;

Sreedaran et al., 2008), oxygenases (Tolman, 1997), nucleases (Zelder et al., 2003; Hegg and Burstyn, 1996; Hegg et al., 1977; Hegg and Burstyn, 1998; An et al., 2006; Belousoff et al., 2008a; Belousoff et al., 2008b), and phosphatases (Sreedaran et al., 2008; Golicnik, 2010; Oliveira et al., 2009; Liang et al., 2007; Belousoff et al., 2006; Fry et al., 2005; Gahan et al., 2009).

Zinc is an outstanding micronutrient with diverse biological, clinical, and public health importance (Hambidge et al., 2010; Sigel et al., 2006; Burdette and Lippard, 2001). There are over 300 natural metalloenzymes (Stehbens, 2003; Lin et al., 2005). Artificial zinc finger proteins and zinc complexes with simple organic ligands have been shown to have sequence-specific DNA binding recognition (Papworth et al., 2000; Nagaoka and Sugiura, 2000; Seng et al., 2010). Some zinc complexes are now beginning to be reported being able to inhibit topoisomerase I and II, which are nuclear enzymes needed for modification of topological state of DNA (Seng et al., 2010; Kikuta et al., 2000; Chuang et al., 1996). An important property of topoisomerase I (Topo I) inhibitors is their anticancer property; in fact, numerous clinical, anticancer drugs are topo I inhibitors (Kukuta et al., 2000; Chuang et al., 1996; Sunami et al., 2009; Pommier, 2006; Beretta et al., 2008; Rothenberg, 1997). However, none of these clinical drugs are zinc complexes. In fact, not many zinc complexes have been studied for their anticancer property (Liguori et al., 2010; Wen et al., 2011).

The above review of cobalt, copper and zinc complexes on their biological activity showed that copper(II) complexes have been extensively studied. These research studies includes DNA interaction, anticancer activity and catalytic oxidation properties as mentioned earlier in this section. Also, similar copper complexes described in the current study, [Cu(phen)(L-thr)(H<sub>2</sub>O)] has been synthesized by Zhang et al. (2004) and was found to have anticancer activity towards HL-60 and SGC-7901 tumour cell lines. Although [Zn(phen)(dipico)(H<sub>2</sub>O)]·H<sub>2</sub>O has been previously synthesized and characterized by Harrison et al. (2006) but the work only covered the X-ray crystallographic data. Unlike copper(II) complexes, not many cobalt(II) and zinc(II) complexes have been studied for their anticancer activity. Motivated by this, selected cobalt(II) and zinc(II) complexes are tested for their DNA recognition, DNA specificity and anticancer properties.

## 2.6 Summary

A list of metal(II)-phen complexes with various *OO'*-, *ONO'*- and *NO*-type coligands are listed in **Table 2.1**. Although there are various *OO'*-, *ONO'*- and *NO*- type coligands reported in the literature, to our knowledge, there are limited studies on the synthesis and biological activities of ternary metal(II) complexes containing 1,10-phenanthroline as main ligand and *OO'*-maltolate, *ONO'*-dipicolinate and *NO*-threoninate coligands. In the review of phen, maltolate, dipicolinate, threoninate and metal(II) ions (Co(II), Cu(II) and Zn(II)) in the earlier sections, it was shown that combination of mentioned

metal and ligand is an interesting topic of research. In the present research, various sets of ternary complexes, described in **section 1.2**, are systematically assembled to study the effect of varying coligands and metal(II) ions on its solid and solution properties.

In short, this review sketches the background for the title of this research and the rationale for choosing the type of metal(II) ions, the type of polypyridyl as main ligand and the selected  $\text{OO}^{\ominus}$ -,  $\text{ONO}^{\ominus}$ - and  $\text{NO}$ -coligands. It is a continuation of the role of inorganic chemists to improve understanding of how the physical and chemical properties of the metal(II) complexes affect their biological activities. Interest in the biological activity of transition metal complexes has attracted the interest of many scientists due to the potential use of metal complexes as therapeutic agents for certain diseases. However, the relationship of the physic-chemical properties and the biological activities of the transition metal complexes are not fully understood. This could be due to diverse structural features of these complexes, resulting from various coordination modes of the ligands and varied coordination geometries of the metal centres.

**Table 2.1:** List of ternary metal(II) complexes with 1,10-phenanthroline as main ligand and various co-ligand

M(phen)(L)X	Type of co-ligand, L			
	OO'-type	ONO'-type	NO-type	Others
<b>Co(II)</b>	[Co(phen)(acac) <sub>2</sub> ]; [Co <sub>2</sub> (μ-OOCCH <sub>3</sub> ) <sub>2</sub> (OOCCH <sub>3</sub> ) <sub>2</sub> (phen) <sub>2</sub> (μ-OH <sub>2</sub> )	[Co(phen)(ida)(H <sub>2</sub> O)]·H <sub>2</sub> O; [Co(phen)(pteridine)(H <sub>2</sub> O)]·3H <sub>2</sub> O	[Co(pico) <sub>2</sub> (phen)]	[Co(phen)(edda)]; [Co(phen)(H <sub>3</sub> L)]Cl·4H <sub>2</sub> O; [Co(bpy)(phen) <sub>2</sub> ](NO <sub>3</sub> ) <sub>2</sub> ·2H <sub>2</sub> O; [Co(4-MPipzcdt)(phen) <sub>2</sub> ]Cl; [Co(L)(phen)Cl]
<b>Cu(II)</b>	[Cu(phen) <sub>2</sub> (ma)]; [Cu(phen)(ma)Cl]; [Cu(phen)(acac)(H <sub>2</sub> O)]ClO <sub>4</sub> ; {[Cu(acac) <sub>2</sub> (phen) <sub>2</sub> Co(NCS) <sub>4</sub> ] ·2[Cu(acac)(phen)(NCS)]}; [Cu(phen) <sub>2</sub> (mal)]·2H <sub>2</sub> O; [Cu(phen)(Sal)]ClO <sub>4</sub>	[Cu(phen)(ida)(H <sub>2</sub> O)]·4H <sub>2</sub> O; [Cu(phen) <sub>2</sub> (μ-ida)]; Cu(phen)](ClO <sub>4</sub> )·CH <sub>3</sub> OH; [Cu <sub>2</sub> (μ-nta)(phen) <sub>3</sub> ](ClO <sub>4</sub> )·2H <sub>2</sub> O; {[Cu(phen) <sub>2</sub> ]{Cr <sub>2</sub> (μ-OH) <sub>2</sub> (nta) <sub>2</sub> }} [Cr <sub>2</sub> (μ-OH) <sub>2</sub> (nta) <sub>2</sub> ]·8H <sub>2</sub> O; [Cu(phen)(SAla)]·H <sub>2</sub> O	[Cu(phen)(L-pro)(H <sub>2</sub> O)](NO <sub>3</sub> ); [Cu(phen)(gly)(H <sub>2</sub> O)](NO <sub>3</sub> ); [Cu(phen)(L-Val-gly)]; [Cu(phen)(gly-L-trp)]; [Cu(phen)(L-thr)(H <sub>2</sub> O)]·ClO <sub>4</sub>	[Cu(phen)(edda)]; [Cu(bpy)(phen)]Cl <sub>2</sub> ·2H <sub>2</sub> O; [Cu(SAla)(phen)]·H <sub>2</sub> O; [CuL(phen) <sub>2</sub> ]Cl <sub>2</sub> ; [Cu(L)(phen)Cl]
<b>Zn(II)</b>	{[Zn(phen)(L-tart)]·6H <sub>2</sub> O} <sub>n</sub> ; [Zn(phen) <sub>2</sub> (pime)]·6H <sub>2</sub> O; [Zn(phen)(acac) <sub>2</sub> ]	[Zn(phen)(dipico)(H <sub>2</sub> O)]·H <sub>2</sub> O; [Zn(phen)(ida)(H <sub>2</sub> O)]·1 $\frac{1}{2}$ H <sub>2</sub> O; [Zn <sub>2</sub> (phen) <sub>3</sub> (nta)]NO <sub>3</sub> ·6H <sub>2</sub> O	[Zn <sub>4</sub> (phen) <sub>4</sub> (pico) <sub>4</sub> ]·11 $\frac{1}{4}$ H <sub>2</sub> O; [Zn(phen)(3-me-pic) <sub>2</sub> ]·5H <sub>2</sub> O	[Zn(phen)(edda)]; [Zn(L)(phen) <sub>2</sub> ]·Cl <sub>2</sub> ; [Zn(L)(phen)Cl]
<b>Other metals</b>	[Ce(phen)(acac) <sub>3</sub> ]; [Mn(phen)(acac)]; [Y(phen)(acac) <sub>3</sub> ]	{[Ni(phen) <sub>3</sub> ][Ni(dipico) <sub>2</sub> ]}·17H <sub>2</sub> O; [Ni(phen)(dipico)(H <sub>2</sub> O)]·H <sub>2</sub> O	[Pt(phen)(gly)]; [Pt(phen)(L-His)]; [Pt(phen)(L-Cys)]; [Pt(phen)(L-Ile)]; [Pt(phen)(L-ala)]; [Pt(phen)(L-pro)]; [Pt(phen)(L-Ser)]; [Pt(phen)(L-Asp)]; [Pt(phen)(L-glu)]; [Pd(phen)(L-Asp)]; [Pd(phen)(L-glu)]	[Ir(η <sup>5</sup> -cp)(phen)Cl] <sup>+</sup> ; [Pt(phen)]Cl <sub>2</sub> ; [Ce(NO <sub>3</sub> )(H <sub>2</sub> O)(phen)(H <sub>3</sub> L)]·5H <sub>2</sub> O; [UO <sub>2</sub> (phen)(H <sub>3</sub> L)]·2H <sub>2</sub> O; [Mn(4-MPipzcdt)(phen) <sub>2</sub> ]Cl] <sup>+</sup>

Note: H<sub>3</sub>L = thiocarbohydrazone; 4-MPipzcdt = 4-methylpiperazine-1-carbodithioate; bpy = 2,2'-bipyridine; SAla = Salicylaldehyde-alanine; L = isatin-based schiff base; ida = iminodiacetic acid; L-tart = L-tartrato; pime = pimelate; acac = acetylacetonate; pico = picolinate; 3-me-pic = 3-methyl-picolinate; mal = malonates; ma = maltolate; dipico = dipicolinate; pteridine = (2-amino-7-methyl-4-oxidopteridine-6-carboxylato-κ<sup>3</sup>O<sup>4</sup>N<sup>5</sup>O<sup>6</sup>); Sal = Salicylaldehyde

### **CHAPTER 3**

#### **SYNTHESIS AND CHARACTERIZATION OF METAL(II)**

#### **1,10-PHENANTHROLINE COMPLEXES WITH *O,O'*-MALTOL,**

**[M(phen)(ma)Cl]·*x*H<sub>2</sub>O (M(II) = Co, Cu, Zn) and [Co(phen)(ma)<sub>2</sub>]·5H<sub>2</sub>O\***

## CHAPTER 3

### SYNTHESIS AND CHARACTERIZATION OF METAL(II)

#### 1,10-PHENANTHROLINE COMPLEXES WITH *O,O'*-MALTOL,

#### $[M(\text{phen})(\text{ma})\text{Cl}] \cdot x\text{H}_2\text{O}$ (M(II) = Co, Cu, Zn) and $[\text{Co}(\text{phen})(\text{ma})_2] \cdot 5\text{H}_2\text{O}^*$

### 3.1 INTRODUCTION

This section describes the attempt to synthesis and characterize two related sets of metal(II)-phen-maltol complexes namely  $[M(\text{phen})(\text{ma})\text{Cl}] \cdot x\text{H}_2\text{O}$  and  $[\text{Co}(\text{phen})(\text{ma})_2] \cdot 5\text{H}_2\text{O}$  (where M = Co, Cu or Zn; phen = 1,10-phenanthroline; ma = maltolate). Metal(II)-phen-maltol complexes were characterized by FTIR, CHN, X-ray, molar conductivity, UV-Vis, fluorescence (FL), electrospray ionization mass spectroscopy, and thermal gravimetric studies. Like the phen ligand, the maltolate is planar. The choice of maltol (3-hydroxy-2-methyl-4-pyrone) was partly influenced by the reported insulin-mimetic property of *bis*(maltolato)cobalt(II), and the reported solubility and thermodynamic stability of neutral metal complexes with maltol (Thompson et al., 2004). Maltol was also reported to be able to inhibit apoptosis of human neuroblastoma cells induced by hydrogen peroxide (Yang et al., 2006). The study was carried out to gain an understanding on the effect of the type of metal ion and number of coordinated maltolate ligand on their structure, solution property and thermal stability of the metal complexes formed.

## 3.2 EXPERIMENTAL

### 3.2.1 Materials and reagents

1,10-phenanthroline monohydrate (99%), 3-hydroxy-2-methyl-4-pyrone (maltol), Copper(II) chloride dihydrate were purchased from Acros Organic. Zinc(II) chloride puriss, cobalt(II) chloride hexahydrate and sodium hydroxide were purchased from Riedel-de Haen, R&M Chemicals, and System AR respectively. All other reagents, such as methanol and ammonia, were of analytical grade and were used as purchased.

### 3.2.2 Preparation of $[M(\text{phen})(\text{ma})\text{Cl}] \cdot x\text{H}_2\text{O}$ ( $M(\text{II}) = \text{Co}, \text{Cu}, \text{Zn}$ ) 1 - 3 and $[\text{Co}(\text{phen})(\text{ma})_2] \cdot 5\text{H}_2\text{O}$ 4

The  $[\text{Cu}(\text{phen})(\text{ma})\text{Cl}] \cdot \frac{1}{2}\text{H}_2\text{O}$  was prepared according to a previously published procedure (Tan et al., 2008). The Co(II) and Zn(II) analogues were similarly prepared. To prepare  $[\text{Co}(\text{phen})(\text{ma})\text{Cl}] \cdot 4\text{H}_2\text{O}$  complex,  $\text{CoCl}_2 \cdot 6\text{H}_2\text{O}$  (0.24 g, 1 mmole) was dissolved in 5 mL of distilled water and the resultant solution was added slowly to a solution of maltol, which was previously prepared by dissolving maltol (0.13 g, 1 mmole) in 20 mL of 0.01 M sodium hydroxide solution. The solution mixture was stirred for 5 minutes (mins). A methanolic solution of phen was prepared separately by dissolving phen (0.20 g, 1 mmole) in 5 mL methanol. The phen solution was then added to the solution mixture of the cobalt chloride and maltol with constant heating (~50 °C) and stirring was continued until an orange precipitate was observed. The final volume of the solution after heating and stirring is *ca.* 5 mL. The solution

was cooled to room temperature, and the resultant solid was collected by suction filtration using a sintered funnel and washed with cold methanol (2 mL), and then dried in vacuo. The yield of orange precipitate (0.40 g, 0.70 mmole, 70%). The pure complex  $[\text{Cu}(\text{phen})(\text{ma})\text{Cl}] \cdot \frac{1}{2}\text{H}_2\text{O}$  was obtained as dark green precipitate (0.37 g, 0.74 mmole, 74 %) whereas  $[\text{Zn}(\text{phen})(\text{ma})\text{Cl}] \cdot 1\frac{1}{2}\text{H}_2\text{O}$  was obtained as yellowish orange precipitate (0.36 g, 0.77 mmole, 77%).

$[\text{Co}(\text{phen})(\text{ma})_2] \cdot 5\text{H}_2\text{O}$  complex was prepared by dissolving  $\text{CoCl}_2 \cdot 6\text{H}_2\text{O}$  (0.24 g, 1 mmole) in 10 mL of distilled water and the solution was added slowly to a solution of maltol. The maltol solution was prepared by dissolving maltol (0.26 g, 2 mmole) in 20 mL sodium hydroxide (0.10 M). The solution mixture was continuously stirred with a magnetic bar at room temperature for 5 minutes. A methanolic solution of phen was prepared by dissolving phen (0.20 g, 1 mmole) in methanol (10 mL). The resultant mixture was heated overnight in water bath at 50 °C. Upon slow evaporation at room temperature, suitable red crystals (0.59 g, 0.84 mmole, 84 %) were obtained for X-ray crystal structure analysis. The attempt to synthesis the other  $[\text{M}(\text{phen})(\text{ma})_2]$  (where M = Cu or Zn) complexes were unsuccessful.

### 3.2.3 Characterization of solids complexes

Elemental analyses (C, H, and N) were carried out on a Perkin Elmer 2400 CHN analyser. CHN elemental analyses were performed in Universiti Kebangsaan Malaysia (UKM). The FTIR spectra of the complex were recorded as KBr disc in the range of 4,000 – 400  $\text{cm}^{-1}$  on a Perkin Elmer FTIR spectrometer. Thermal analyses were performed using a Mettler Toledo TGA/DTG 851<sup>e</sup> instrument under nitrogen atmosphere. The samples were heated in the temperature range of 25 - 800  $^{\circ}\text{C}$  and the heating rate was 10  $^{\circ}\text{C}/\text{min}$ . The flow rate of nitrogen gas,  $\text{N}_2$ , was 20 mL/min.

### 3.2.4 Determination of crystal structure of complex 4

The crystal structure of complex 4 was solved by Prof. Teoh Siang Guan from Universiti Sains Malaysia (USM). The intensity data for a red crystal, 0.45 x 0.30 x 0.09 mm, were collected at 293 K on a Bruker SMART APEX area-detector using Mo  $\text{K}\alpha$  radiation,  $\lambda = 0.71073 \text{ \AA}$ , over the range  $1.81^{\circ} < \theta < 30.15^{\circ}$ . APEX2 software was used for data collection and refinement (Bruker, 2007). Absorption corrections were made using SADABS (Sheldrick, 1996). The structure was solved by direct-methods and refined by a full-matrix least-squares procedure on  $F^2$  with anisotropic displacement parameters for non-hydrogen atoms, C and N-bound hydrogen atoms in their calculated positions and a weighting scheme of the form calculated  $w = 1/[s^2(F_o^2)]$   $w = 1/[s^2(F_o^2) + (0.1040P)^2 + 0.0000P]$  where  $P = (F_o^2 + 2F_c^2)/3$

(Sheldrick, 2008). The complex was found to crystallise with six water molecules of solvation; two of these were disordered and were refined with a 50% occupancy factor each. Data collection and experimental details for the complex are summarised in **Table 3.1**.

**Table 3.1:** Crystal data and structure refinement for  $[\text{Co}(\text{phen})(\text{ma})_2] \cdot 5\text{H}_2\text{O}$  **4**

Empirical formula	$\text{CoC}_{24}\text{H}_{28}\text{N}_2\text{O}_{11}$
Formula weight	579.41
Temperature ( $^{\circ}\text{C}$ )	20
Crystal system	Monoclinic
Space group	$P2_1/c$
Unit cell dimensions ( $\text{\AA}$ )	$a = 10.4432(2)$ ; $b = 16.3806(3)$ ; $c = 16.6834(3)$
Volume ( $\text{\AA}^3$ )	2645.04
Z	4
Density (calculated)( $\text{Mg/m}^3$ )	1.455
Absorption coefficient ( $\text{mm}^{-1}$ )	0.711
F(000) (mm)	1204
Crystal size (mm)	0.45 x 0.30 x 0.09
$\theta$ range for data collection ( $^{\circ}$ )	1.81 – 30.15
Index ranges	$-12 \leq h \leq 14$ ; $-22 \leq k \leq 23$ ; $-23 \leq l \leq 22$
Reflections collected	34,313
Independent reflections	7793
Data/restraints/parameters	7793/0/355
Goodness-of-fit on $F^2$	0.969
Final $R$ indices [ $I > 2(\sigma)I$ ]	$R = 0.0632$ ; $wR = 0.1686$
$R$ indices (all data)	$R = 0.1653$ ; $wR = 0.2161$
Largest dif. Peak and hole ( $e \text{\AA}^{-3}$ )	0.340, - 0.407

### 3.2.5 Characterization of aqueous solutions of complexes

A CON 700 bench top conductivity meter from EUTECH Instruments was used to measure the conductivity of the solvent and methanol-water (1:1 v/v) solutions of the metal(II) complexes. The conductivity meter was calibrated using KCl as a calibrant. For conductivity measurements, deionised water and the HPLC grade methanol were used for preparing solutions of the

metal(II) complexes. A 1:1(volume : volume) water-methanol mixture was used as solvent to dissolve the complexes and metal(II) chloride salts to give  $1.0 \times 10^{-3}$  M solutions. The conductivity meter was checked with a calibration of KCl standard solution (1413  $\mu$ S) or recalibrated when necessary. The rinsed conductivity electrode was dipped in each solution and the reading was recorded after it stabilised.

UV-visible spectroscopic measurements of the aqueous sample solutions were carried out on a Perkin Elmer Lamda 35 spectrophotometer in the range of 200 – 900 nm. The solutions of samples, free ligands and metal(II) chloride were prepared by using 1:1 (v/v) water-methanol mixture to give  $1.0 \times 10^{-3}$  M stock solutions. All the sample solutions were further diluted to  $1.0 \times 10^{-5}$  to  $5.0 \times 10^{-5}$  M for UV dilution experiments. For visible spectroscopic measurements, the solutions of samples and metal(II) chloride were prepared by using 1:1 (v/v) water-methanol mixture to give  $1.0 \times 10^{-2}$  M. Water-methanol was filled into the reference cell while the sample cell was filled with sample solutions.

The fluorescence study was carried out with a Perkin Elmer LS55 Fluorescence spectrometer at room temperature. The stock solutions of samples, free ligands and metal(II) chloride solutions were prepared in the same way as the stock solutions used for UV-Vis spectroscopic study. All the sample solutions were further diluted to  $1.0 \times 10^{-6}$  M for fluorescence study.

The measurements of Electrospray ionisation mass spectra (ESI) of the metal(II) complexes were done at Centre for Chemical, Molecular and Materials Analysis Centre (CMMAC), National University of Singapore (NUS). The ESI spectra were recorded in positive and negative modes using a Thermo Finnigan LCQ spectrometer. In ESI-MS analysis, solution samples of all the complexes were fixed at 50 pMol/ $\mu$ L. The samples were introduced into the mass spectrometer either through a LC pump or injection using a syringe pump. The capillary temperature was set at 150 °C.

### **3.3 RESULT AND DISCUSSION**

#### **3.3.1 Characterization of solids complexes**

According to Tan and co-workers,  $[\text{Cu}(\text{phen})(\text{ma})\text{Cl}] \cdot \frac{1}{2}\text{H}_2\text{O}$  has a square pyramidal geometry. Both coordinated phen and maltolate ligands in the Cu(II) complexes occupy the basal plane with the chloride occupying the apical position. The Co(II), Cu(II) and Zn(II) products of  $[\text{M}(\text{phen})(\text{ma})\text{Cl}] \cdot x\text{H}_2\text{O}$  were orange, dark green and yellowish orange in colour. Red crystals of  $[\text{Co}(\text{phen})(\text{ma})_2] \cdot 5\text{H}_2\text{O}$  were obtained. Samples collected were used to carry out the characterization studies. Results for  $[\text{Co}(\text{phen})(\text{ma})\text{Cl}] \cdot 4\text{H}_2\text{O}$  and  $[\text{Co}(\text{phen})(\text{ma})_2] \cdot 5\text{H}_2\text{O}$  in this chapter were published during the course of this research (Chin et al., 2011). Attempt in synthesis of  $[\text{Cu}(\text{phen})(\text{ma})_2]$  resulted in the isolation of  $[\text{Cu}(\text{phen})(\text{ma})\text{Cl}] \cdot \frac{1}{2}\text{H}_2\text{O}$ . This may be due to the Jahn-Teller effect is profound in Cu(II) centre (Kang et al., 2005; Zhang et al., 2000). On the other hand, a brownish gel was obtained in the attempt to prepare the analogous Zn(II)

complex,  $[\text{Zn}(\text{phen})(\text{ma})_2]$ . Several types of solvent such as acetone, ether, acetonitrile, dichloromethane and hexane were used to isolate the product from brownish gel substance. The gel substance dissolved in the mentioned solvents to form a clear brownish solution. Slow evaporation of solution form back gel substance. Unfortunately, this method was unable to isolate any characterisable product from the gel. Hence, formation of  $[\text{Cu}(\text{phen})(\text{ma})\text{Cl}] \cdot \frac{1}{2}\text{H}_2\text{O}$  and  $[\text{Zn}(\text{phen})(\text{ma})\text{Cl}] \cdot \frac{1}{2}\text{H}_2\text{O}$  are much more favourable compared to  $[\text{Cu}(\text{phen})(\text{ma})_2]$  and  $[\text{Zn}(\text{phen})(\text{ma})_2]$  complexes. Based on microanalysis results, the complexes can be formulated as  $[\text{Co}(\text{phen})(\text{ma})\text{Cl}] \cdot 4\text{H}_2\text{O}$  **1**,  $[\text{Cu}(\text{phen})(\text{ma})\text{Cl}] \cdot \frac{1}{2}\text{H}_2\text{O}$  **2**,  $[\text{Zn}(\text{phen})(\text{ma})\text{Cl}] \cdot \frac{1}{2}\text{H}_2\text{O}$  **3** and  $[\text{Co}(\text{phen})(\text{ma})_2] \cdot 5\text{H}_2\text{O}$  **4** as listed in **Table 3.2**.

**Table 3.2:** Physical and chemical data of metal(II) complexes, **1 - 4**

Complex		1	2	3	4
Molecular formulae		$[\text{Co}(\text{C}_{12}\text{H}_8\text{N}_2)(\text{C}_6\text{H}_5\text{O}_3)\text{Cl}] \cdot 4\text{H}_2\text{O}$	$[\text{Cu}(\text{C}_{12}\text{H}_8\text{N}_2)(\text{C}_6\text{H}_5\text{O}_3)\text{Cl}] \cdot \frac{1}{2}\text{H}_2\text{O}$	$[\text{Zn}(\text{C}_{12}\text{H}_8\text{N}_2)(\text{C}_6\text{H}_5\text{O}_3)\text{Cl}] \cdot \frac{1}{2}\text{H}_2\text{O}$	$[\text{Co}(\text{C}_{12}\text{H}_8\text{N}_2)(\text{C}_6\text{H}_5\text{O}_3)_2] \cdot 5\text{H}_2\text{O}$
Molecular weight (g/mol)		471.75	413.32	433.18	579.39
% yield		~ 70 %	~ 73 %	~ 78 %	~ 85 %
Colour		Orange ppt.	Dark green ppt.	Yellowish orange ppt.	Red crystals
CHN elemental analysis, % Calculated (Found)	C	45.83 (45.51)	52.31 (52.48)	49.91 (49.65)	49.75 (49.83)
	H	4.49 (4.25)	3.41 (3.20)	3.72 (4.07)	4.87 (4.33)
	N	5.94 (5.88)	6.78 (6.53)	6.47 (7.07)	4.83 (4.88)

FTIR spectra of complexes **1 - 4** are shown in **Appendix 3.1** and assignments of the characteristic peaks are tabulated in **Table 3.3**. The broad

bands at 3405, 3422, 3401 and 3407  $\text{cm}^{-1}$  in the FTIR spectra were attributed to the OH stretching of the lattice water molecule(s) in metal complexes, **1 - 4**, respectively (Dutt et al., 1975; Nakamoto, 1977; Hsieh et al., 2006; Maurya et al., 2011). The peaks correspond to the ring stretching frequencies ( $\nu(\text{C}=\text{C})$  and  $\nu(\text{C}=\text{N})$ ) of phen were observed at 1508-1518  $\text{cm}^{-1}$  and 1424-1432  $\text{cm}^{-1}$  for complexes **1-4** respectively. By comparing the FTIR spectrum of free phen ligand (**Appendix 3.2**) with metal complexes, **1 - 4**, it was found that both  $\nu(\text{C}=\text{C})$  and  $\nu(\text{C}=\text{N})$  peaks of the phen observed were slightly shifted to higher frequencies upon coordinated to the metal centre (Schilt and Taylor, 1958; Garcia-Raso et al., 2003; Tang et al., 2007). Two strong absorption peaks at  $\sim 848 \text{ cm}^{-1}$  and  $\sim 727 \text{ cm}^{-1}$  were observed. These were ascribed to out-of-plane  $\nu(\text{C}-\text{H})$  modes suggesting the coordination of the phen (Garcia-Raso et al., 2003; Zhang et al., 2004; Jin et al., 2000).

Three typical peaks of coordinated maltolate ligand were found in the region of 1400 – 1602  $\text{cm}^{-1}$  (Lambooy et al., 2007; Fernandes et al., 2008). The peak at 1655  $\text{cm}^{-1}$ , which corresponds to  $\nu(\text{C}=\text{O})$  in the free maltolate ligand, is blue shifted to 1602  $\text{cm}^{-1}$  in complex **1**, to 1591  $\text{cm}^{-1}$  in complex **2**, to 1598  $\text{cm}^{-1}$  in complex **3** and to 1596  $\text{cm}^{-1}$  in complex **4** (Greaves et al., 1988; Brito et al., 2008). The shift mentioned here, suggests the coordination of the  $\text{C}=\text{O}$  of maltolate ligand (Bruto et al., 2008). Both  $\nu(\text{C}=\text{O})$  and  $\nu(\text{C}=\text{C})$  bands of the pyrone ring were observed at 1618  $\text{cm}^{-1}$  and 1561  $\text{cm}^{-1}$  were blue shifted to 1575  $\text{cm}^{-1}$  and 1509  $\text{cm}^{-1}$  in complex **1**, and to 1560  $\text{cm}^{-1}$  and 1508  $\text{cm}^{-1}$  in complex **2**. Similarly, the bands for  $\nu(\text{C}=\text{O})$  and  $\nu(\text{C}=\text{C})$  vibration of the

maltolate ligand are found to shift to a lower wavenumber in the infrared spectra of complexes **3** and **4**. These peaks were also observed in FTIR spectra of complexes **3** and **4** with the value of  $1571\text{ cm}^{-1}$  and  $1508\text{ cm}^{-1}$  (Thompson et al., 2004; Marwaha et al., 1994).

IR band at the wavelength,  $\sim 1461\text{ cm}^{-1}$ , has been assigned to the stretching of the C=C double bond located at the opposite side of the  $\text{H}_3\text{C}-\text{C}=\text{C}-\text{O}^-$  (Parajón – Costa and Baran, 2011) in the maltolate ligand. The bands at  $1266\text{ cm}^{-1}$  in complex **1**,  $1271\text{ cm}^{-1}$  in complex **2**,  $1281\text{ cm}^{-1}$  in complex **3** and  $1278\text{ cm}^{-1}$  in complex **4** have been assigned to the C-O-C stretching mode of the pyrone ring. The bands for  $\nu_{\text{as}}(\text{C}-\text{O}-\text{C})$  and  $\nu(\text{C}-\text{H})$  of the coordinated maltolate ligand were observed at  $1103\text{ cm}^{-1}$  and  $1043\text{ cm}^{-1}$  in the infrared spectrum of complex **1** whereas corresponding bands for complex **2** were observed at  $1107\text{ cm}^{-1}$  and  $1039\text{ cm}^{-1}$ . These bands were again observed at  $1103\text{ cm}^{-1}$  and  $1042\text{ cm}^{-1}$  for complex **3**, and at  $1101\text{ cm}^{-1}$  and  $1042\text{ cm}^{-1}$  for complex **4**. The medium bands at  $923\text{ cm}^{-1}$  (complex **1**),  $915\text{ cm}^{-1}$  (complex **2**),  $918\text{ cm}^{-1}$  (complexes **3** and **4**) have been assigned to the maltolate symmetric C-O-C stretching frequency (Parajón – Costa and Baran, 2011; Dutt et al., 1975; Marwaha et al., 1994; Maurya et al., 2011).

FTIR spectra of complexes **1** and **4** did not show any significant difference although the monodentate chloride ligand in complex **1** been replaced by a bidentate maltolate ligand in complex **4**. It was proposed in the

earlier discussion that the planar phen coordinates to the metal ions through the nitrogen atoms of aromatic rings. In general, the  $\nu(\text{M-N})$  bands are normally found in the low frequency region. The  $\nu(\text{M-N})$  peak of these metals are in the  $180 - 290 \text{ cm}^{-1}$  region (Nakamoto, 1977). The peak of coordinated chloride ligand,  $\nu(\text{M-Cl})$ , was previously observed in the infrared spectrum at  $280 - 290 \text{ cm}^{-1}$  region (Nakamoto, 1977; Reddy et al., 2007; Li et al., 2007). These  $\nu(\text{M-Cl})$  peaks are beyond the detection of the FTIR spectrophotometer used here (Nakamoto, 1977; Reddy et al., 2007; Li et al., 2007). In conclusion, analysis of FTIR data supports the postulated formulae of the synthesized complexes **1 - 4**.

**Table 3.3:** Characteristic Infrared band assignments of metal(II) complexes, **1 - 4**

Bond	1	2	3	4	Remarks
$\nu(\text{O-H})$	3402(b)	3422 (b)	3401 (b)	3393 (b)	Water
$\nu(\text{C-H})$	-	3042 (w)	3056 (w)	3063 (w)	Phen
$\nu(\text{C=N})$	1424 (m)	1432 (m)	1426 (s)	1421 (m)	
$\nu(\text{C=C})$	1509 (m)	1518 (m)	1517 (m)	1508 (m)	
$\nu(\text{C-H})$ Out-of-plane	728 (s), 848 (s)	723 (s), 847(s)	727 (s), 849 (s)	727 (s), 847 (s)	
$\nu(\text{C=O})$	1602 (s)	1591 (m)	1598 (s)	1596 (s)	Maltol
[ $\nu(\text{C=O})$ + $\nu(\text{C=C})$ ]	1575 (s) 1509 (m)	1560 (s) 1508 (w)	1571 (s) 1508 (m)	1571 (s) 1508 (m)	
[ $\nu(\text{C=C})$ + $\nu(\text{C-O})$ + $\delta_{\text{as}}(\text{CH}_3)$ ]	1461 (m)	1471 (s)	1459 (m)	1460 (m)	
(C-H)rock	1340 (w)	1345 (w)	1342 (w)	1340 (w)	
$\nu(\text{C-O-C})_{\text{aromatic}}$	1266 (m)	1271 (s)	1281 (s)	1278 (w)	
$\nu_{\text{as}}(\text{C-O-C})$ + $\nu_{\text{ring}}$	1103 (w) 1043 (w)	1107 (w) 1039 (w)	1103 (m) 1042 (w)	1101 (w) 1042 (w)	
$\nu_{\text{s}}(\text{C-O-C})$	923 (m)	915 (m)	918 (m)	918 (m)	

The thermograms of four complexes,  $[\text{Co}(\text{phen})(\text{ma})\text{Cl}]\cdot 4\text{H}_2\text{O}$  **1**,  $[\text{Cu}(\text{phen})(\text{ma})\text{Cl}]\cdot \frac{1}{2}\text{H}_2\text{O}$  **2**,  $[\text{Zn}(\text{phen})(\text{ma})\text{Cl}]\cdot 1\frac{1}{2}\text{H}_2\text{O}$  **3** and  $[\text{Co}(\text{phen})(\text{ma})_2]\cdot 5\text{H}_2\text{O}$  **4** were recorded in the temperature range of 25 – 800 °C at heating rate of 10 °C/min. Thermal data of complexes **1 - 4** are presented in **Table 3.4**. The thermogram (TGA and DTG curves) of complex **1**,  $[\text{Co}(\text{phen})(\text{ma})\text{Cl}]\cdot 4\text{H}_2\text{O}$  shows four steps of decomposition in the range of 25 – 800 °C (**Appendix 3.3**). The derivative thermogravimetric analysis (DTG) curves for **1** show that all four the decomposition steps are endothermic processes. A peak corresponds to the loss of four water molecules (Calc.: 15.3 %, Found: 15.2 %) in the temperature range of 26 – 130 °C was observed. The loss of water molecules at 98 °C indicates that they are lattice water molecules and not coordinated water molecules. A second weight loss of 5.4 % (Calc.: 7.5 %) was observed at 306 °C for the removal of the chloride ligand from complex **1**. The high temperature required to remove the ligand suggests that chloride was coordinated to the Co(II). This analysis of thermal data is consistent with the earlier postulated formula from CHN analytical data (**Table 3.2**) and with the infrared spectroscopic analyses.

TGA curve of complex **2**,  $[\text{Cu}(\text{phen})(\text{ma})\text{Cl}]\cdot \frac{1}{2}\text{H}_2\text{O}$  (**Appendix 3.4**) shows four decomposition steps in the range of 25 – 800 °C. The DTG curve for **2** shows that all four decomposition steps are endothermic processes. First step of decomposition occurred at decomposition temperature in the range of 40 - 77 °C. The loss of half molecule of water (Calc.: 2.2 %, Found: 2.2 %) at 50 °C indicates that it is lattice water molecule. The existence of half water

molecule is in agreement with the elemental analysis of **2**. **Appendix 3.5** shows thermogram of complex **3**,  $[\text{Zn}(\text{phen})(\text{ma})\text{Cl}] \cdot 1\frac{1}{2} \text{H}_2\text{O}$ . In the range of 25 - 800 °C, there were three steps of decomposition. A weight loss of 12.5 % (Calc.: 14.4 %) was observed at 51 °C could be due to dehydration and loss of the chloride ligand.

The DTG curve of complex **4**,  $[\text{Co}(\text{phen})(\text{ma})_2] \cdot 5\text{H}_2\text{O}$  (**Appendix 3.6**) shows decomposition pattern with three steps in the range of 25 – 800 °C. The first step occurred at 65 °C was due to the loss of five water molecules (Calc.: 15.5 %, Found: 14.3 %). This suggests the presence of five lattice molecules in this complex. The second step of decomposition took place at 292 °C, which was likely due to the loss of one maltol ligand (Calc.: 21.6 %, Found: 21.6 %). The final step of decomposition, which occurred at 653 °C, could be assigned to the removal of all the ligand moieties *i.e.* one maltol molecule and one phen molecule (Calc.: 52.7 %, Found : 56.4 %) from the complex (Dutt et al., 1975; Marwaha et al., 1994; Reddy et al., 2007; Maurya et al., 2008; Shebl et al., 2010; Maurya et al., 2011). The organic moieties in all maltolate compounds underwent decomposition above 800 °C, leading to the formation of metal oxide (Tunçel et al., 2006). The metal complexes **1** - **4** showed similar decomposition sequences. The decomposition began with the dehydration process. The dehydration was then followed by the loss of chloride, maltol and phen ligand. The TGA data appear to suggest that the decomposition of the maltol ligand occurred prior to the phen ligand, which

seems to imply that the phen ligand was bonded to the metal center more strongly.

**Table 3.4:** TGA data<sup>a</sup> of metal(II) complexes, **1 - 4**

Molecular formulae	Decomposition range (°C)	Wt. % loss Calc. (Found)	Assignment (Removal)
[Co(C <sub>12</sub> H <sub>8</sub> N <sub>2</sub> )(C <sub>6</sub> H <sub>5</sub> O <sub>3</sub> )Cl]·4H <sub>2</sub> O <b>(1)</b>	26 - 130 (98) <sup>b</sup> 130 - 315 (306) <sup>b</sup>	15.3 (15.2) 7.5 (5.4)	4 mole of lattice water 1 mole of chloride
[Cu(C <sub>12</sub> H <sub>8</sub> N <sub>2</sub> )(C <sub>6</sub> H <sub>5</sub> O <sub>3</sub> )Cl]·1/2 H <sub>2</sub> O <b>(2)</b>	40 - 77 (50) <sup>b</sup>	2.2 (2.2)	1/2 mole of lattice water
[Zn(C <sub>12</sub> H <sub>8</sub> N <sub>2</sub> )(C <sub>6</sub> H <sub>5</sub> O <sub>3</sub> )Cl]·1 1/2 H <sub>2</sub> O <b>(3)</b>	27 - 177 (51) <sup>b</sup>	14.4 (12.5)	1 1/2 mole of lattice water + 1 mole of chloride
[Co(C <sub>12</sub> H <sub>8</sub> N <sub>2</sub> )(C <sub>6</sub> H <sub>5</sub> O <sub>3</sub> ) <sub>2</sub> ]·5H <sub>2</sub> O <b>(4)</b>	26 - 177 (65) <sup>b</sup> 162 - 519 (292) <sup>b</sup> 533 - 799 (653) <sup>b</sup>	15.5 (14.3) 21.6 (21.6) 52.7 (56.4)	5 mole of lattice water 1 mole of maltol 1 mole of maltol + 1 mole of phen

<sup>a</sup> Only the decomposition steps of water molecules and chloride was tabulated in the table due to its importance to determine the properties of water molecules and chloride atom.

<sup>b</sup> Value in the brackets refers to the inflection points of each decomposition step.

### 3.3.2 Analysis of crystal structure of complex 4

The ORTEP structure of the complex **4** is shown in **Figure 3.1** and selected bond lengths and bond angles are tabulated in **Table 3.5**. There are six lattice water molecules but the OW5A and OW5B water molecules are

disordered with half (50:50) occupancy. The structure shows the coordination of two maltolate ligands and phen in a distorted octahedral environment around the Co(II) atom. The planar heterocyclic phen coordinated to the Co(II) *via* two nitrogen atoms (N(1) and N(2)) while each of the two maltolate ligands coordinate *via* two oxygen atoms (O(1), O(2); O(3), O(4)).

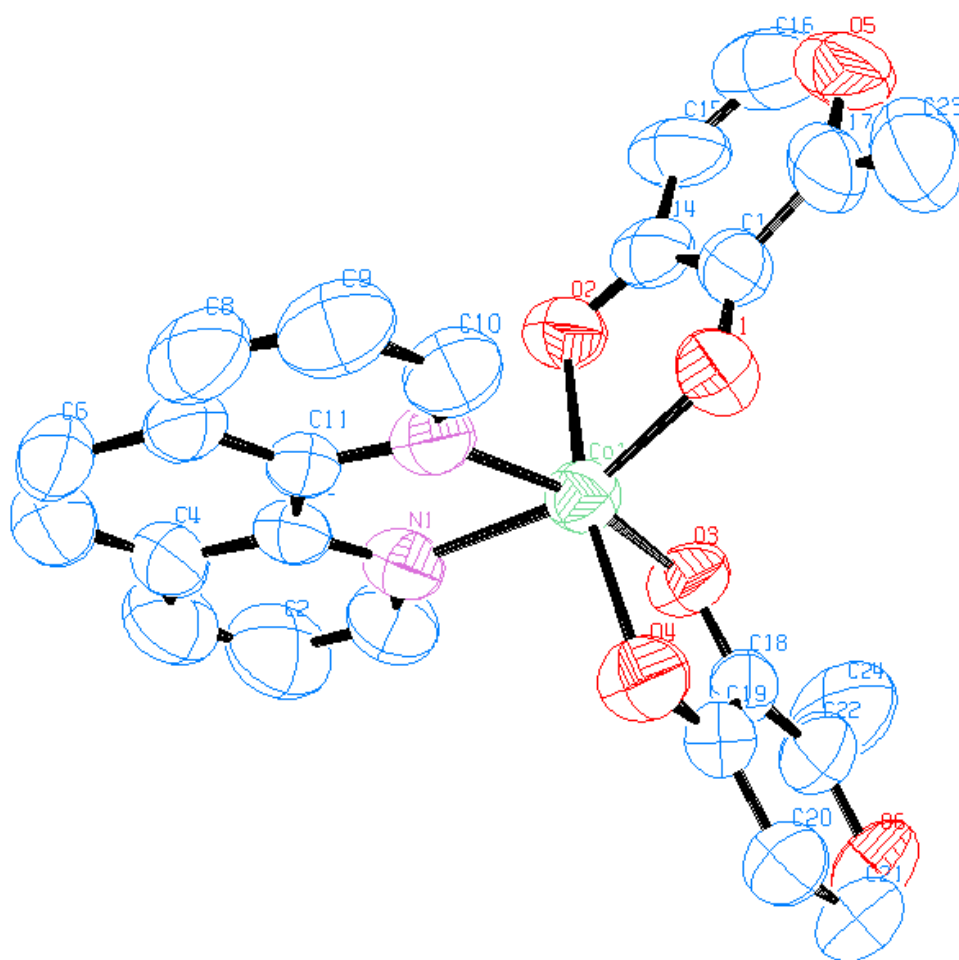


**Figure 3.1:** ORTEP structure of [Co(phen)(ma)<sub>2</sub>] $\cdot$ 5H<sub>2</sub>O **4** with ellipsoids at 50%.

The bite angles (79 – 80°) observed for the coordinated maltolate ligands are relatively smaller than those reported elsewhere, which ranges

from 81.50° to 85.57 ° (Fernandes et al., 2008; Ahmed et al., 2000; Archer et al., 1991; Tan et al., 2008; Carland et al., 2005). The Co-N bond distances (2.145 and 2.161 Å) and the bite angle (76.05°) of the coordinated phen were similar to other cobalt(II) complexes with variable number (1-3) of coordinated phen (Papadopoulos et al., 2007; Liu et al., 2009; Kumar et al., 2009; Harding et al., 2008). The small bite angles (76 – 80°) observed for all the three coordinated bidentate ligands are the consequence of their structural rigidity. In contrast, the bite angles of the maltolate and phen ligands in the square pyramidal [Cu(phen)(ma)Cl]· ½H<sub>2</sub>O are wider (82 – 85°) with shorter Cu-N (phen) bond distances (2.001 and 2.010 Å) (Tan et al., 2008).

**Table 3.5:** Selected bond lengths (Å) and angles (°) for complex **4**

Bond lengths (Å)					
Co(1) – O(1)	2.024 (3)	Co(1) – O(4)	2.144 (3)	O(1) – C(13)	1.302 (5)
Co(1) – O(3)	2.038 (2)	Co(1) – N(1)	2.145 (3)	O(2) – C(14)	1.261 (5)
Co(1) – O(2)	2.129 (2)	Co(1) – N(2)	2.161 (3)	O(3) – C(18)	1.310 (4)
				O(4) – C(19)	1.255 (4)
Bond angles (°)					
O(1) – Co(1) – O(3)	102.60 (11)	O(2) – Co(1) – O(4)	166.63 (10)	O(1) – Co(1) – N(2)	89.03 (11)
O(1) – Co(1) – O(2)	80.24 (11)	O(1) – Co(1) – N(1)	159.68 (12)	O(3) – Co(1) – N(2)	167.60 (11)
O(3) – Co(1) – O(2)	88.34 (10)	O(3) – Co(1) – N(1)	93.61 (12)	O(2) – Co(1) – N(2)	98.00 (10)
O(1) – Co(1) – O(4)	96.71 (11)	O(2) – Co(1) – N(1)	88.15 (11)	O(4) – Co(1) – N(2)	94.95 (10)
O(3) – Co(1) – O(4)	79.58 (10)	O(4) – Co(1) – N(1)	98.23 (11)	N(1) – Co(1) – N(2)	76.05 (12)

The centroid-centroid distance between both phen rings (3.181 Å) of adjacent [Co(phen)(ma)<sub>2</sub>].5H<sub>2</sub>O molecule in molecular packing are near to the reported values (3.3 - 3.8 Å) (He et al., 2012; Chen et al., 2012; Castiñeiras et al., 2002; Lin et al., 2009; Janiak, 2000). This indicates the presence of intermolecular  $\pi$ - $\pi$  stacking interaction between the aromatic phen rings of adjacent molecules (**Figure 3.2**) which is a common phenomenon if planar heterocyclic phen ligand is present in the metal complex (Zhang et al., 2004; Yodoshi et al., 2007; Jia et al., 2010; Bodoki et al., 2009; Paulovicova et al., 2001). Besides, each maltolate ligand acts as a H-acceptor site and the lattice water molecules act as H-donor sites. Hydrogen bonding links each [Co(phen)(ma)<sub>2</sub>].5H<sub>2</sub>O molecule with adjacent molecules in the lattice into an inter-linking network. The overall complex are stabilised by the  $\pi$ - $\pi$  interaction of planar phen rings and H-bond network. Supplementary data for this crystal structure (CCDC No. 774861) can be found online at [doi:10.1016/j.jinorgbio.2010.11.018](https://doi.org/10.1016/j.jinorgbio.2010.11.018).

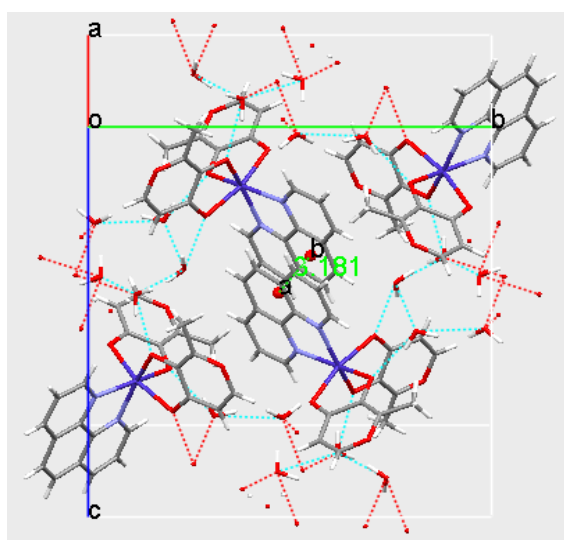


**Figure 3.2:** Packing diagram of complex **4** viewing along a\* axis (light blue dotted lines are H-bonds).

### 3.3.3 Characterization of aqueous solutions of complexes

The ternary metal(II) complexes (**1 - 4**) synthesized in this work were analyzed using Electrospray Ionisation Mass Spectrometry (ESI-MS) at positive ion mode (**Table 3.6**). The base peak was observed at an  $m/z$  value of 364.2 (calc.: 364.2, relative abundance: 100 %) in the mass spectrum of  $[\text{Co}(\text{phen})(\text{ma})\text{Cl}]\cdot 4\text{H}_2\text{O}$  **1**. The peak could be assigned to  $[\text{Co}(\text{phen})(\text{ma})]^+$ . The base peaks observed at  $m/z$  368.8 in the ESI-MS of complex **2** matched well with the calculated mass for  $[\text{}^{63}\text{Cu}(\text{phen})(\text{ma})]^+$  (calc.: 368.0, relative abundance: 100 %) and the isotopic peaks for  $[\text{}^{65}\text{Cu}(\text{phen})(\text{ma})]^+$  was observed at  $m/z$  370.0 (calc.: 370.0, relative abundance: 48 %). In the case of complex **3**, the base peak observed at  $m/z$  369.2 is assigned to  $[\text{}^{64}\text{Zn}(\text{phen})(\text{ma})]^+$  (calc.: 369.2, relative abundance: 100 %). The isotopic peaks observed at  $m/z$  371.2 (calc.: 371.2, relative abundance: 55 %), 372.2 (calc.: 373.2, relative abundance: 38 %), 374.3 (calc.: 373.2, relative abundance: 8 %) and 375.1 (calc.: 375.2, relative abundance: 2 %) are due to Zn isotopes ( $^{66}\text{Zn}$ ,  $^{67}\text{Zn}$ ,  $^{68}\text{Zn}$  and  $^{70}\text{Zn}$ ). Complex **4** is a neutral molecule. The base peak observed at  $m/z$  364.2 can be assigned to  $[\text{Co}(\text{phen})(\text{ma})]^+$  (calc.: 364.2, relative abundance: 100 %), a ion fragment that can be generated from complex **4**. The formation of  $[\text{Co}(\text{phen})(\text{ma})]^+$  might have caused by the dissociation of one maltolate ligand from complex **4**. In order to verify the hypothesis, complex **4** was further investigated using ESI-MS where the mass spectrum was recorded in a negative mode. The base peak was observed at  $m/z$  125.2 in the negative mode ESI mass spectrum of complex **4**, which could be assigned to  $[\text{ma}]^-$ . The result provided indirect evidence to the formation of complex **4** as the related

fragments were identified in the mass spectra. Complex **4** seems to be not stable under the ESI-MS conditions (capillary temperature, 150 °C) used. Molar conductivity experiment was carried out to further study the stability and chemical nature of complex **4** in solution.

**Table 3.6:** ESI-MS data for metal(II) complexes, **1 - 4**

Complex	Fragment	<i>m/z</i> (calculated)	<i>m/z</i> (Found)	Relative abundance, %
<b>1</b>	[Co(phen)(ma)] <sup>+</sup>	364.2	364.2	100
<b>2</b>	[ <sup>63</sup> Cu(phen)(ma)] <sup>+</sup>	368.0	368.8	100
	[ <sup>65</sup> Cu(phen)(ma)] <sup>+</sup>	370.0	370.0	48
<b>3</b>	[ <sup>64</sup> Zn(phen)(ma)] <sup>+</sup>	369.2	369.2	100
	[ <sup>66</sup> Zn(phen)(ma)] <sup>+</sup>	371.2	371.2	55
	[ <sup>67</sup> Zn(phen)(ma)] <sup>+</sup>	372.2	373.2	38
	[ <sup>68</sup> Zn(phen)(ma)] <sup>+</sup>	373.2	374.3	8
	[ <sup>70</sup> Zn(phen)(ma)] <sup>+</sup>	375.2	375.1	2
<b>4</b>	[Co(phen)(ma)] <sup>+</sup>	364.2	364.2	100
	[ma]	125.2	125.2	100

Conductivity measurement of 1 mM of individual solutions of CoCl<sub>2</sub>, CuCl<sub>2</sub>, ZnCl<sub>2</sub>, phen, maltol, complexes **1 - 4** in water-methanol (1:1 v/v) was carried out at 25 °C. The results are summarised in the form of a bar chart shown in **Figure 3.3**. The solution of [Co(phen)(ma)Cl]·4H<sub>2</sub>O complex **1** and CoCl<sub>2</sub> gave molar conductivity values of about 59 and 118 Ω<sup>-1</sup> cm<sup>2</sup> mol<sup>-1</sup> respectively. On the other hand, the solution of [Cu(phen)(ma)Cl]·1/2H<sub>2</sub>O complex **2** and [Zn(phen)(ma)Cl]·1 1/2 H<sub>2</sub>O complex **3** gave molar conductivity values of about 57 Ω<sup>-1</sup> cm<sup>2</sup> mol<sup>-1</sup>. The solution of the complexes **1 - 3** gave lower molar conductivity than the CuCl<sub>2</sub> (119 Ω<sup>-1</sup> cm<sup>2</sup> mol<sup>-1</sup>) and ZnCl<sub>2</sub> (112 Ω<sup>-1</sup> cm<sup>2</sup> mol<sup>-1</sup>) solution. Same molar conductivity values were obtained when the solutions were measured after 24 hours. Complexes **1 - 3**

gave slightly lower molar conductivity values than those previous known cationic metal (Co(II), Ni(II), Cu(II)) complexes with uncoordinated  $\text{Cl}^-$  anion ( $66 - 73 \Omega^{-1} \text{ cm}^2 \text{ mol}^{-1}$ ) (Shebl et al., 2010; Geary, 1971; Coury, 1999). The molar conductivity measurement of the solutions of complexes **1** – **3** suggested that the complexes exist as 1:1 electrolyte in solution, and they consist of  $[\text{M}(\text{phen})(\text{ma})]^+$  and  $\text{Cl}^-$  ions.

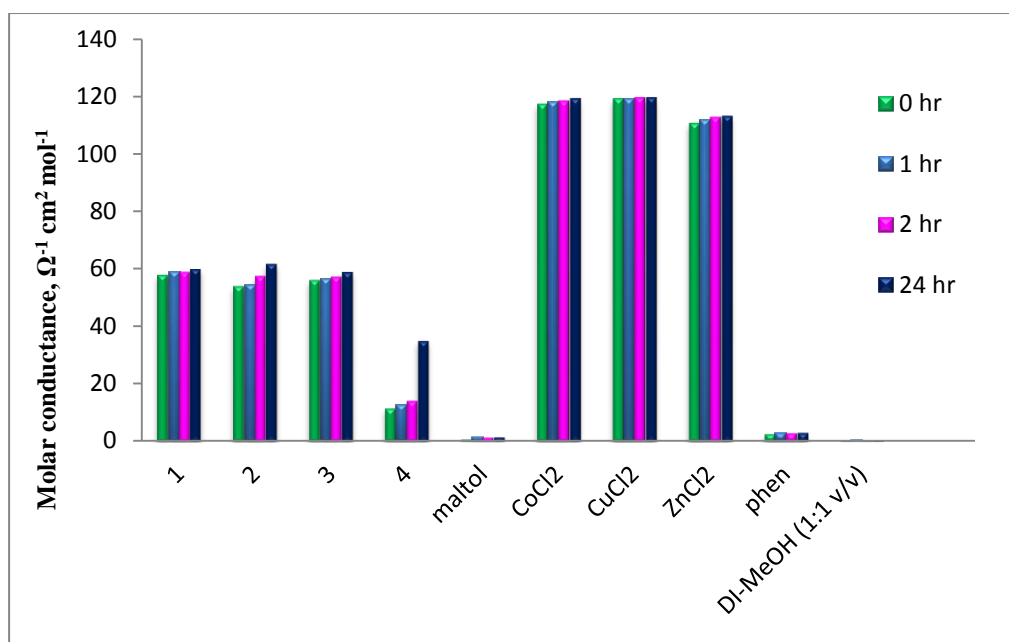


**Figure 3.3:** Molar conductivity ( $\Omega^{-1} \text{ cm}^2 \text{ mol}^{-1}$ ) for metal(II) complexes, **1** - **4**.

The molar conductivity of  $[\text{Co}(\text{phen})(\text{ma})_2] \cdot 5\text{H}_2\text{O}$  complex **4** was similarly measured as for complexes **1-3**. Measurement of the solution of complex **4** gave a molar conductivity value of  $11 - 14 \Omega^{-1} \text{ cm}^2 \text{ mol}^{-1}$  and the value remains constant for the first 2 hours. The low conductivity indicates the non-electrolytic nature of complex **4**. The results obtained is consistent with

those values found for the previously reported neutral Co(II) and other metal(II) complexes ( $10 - 24 \Omega^{-1} \text{ cm}^2 \text{ mol}^{-1}$ ) (Chandra and Kumar, 2005; Tuncel and Serin, 2006; Maurya et al., 2008; Shebl et al., 2010; Reddy et al., 2007; Maurya et al., 2011; García-Raso et al., 2003). However, its molar conductivity increases to  $35 \Omega^{-1} \text{ cm}^2 \text{ mol}^{-1}$  at 24 hours, suggesting partial ligand dissociation. This data is consistent with the ESI-MS result. Although Co(II) complexes are said to be usually labile, coordinated phen and maltolate ligands in complexes **1** and **4** seem to be relatively stable, within the duration of the measurement.

UV-Visible spectroscopy is a useful technique in the characterisation of inorganic species. In UV-Visible region of the electromagnetic spectrum, molecules undergo electronic transitions. As a molecule absorbs energy, an electron is promoted from an occupied orbital to an unoccupied orbital of greater potential energy ( $\sigma \rightarrow \sigma^*$ ,  $n \rightarrow \sigma^*$ ,  $n \rightarrow \pi^*$  or  $\pi \rightarrow \pi^*$ ). Generally, the most probable transition takes place from the highest occupied molecular orbital (HOMO) to the lowest unoccupied molecular orbital (LUMO) (Pavia et al., 2001). Electronic spectra of four complexes **1** - **4** were recorded in water-methanol (1:1 v/v) solutions (UV:  $1.0$  to  $5.0 \times 10^{-5}$  M; Visible: 0.01 M). The assignments of electronic spectral peaks observed in each of the complexes along with the molar extinction coefficients are tabulated in **Table 3.7**. In the visible region,  $[\text{Cu}(\text{phen})(\text{ma})\text{Cl}] \cdot \frac{1}{2}\text{H}_2\text{O}$  (0.01 M) exhibit  $\lambda_{\text{max}}$  at 645 nm ( $\epsilon = 55$ ) whereas no visible absorptions for  $[\text{Co}(\text{phen})(\text{ma})\text{Cl}] \cdot 4\text{H}_2\text{O}$ ,  $[\text{Zn}(\text{phen})(\text{ma})\text{Cl}] \cdot \frac{1}{2} \text{H}_2\text{O}$  and  $[\text{Co}(\text{phen})(\text{ma})_2] \cdot 5\text{H}_2\text{O}$  were observed

(**Appendix 3.7**). This 645 nm band (**Appendix 3.8**) of the Cu(II) complex with low molar absorptivity was assigned to d-d transition. In the case of Co(II) complexes, d-d transitions are forbidden by the Laporte rule.

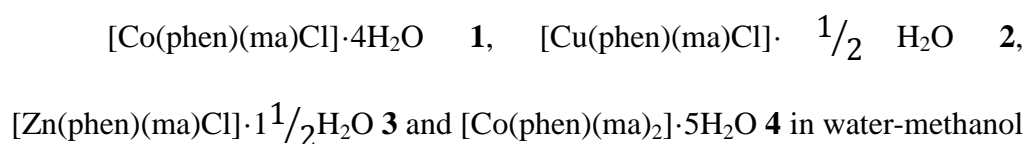
**Table 3.7:** Absorption spectral data for metal(II) complexes, **1 - 4**

Complex	$\lambda_{\max}$ (nm), $\epsilon$ ( $\text{mol}^{-1}\text{dm}^3\text{cm}^{-1}$ )	Assignment
[Co(phen)(ma)Cl]·4H <sub>2</sub> O ( <b>1</b> )	225 ( $\epsilon = 38\ 750$ )	$\pi \rightarrow \pi^*$ (phen)
	269 ( $\epsilon = 34\ 730$ )	$\pi \rightarrow \pi^*$ (phen)
[Cu(phen)(ma)Cl]· $\frac{1}{2}$ H <sub>2</sub> O ( <b>2</b> )	225 ( $\epsilon = 44\ 260$ )	$\pi \rightarrow \pi^*$ (phen)
	271 ( $\epsilon = 36\ 320$ )	$\pi \rightarrow \pi^*$ (phen)
	645 ( $\epsilon = 55$ )	d-d
[Zn(phen)(ma)Cl]· $\frac{1}{2}$ H <sub>2</sub> O ( <b>3</b> )	225 ( $\epsilon = 40\ 670$ )	$\pi \rightarrow \pi^*$ (phen)
	270 ( $\epsilon = 35\ 250$ )	$\pi \rightarrow \pi^*$ (phen)
[Co(phen)(ma) <sub>2</sub> ]·5H <sub>2</sub> O ( <b>4</b> )	227 ( $\epsilon = 43\ 720$ )	$\pi \rightarrow \pi^*$ (phen)
	269 ( $\epsilon = 34\ 610$ )	$\pi \rightarrow \pi^*$ (phen)

In UV spectra, aqueous solutions of complexes **1 - 4** have two bands at  $\lambda_{\max}$  of 225 nm and another  $\lambda_{\max}$  within the range of 269 - 271 nm respectively. Phenanthroline complexes have been extensively studied previously and many of these work have reported the two intense peaks observed in the UV region at about 226 nm and 269 nm which aroused from the  $\pi \rightarrow \pi^*$  transition of the coordinated phenanthroline ligand (Zhang et al., 2004). Comparing the UV spectra of complexes **1 - 4** with those of MCl<sub>2</sub> (no UV absorption), 1,10-phenanthroline ( $\lambda_{\max}$ : 229 nm and 265 nm) and maltol ( $\lambda_{\max}$ : 213 nm and 273 nm), the presence of coordinated phen and maltolate ligands in the solution of complexes **1 - 4** are inferred (Radanović et al., 2003; Papadopoulos et al., 2007; Ni et al., 2005). Intraligand transitions of respective ligands help to identify the coordinated ligand in metal complexes. The results obtained from

the UV-Vis study matched well with the FTIR data. A plot of absorbance versus concentration for the two maximum absorption peaks in the UV region for four ternary complexes **1 - 4** are shown in **Appendix 3.9 - 3.12** (inset). A regression line for each plot has been drawn by using the least-squares method generated by using Microsoft Office Excel 2007 software. The correlation coefficient ( $R^2$ ) values for all the plotted graphs are very close to 1.0000 showing that the data obtained fit in the regression line and obeyed the Beer-Lamberts Law. The average molar absorptivity values were obtained for all four ternary complexes based on the Beer-Lambert Law and the general linear equations.

The *N,N'*-phen ligand was used in the current study as the main ligand and *O,O'*-maltol was used as the coligand to synthesise metal complexes **1 - 4**. Many researchers have reported that phen is a fluorescent molecule. According to Peter and Chen (2002), fluorescence is a photonic process involving transition between electronic and vibration states of fluorophores. It would be interesting to obtain the fluorescence spectra of metal complexes **1 - 4** in order to study the effect of the type of metal ions on the emission properties. The fluorescence (FL) spectra of maltolate complexes **1 - 4**, maltol and phen ligands are shown in **Figure 3.4**.



still retain the FL emission property of the free phen ligand in the same solvent mixture. There is no change in the shape of the FL emission bands but there is slight red shift in  $\lambda_{\text{max}}$ . The FL emission in the metal complexes arises from the coordinated phen ligand. The FL emission intensities of complexes **1**, **2** and **4** are lower than the free phen ligand. This lower FL intensity is due to quenching of phen FL by the Co(II) and Cu(II) ion. The quenching mechanism has previously been ascribed to static quenching (Seng et al., 2008). Maltol has no FL emission. [Co(phen)(ma)<sub>2</sub>] $\cdot$ 5H<sub>2</sub>O has a lower FL emission intensity than [Co(phen)(ma)Cl] $\cdot$ 4H<sub>2</sub>O. The results appear to suggest that the change in geometry and the number of coordinated maltolate ligands influence the FL emission intensity but not the  $\lambda_{\text{max}}$  and shape of the FL emission bands (**Figure 3.10; spectra III and IV**). Seng and coworkers has reported the amount of quenching of the coordinated phen is influenced by the type of the transition metal(II) ion in the octahedral [M(phen)(edda)] complexes.

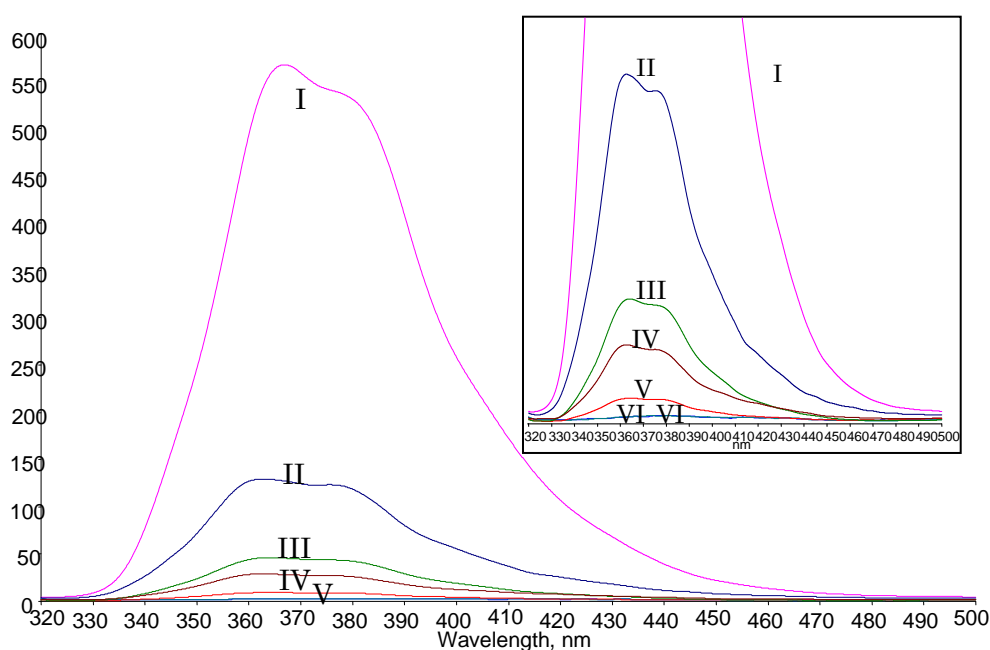


**Figure 3.4:** Fluorescence spectra of **3** (I), phen (II), **1** (III), **4** (IV), **2** (V), maltol (VI) and water-methanol mixture (1:1 v/v) (VII) at 1  $\mu$ M.

[Zn(phen)(ma)Cl]·1 1/2H<sub>2</sub>O in water-methanol shows an enhancement in FL spectra which is different from the Co(II) and Cu(II) analogues. The enhancement of FL emission spectra of the Zn(II) complex cannot be explained by static quenching mechanism (Seng et al., 2008). Higher FL emission observed for the Zn(II) complex (compared to the Co(II) and Cu(II) complexes) has been attributed to the full d<sup>10</sup> electron configuration of the Zn(II) ion (Hu et al., 2010). In a previous study on the fluorescence of solid samples of a series ZnX<sub>2</sub>(phen) complexes (X = Cl, Br, I), the type of halides was found to affect the FL emission intensity and the order was found to be ZnCl<sub>2</sub>(phen) < phen < ZnBr<sub>2</sub>(phen) < ZnI<sub>2</sub>(phen) (Ikeda et al., 1996). The FL emission enhancement was explained by the dependence of intersystem crossing rate on the halide, and the mechanism involved a Heitler-London type mixing between the phen locally excited and the ρ (halogen) → δ\* (phen) ligand-to-ligand charge-transfer (LLCT) electronic configurations and 1,3(n, δ\*) energy level change due to the coordination. The order of complexes in terms of increasing FL intensity is **2** < **4** < **1** < phen < **3**.

### 3.4 CONCLUSION

Four metal complexes containing phen and maltolate ligands namely [Co(phen)(ma)Cl]·4H<sub>2</sub>O **1**, [Cu(phen)(ma)Cl]· 1/2 H<sub>2</sub>O **2**, [Zn(phen)(ma)Cl]·1 1/2H<sub>2</sub>O **3** and [Co(phen)(ma)<sub>2</sub>]·5H<sub>2</sub>O **4** were prepared. Fourier Transform Infrared Spectroscopy (FTIR), elemental analysis and ESI-MS study confirmed their formation. Generally, all four metal complexes are

thermally stable at room temperature. The decomposition began with the dehydration process. The dehydration was then followed by the loss of chloride, maltol and phen ligand. It can be concluded from the discussion in the previous **section 3.3.3**, complexes **1 - 3** exist as  $[\text{Co}(\text{phen})(\text{ma})]^+$ ,  $[\text{Cu}(\text{phen})(\text{ma})]^+$  and  $[\text{Zn}(\text{phen})(\text{ma})]^+$  or its hydrated species and  $\text{Cl}^-$  in solution while complex **4** exists as the neutral  $[\text{Co}(\text{phen})(\text{ma})_2]$  species in aqueous solution. Based on the molar conductivity obtained, complexes **1 - 3** are categorized as 1:1 electrolyte while complex **4** is non-electrolyte in water-methanol (1:1 v/v) solution. The dissociation of phen and maltolate ligands in complexes **1** and **4** were not observed within the duration of the conductivity experiments, which appear to suggest that the ligands are bound strongly to the metal centres. FL emission intensities are increasing in the order of  $\mathbf{2} < \mathbf{4} < \mathbf{1} < \text{phen} < \mathbf{3}$ . Different quenching of phen FL by the type of metal ion and number of coordinated ligands resulted in the differential FL emission of this set of complexes. Zn(II) enhances the FL of the coordinated phen while Co(II) and Cu(II) partially quenches the FL of the coordinated phen. The UV absorption bands observed in the UV-Vis spectra of the metal complexes arose from the  $\pi \rightarrow \pi^*$  transition of the coordinated phenanthroline ligand. However, no visible absorption spectra were obtained for  $[\text{Co}(\text{phen})(\text{ma})\text{Cl}] \cdot 4\text{H}_2\text{O}$ ,  $[\text{Zn}(\text{phen})(\text{ma})\text{Cl}] \cdot 1\frac{1}{2}\text{H}_2\text{O}$  and  $[\text{Co}(\text{phen})(\text{ma})_2] \cdot 5\text{H}_2\text{O}$ . In the case of Co(II) complexes, d-d transitions are forbidden by the Laporte rule.

**CHAPTER 4**  
**SYNTHESIS AND CHARACTERIZATION OF METAL(II)**  
**1,10-PHENANTHROLINE COMPLEXES WITH**  
***O,N,O'*-DIPICOLINIC ACID**

**CHAPTER 4**  
**SYNTHESIS AND CHARACTERIZATION OF METAL(II)**  
**1,10-PHENANTHROLINE COMPLEXES WITH**  
***O,N,O'*-DIPICOLINIC ACID**

**4.1 INTRODUCTION**

In the previous chapter, two series of metal(II)-phen-maltolate complexes were synthesized and characterized to study the effect of the type of metal ion and the number of coordinated ligands on the solution properties and thermal stability of the metal(II) complexes. In this chapter, the subsidiary ligand has been replaced by dipicolinate ligand to synthesize  $[M(\text{phen})(\text{dipico})(\text{H}_2\text{O})] \cdot x\text{H}_2\text{O}$  (where  $M = \text{Co}$  or  $\text{Zn}$ ;  $x = 1$  or  $2$ ) and  $[\text{Cu}_2(\text{phen})_3(\text{dipico})(\text{H}_2\text{O})][\text{Cu}(\text{dipico})_2] \cdot [(11\text{H}_2\text{O})(\text{CH}_3\text{OH})]$  complexes. These dipicolinate complexes were characterized by Fourier Transform Infrared spectroscopy (FTIR), CHN elemental analysis, X-ray crystallography, molar conductivity, UV-Visible spectroscopy (UV-Vis) and fluorescence spectroscopy (FL). Dipicolinate ligand has been chosen as coligand partly because its non-toxicity may results in lower toxicity of metal(II) complexes. In addition, dipicolinate-based complexes were reported to exhibit various biological functions, *viz.* insulin mimetic, antibacterial and anticancer (Yang et al., 2002; Cai et al., 2010; Martin et al., 1997; Pocker et al., 1980; Tochikubo et al., 1974; Murakami et al., 2003). This chapter also investigated the effect of the type of metal ion on the solution properties of the set of metal(II)-phen-dipicolinate complexes.

## 4.2 EXPERIMENTAL

### 4.2.1 Materials and reagents

1,10-phenanthroline monohydrate (99%), pyridine-2,6-dicarboxylic acid (dipico), zinc(II) chloride puriss were purchased from Riedel-de Haen. Cobalt(II) chloride hexahydrate was purchased from R&M Chemicals. Copper(II) chloride dihydrate and sodium hydroxide were bought from Acros Organic and System AR respectively. All reagents and solvents (Analytical grade or HPLC grade methanol) were used as purchased.

### 4.2.2 Preparation of $[M(\text{phen})(\text{dipico})(\text{H}_2\text{O})] \cdot x\text{H}_2\text{O}$ ( $M = \text{Co}$ or $\text{Zn}$ ; $x = 1, 2$ ) (**5** and **7**) and $[\text{Cu}_2(\text{phen})_3(\text{dipico})(\text{H}_2\text{O})][\text{Cu}(\text{dipico})_2] \cdot [(11\text{H}_2\text{O})(\text{CH}_3\text{OH})]$ **6**

To prepare  $[\text{Co}(\text{phen})(\text{dipico})(\text{H}_2\text{O})] \cdot 2\text{H}_2\text{O}$  **5**, cobalt(II) chloride (0.24 g, 1 mmole) in deionised water (10 mL) and dipicolinic acid (0.17 g, 1 mmole) in 0.1 M NaOH (20 mL) were mixed and stirred for 30 minutes. This was followed by addition of a methanolic solution (5 mL) of phen (0.18 g, 1 mmole) to the solution mixture. The solution was heated to reduce the volume of the solution to *c.a.* 5 mL. The solution was then allowed to stand overnight. The product was collected on the following day by suction filtration and washed with cold deionised water, then dried *in vacuo*. The yield of brownish orange crystals (0.40 g, 69 %).

The above procedure was used to prepare the Cu(II) and Zn(II) analogues. The attempt to synthesis the other [Cu(phen)(dipico)(H<sub>2</sub>O)] complex was unsuccessful. The recovered product was [Cu<sub>2</sub>(phen)<sub>3</sub>(dipico)(H<sub>2</sub>O)][Cu(dipico)<sub>2</sub>].[(11H<sub>2</sub>O)(CH<sub>3</sub>OH)] **6**. The pure complex **6** was obtained as blue crystals (0.35 g, 75 %) whereas [Zn(phen)(dipico)(H<sub>2</sub>O)].H<sub>2</sub>O **7** was obtained as white crystals (0.32 g, 72%).

#### **4.2.3 Characterization of solids complexes**

Elemental analyses (C, H, and N) and FTIR spectra were similarly performed as ascribed in Chapter 3 section 3.2.3.

#### **4.2.4 Determination of crystal structures**

The X-ray diffraction data was obtained with a Bruker AXS CCD diffractometer with Mo K $\alpha$  radiation ( $\lambda = 0.71073 \text{ \AA}$ ). The SMART (Version 5.631) & SAINT (Version 6.63) (Bruker, 2000) softwares were used for data collection. The integration of intensity of reflections and scaling were done by SMART (Version 5.631) & SAINT (Version 6.63) (Bruker, 2000); SADABS (Sheldrick, 2001) was used for empirical absorption correction. SHELXTL (Bruker, 2000) was used for space group determination, structure refinement, graphics and structure reporting. The structures were solved by direct-methods and refined by a full-matrix least-squares procedure of  $F^2$  with anisotropic

displacement parameters for non-hydrogen atoms, C and N-bound hydrogen atoms in their calculated positions and using a weighting scheme of the form calculated  $w = 1/[s^2(F_o^2) + (0.0996P)^2 + 0.0491P]$  where  $P = (F_o^2 + 2F_c^2)/3$  **5**; calculated  $w = 1/[s^2(F_o^2) + (0.1603P)^2 + 10.9481P]$  where  $P = (F_o^2 + 2F_c^2)/3$  **6**; calculated  $w = 1/[s^2(F_o^2) + (0.0384P)^2 + 0.9832P]$  where  $P = (F_o^2 + 2F_c^2)/3$  **7** (Sheldrick, 2008). Hydrogen atoms in their calculated positions were refined using a riding model. Data collection and experimental details for the complexes are summarized in **Table 4.1**.

**Table 4.1:** Crystal data and structure refinement for metal(II) complexes **5 - 7**

	<b>5</b>	<b>6</b>	<b>7</b>
Empirical formula	CoC <sub>19</sub> H <sub>17</sub> N <sub>3</sub> O <sub>7</sub>	Cu <sub>3</sub> C <sub>58</sub> H <sub>59</sub> N <sub>9</sub> O <sub>24.5</sub>	ZnC <sub>19</sub> H <sub>15</sub> N <sub>3</sub> O <sub>6</sub>
Formula weight	458.29	1464.78	446.73
Temperature (K)	223	223	223
Crystal system	Triclinic	Triclinic	Monoclinic
Space group	P-1	P-1	P2(1)/c
Unit cell dimensions (Å)	a = 7.7873(13); b = 9.2814(16); c = 14.034(2)	a = 14.481(5); b = 15.569(5); c = 15.863(5)	a = 7.4836(3); b = 20.7987(9); c = 11.5801(5)
Volume (Å <sup>3</sup> )	953.7(3)	3137.4(18)	177.90(13)
Z	2	2	4
Density (calculated) (mg/m <sup>3</sup> )	1.596	1.523	1.674
Absorption coefficient (mm <sup>-1</sup> )	0.949	1.096	1.431
F(000) (mm)	470	1454	912
Crystal size (mm)	0.30 x 0.12 x 0.10	0.56 x 0.36 x 0.16	0.28 x 0.12 x 0.10
θ range for data collection (°)	2.31 – 27.50	2.31 - 21.15	1.96 – 27.50
Index ranges	-10 ≤ h ≤ 10; -11 ≤ k ≤ 11; -18 ≤ l ≤ 18	-17 ≤ h ≤ 17; -18 ≤ k ≤ 18; -18 ≤ l ≤ 18	-9 ≤ h ≤ 9; -25 ≤ k ≤ 27; -12 ≤ l ≤ 15
Reflections collected	10238	32739	12418
Independent reflections	4340	11022	4060
Data/restraints/parameters	4340/6/289	11022/18/874	4060/4/278
Goodness-of-fit on F <sup>2</sup>	1.067	1.077	1.060
Final R indices [I > 2(σ)]	R = 0.0665; wR = 0.1632	R = 0.1141; wR = 0.2994	R = 0.0364; wR = 0.0849
R indices (all data)	R = 0.0833; wR = 0.1729	R = 0.1720; wR = 0.3279	R = 0.0428; wR = 0.0878
Largest dif. Peak and hole (eÅ <sup>3</sup> )	1.435, -0.857	1.558, -0.862	0.428, -0.277

#### 4.2.5 Characterization of aqueous solutions of complexes

A CON 700 bench top conductivity meter from EUTECH Instruments was used to measure the conductivity of the solvent mixture used and methanol-water (1:1 v/v) solutions of the ternary metal(II) complexes, using KCl as calibrant. The preparation of the water-methanolic (1:1 v/v) solutions of metal(II) complexes (**5 - 7**) and procedures for the conductivity measurement were the same as in Chapter 3 section 3.2.6. UV-visible spectra of aqueous solutions of these complexes were obtained with a Perkin Elmer Lambda 35 spectrophotometer in the range of 200 – 900 nm. These solutions were prepared by using 1:1 (v/v) water-methanol mixture to give  $1.0 \times 10^{-3}$  M stock solutions. The solutions of the free ligands and the metal(II) chloride were similarly prepared. The reference cell was filled with water-methanol (1:1 v/v) while the sample cell was filled with the sample solution. The fluorescence study was carried out with a Perkin Elmer LS55 Fluorescence spectrometer at 272 nm (excitation wavelength). The stock solutions of the metal(II) complexes and the stock solutions of the free ligands and metal(II) chlorides for fluorescence study were prepared as described for sample solutions for UV-Vis spectra measurements. The sample solutions were further diluted to  $1.0 \times 10^{-6}$  M for the fluorescence study.

## 4.3 RESULT AND DISCUSSION

### 4.3.1 Characterization of solids complexes

All three dipicolinate complexes, **5 - 7** were synthesized by modifying the method published elsewhere (Kirillova et al., 2007; Ma et al., 2002; Hadadzadeh et al., 2009). The complexes **5 - 7**, were characterized by Fourier Transform Infrared Spectroscopy, elemental analysis and X-ray crystallography. The modified preparations gave yield of up to ~ 69 % for complex **5**, ~ 75% for complex **6** and ~ 72 % for complex **7**. Based on microanalysis results, the complexes can be formulated as  $[\text{Co}(\text{phen})(\text{dipico})(\text{H}_2\text{O})] \cdot 2\text{H}_2\text{O}$  **5**,  $[\text{Cu}_2(\text{phen})_3(\text{dipico})(\text{H}_2\text{O})][\text{Cu}(\text{dipico})_2] \cdot [(11\text{H}_2\text{O})(\text{CH}_3\text{OH})]$  **6** and  $[\text{Zn}(\text{phen})(\text{dipico})(\text{H}_2\text{O})] \cdot \text{H}_2\text{O}$  **7** as listed in **Table 4.2**.

**Table 4.2:** Physical and chemical data of metal(II) complexes, **5 - 7**

Complex	5	6	7
Molecular formulae	$[\text{Co}(\text{C}_{12}\text{H}_8\text{N}_2)(\text{C}_7\text{H}_3\text{NO}_4)(\text{H}_2\text{O})] \cdot 2\text{H}_2\text{O}$	$[\text{Cu}_2(\text{C}_{12}\text{H}_8\text{N}_2)_3(\text{C}_7\text{H}_3\text{NO}_4)(\text{H}_2\text{O})][\text{Cu}(\text{C}_7\text{H}_3\text{NO}_4)_2] \cdot [(11\text{H}_2\text{O})(\text{CH}_3\text{OH})]$	$[\text{Zn}(\text{C}_{12}\text{H}_8\text{N}_2)(\text{C}_7\text{H}_3\text{NO}_4)(\text{H}_2\text{O})] \cdot \text{H}_2\text{O}$
Molecular weight (g/mol)	458.28	1464.78	446.73
% yield	~ 69 %	~ 75 %	~ 72 %
Colour	Brown crystals	Blue crystals	White crystals
CHN elemental analysis, % Calculated (Found)	C	49.80 (49.60)	51.08 (51.04)
	H	3.74 (3.59)	3.38 (3.18)
	N	9.17 (9.28)	9.41 (9.44)

FTIR spectra of complexes **5 - 7** are shown in **Appendix 4.1** and assignments of the characteristic bands are listed in **Table 4.3**. In the higher wavenumber,  $\nu(\text{H}_2\text{O})$  vibrations bands ( $3518 - 3254 \text{ cm}^{-1}$ ) suggests presence

of coordinated water or lattice water molecule(s) for complexes **5**, **6** and **7** (Nakamoto, 1977; Hadadzadeh et al., 2010; Yenikaya et al., 2009; Kirillova et al., 2007; Vargová et al., 2004). This strong, broad and intense band is indicative of O-H stretching (Kirillova et al., 2007; Nakamoto, 1977). The relatively weak aromatic  $\nu(\text{C-H})$  bands in the range of  $3098 - 3052 \text{ cm}^{-1}$  for complexes **5** and **7** suggest the presence of phen ligand (Yenikaya et al., 2009; Kirillova et al., 2007; Gonzalez-Baró et al., 2005; Bulut et al., 2009).

A weak absorption of  $\nu(\text{C=N})$  and strong absorption of aromatic  $\nu(\text{C=C})$  typical of coordinated phen are observed for **5 - 7** in the range of  $1516 - 1520 \text{ cm}^{-1}$  and  $1426 - 1428 \text{ cm}^{-1}$  respectively (Schilt and Taylor, 1958; Garcia-Raso et al., 2003; Tang et al., 2007). Several ring stretching modes of the phen are found in the range of  $1031 - 1106 \text{ cm}^{-1}$  (Shani et al., 1977). Two medium  $\nu(\text{C-H})$  out of plane vibration bands at  $\sim 723 \text{ cm}^{-1}$  and  $\sim 855 \text{ cm}^{-1}$  suggest the coordination of phen (Garcia-Raso et al., 2003; Zhang et al., 2004; Jin et al., 2000). The presence of the  $\nu(\text{M-N})$  vibration bands in the range of  $180 - 290 \text{ cm}^{-1}$  observed for M(II)-phen complexes could not be verified for complexes **5 - 7** as they were out of range for the FTIR spectrophotometer used (Schilt and Taylor, 1958; Papadopoulos et al., 2007; Shebl et al., 2010; García-Raso et al., 2003; Yenikaya et al., 2009).

The  $\nu(\text{C=O})$  and  $\nu(\text{C-O})$  vibrations of -COOH group of the free dipicolinic acid occurred at  $1701 \text{ cm}^{-1}$  and  $1290 \text{ cm}^{-1}$  respectively (**Appendix**

**3.2).** These two peaks were found to have shifted to a lower frequency in complexes **5 - 7** and this shift is due to coordination of the dipicolinate ligand to the Co(II), Cu(II) and Zn(II) centre. Strong  $\nu_{\text{as}}(\text{COO}^-)$  and  $\nu_{\text{s}}(\text{COO}^-)$  absorption bands were observed for **5 - 7** in the range of 1618 - 1629  $\text{cm}^{-1}$  and 1368 - 1379  $\text{cm}^{-1}$  respectively (Hadadzadeh et al., 2010; Dutta et al., 1981; Allan et al., 1989; Dutta et al., 1980; Sukanya et al., 2006; Yenikaya et al., 2009; Kirillova et al., 2007; Bulut et al., 2009; Zhou et al., 2009; Cai et al., 2010). Coordinated dipicolinate exhibit  $\nu(\text{C}=\text{N})$  and  $\nu(\text{C}=\text{C})$  stretching vibrations at 1585  $\text{cm}^{-1}$  (Dutta et al., 1980; Vargová et al., 2004; Shani et al., 1977; Rana et al., 1979). These were similarly observed for complexes **5 - 7** (1583 – 1589  $\text{cm}^{-1}$ ).

The  $\nu(\text{C}-\text{N})$  and  $\nu(\text{C}-\text{H})$  vibrations of the pyridine moiety of the dipicolinate in complexes **5 - 7** were observed in the range of 1077 – 1283  $\text{cm}^{-1}$  and 911 – 914  $\text{cm}^{-1}$  respectively (Cai et al., 2010; Bulut et al., 2009). The ring wagging vibration of the pyridine moiety was also observed at 766 - 772  $\text{cm}^{-1}$  (Yenikaya et al., 2009; Bulut et al, 2009). The medium intensity of  $\nu(\text{Co}-\text{O})$  and  $\nu(\text{Cu}-\text{O})$  vibration bands were observed at 422  $\text{cm}^{-1}$  (**5**) and 429  $\text{cm}^{-1}$  (**6**) (Liu et al., 2005; Zhang et al., 2008; Yenikaya et al., 2009). However, the  $\nu(\text{Zn}-\text{O})$  vibration band in complex **7** was not observed. The  $\nu(\text{Zn}-\text{O})$  vibration band ( $< 300 \text{ cm}^{-1}$ ) of complex **7** is beyond the detection of the FTIR spectrophotometer used. Observation of the  $\nu(\text{M}-\text{O})$  vibration bands can be used to show coordination of the oxygen atom of the carboxylate group to the Co(II), Cu(II) and Zn(II) centres (Allan et al., 1989; Yenikaya et al; 2009; Cai

et al., 2010; Tunçel et al., 2006; García-Raso et al., 2003). The FTIR spectral of complexes **5 - 7** (**Appendix 4.1**) suggested that both phen and dipicolinate ligands were coordinated to the metal (Co(II), Cu(II) and Zn(II)) centres respectively.

**Table 4.3:** Characteristic Infrared band assignments of metal(II) complexes **5 - 7**

Bond	5	6	7	Remarks
v(O-H)	3494 (m)		3518 (s)	Water
	3436 (w)	3401 (b)	3447 (m)	
	3369 (b)		3254 (b)	
v(C-H) <sub>aromatic</sub>	3052 (w)	-	3071 (w) 3098 (w)	Phen
v(C=N)	1516 (m)	1520 (m)	1519 (m)	
v(C=C)	1426 (s)	1428 (s)	1427 (s)	
V <sub>ring</sub>	1098 (w)	1106 (m)	1104 (m)	
	1077 (m)	1084 (m)	1079 (m)	
	1032 (w)	1036 (w)	1031 (m)	
v(C-H) Out-of-plane	727(m),	723 (m)	727 (s),	
	855(m)	854 (m)	848 (m)	
v(M-N)	529 (w)	-	438 (m)	
v <sub>as</sub> (COO <sup>-</sup> )	1618 (s)	1629 (s)	-	Dipicolinate
v <sub>s</sub> (COO <sup>-</sup> )	1379 (s)	1370 (s)	1368 (s)	
V <sub>pyridine</sub> = [v(C=N) + v(C=C)]	1586 (b)	1589 (b)	1583 (b)	
v(C-N)	1283 (s)	1276 (s)	1283 (s)	
	1077 (m)	1084 (m)	1079 (m)	
[v(C=C) + v(C-O <sup>-</sup> )]	1459 (w)	1459 (w)	1460 (w)	
v(C-H)	914 (m)	912 (m)	911 (m)	
(pyridine) <sub>wagging</sub>	767 (m)	772 (m)	766 (m)	
v(M-O)	422 (m)	429 (m)	-	

#### 4.3.2 Analysis of crystal structures

**Figures 4.1 - 4.3** showed the crystal structures of  $[\text{Co}(\text{phen})(\text{dipico})(\text{H}_2\text{O})] \cdot 2\text{H}_2\text{O}$  **5**,

$[\text{Cu}_2(\text{phen})_3(\text{dipico})(\text{H}_2\text{O})][\text{Cu}(\text{dipico})_2] \cdot [(11\text{H}_2\text{O})(\text{CH}_3\text{OH})]$  **6** and

[Zn(phen)(dipico)(H<sub>2</sub>O)]·H<sub>2</sub>O **7**. Both complexes, **5** and **7** are isostructural to their manganese(II) (Ma et al., 2002), zinc(II) (Harrison et al., 2006) and nickel(II) analogues (Hadadzadeh et al., 2010) which are all octahedral. The dipicolinate ligand served as a tridentate ligand, the ligand bounds to the metal centres through the *O,N,O'* donor atoms. On the other hand, the phen ligand coordinates to the metal centres through its two nitrogen donor atoms and acts as a bidentate chelating ligand. The sixth coordination site is filled by a monodentate aqua ligand. These ligating atoms, O<sub>3</sub>N<sub>3</sub>, forms a distorted octahedral coordination sphere around each metal(II) center of the complexes **5** and **7**. Complex **7** is highly distorted owing to the planarity, rigidity and denticity of phen and dipico ligands. Besides, the limited span width of the terminal O(1) and O(3) ligating atoms of dipico caused phen and dipico cannot chelate to Zn(II) in the same plane (Harrison et al., 2006; Hadadzadeh et al., 2010).

The Co(1) - N(3) (2.047 Å) and Co(1) - O5W (2.099 Å) bonds of complex **5** are significantly shorter than the other four octahedral bonds (2.104 - 2.154 Å) in **5**. Similarly, the Zn(1) - N(3) (2.0547 Å) and Zn(1) - O1W (2.0478 Å) bonds of complex **7** are significantly shorter than the other four octahedral bonds (2.1142 - 2.2617 Å) in **7**. The M - N<sub>phen</sub> bond lengths of complexes **5** and **7** are similar to those reported for other Co-phen and Zn-phen complexes (Papadopoulos et al., 2007; Harrison et al., 2006; Xiao et al., 2005; Rubin-Preminger et al., 2008; Hanauer et al., 2008; He et al., 2007; Song et al., 2011; Wang et al., 2000). Co(1) - O5W and Zn(1) - O1W bond

lengths are shorter than  $\text{Co} - \text{O}_{\text{dipico}}$  and  $\text{Zn} - \text{O}_{\text{dipico}}$  observed for other similar metal(II)-dipico complexes (Harrison et al., 2006; Hakansson et al., 1993; Ma et al., 2002; Hadadzadeh et al., 2010; Bulut et al., 2009). The  $\text{M} - \text{N}_{\text{dipico}}$  bond is shorter than the two  $\text{M} - \text{N}_{\text{phen}}$  bond lengths, indicating that  $\text{N}_{\text{dipico}}$  is a stronger donor, since the two carboxylate groups in ortho positions enhance the electron density (basicity) on this N-atom (Uçar et al., 2007; Ma et al., 2002; Bulut et al., 2009).

The N(1), O(1), O(3) and N(3) ligating atoms are equatorial ligating atoms in complex **7**. These equatorial atoms are not coplanar as the N(1) atom is slightly displaced from the O(1)-O(3)-N(3) plane. The bite angles for the dipico ligand in complex **5** ( $\text{N}(3)\text{-Co}(1)\text{-O}(1) = 75.97^\circ$  and  $\text{N}(3)\text{-Co}(1)\text{-O}(3) = 75.92^\circ$ ) and complex **7** ( $\text{N}(3)\text{-Zn}(1)\text{-O}(3) = 73.86^\circ$  and  $\text{N}(3)\text{-Zn}(1)\text{-O}(3) = 76.37^\circ$ ) are similar to those reported for dipicolinate-metal complexes (Gonzalez-Baró et al., 2005; Sukanya et al., 2006; Xie et al., 2004; Okabe and Oya, 2000; Hakansson et al., 1993; Uçar et al., 2007). The equatorial N(1) atom (phen) is almost directly opposite the equatorial N(3) atom (dipico) as the  $\text{N}(1)\text{-Co}(1)\text{-N}(3)$  bond angle is  $171^\circ$ . The bite angle of the phen ligand in complex **5** ( $78.50^\circ$ ) and **7** ( $77.03^\circ$ ) are smaller than those observed for the phen ligands in the less distorted octahedral complexes (Ng et al., 2009; Jhong et al., 2007; Li et al., 2007; Hadadzadeh et al., 2010; Wang et al., 2000). The chelated phen ligand can be considered to be rotated about its N(1)-ligating atom such that its other nitrogen-ligating atom (N(2)) latches onto the Zn(1) atom of the Zn(1)-dipico moiety from above, and the phen plane is

perpendicular to the O(1)-O(3)-N(3) plane of the dipico ligand. Interestingly, the coordinated water (O5W or O1W) are opposite to N(2), but the O(5)-Co(1)-N(2) and N(2)-Zn(1)-O1w bond deviates greatly from linearity ( $167^\circ$  and  $161^\circ$ ) in complexes **5** and **7** respectively.

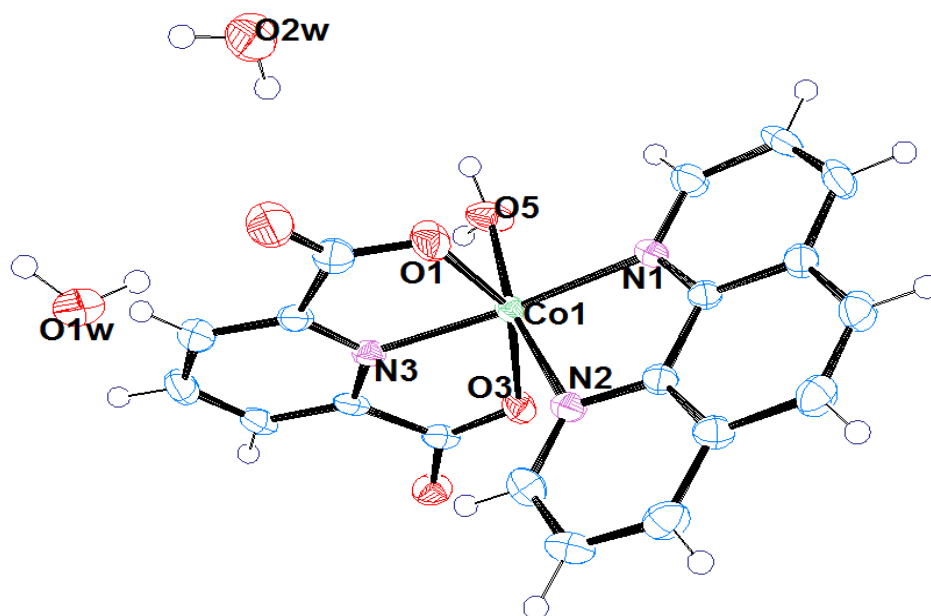


**Figure 4.1:** An ORTEP structure of  $[\text{Co}(\text{phen})(\text{dipico})(\text{H}_2\text{O})].2\text{H}_2\text{O}$ , **5** with ellipsoid at 50%.

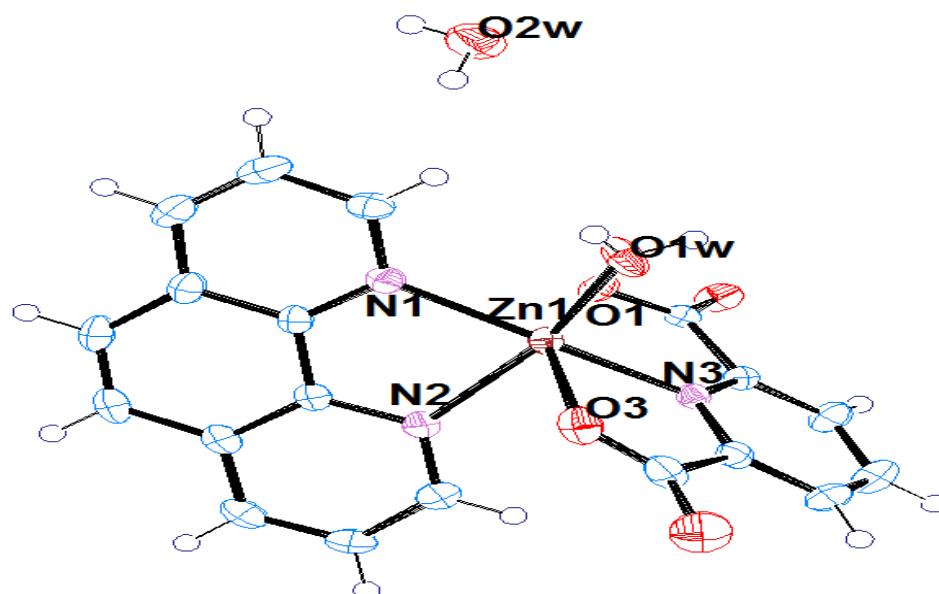


**Figure 4.2:** An ORTEP structure of  $[\text{Zn}(\text{phen})(\text{dipico})(\text{H}_2\text{O})].\text{H}_2\text{O}$ , **7** with ellipsoids at 50%.

The crystal structure of  $[\text{Cu}_2(\text{phen})_3(\text{dipico})(\text{H}_2\text{O})][\text{Cu}(\text{dipico})_2] \cdot [(\text{11H}_2\text{O})(\text{CH}_3\text{OH})]$  **6** is shown in **Figure 4.3**. The crystal quality is not good but it managed to provide some important information about the chemical structure and the coordination geometry of the complex. The crystal structure suggested that the isolated copper complex can be formulated as  $[\text{Cu}_2(\text{phen})_3(\text{dipico})(\text{H}_2\text{O})][\text{Cu}(\text{dipico})_2] \cdot [(\text{11H}_2\text{O})(\text{CH}_3\text{OH})]$  and that it is a trinuclear ionic compound, consisting of  $[\text{Cu}_2(\text{phen})_3(\text{dipico})(\text{H}_2\text{O})]^{2+}$  cation and  $[\text{Cu}(\text{dipico})_2]^{2-}$  anion. In the dicopper(II) cation  $[\text{Cu}_2(\text{phen})_3(\text{dipico})(\text{H}_2\text{O})]^{2+}$ , the dipicolinate ligand is coordinated to the Cu(1) center *via* O and N atoms and the other carboxylate oxygen atom bridges the Cu(1) and Cu(2) atoms. A phen ligand along with an aqua ligand are coordinated to the Cu(1), resulting in the formation of a distorted square pyramidal environment about Cu(1). Similarly, the Cu(2) center adopts a distorted square pyramidal. The Cu(2) ion of the dinuclear cation is bridged by one of the carboxylate oxygen atoms of dipicolinate ligand to Cu(1) and it has two phen ligands attached through nitrogen donors. The copper center of the counter anion,  $[\text{Cu}(\text{dipico})_2]^{2-}$ , has a distorted octahedral environment resulting from the coordination of two dipicolinate ligands.

The Cu – N<sub>phen</sub> bond lengths (1.995 - 2.193 Å) in complex **6** are similar to those reported for other Cu-phen complexes (García-Raso et al., 2003; Zhou et al., 2011). Cu(1) - O1W bond length (2.009 Å) is shorter than those observed for complexes **5** [Co(1) – O5W (2.099 Å)] and **7** [Zn(1) – O1W

(2.0478 Å)]. Both Cu(3) - N<sub>dipico</sub> bond lengths of [Cu(dipico)<sub>2</sub>]<sup>2-</sup> are shorter than Cu(1) - N<sub>dipico</sub> of [Cu<sub>2</sub>(phen)<sub>3</sub>(dipico)(H<sub>2</sub>O)]<sup>2+</sup>, Co(1) - N<sub>dipico</sub> and Zn(1) - N<sub>dipico</sub>. The Cu(2) - O(1) bond lengths (2.007 Å) of bridged carboxylate O atom of dipicolinate is shorter than all M - O<sub>dipico</sub> (M = Co, Cu and Zn) bond lengths (2.007 - 2.2617 Å). All M - O<sub>dipico</sub> bond lengths except for Cu(2) - O(1) bond length are similar to those reported metal(II)-dipico complexes (Harrison et al., 2006; Hakansson et al., 1993; Ma et al., 2002; Hadadzadeh et al., 2010; Bulut et al., 2009). Like those M - N<sub>dipico</sub> and M - N<sub>phen</sub> bond lengths for Co(II) and Zn(II) complexes, Cu - N<sub>dipico</sub> bond are shorter than Cu - N<sub>phen</sub> bond lengths, indicates that N<sub>dipico</sub> is a stronger donor, since the two carboxylate groups in ortho positions enhance the electron density (basicity) on this N-atom (Uçar et al., 2007; Ma et al., 2002; Bulut et al., 2009).

The bite angles for the dipico ligands in complex **6** (N(7)-Cu(1)-O(3) = 77.6°; N(8)-Cu(3)-O(5) = 78.4°; N(8)-Cu(3)-O(7) = 77.1°; N(9)-Cu(3)-O(9) = 77.7 °; N(9)-Cu(3)-O(11) = 78.6°) are similar to those reported for dipicolinate-metal complexes (Gonzalez-Baró et al., 2005; Sukanya et al., 2006; Xie et al., 2004; Okabe and Oya, 2000; Hakansson et al., 1993; Uçar et al., 2007). The N(6) atom (phen) is almost directly opposite N(4) atom (phen) as N(6)-Cu(2)-N(4) bond angle is 175°. Also, the N(8) atom (dipico) and N(9) atom (dipico) is almost directly opposite to each other as N(8)-Cu(3)-N(9) bond angle is 175°. The bite angle of the phen ligand in complex **6** (79.4 - 82.0°) are slightly bigger than those observed for the phen ligands in complexes **5** and **7**, but is consistent to those reported distorted octahedral

complexes (Ng et al., 2009; Jhong et al., 2007; Li et al., 2007; Hadadzadeh et al., 2010; Wang et al., 2000). Interestingly, the bridging carboxylate O atom is opposite to N(5) atom of phen, but the N(5)-Cu(2)-O(1) bond deviate greatly from linearity ( $158^\circ$ ) in complex **6**.

The centroid-centroid distance of the two phen ligands that coordinated to Cu(1) and Cu(2) in the cation  $[\text{Cu}_2(\text{phen})_3(\text{dipico})(\text{H}_2\text{O})]^{2+}$  is 3.799 Å. Also, the centroid-centroid distance between both phen ligands of adjacent  $[\text{Cu}_2(\text{phen})_3(\text{dipico})(\text{H}_2\text{O})]^{2+}$  cations is 3.480 Å. Besides, the centroid-centroid distance between the phen ligand of  $[\text{Cu}_2(\text{phen})_3(\text{dipico})(\text{H}_2\text{O})]^{2+}$  cation and dipicolinate ligand of the  $[\text{Cu}(\text{dipico})_2]^{2-}$  anion is 3.635 Å. All the mentioned centroid-centroid distance are consistent to reported values (3.3 - 3.8 Å) (He et al., 2012; Chen et al., 2012; Castiñeiras et al., 2002; Lin et al., 2009; Janiak, 2000). These centroid-centroid distances suggest presence of intermolecular  $\pi$ - $\pi$  stacking interaction between the aromatic phen rings and pyridine rings of dipicolinate (**Figure 4.4**). (Zhang et al., 2004; Yodoshi et al., 2007; Jia et al., 2010; Bodoki et al., 2009; Paulovicova et al., 2001). The hydrogen bonding is not indicated due to the H atoms of the water and methanol molecules are not located. Overall, the crystal structure of complex **6** is stabilized by electrostatic interactions and the  $\pi$ - $\pi$  stacking interaction between the aromatic rings of phen ligands and pyridine rings of dipicolinate ligands.

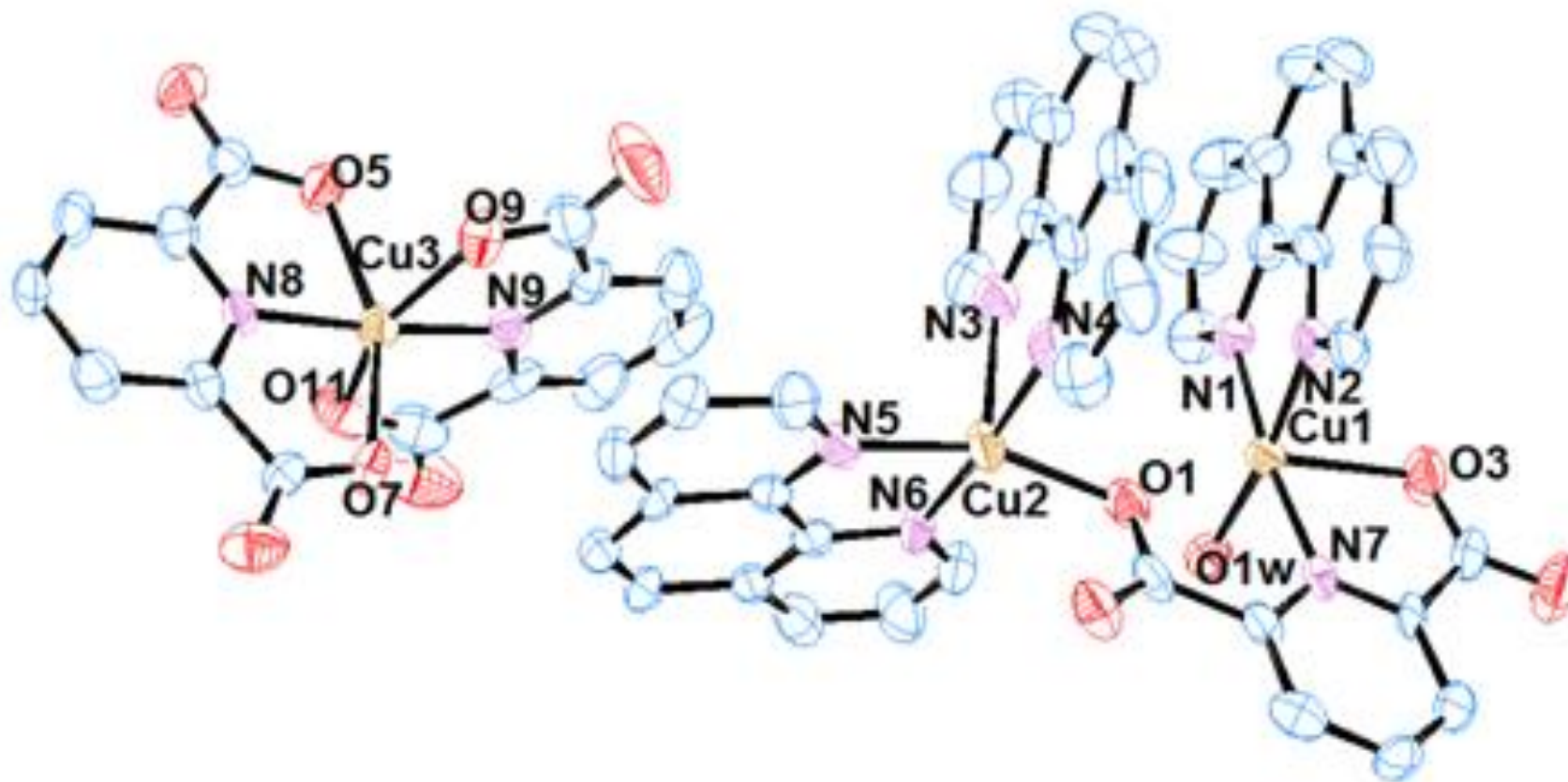


**Figure 4.3:** ORTEP structure of  $[\text{Cu}_2(\text{phen})_3(\text{dipico})(\text{H}_2\text{O})][\text{Cu}(\text{dipico})_2] \cdot [(11\text{H}_2\text{O})(\text{CH}_3\text{OH})]$  **6**, with ellipsoid at 50 %

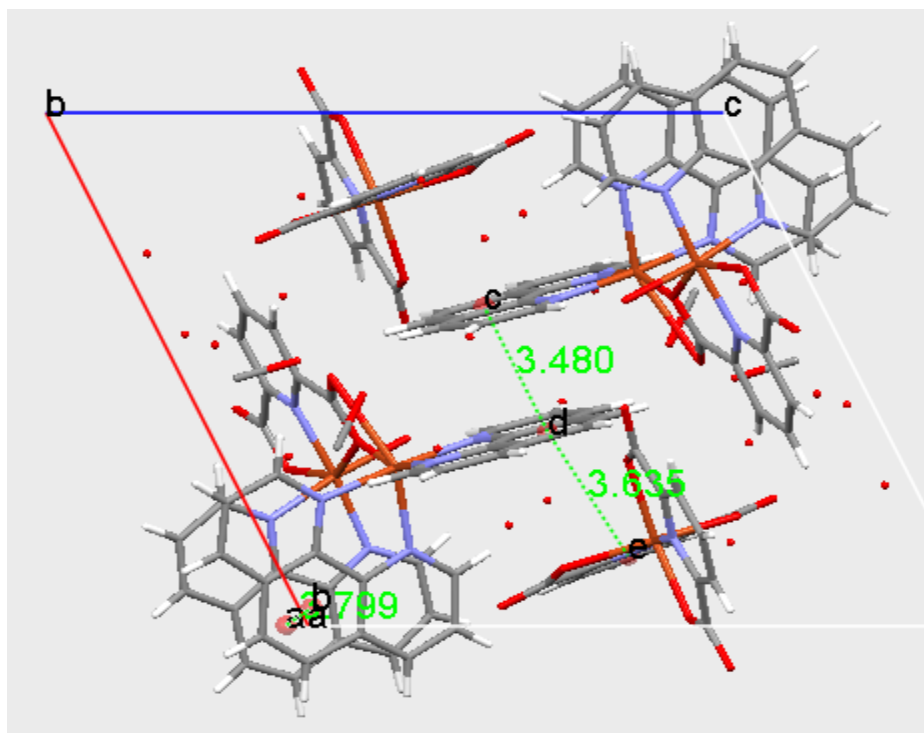


**Figure 4.4:** Packing diagram of complex **6** viewing along *b* axis

**Table 4.4:** Selected bond lengths (Å) for metal(II) complexes **5 - 7**

Bond lengths (Å)		5	6	7		
M-dipico	Co(1) – O(1)	2.140(3)	Cu(1) - O(3)	2.238 (8)	Zn(1) – O(1)	2.2617(15)
	Co(1) – O(3)	2.154(3)	Cu(1) - N(7)	2.013 (8)	Zn(1) – O(3)	2.1943(16)
	Co(1) – N(3)	2.047(3)	Cu(2) - O(1)	2.007 (7)	Zn(1) – N(3)	2.0547(17)
			Cu(3) - O(5)	2.178 (7)		
			Cu(3) - N(8)	1.929 (8)		
			Cu(3) - O(7)	2.202 (7)		
			Cu(3) - O(9)	2.225 (8)		
			Cu(3) - N(9)	1.914 (9)		
			Cu(3) - O(11)	2.167 (9)		
M-H <sub>2</sub> O	Co(1) – O5W	2.099(3)	Cu(1) - O1W	2.009 (7)	Zn(1) – O1W	2.0478(18)
M-phen	Co(1) – N(1)	2.104(3)	Cu(1) - N(1)	2.004 (8)	Zn(1) – N(1)	2.1142(18)
	Co(1) – N(2)	2.130(3)	Cu(1) - N(2)	2.027 (9)	Zn(1) – N(2)	2.2028(18)
			Cu(2) - N(3)	2.193 (9)		
			Cu(2) - N(4)	1.999 (10)		
			Cu(2) - N(5)	2.027 (9)		
			Cu(2) - N(6)	1.995 (9)		

**Table 4.5:** Selected bond angles ( $^{\circ}$ ) for metal(II) complexes **5 - 7**

5		6		7	
N(3)-Co(1)-O(5)	91.20(11)	N(1)-Cu(1)-O1W	93.5(3)	O(1W)-Zn(1)-N(3)	100.12(7)
N(3)-Co(1)-N(1)	171.20(11)	N(1)-Cu(1)-N(7)	173.0(3)	O(1W)-Zn(1)-N(1)	92.24(8)
O(5)-Co(1)-N(1)	90.67(11)	O1W-Cu(1)-N(7)	90.0(3)	N(3)-Zn(1)-N(1)	157.61(7)
N(3)-Co(1)-N(2)	100.47(11)	N(1)-Cu(1)-N(2)	81.6(3)	O(1W)-Zn(1)-O(3)	88.76(8)
O(5)-Co(1)-N(2)	167.46(11)	O1W-Cu(1)-N(2)	172.6(3)	N(3)-Zn(1)-O(3)	76.37(6)
N(1)-Co(1)-N(2)	78.50(11)	N(7)-Cu(1)-N(2)	95.4(3)	N(1)-Zn(1)-O(3)	122.86(6)
N(3)-Co(1)-O(1)	75.97(11)	N(1)-Cu(1)-O(3)	96.1(3)	O(1W)-Zn(1)-N(2)	161.04(7)
O(5)-Co(1)-O(1)	98.59(12)	O1W-Cu(1)-O(3)	94.2(3)	N(3)-Zn(1)-N(2)	95.32(7)
N(1)-Co(1)-O(1)	95.25(11)	N(7)-Cu(1)-O(3)	77.6(3)	N(1)-Zn(1)-N(2)	77.03(7)
N(2)-Co(1)-O(1)	88.77(11)	N(2)-Cu(1)-O(3)	91.8(3)	O(3)-Zn(1)-N(2)	84.22(6)
N(3)-Co(1)-O(3)	75.92(10)	N(1)-Cu(1)-O(1)	112.7(3)	O(1W)-Zn(1)-O(1)	94.00(7)
O(5)-Co(1)-O(3)	88.96(11)	O1W-Cu(1)-O(1)	87.5(3)	N(3)-Zn(1)-O(1)	73.98(6)
N(1)-Co(1)-O(3)	112.72(10)	N(7)-Cu(1)-O(1)	73.4(3)	N(1)-Zn(1)-O(1)	86.68(6)
N(2)-Co(1)-O(3)	89.43(11)	N(2)-Cu(1)-O(1)	89.3(3)		
		O(3)-Cu(1)-O(1)	151.0(3)		
		N(6)-Cu(2)-N(4)	175.4(4)		
		N(6)-Cu(2)-O(1)	92.7(3)		
		N(4)-Cu(2)-O(1)	91.0(3)		
		N(6)-Cu(2)-N(5)	82.0(4)		
		N(4)-Cu(2)-N(5)	95.5(4)		
		O(1)-Cu(2)-N(5)	158.0(3)		
		N(6)-Cu(2)-N(3)	97.3(4)		
		N(4)-Cu(2)-N(3)	79.4(4)		
		O(1)-Cu(2)-N(3)	97.8(3)		
		N(5)-Cu(2)-N(3)	104.0(3)		
		N(9)-Cu(3)-N(8)	175.0(3)		
		N(9)-Cu(3)-O(11)	78.6(4)		
		N(8)-Cu(3)-O(11)	101.5(3)		
		N(9)-Cu(3)-O(5)	96.7(3)		
		N(8)-Cu(3)-O(5)	78.4(3)		
		O(11)-Cu(3)-O(5)	89.7(3)		
		N(9)-Cu(3)-O(7)	107.9(3)		
		N(8)-Cu(3)-O(7)	77.1(3)		
		O(11)-Cu(3)-O(7)	95.5(3)		
		O(5)-Cu(3)-O(7)	155.4(3)		
		N(9)-Cu(3)-O(9)	77.7(3)		
		N(8)-Cu(3)-O(9)	102.2(3)		
		O(11)-Cu(3)-O(9)	156.2(3)		
		O(5)-Cu(3)-O(9)	93.0(3)		
		O(7)-Cu(3)-O(9)	91.7(3)		

### 4.3.3 Characterization of aqueous solutions of complexes

The aqueous solutions of complexes **5** - **7** were characterized by molar conductivity, UV-visible and fluorescence studies. To investigate the species in solution, the molar conductivities of metal(II) chloride, ligands, complexes **5** - **7** were determined for time points of up to 24 hours (**Figure 4.5**). Conductivity measurement is useful for studying the stability of the metal complexes in solution and analysing the species in solution. The metal complexes **5** - **7**, metal(II) chlorides and ligands were dissolved in a 1:1 (v/v) water-methanol mixture and their conductivities were measured at 25 °C. The molar conductivity of CoCl<sub>2</sub>, CuCl<sub>2</sub> and ZnCl<sub>2</sub> were about 118, 119 and 112 Ω<sup>-1</sup> cm<sup>2</sup> mol<sup>-1</sup>, respectively. These values remained unchanged up to 24 hours. Molar conductivity of the metal(II) chloride, CoCl<sub>2</sub>, CuCl<sub>2</sub> and ZnCl<sub>2</sub> are similar to the known 1:2 electrolytes, [Zn(L)(phen)<sub>2</sub>]Cl<sub>2</sub> and [ZnL(bpy)<sub>2</sub>]Cl<sub>2</sub> (Nakabayashi et al., 2006; Snow and Sheardy, 2001; Gallori et al., 2000).

Recently, Sharma and co-workers (2011) reported that the range of the molar conductivity value for non-electrolyte is within 8 to 14 Ω<sup>-1</sup> cm<sup>2</sup> mol<sup>-1</sup> in water-methanol (1:1 v/v). The low molar conductivity values of freshly prepared solvent mixture (0.52 Ω<sup>-1</sup> cm<sup>2</sup> mol<sup>-1</sup>), free phen ligand (2.98 Ω<sup>-1</sup> cm<sup>2</sup> mol<sup>-1</sup>), **5** (9.45 Ω<sup>-1</sup> cm<sup>2</sup> mol<sup>-1</sup>) and **7** (13.86 Ω<sup>-1</sup> cm<sup>2</sup> mol<sup>-1</sup>) indicate the non-electrolyte nature of the solvent, phen and the complexes **5** and **7** (Papadopoulos et al., 2007). This suggests complexes **5** and **7** exist as neutral complex species in aqueous solution and dissolving them did not lead to any

dissociation of coordinated ligand. The molar conductivity of complex **6** ( $44 \Omega^{-1} \text{ cm}^2 \text{ mol}^{-1}$ ) is near to those 1:1 electrolyte ( $37 - 43 \Omega^{-1} \text{ cm}^2 \text{ mol}^{-1}$ ) compounds reported by Arjmand et al. (2010). The molar conductivity of complex **6** is much lower than theoretical values of 1:1 electrolyte ( $75 - 95 \Omega^{-1} \text{ cm}^2 \text{ mol}^{-1}$ ) (Geary, 1971). This might be due to low mobility of bulky cations,  $[\text{Cu}_2(\text{phen})_3(\text{dipico})(\text{H}_2\text{O})]^{2+}$  and anions  $[\text{Cu}(\text{dipico})_2]^{2-}$  of an ionic metal complex in the solution (Golchoubian and Fazilati, 2012; Apelblat, 2011). The insignificant increase in the conductivity value of every sample over the time might be due to the changes in the ion mobility. This phenomenon might have caused by the evaporation of the volatile methanol in the mixture solutions with time, as reported by Bald and co-workers in 2007. Over 24 hours, the molar conductivity of complexes **5 - 7** did not change significantly, suggesting no dissociation of the neutral species of complexes **5** and **7**, and no dissociation of the ionic species of complex **6**. Hence, it is concluded that dipicolinate complexes **5 - 7** are stable in solution. Dipicolinate complexes **5** and **7**, in aqueous solutions, could have existed as  $[\text{Co}(\text{phen})(\text{dipico})(\text{H}_2\text{O})]$  and  $[\text{Zn}(\text{phen})(\text{dipico})(\text{H}_2\text{O})]$  species respectively. Complex **6** could have exists as individual cation  $[\text{Cu}_2(\text{phen})_3(\text{dipico})(\text{H}_2\text{O})]^{2+}$  and anion  $[\text{Cu}(\text{dipico})_2]^{2-}$ .

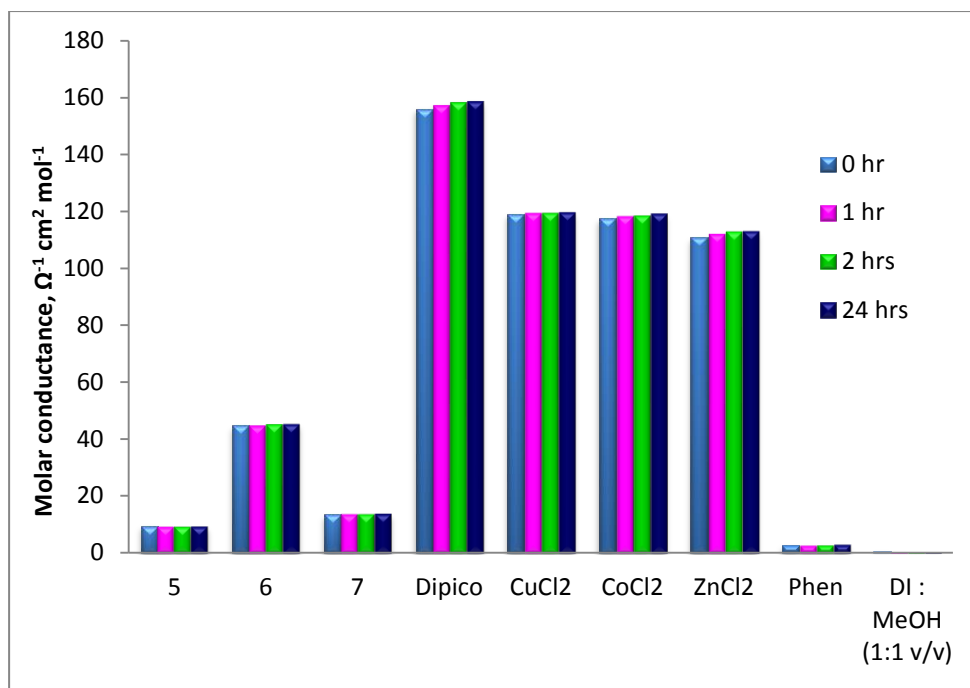


**Figure 4.5:** Molar conductivity of 1 mM of metal(II) complexes **5 - 7**, metal(II) chloride, phen and dipicolinate ligand in deionised water-methanol (1:1 v/v) at 25 °C.

The UV-visible spectra of the complexes and the pure ligands were recorded in deionised water-methanol (1:1 v/v) solutions. The peak assignments of these spectra of complexes **5 - 7** along with the molar extinction coefficients ( $\epsilon$  value) are tabulated in **Table 4.6. Appendix 4.2 - 4.4** are the UV spectra of the complexes **5 - 7**. A d-d band was observed at 729 nm for complex **6** (**Appendix 4.5**). The coordination of phen and dipicolinate ligands to Cu(II) ion causes a blue shift of the d-d band position with respect to that in the CuCl<sub>2</sub> solution (831 nm) (Ng et al., 2006). No visible absorption spectra were observed for complexes **5** and **7**. In this case, d-d transitions are forbidden by the Laporte rule.

The spectrum of pure phen ligand gave two dominant bands at 229 nm and 265 nm. Two intense bands at 228 nm ( $\epsilon = 53130$ ) and 271 nm ( $\epsilon = 43660$ ) were observed in the UV spectrum of complex **5**. Two intense bands at 222 nm ( $\epsilon = 12530$ ) and 272 nm ( $\epsilon = 10560$ ) were also observed in the UV spectrum of complex **6**. Similarly, two peaks were observed in the UV spectrum of complex **7** at 227 nm ( $\epsilon = 48500$ ) and 272 nm ( $\epsilon = 39500$ ). By comparing with the spectra of the corresponding dipicolinic acid and phen ligands (**Appendix 4.6**) for the position of the  $\lambda_{\text{max}}$  and intensity of the absorbance, it can be concluded that both intense peaks at  $\sim 227$  nm and  $\sim 272$  nm can be ascribed to the coordinated phen ligand. Bonghaei et al. (2007) and Bencini et al. (2010) have reported the two intense peaks observed in the UV region of the electronic spectra for phen containing complexes aroused from intra ligand  $\pi \rightarrow \pi^*$  transition. The observations matched well with the results for the phenanthroline complexes in Chapter 3, section 3.3.3.

Regression lines and correlation coefficient ( $R^2$ ) values for each plot are drawn as described in Chapter 3, section 3.3.3. The correlation coefficient ( $R^2$ ) values for all the plotted graphs obtained for complexes **5 - 7** are very close to 1.0000, showing that the data obtained fit in the regression line and obeyed the Beer-Lambert Law. The average molar absorptivity values of complexes **5 - 7** were obtained by using the Beer-Lambert Law and the general linear equation.

**Table 4.6:** Absorption spectral data of metal(II) complexes, **5 - 7**

Complex	$\lambda_{\max}$ (nm), $\epsilon$ ( $\text{mol}^{-1}\text{dm}^3 \text{cm}^{-1}$ )	Assignment
<b>5</b>	228 ( $\epsilon = 53\ 130$ )	$\pi \rightarrow \pi^*(\text{phen})$
	271 ( $\epsilon = 43\ 660$ )	$\pi \rightarrow \pi^*(\text{phen})$
<b>6</b>	222 ( $\epsilon = 12530$ )	$\pi \rightarrow \pi^*(\text{phen})$
	272 ( $\epsilon = 10560$ )	$\pi \rightarrow \pi^*(\text{phen})$
	729	d-d
<b>7</b>	227 ( $\epsilon = 48\ 500$ )	$\pi \rightarrow \pi^*(\text{phen})$
	272 ( $\epsilon = 39\ 500$ )	$\pi \rightarrow \pi^*(\text{phen})$
phen	229	$\pi \rightarrow \pi^*$
	265	$\pi \rightarrow \pi^*$

The FL emission spectra for complexes **5**,  $[\text{Co}(\text{phen})(\text{dipico})(\text{H}_2\text{O})] \cdot 2\text{H}_2\text{O}$ , **6** and  $[\text{Cu}_2(\text{phen})_3(\text{dipico})(\text{H}_2\text{O})][\text{Cu}(\text{dipico})_2] \cdot [(11\text{H}_2\text{O})(\text{CH}_3\text{OH})]$  and **7**  $[\text{Zn}(\text{phen})(\text{dipico})(\text{H}_2\text{O})] \cdot \text{H}_2\text{O}$  are shown in **Figure 4.6**. All three complexes **5 - 7** can emit fluorescence in deionised water-methanol (1:1 v/v) solution. Complexes **5 - 7** gave two bands with the  $\lambda_{\max}$  values in the range of 364 - 366 nm and at 377 nm. By comparing with FL spectra of free phen and dipico ligands in the same solvent mixture, it is concluded that both peaks arise from coordinated phen as dipicolinate ligand has no FL emission. The FL emission spectrum of complex **5** (**Figure 4.6; spectra III**) showed that Co(II) partially quenched the highly emissive free phen ligand. Similarly, Cu(II) quenched the highly emissive free phen ligand too as shown in spectrum of complex **6** (**Figure 4.6; spectra IV**). Seng and co-workers (2008) have described this quenching mechanism as static quenching.

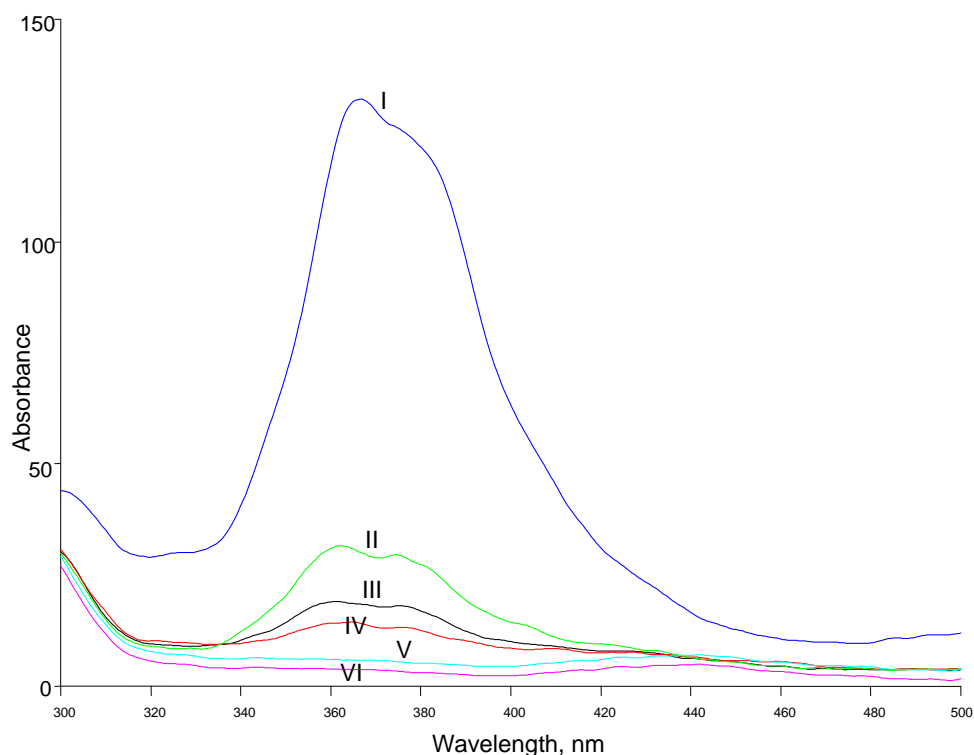


**Figure 4.6:** Fluorescence spectra of **7** (I), phen (II), **5** (III), **6** (IV), dipico (V) and solvent mixture (VI) at 0.1  $\mu\text{M}$ .

Seng et al., (2008) found that the amount of quenching of the coordinated phen is influenced by the type of transition metal(II) ion in the octahedral  $[\text{M}(\text{phen})(\text{edda})]$  complexes. Diamagnetic Zn(II) enhances the FL of the coordinated phen while paramagnetic Co(II) and Cu(II) partially quenches the highly emissive free phen ligand. Higher FL emission observed for Zn(II) complex (compared to the Co(II) and Cu(II) complexes) has been attributed to the full  $d^{10}$  electron configuration of the Zn(II) ion (Hu *et al.*, 2010). In a previous study on the fluorescence of solid samples of a series  $\text{ZnX}_2(\text{phen})$  complexes ( $\text{X} = \text{Cl}, \text{Br}, \text{I}$ ), the type of halide was found to affect the FL emission intensity and the order was found to be  $\text{ZnCl}_2(\text{phen}) < \text{phen} < \text{ZnBr}_2(\text{phen}) < \text{ZnI}_2(\text{phen})$  (Ikeda et al., 1996). The FL emission enhancement

was explained by the dependence of intersystem crossing rate on the halide, and the mechanism involved a Heitler-London type mixing between the phen locally excited and the  $\rho$  (halogen)  $\rightarrow$   $\delta^*$  (phen) ligand-to-ligand charge-transfer (LLCT) electronic configurations and 1,3(n,  $\delta^*$ ) energy level change due to the coordination. Analysis of the data in **Figure 4.6** shows that a change of the type of metal(II) ion influences the FL emission intensity but not the  $\lambda_{\text{max}}$  and shape of the FL emission bands. The order of complexes in terms of increasing FL intensity is **6** < **5** < phen < **7**.

#### 4.4 CONCLUSION

Reactions between phen, dipicolinate and metal(II) chloride (metal(II) = Co(II), Cu(II) or Zn(II)) yielded metal complexes [Co(phen)(dipico)(H<sub>2</sub>O)]·2H<sub>2</sub>O **5**, [Cu<sub>2</sub>(phen)<sub>3</sub>(dipico)(H<sub>2</sub>O)][Cu(dipico)<sub>2</sub>].[(11H<sub>2</sub>O)(CH<sub>3</sub>OH)] **6** and [Zn(phen)(dipico)(H<sub>2</sub>O)]·H<sub>2</sub>O **7**. The chemical structures and chemical formulae have been established by Fourier Transform infrared spectroscopy (FTIR), CHN elemental analysis and X-ray crystallography. It can be concluded from the above discussion that complexes **5** and **6** exist as non-electrolyte in aqueous solution. The neutral complexes **5** and **6** exists as [Co(phen)(dipico)(H<sub>2</sub>O)] and [Zn(phen)(dipico)(H<sub>2</sub>O)] species in aqueous solution. The molar conductivity measurements suggest that complexes **5** and **7** seem to be stable within the duration of conductivity measurement. Complex **6** is a 1:1 electrolyte. The lower molar conductivity of complex **6** might be due

to low mobility of bulky cation and anion of the complexes in the solution. UV absorption peaks observed in the electronic spectra of the complexes could arise from the  $\pi \rightarrow \pi^*$  transition of the coordinated phenanthroline ligand. However, no visible absorption peaks was found in the electronic spectra obtained for complexes **5** and **7**. Zn(II) enhances the FL of the coordinated phen while Co(II) and Cu(II) partially quenches the FL of the coordinated phen. The order of compounds in terms of increasing FL intensity is **6** < **5** < phen < **7**.

## CHAPTER 5

### SYNTHESIS AND CHARACTERIZATION OF METAL(II)

1,10-PHENANTHROLINE COMPLEXES WITH *N,O*- THREONINE,

$[M(\text{phen})(\text{AA})(\text{H}_2\text{O})\text{Cl}] \cdot 2\text{H}_2\text{O}$  (M(II) = Cu, Zn; AA = L-thr, D-thr)

**CHAPTER 5**  
**SYNTHESIS AND CHARACTERIZATION OF METAL(II)**  
**1,10-PHENANTHROLINE COMPLEXES WITH *N,O*- THREONINE,**  
**[M(phen)(AA)(H<sub>2</sub>O)Cl]·2H<sub>2</sub>O (M(II) = Cu, Zn; AA = L-thr, D-thr)**

**5.1 INTRODUCTION**

Previous chapters investigated ternary metal(II) polypyridyl complexes with *OO'*-maltolate (chapter 3) or *ONO'*-dipicolinate (chapter 4) as coligand in the solid (FTIR, elemental CHN and X-ray crystallography) state and in the aqueous solution form (UV-visible, molar conductivity and fluorescence). In this chapter, another set of similar metal(II) complexes was constructed by retaining the main ligand 1,10-phenanthroline, by choosing two types of metal(II), and changing the coligand to threonine. Here, L-threonine (L-thr) and D-threonine (D-thr) were used. Thus, two pairs of enantiomeric ternary metal(II) complexes were prepared and their general formula is [M(phen)(AA)(H<sub>2</sub>O)Cl]·2H<sub>2</sub>O (M(II) = Cu, Zn; AA = L-thr, D-thr). Both coordinated L-threoninate and D-threoninate have H-donor and H-acceptor sites and are optically active. Many optically-active transition metal complexes have been synthesized and studied (Bryan and Dabrowiak, 1975; Douglas and Saito, 1980; Brunner et al., 2000). Enantiomers of chiral metal complexes have attracted considerable attention as potential structural probes of DNA conformation (Nakabayashi et al., 2004; Chetana et al., 2009; Zhang et al., 2009; Jin and Ranford, 2000; Rao et al., 2007). Chiral octahedral metal

complexes involving delta ( $\Delta$ ) and lamda ( $\Lambda$ ) enantiomers have been extensively investigated (Svensson et al., 2011; Hall et al., 2011). However, less research on the L- and D- chiral metal complexes has been carried out (Arjmand et al., 2010). As was done for the previous two series of metal(II) complexes, this chapter also investigated the effect of changing the type of metal(II) ion and chiral coligand of  $[M(\text{phen})(\text{AA})(\text{H}_2\text{O})\text{Cl}]\cdot 2\text{H}_2\text{O}$  complexes ( $M(\text{II}) = \text{Cu}, \text{Zn}$ ;  $\text{AA} = \text{L-thr}, \text{D-thr}$ ) on their structures, thermal stability and solution properties (UV-Visible, molar conductivity and fluorescence).

## **5.2 EXPERIMENTAL**

### **5.2.1 Materials and Reagents**

1,10-phenanthroline monohydrate (99%), L-threonine (98 %), D-threonine (98 %), Copper(II) chloride dihydrate were purchased from Acros Organic. Zinc(II) chloride puriss was purchased from Riedel-de Haen. Methanol and ammonia were of analytical grade and were used as purchased. Deionised water was used as solvent.

### **5.2.2 Preparation of $[M(\text{phen})(\text{AA})(\text{H}_2\text{O})\text{Cl}]\cdot 2\text{H}_2\text{O}$ ( $M(\text{II}) = \text{Cu}, \text{Zn}$ ; $\text{AA} = \text{L-thr}, \text{D-thr}$ ) **8 - 11****

In the preparation of  $[\text{Cu}(\text{phen})(\text{L-thr})(\text{H}_2\text{O})\text{Cl}]\cdot 2\text{H}_2\text{O}$  **8**, copper(II) chloride (0.17 g, 1 mmol) in deionised water (10 mL) and L-threonine (0.12 g, 1 mmol) in 1.0 M  $\text{NH}_3$  solution (20 mL) were mixed and stirred continuously

at room temperature for 10 minutes. This was followed by addition of a methanolic solution (5 mL) of phenanthroline (0.18 g, 1 mmol) to the above mixture. The resultant mixture was heated until the volume of the solution reached approximately 5 mL. The solution was then allowed to stand overnight. The solid product formed was collected on the following day by suction filtration and washed with cold deionised water. The complex, **8**, was obtained as blue crystals (0.40 g, 85 %). The  $[\text{Cu}(\text{phen})(\text{D-thr})(\text{H}_2\text{O})\text{Cl}]\cdot 2\text{H}_2\text{O}$  **9**, was similarly prepared. In the preparation of complex **9**, the L-threonine solution was replaced by D-threonine solution. The D-threonine solution was prepared by dissolving D-threonine (0.12 g, 1 mmol) in 1.0 M  $\text{NH}_3$  solution (20 mL). On standing, blue crystals formed in the reaction mixture. The crystals were filtered and washed with cold deionised water (0.38 g, 82 %). The zinc(II) analogues, *viz.*  $[\text{Zn}(\text{phen})(\text{L-thr})(\text{H}_2\text{O})\text{Cl}]\cdot 2\text{H}_2\text{O}$  **10** and  $[\text{Zn}(\text{phen})(\text{D-thr})(\text{H}_2\text{O})\text{Cl}]\cdot 2\text{H}_2\text{O}$  **11**, were similarly prepared. The copper(II) chloride solutions were replaced by zinc(II) chloride solutions. The colourless crystals of **10** and **11** formed in their respective reaction mixtures on standing overnight. These crystals were filtered and washed with cold deionised water (Complex **10**: 0.35 g, 80 %; complex **11**: 0.36 g, 82 %).

### 5.2.3 Characterization of solids complexes

Elemental analyses (C, H, and N) and FTIR spectral of the complexes were similarly carried out as described in chapter 3.2.3. In this chapter, thermogravimetric analyses of the complexes were performed with a Mettler

Toledo TGA/DTG 851<sup>o</sup> instrument as described in Chapter 3 (Section 3.2.3) with a slight change in program setting. The samples were heated in the range of 25 - 800 °C and the heating rate was 15 °C/min. The nitrogen gas (N<sub>2</sub>) flow rate was set at 20 mL/min.

#### 5.2.4 Determination of crystal structure

Crystal structures of complexes **8**, **10** and **11** were solved by Prof. Ng Seik Weng from University of Malaya (UM), Malaysia. Crystal data of complexes **8**, **10** and **11** were collected on a Bruker SMART APEX-II CCD area-detector using Mo K $\alpha$  radiation ( $\lambda = 0.71073 \text{ \AA}$ ), using  $\omega$ -scan mode. The SMART and SAINT softwares (2000) were used for data acquisition, cell refinement and data reduction. SADABS (Sheldrick 2001) was used for empirical absorption correction. The structures were solved by direct methods and refined by full-matrix, least-squares method using the SHELXS-97 program (Sheldrick 1997).

Crystal structure of complex **9** was solved by Assoc. Prof. Leong Weng Kee from Nanyang Technological University (NTU), Singapore. Crystal data of complex **9** was collected at 103 K on a Bruker APEX-II CCD area-detector using Mo K $\alpha$  radiation ( $\lambda = 0.71073 \text{ \AA}$ ), over the range  $2.57^\circ < \theta < 36.48^\circ$ . Bruker APEX2 and SAINT softwares (2007) were used for data collection, refinement and reduction. Absorption corrections were made using SADABS

(Sheldrick 1997). Bruker SHELXTL (2000) was used for space group determination, structure refinement, graphics and structure reporting. Crystal parameters, data collection details and results of the refinements are summarized in **Table 5.1**.

### **5.2.5 Characterization of aqueous solutions of complexes**

The preparation of the water-methanolic (1:1 v/v) solutions of metal(II) complexes (**8 - 11**) and procedures for the conductivity measurement, ESI-MS, UV-visible and fluorescence study were the same as those in Chapter 3 Section 3.2.5. Circular dichroism (CD) study of the chirality of metal complexes was carried out with a 1.0 mm quartz cell using a Jasco J-810 spectropolarimeter. Solutions of copper complex ( $2.5 \times 10^{-4}$  M) and zinc complex (1.0 mM) were prepared by using deionised water.

**Table 5.1:** Crystal data and structure refinement for metal(II) complexes, 7 - 10

	8	9	10	11
Empirical formula	CuC <sub>16</sub> H <sub>22</sub> N <sub>3</sub> O <sub>6</sub> Cl	CuC <sub>16</sub> H <sub>22</sub> N <sub>3</sub> O <sub>6</sub> Cl	ZnC <sub>16</sub> H <sub>22</sub> N <sub>3</sub> O <sub>6</sub> Cl	ZnC <sub>16</sub> H <sub>22</sub> N <sub>3</sub> O <sub>6</sub> Cl
Formula weight	451.36	451.36	453.19	453.19
Temperature (°C)	25	- 170	20	20
Crystal system and Space group	Monoclinic, P2(1)	Monoclinic, P2(1)	Monoclinic, P2(1)	Monoclinic, P2(1)
Unit cell dimensions (Å)	a = 7.0809(13) b = 10.3455(18) c = 12.564(2)	a = 6.9777(2); b = 10.2734(4); c = 12.5168(4)	a = 6.9963(7) b = 10.3330(10) c = 12.7290(12)	a = 7.0809(13) b = 10.3455(18) c = 12.564(2)
Volume (Å <sup>3</sup> )	915.2	893.47	914.9(15)	937.3(3)
Z	2	2	2	2
Density (calculated) (Mg/m <sup>3</sup> )	1.638	1.678	1.645	1.606
Absorption coefficient (mm <sup>-1</sup> )	1.379	1.412	1.528	1.491
F(000) (mm)	466	466	468	468
Crystal size (mm)	0.49 x 0.16 x 0.09	0.40 x 0.36 x 0.32	0.35 x 0.25 x 0.15	0.25 x 0.10 x 0.05
θ range for data collection (°)	1.60 – 25.50	2.57 – 36.48	1.61 – 27.49	1.60 – 25.00
Index ranges	-7 ≤ h ≤ 8 -12 ≤ k ≤ 12 -15 ≤ l ≤ 15	-11 ≤ h ≤ 11; -17 ≤ k ≤ 17; 0 ≤ l ≤ 20	-9 ≤ h ≤ 9 -13 ≤ k ≤ 13 -15 ≤ l ≤ 16	-8 ≤ h ≤ 8 -12 ≤ k ≤ 12 -15 ≤ l ≤ 15
Reflections collected	5526	19941	8550	7316
Independent reflections	3238	8146	4058	3250
Data/restraints/parameters	3238/10/280	8146/1/263	4058/10/272	3250/10/264
Goodness-of-fit on F <sup>2</sup>	1.030	1.049	1.075	1.007
Final R indices [I > 2(σ)]	R = 0.031; wR = 0.071	R = 0.0274; wR = 0.0640	R = 0.0523; wR = 0.1491	R = 0.0579; wR = 0.1348
R indices (all data)	R = 0.033; wR = 0.072	R = 0.0309; wR = 0.0640	R = 0.0585; wR = 0.1530	R = 0.0811; wR = 0.1476
Largest dif. Peak and hole (e Å <sup>-3</sup> )	0.29, -0.27	0.387, - 0.787	1.535, -0.741	0.994, -0.694

## 5.3 RESULT AND DISCUSSION

### 5.3.1 Characterization of solids complexes

A series of threoninate complexes were prepared with heterocyclic phen ligand and two chosen late transition metal ( $\text{Cu}^{2+}$  and  $\text{Zn}^{2+}$ ).  $[\text{M}(\text{phen})(\text{AA})(\text{H}_2\text{O})\text{Cl}]\cdot 2\text{H}_2\text{O}$  complexes were prepared by modifying previously published methods (Abdel-Rahman et al., 1996; Zhang et al., 2004; Rizzi et al., 2000; Yodoshi et al., 2007). AA represents amino acid used, L-threonine or D-threonine. Blue crystals were obtained for both Cu(II) complexes,  $[\text{Cu}(\text{phen})(\text{L-thr})(\text{H}_2\text{O})\text{Cl}]\cdot 2\text{H}_2\text{O}$  **8** (yield, ~85 %) and  $[\text{Cu}(\text{phen})(\text{D-thr})(\text{H}_2\text{O})\text{Cl}]\cdot 2\text{H}_2\text{O}$  **9** (yield, ~82 %). For  $[\text{Zn}(\text{phen})(\text{L-thr})(\text{H}_2\text{O})\text{Cl}]\cdot 2\text{H}_2\text{O}$  **10** (yield, ~80 %) and  $[\text{Zn}(\text{phen})(\text{D-thr})(\text{H}_2\text{O})\text{Cl}]\cdot 2\text{H}_2\text{O}$  **11** (yield, ~82 %), white crystals were obtained. Based on microanalysis results, the complexes can be formulated as  $[\text{Cu}(\text{phen})(\text{L-thr})(\text{H}_2\text{O})\text{Cl}]\cdot 2\text{H}_2\text{O}$  **8**,  $[\text{Cu}(\text{phen})(\text{D-thr})(\text{H}_2\text{O})\text{Cl}]\cdot 2\text{H}_2\text{O}$  **9**,  $[\text{Zn}(\text{phen})(\text{L-thr})(\text{H}_2\text{O})\text{Cl}]\cdot 2\text{H}_2\text{O}$  **10** and  $[\text{Zn}(\text{phen})(\text{D-thr})(\text{H}_2\text{O})\text{Cl}]\cdot 2\text{H}_2\text{O}$  **11**. These and other physicochemical data are listed in **Table 5.2**.

**Table 5.2:** Physical and chemical data of metal(II) complexes, **8 - 11**

Complex	<b>8</b>	<b>9</b>	<b>10</b>	<b>11</b>	
Molecular formulae	$[\text{Cu}(\text{C}_4\text{H}_8\text{NO}_3)(\text{C}_{12}\text{H}_8\text{N}_2)(\text{H}_2\text{O})\text{Cl}]\cdot 2\text{H}_2\text{O}$	$[\text{Cu}(\text{C}_4\text{H}_8\text{NO}_3)(\text{C}_{12}\text{H}_8\text{N}_2)(\text{H}_2\text{O})\text{Cl}]\cdot 2\text{H}_2\text{O}$	$[\text{Zn}(\text{C}_4\text{H}_8\text{NO}_3)(\text{C}_{12}\text{H}_8\text{N}_2)(\text{H}_2\text{O})\text{Cl}]\cdot 2\text{H}_2\text{O}$	$[\text{Zn}(\text{C}_4\text{H}_8\text{NO}_3)(\text{C}_{12}\text{H}_8\text{N}_2)(\text{H}_2\text{O})\text{Cl}]\cdot 2\text{H}_2\text{O}$	
Molecular weight (g/mol)	451.36	451.36	453.19	453.19	
% yield	~ 85 %	~ 82 %	~ 80 %	~ 82 %	
Colour	Blue crystals	Blue crystals	White crystals	White crystals	
CHN elemental analysis, % Calculated (Found)	C	42.58 (42.26)	42.58 (42.21)	42.40 (42.50)	42.40 (42.70)
	H	4.91 (4.61)	4.91 (4.38)	4.89 (4.71)	4.89 (4.70)
	N	9.31 (9.31)	9.31 (9.18)	9.27 (9.64)	9.27 (9.73)

The vibration peaks observed at 3421 (complexes **8 - 9**) and 3391  $\text{cm}^{-1}$  (complexes **10 - 11**) suggested the presence of coordinated water or lattice water molecule(s) (Abdel-Rahman et al., 1996). All the four complexes exhibit two bands, one in the range of 1615 - 1623  $\text{cm}^{-1}$  and another at about 1395  $\text{cm}^{-1}$ , which are characteristic for  $\nu_{\text{asy}}(\text{COO}^-)$  and  $\nu_{\text{sym}}(\text{COO}^-)$  of the  $\text{COO}^-$  group present in amino acid. The free amino acid  $\nu_{\text{asy}}(\text{COO}^-)$  is observed at frequency 1630  $\text{cm}^{-1}$  (**Appendix 5.1**) while the corresponding  $\nu_{\text{asy}}(\text{COO}^-)$  stretching vibrations of the four complexes were shifted to lower frequencies suggesting the terminal coordination mode of carboxylate group of threonine to the copper/zinc ion (Yang et al., 2003). The difference between  $\nu_{\text{asy}}(\text{COO}^-)$  and  $\nu_{\text{sym}}(\text{COO}^-)$  stretching frequencies ( $\Delta\nu$ ) value was used to determine the nature of binding of carboxylate to metal ion. The  $\Delta\nu$  values of all four complexes are more than 200  $\text{cm}^{-1}$ , which clearly indicate unidentate binding of carboxylate group to metal ion (Abdel-Rahman et al., 1996; Jin and Ranford, 2000; Zhang et al., 2004; Jia et al., 2010; Arjmand et al., 2010). The free amino acid  $\nu(\text{C-N})$  stretching is at approximately 1184  $\text{cm}^{-1}$  and this band shifted to lower frequency at 1165  $\text{cm}^{-1}$  for its complex, suggesting coordination of the amino nitrogen atom. In other words, FTIR analyses suggest the bidentate coordination of amino acid ligand to metal through  $\text{COO}^-$  and  $\text{-NH}_2$  groups (Nakamoto et al., 1978; Abdel-Rahman et al., 1996; Versiane et al., 2006).

Also, the  $\nu(\text{C=N})$  and  $\nu(\text{C=C})$  stretching frequencies of free phen ligand are observed at 1505 and 1422  $\text{cm}^{-1}$  (**Appendix 3.2**). In the infrared

spectra of complexes **8** - **11**, the  $\nu(\text{C}=\text{N})$  stretching band shifted to a higher frequencies at  $1524\text{ cm}^{-1}$  (complexes **8** and **9**) and  $1520\text{ cm}^{-1}$  (complexes **10** and **11**). The  $\nu(\text{C}=\text{C})$  stretching peaks are also observed at a higher frequencies compared to those of free phen ligand, at  $1434$  and  $1590\text{ cm}^{-1}$  in both Cu(II) complexes **8** and **9**. In Zn(II) complexes (**10** and **11**), the  $\nu(\text{C}=\text{C})$  stretching peaks are observed at  $1432$  and  $1583\text{ cm}^{-1}$ . Both  $\nu(\text{C}=\text{N})$  and  $\nu(\text{C}=\text{C})$  stretching shifted to a higher frequency upon complexation (Jin and Ranford 2000; Zhang et al., 2004). The literature value of  $\nu(\text{M}-\text{N})$ ,  $\nu(\text{M}-\text{O})$  and  $\nu(\text{M}-\text{Cl})$  stretching frequencies are found below  $400\text{ cm}^{-1}$ . These peaks are beyond the detection of the FTIR spectrophotometer used (Nakamoto 1977; Reddy et al., 2006). In conclusion, FTIR spectral analysis of complexes **8** - **11** (**Appendix 5.2**) shows that both phen and threoninate ligands are coordinated to the metal (Cu(II) and Zn(II)) centres respectively.

**Table 5.3:** Characteristic Infrared band assignments of metal(II) complexes, **8** - **11**

Bond	8	9	10	11	Remarks
$\nu(\text{O}-\text{H})$	3421(b)	3421(b)	3391(b)	3391(b)	water
$\nu(\text{C}-\text{H})$	3048(w)	3048(w)	3054(w)	3054(w)	Phen
$\nu(\text{C}-\text{C})$	1590(sh) 1434(m)	1590(sh) 1434(m)	1583(sh) 1432(m)	1583(sh) 1433(m)	
$\nu(\text{C}=\text{N})$	1524(m)	1524(m)	1520(m)	1520(m)	
$\nu(\text{C}-\text{H})$ Out-of-plane	725(s), 738(w), 790(w), 851(s), 900(m)	725(s), 738(w), 790(w), 851(s), 900(m)	729(s), 787(w), 851(s), 898(m)	729(s), 788(w), 851(s), 898(m)	
$\nu(\text{COO}^-)_{\text{as}}$	1623(s)	1623(s)	1616(s)	1615(s)	
$\nu(\text{COO}^-)_{\text{sv}}$	1395(s)	1395(s)	1395(s)	1395(s)	
$\nu(\text{N}-\text{H})$	3313(b)	3313(b)	3329(b)	3329(b)	
$\nu(\text{C}-\text{H})$	2973(w)	2973(w)	2976(m) 2990(w)	2976(m) 2990(w)	
(C-H)bend	1458(m)	1458(m)	1452(m)	1453(m)	
(C-H)rock	1347(m)	1347(m)	1351(m)	1351(m)	
$\nu(\text{C}-\text{N})$	1165(m)	1165(m)	1154(m)	1154(m)	
$\nu(\text{C}-\text{C}) + \nu(\text{C}-\text{O})$	872(w)	872(w)	866(w)	867(w)	
$\rho(\text{CH}_3) + \rho(\text{NH}_2)$	1308(w), 936(w), 972(w)	1307(w) 971(w)	1311(w) 966(w)	1311(w) 966(w)	
$\rho(\text{C}=\text{O})$	648(w)	648(w)	643(w)	643(w)	
$\delta(\text{NH}_2)_{\text{wagg}} + \nu(\text{C}-\text{N})$	1052(m)	1052(m)	1047(m)	1047(m)	
$\delta(\text{NH}_2)_{\text{wagg}}$	807(m)	807(m)	802(w)	802(w)	

Elemental analysis of complexes **8** and **9** allows their formulation as  $[\text{Cu}(\text{phen})(\text{L-thr})(\text{H}_2\text{O})\text{Cl}]\cdot 2\text{H}_2\text{O}$  and  $[\text{Cu}(\text{phen})(\text{D-thr})(\text{H}_2\text{O})\text{Cl}]\cdot 2\text{H}_2\text{O}$ . The TG-DTG curves (**Appendices 5.3 - 5.4**) of the pair of enantiomeric Cu(II) complexes **8** and **9** have five decomposition peaks (**Table 5.4**). In the DTG curves for complexes **8** and **9**, it can be seen that all five decomposition steps are endothermic processes. The loss of two water molecules (Calc.: 8.0 %; Found: 7.9 % (**8**); 7.8 % (**9**)) for both Cu(II) complexes occurred in the first step of decomposition at around 100 °C, suggesting that they are lattice water molecules. In the second decomposition step, loss of another water molecule (Calc.: 4.0 %; Found: 3.9 % (**8**); 3.3 % (**9**)) for both Cu(II) complexes at above 100 °C suggests coordinated water molecule. This means that both complexes **8** and **9** have two lattice water molecules and one coordinated water molecule (*i.e.* aqua ligand). A weight loss of 7.8 % (complex **8**) and 7.3 % (complex **9**) (Calc.: 7.9 %) were observed at around 168 °C. These can be assigned to the removal of one chloro ligand from each of the complexes. The high decomposition temperature suggests that the chloro ligand is coordinated into the Cu(II) center as reported elsewhere (Fouad et al., 2010; Mishra et al., 2012). The above analyses of thermal data are consistent with the earlier CHN analytical data (**Table 5.2**), infrared spectroscopic analyses (**Table 5.3**) and X-ray data (**Table 5.5**) which show the presence of coordinated chloride, one coordinated water molecule and two lattice water molecules. The last two decomposition steps could not be interpreted.

The TGA curves of Zn(II) complexes **10** and **11** also showed five steps of decomposition in the range of 25 – 800 °C. In the first decomposition step, a peak (Calc.: 7.9 %, Found: 7.6 % (**10**); 6.7 % (**11**)) was observed at around 60 °C, which corresponds to the loss of two water molecules. The expulsion of water molecules at low temperature seems to suggest that they are lattice water molecules and not coordinated water molecules. The second weight loss was observed at *ca.* 90 °C. This involved a weight loss of 4.0 % and 3.8 % (Calc.: 4.0 %) which can be ascribed to loss of one water molecule for complexes **10** and **11** respectively. Because of the higher decomposition temperature, this water molecule could be the aqua ligand, *i.e.* coordinated water. Both dehydration process, *i.e.* first and second decomposition steps, in Zn(II) complexes, are endothermic reactions as shown in DTG curve (**Appendices 5.5 - 5.6**). The third decomposition step at ~204 °C for both Zn(II) complexes can be interpreted as removal of chloro ligand as the weight loss of 6.0 % (**10**) and 4.1 % (**11**) approximately matched the theoretical loss of a chloride (Calc.: 7.8 %). This thermal data matched well with the CHN analytical data, X-ray data and infrared result. In the final decomposition stage, a broad curve and large weight loss was observed for both Zn(II) complexes. This decomposition step could have involved more than one chemical processes. As a result, it is difficult to correlate these steps accurately with proper decomposition products. All four TGA curves for Cu(II) and Zn(II) complexes show that they underwent similar dissociation processes at the first three stages. Firstly, dehydration of two lattice water molecules followed by removal of one aqua molecule from the metal(II) complexes. Decomposition process continue with the removal of chloro ligand from both Cu(II) and Zn(II) complexes.

**Table 5.4:** TGA data<sup>a</sup> for metal(II) complexes, **8 - 11**.

Molecular formulae	Decomposition range (°C)	Wt. % loss Calc. (Found)	Assignment (Removal)
[Cu(C <sub>12</sub> H <sub>8</sub> N <sub>2</sub> )(C <sub>4</sub> H <sub>8</sub> NO <sub>3</sub> )(H <sub>2</sub> O)Cl]·2H <sub>2</sub> O <b>(8)</b>	28 - 98 (48) <sup>b</sup>	8.0 (7.9)	2 mole of lattice water
	105 - 144 (134) <sup>b</sup>	4.0 (3.9)	1 mole of coordinated water molecule
	164 - 178 (169) <sup>b</sup>	7.9 (7.8)	1 mole of Cl <sup>-</sup>
[Cu(C <sub>12</sub> H <sub>8</sub> N <sub>2</sub> )(C <sub>4</sub> H <sub>8</sub> NO <sub>3</sub> )(H <sub>2</sub> O)Cl]·2H <sub>2</sub> O <b>(9)</b>	29 - 115 (44) <sup>b</sup>	8.0 (7.8)	2 mole of lattice water
	115 - 147 (129) <sup>b</sup>	4.0 (3.3)	1 mole of coordinated water molecule
	147 - 180 (167) <sup>b</sup>	7.9 (7.3)	1 mole of Cl <sup>-</sup>
[Zn(C <sub>12</sub> H <sub>8</sub> N <sub>2</sub> )(C <sub>4</sub> H <sub>8</sub> NO <sub>3</sub> )(H <sub>2</sub> O)Cl]·2H <sub>2</sub> O <b>(10)</b>	39 - 79 (60) <sup>b</sup>	7.9 (7.6)	2 mole of lattice water
	79 - 132 (91) <sup>b</sup>	4.0 (4.0)	1 mole of coordinated water molecule
	132 - 232 (204) <sup>b</sup>	7.8 (6.0)	1 mole of Cl <sup>-</sup>
[Zn(C <sub>12</sub> H <sub>8</sub> N <sub>2</sub> )(C <sub>4</sub> H <sub>8</sub> NO <sub>3</sub> )(H <sub>2</sub> O)Cl]·2H <sub>2</sub> O <b>(11)</b>	26 - 72 (60) <sup>b</sup>	7.9 (6.7)	2 mole of lattice water
	73 - 99 (88) <sup>b</sup>	4.0 (3.8)	1 mole of coordinated water molecule
	99 - 225 (204) <sup>b</sup>	7.8 (4.1)	1 mole of Cl <sup>-</sup>

<sup>a</sup> Only the first three decomposition steps was tabulated in the table due to its importance to determine the properties of water molecules and chloride atom.

<sup>b</sup> Value in the brackets refers to the inflection points of each decomposition stage.

### 5.3.2 Analysis of crystal structures

The crystal structures of Cu(II) complexes (**8** and **9**) and Zn(II) complexes (**10** and **11**) are shown in **Figure 5.1** and **Figure 5.2** and these structures are similar. Each of these structures depicts a neutral compound which can be formulated as [M(phen)(AA)(H<sub>2</sub>O)Cl] and two lattice water molecules. Thus, all of them can be formulated as [M(phen)(AA)(H<sub>2</sub>O)Cl]·2H<sub>2</sub>O (M is Cu(II) or Zn(II); AA is L-thr or D-thr).

The central M(II) ion is six-coordinated and has a distorted octahedral geometry. The phen ligand behaves as a *N,N*-bidentate ligand. Phen ligand coordinated to the metal centre *via* its two nitrogen atoms. The threoninate ligand behave as a *N,O*-bidentate ligand. The threoninate ligand is coordinated *via* its amino nitrogen atom and carboxylate oxygen atom. Both threoninate and phen ligands coordinated to the metal centre at the equatorial positions. The fifth and sixth vacant coordination sites at the axial positions are filled by one aqua ligand and one coordinated chloride ion, Cl(1). Selected bond lengths and angles are listed in **Table 5.5**.

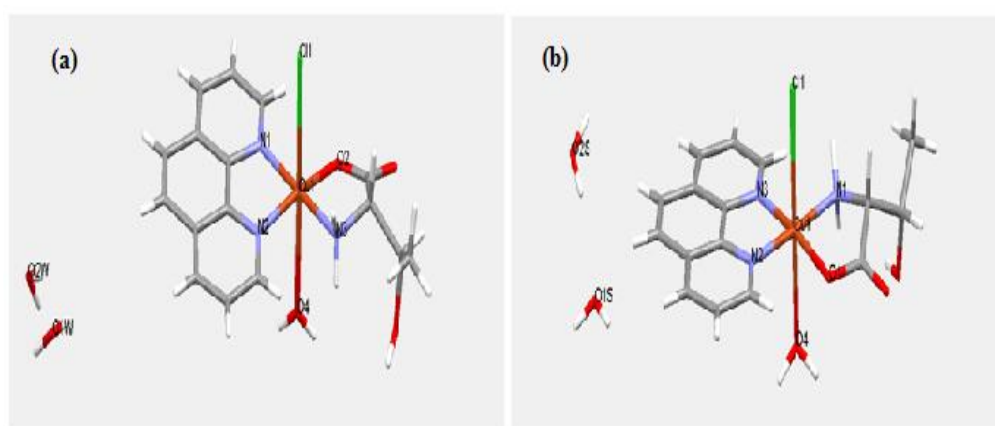


**Figure 5.1:** Crystal structure of (a)  $[\text{Cu}(\text{phen})(\text{L-thr})(\text{H}_2\text{O})\text{Cl}] \cdot 2\text{H}_2\text{O}$  **8**; (b)  $[\text{Cu}(\text{phen})(\text{D-thr})(\text{H}_2\text{O})\text{Cl}] \cdot 2\text{H}_2\text{O}$  **9**

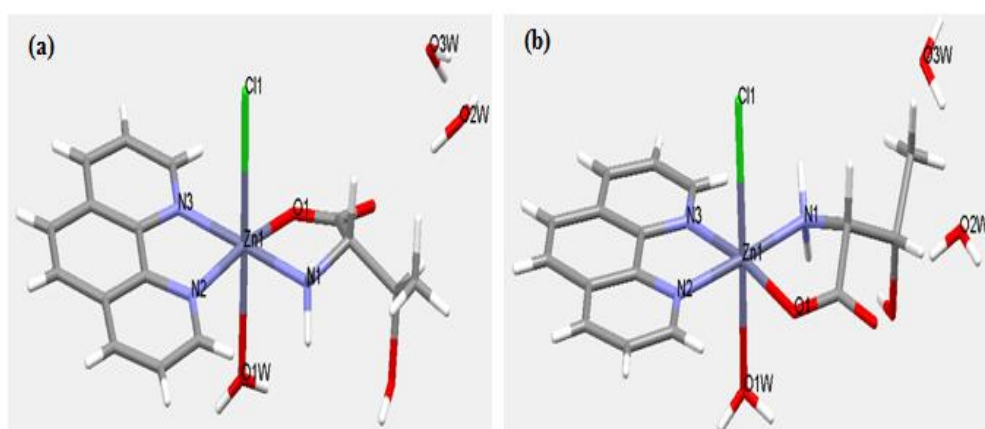


**Figure 5.2:** Crystal structure of (a)  $[\text{Zn}(\text{phen})(\text{L-thr})(\text{H}_2\text{O})\text{Cl}] \cdot 2\text{H}_2\text{O}$  **10**; (b)  $[\text{Zn}(\text{phen})(\text{D-thr})(\text{H}_2\text{O})\text{Cl}] \cdot 2\text{H}_2\text{O}$  **11**

The equatorial Cu(1)-O(2) and Cu(1)-N(3) bond lengths are 1.969(2) Å, 1.990(3) Å in complex **8** and the Cu(1)-O(1) and Cu(1)-N(1) bond lengths are 1.9742(10) Å, 1.9959(12) Å in complex **9**. The bond lengths of threoninate to the metal centre are similar to those found in other copper-amino acid complexes such as [Cu(phen)(L-thr)(H<sub>2</sub>O)](ClO<sub>4</sub>), [Cu(OH<sub>2</sub>)(phen)(L-phe)]NO<sub>3</sub>·H<sub>2</sub>O, [Cu(L-thr)<sub>2</sub>]·H<sub>2</sub>O, [Cu(phen)(Gly)Cl]<sub>2</sub>·7H<sub>2</sub>O, [Cu(bpy)(L-pro)(H<sub>2</sub>O)]·NO<sub>3</sub> (L-thr = L-threoninate and L-phe = L-phenylalanine; Gly = glycine; bpy = 2,2'-bipyridine) (Abdel-Rahman et al., 1996; Rizzi et al., 2000; Zhang et al., 2004; Rao et al., 2007; Yodoshi et al., 2007). The bond lengths of Zn-O<sub>thr</sub> and Zn-N<sub>thr</sub> are 2.057(4) Å, 2.083(5) Å in complex **10** and 2.118(5) Å and 2.161(6) Å in complex **11**, respectively. The bite angles O<sub>thr</sub> – M(1) – N<sub>thr</sub> for chelated amino acids to the metal centres in complexes **8** - **11** are in the range of 82 - 84°.

Bond lengths of the coordinated phen nitrogen atoms to the Cu(II) and Zn(II) centres are close to the corresponding literature values of Cu(II)-phen and Zn(II)-phen complexes. The bite angle N<sub>phen</sub> – M(1) – N<sub>phen</sub> of both Cu(II) and Zn(II) complexes are in the range of 78 - 82°, which are close to the corresponding values reported for some phenanthroline complexes (Abdel-Rahman et al., 1996; Paulovicova et al., 2001; Zhang et al., 2004; Yodoshi et al., 2007; Jia et al., 2010). On the other hand, the M(1)-Cl(1) distance and M(1)-O<sub>aqua</sub> distance are longer than the corresponding values reported for the known Cu(II) and Zn(II) complexes with aqua and chloro ligands (Su et al., 1993; Abdel-Rahman et al., 1996; Ng et al., 2003; Zhang et al., 2004; Jia et al.,

2010). Thus, the chloro and aqua ligands are probably weakly bounded to the M(II) atom and they may dissociate when dissolved in water.

Basically, each of the threoninate ligand has both H-acceptor and H-donor sites and the lattice water molecules act as H-donor sites. Hydrogen bonding links each  $[M(\text{phen})(\text{AA})(\text{H}_2\text{O})\text{Cl}] \cdot 2\text{H}_2\text{O}$  ( $M = \text{Cu}$  or  $\text{Zn}$ ) molecule with adjacent molecules in the lattice into 3D supramolecular frameworks. Interestingly, both pairs of Cu(II) and Zn(II) enantiomers show a mirror image in the direction of  $a$ -axis (**Figures 5.3 – 5.4**). This suggests that the chirality of complexes **8 - 11** are controlled by the chirality of ligands like those Cu(II) and Cd(II) complexes reported by Li and co-workers (2013).

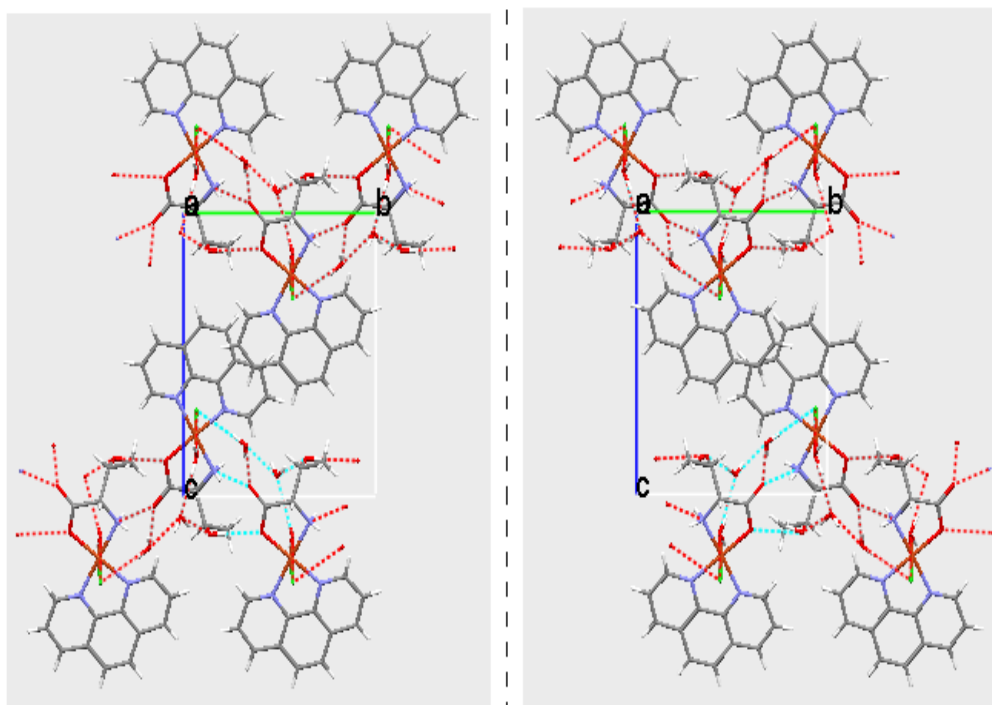


**Figure 5.3:** The molecular packing with hydrogen-bonding of complex **8** (left) and its enantiomer, complex **9** (right) in the direction of  $a$ -axis. The mirror is drawn as a dash line.

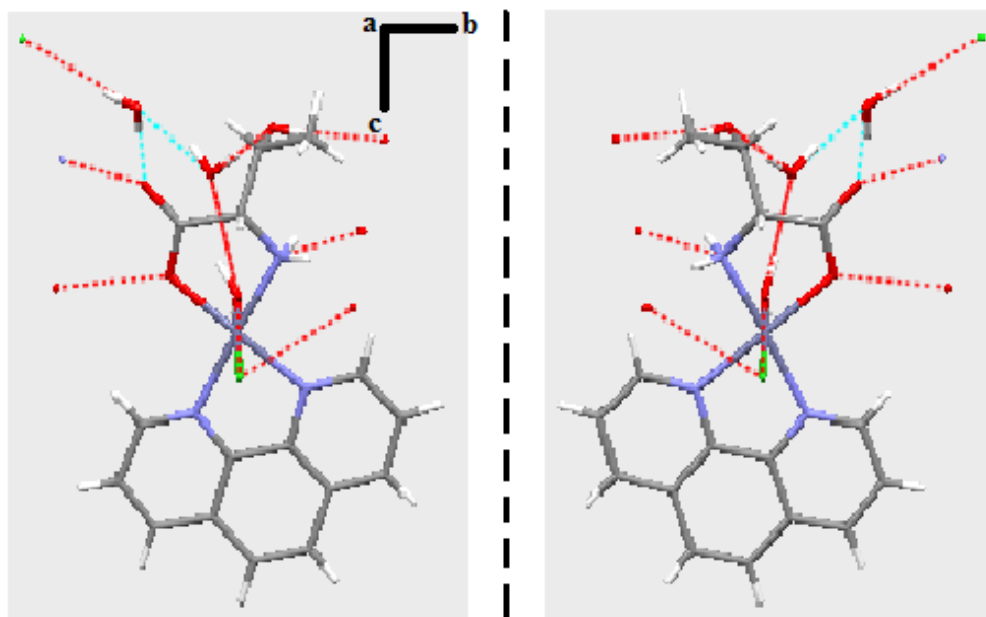


**Figure 5.4:** The molecular structure with hydrogen-bonding of complex **10** (left) and its enantiomer, complex **11** (right) in the direction of *a*-axis. The mirror is drawn as a dash line.

**Table 5.5:** Selected bond lengths, (Å) and bond angles (°) for complexes **8 - 11**.

Bond lengths, (Å)							
8		9		10		11	
Cu(1) - N(1)	2.015(3)	Cu(1) - N(2)	2.0121(12)	Zn(1) - N(1)	2.073(5)	Zn(1) - N(1)	2.078(6)
Cu(1) - N(2)	2.031(3)	Cu(1) - N(3)	2.0296(12)	Zn(1) - N(2)	2.136(5)	Zn(1) - N(2)	2.131(7)
Cu(1) - N(3)	1.990(3)	Cu(1) - N(1)	1.9959(12)	Zn(1) - O(1)	2.057(4)	Zn(1) - O(1)	2.083(5)
Cu(1) - O(2)	1.969(2)	Cu(1) - O(1)	1.9742(10)	Zn(1) - N(3)	2.118(5)	Zn(1) - N(3)	2.161(6)
Cu(1) - O(4)	2.404(3)	Cu(1) - O(4)	2.3465(10)	Zn(1) - O1W	2.201(4)	Zn(1) - O1W	2.222(5)
Cu(1) - Cl(1)	2.780(3)	Cu(1) - Cl(1)	2.772(3)	Zn(1) - Cl(1)	2.5729(13)	Zn(1) - Cl(1)	2.5929(19)
Bond angles, (°)							
8		9		10		11	
O(2) - Cu(1) - N(3)	84.45(11)	O(1) - Cu(1) - N(1)	84.43(5)	O(1) - Zn(1) - N(1)	81.96(18)	O(1) - Zn(1) - N(1)	81.8(2)
O(2) - Cu(1) - N(1)	96.35(9)	O(1) - Cu(1) - N(2)	96.61(12)	O(1) - Zn(1) - N(3)	100.26(16)	O(1) - Zn(1) - N(3)	172.0(2)
O(2) - Cu(1) - N(2)	172.04(10)	O(1) - Cu(1) - N(3)	172.77(4)	O(1) - Zn(1) - N(2)	171.49(17)	O(1) - Zn(1) - N(2)	100.3(2)
O(2) - Cu(1) - O(4)	86.01(11)	O(1) - Cu(1) - O(4)	86.80(4)	O(1) - Zn(1) - O1W	85.59(19)	O(1) - Zn(1) - O1W	86.1(3)
N(3) - Cu(1) - N(1)	178.54(12)	N(1) - Cu(1) - N(2)	177.71(5)	N(1) - Zn(1) - N(3)	177.8(2)	N(1) - Zn(1) - N(3)	99.7(2)
N(3) - Cu(1) - N(2)	97.29(10)	N(1) - Cu(1) - N(3)	97.16(5)	N(1) - Zn(1) - N(2)	99.56(17)	N(1) - Zn(1) - N(2)	177.9(3)
N(3) - Cu(1) - O(4)	88.18(11)	N(2) - Cu(1) - N(3)	82.06(5)	N(3) - Zn(1) - N(2)	78.3(2)	N(3) - Zn(1) - N(2)	78.4(3)
N(1) - Cu(1) - O(4)	93.09(10)	N(1) - Cu(1) - O(4)	88.24(4)	N(1) - Zn(1) - O1W	89.33(18)	N(1) - Zn(1) - O1W	89.7(3)
N(2) - Cu(1) - O(4)	86.28(11)	N(2) - Cu(1) - O(4)	93.85(4)	N(3) - Zn(1) - O1W	91.07(18)	N(3) - Zn(1) - O1W	86.0(3)
N(1) - Cu(1) - N(2)	82.09(12)	N(3) - Cu(1) - O(4)	86.20(4)	N(2) - Zn(1) - O1W	86.06(19)	N(2) - Zn(1) - O1W	90.9(2)

### 5.3.3 Characterization of aqueous solutions of complexes

To study the species of metal(II)-phen-threoninate complexes **8** - **11** respectively in solution, complexes were dissolved in water-methanol (1:1 v/v) mixture and each solution was analysed by using Electrospray Ionisation Mass Spectrometry (ESI-MS). All the metal(II) complexes were studied by ESI-MS in positive ion mode. The mass spectrum of complex **8** shows a base peak at an  $m/z$  value of 360.8 (calc. 361.8, relative abundance: 100 %) could be assigned to  $[\text{}^{63}\text{Cu}(\text{phen})(\text{L-thr})]^+$ . The isotopic peak at  $m/z$  value of 362.8 (calc. 362.9, relative abundance: 42 %) could be assigned to  $[\text{}^{64}\text{Cu}(\text{phen})(\text{L-thr})]^+$ . The mass spectrum of complex **9** shows a base peak at an  $m/z$  value of 360.9 (calc. 361.8, relative abundance: 100 %) and an isotopic peak at  $m/z$  value of 362.9 (calc. 362.8, relative abundance: 46 %). These peaks could be assigned to  $[\text{}^{63}\text{Cu}(\text{phen})(\text{D-thr})]^+$  and  $[\text{}^{64}\text{Cu}(\text{phen})(\text{D-thr})]^+$ , respectively. The high intensity peak at  $m/z$  274 is due to the presence of low amount of impurity in the sample. The same peak ( $m/z$  274) is observed in the ESI mass spectrum of phen ligand.

The base peak observed at  $m/z$  361.7 in the ESI mass spectrum of complex **10** matched well with the calculated mass for  $[\text{}^{67}\text{Zn}(\text{phen})(\text{L-thr})]^+$  (calc.: 363.7, relative abundance: 100 %). The isotopic peaks at  $m/z$  values of 359.7 (calc. 360.9, relative abundance: 9 %), 360.8 (calc. 362.9, relative abundance: 15 %), 363.7 (calc. 364.9, relative abundance: 53 %) and 365.7 (calc. 366.9, relative abundance: 31 %) in the ESI mass spectrum of complex

**10** are assigned to  $[\text{Zn}(\text{phen})(\text{L-threo})]^+$  species with different zinc isotopes ( $^{64}\text{Zn}$ ,  $^{66}\text{Zn}$ ,  $^{68}\text{Zn}$  and  $^{70}\text{Zn}$ ). In the case of complex **11**, peak at  $m/z$  361.8 matched well with the calculated mass for  $[\text{Zn}(\text{phen})(\text{D-thr})]^+$  (calc.: 360.9, relative abundance: 45 %). There are two explanations for the lower relative abundance in  $[\text{Zn}(\text{phen})(\text{D-thr})]^+$ . This phenomenon might be due to the lower concentration used or the high temperature applied to the capillary system. The temperature used (150 °C) to obtain ESI mass spectrum might be too high temperature and lead to degradation or break down of the complexes. The isotopic peaks at  $m/z$  values of 363.7 (calc. 362.9, relative abundance: 21 %), 364.7 (calc. 363.9, relative abundance: 8 %), 365.7 (calc. 364.9, relative abundance: 16 %) and 366.7 (calc. 366.9, relative abundance: 2 %) in the ESI mass spectrum of complex **11** are similarly assigned to  $[\text{Zn}(\text{phen})(\text{L-threo})]^+$  species with different zinc isotopes ( $^{66}\text{Zn}$ ,  $^{67}\text{Zn}$ ,  $^{68}\text{Zn}$  and  $^{70}\text{Zn}$ ).

The messy mass spectra of complexes **10** and **11** might be due to the presence of impurity in the sample. By comparing ESI mass spectra of complexes **10** and **11** with those of phen and threonine ligands, the impurity could be assigned to unreacted phen and threonine. Two similar peaks at  $m/z$  212 and 302 in ESI mass spectra of complexes **10** and **11** were observed at ESI mass spectrum of phen ligand. Other peaks at  $m/z$  289, 482 and 541 were observed at ESI mass spectrum of L-threonine ligand too. All the cationic complex species detected in the ESI mass spectra were formed *via* dissociation of the aqua and the anionic chloride ligands from their respective complexes **8** - **11** (Ng et al., 2006; Arjmand et al., 2010).

**Table 5.6:** ESI-MS data for metal(II) complexes, **8 - 11**

Complex	Fragment	<i>m/z</i> (calculated)	<i>m/z</i> (Found)
<b>8</b>	[ <sup>63</sup> Cu(phen)(L-thr)] <sup>+</sup>	361.8	360.8
	[ <sup>64</sup> Cu(phen)(L-thr)] <sup>+</sup>	362.8	362.9
<b>9</b>	[ <sup>63</sup> Cu(phen)(D-thr)] <sup>+</sup>	361.8	360.9
	[ <sup>64</sup> Cu(phen)(D-thr)] <sup>+</sup>	362.8	362.9
<b>10</b>	[ <sup>64</sup> Zn(phen)(L-thr)] <sup>+</sup>	360.9	359.7
	[ <sup>66</sup> Zn(phen)(L-thr)] <sup>+</sup>	362.9	360.8
	[ <sup>67</sup> Zn(phen)(L-thr)] <sup>+</sup>	363.9	361.7
	[ <sup>68</sup> Zn(phen)(L-thr)] <sup>+</sup>	364.9	363.7
	[ <sup>70</sup> Zn(phen)(L-thr)] <sup>+</sup>	366.9	365.7
<b>11</b>	[ <sup>64</sup> Zn(phen)(D-thr)] <sup>+</sup>	360.9	361.8
	[ <sup>66</sup> Zn(phen)(D-thr)] <sup>+</sup>	362.9	363.7
	[ <sup>67</sup> Zn(phen)(D-thr)] <sup>+</sup>	363.9	364.7
	[ <sup>68</sup> Zn(phen)(D-thr)] <sup>+</sup>	364.9	365.7
	[ <sup>70</sup> Zn(phen)(D-thr)] <sup>+</sup>	366.9	366.7

Conductivity measurement is a useful technique to study the type of species in solution. The molar conductivities of copper(II) chloride, zinc(II) chloride, phen, L-threonine, D-threonine, Cu(II) and Zn(II) complexes were determined for time points of up to 24 hours (**Figure 5.5**). Complexes **8 - 11**, copper(II) chloride, zinc(II) chloride, phen, L-threonine and D-threonine were dissolved in a 1:1 (v/v) water-methanol mixture and their conductivities were measured at 25 °C. The molar conductivity of Cu(II) ( $52 - 53 \Omega^{-1} \text{ cm}^2 \text{ mol}^{-1}$ ) and Zn(II) ( $62 - 65 \Omega^{-1} \text{ cm}^2 \text{ mol}^{-1}$ ) complex solutions remains unchanged from 0 to 24 hours. The CuCl<sub>2</sub> and ZnCl<sub>2</sub> solutions have molar conductivity values of about 119 and 110  $\Omega^{-1} \text{ cm}^2 \text{ mol}^{-1}$  respectively, typical of 2:1 electrolytes. These values remain unchanged up to 24 hours. Metal(II) salts (CuCl<sub>2</sub> and ZnCl<sub>2</sub>) in aqueous solutions exist as M<sup>2+</sup> and Cl<sup>-</sup> ions. Low molar conductivities ( $< 5 \Omega^{-1} \text{ cm}^2 \text{ mol}^{-1}$ ) of respective solutions of the free ligands (phen, L-thr and D-thr) indicate their non-electrolyte in nature. Molar conductivities of complexes **8 - 11** are lower than those reported cationic metal complexes with uncoordinated Cl<sup>-</sup> anion ( $66 - 73 \Omega^{-1} \text{ cm}^2 \text{ mol}^{-1}$ ) ( $[(\text{H}_2\text{L})\text{Co}(\text{phen})]\text{Cl}\cdot 4\text{H}_2\text{O}$ ,  $[(\text{H}_2\text{L})\text{Cu}(\text{ox})]\text{Cl}\cdot 3\text{H}_2\text{O}$ ,  $[(\text{H}_2\text{L})\text{Zn}(\text{ox})]\text{Cl}\cdot 4\text{H}_2\text{O}$  where H<sub>2</sub>L = thiocarbohydrazone; ox = oxalate) (Shebl et al., 2010). From the

results obtained, all metal(II) complexes **8** - **11** are classified as 1:1 electrolytes and probably exist as  $[M(\text{phen})(\text{AA})]^+$  or  $[M(\text{phen})(\text{AA})(\text{H}_2\text{O})]^+$  (where M = Cu or Zn; AA = L-thr or D-thr) and  $\text{Cl}^-$  ions (Jin and Ranford 2000; Ng et al., 2006; Arjmand et al., 2010; Shebl et al., 2010). The conductivity measurements results obtained are consistent with the ESI-MS data obtained earlier.

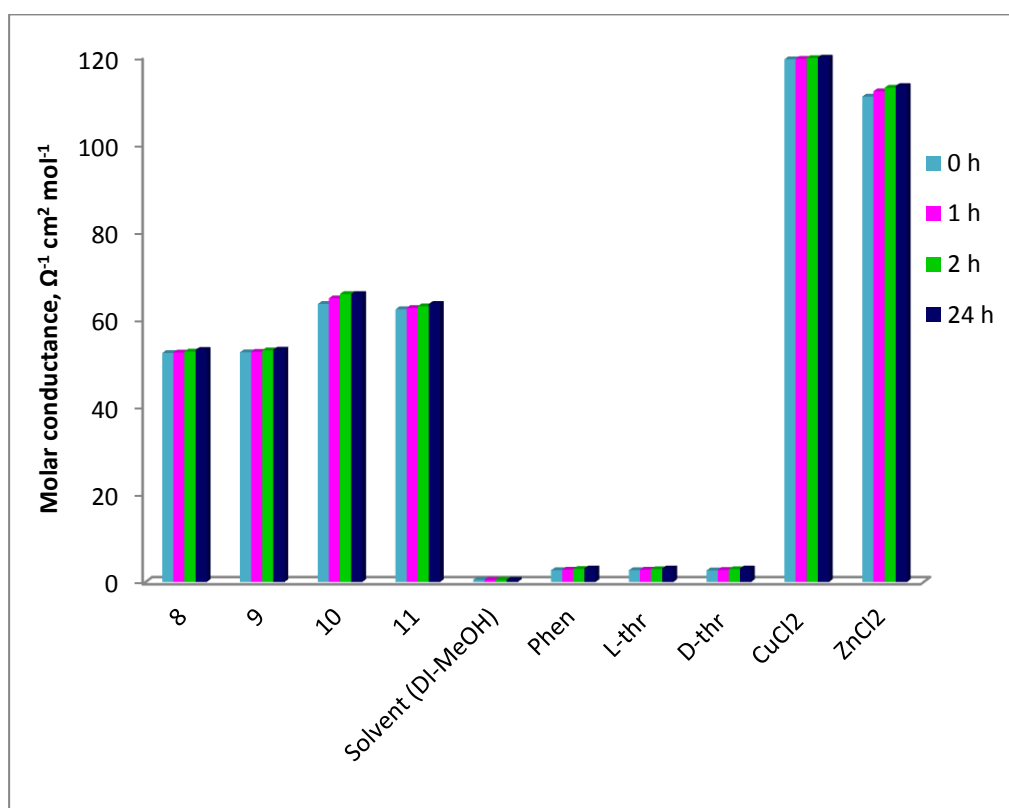


**Figure 5.5:** Molar conductivity of 1 mM of **8** - **11** and other compounds in deionised water-methanol (1:1 v/v) at 25 °C.

Both Cu(II) complexes **8** and **9** in aqueous medium (deionised water: methanol 1:1 v/v) show a broad d-d transition band centred at 611 nm in their respective visible spectra (Paulovicova et al., 2001; Rao et al., 2007; Chetana et al., 2009). The shift of the d-d band position with respect to that in the

CuCl<sub>2</sub> solution (**Appendix 5.11**) is a consequence of the coordination of phen and threonine ligands to Cu(II) ion. As these values are far from that of aqueous CuCl<sub>2</sub> at 831 nm (Ng et al., 2006), it is reasonable to assume that most of the complexes **8** and **9** species are not dissociated in an aqueous medium. The electronic spectra of the complexes **8** and **9** matched well with the previously reported square pyramidal Cu(II) complexes, [Cu(phen)(L-ala)(H<sub>2</sub>O)]NO<sub>3</sub>, [Cu(phen)(L-thr)(H<sub>2</sub>O)]NO<sub>3</sub>·ClO<sub>4</sub> and [Cu(phen)(L-pro)(H<sub>2</sub>O)]NO<sub>3</sub> (L-ala = L-alanine; L-thr = L-threonine; L-pro = L-proline) (Paulovicova et al., 2001; Rao et al., 2007; Chetana et al., 2009). By comparing the  $\lambda_{\text{max}}$  at visible spectra (611 nm) with the literature values (611 - 615 nm), it suggests that Cu(II) complexes, **8** and **9** could adopt a square pyramidal geometry in the solution (Paulovicova et al., 2001; Rao et al., 2007; Chetana et al., 2009). In contrast, the X-ray data show that the metal centre of both copper(II) complexes adopted an octahedral coordination geometry in solid state. The weakly bonded chloro ligand dissociated in aqueous solutions of complexes **8** and **9**, and is likely to be replaced by solvent water molecule.

**Table 5.7:** Electronic absorption and emission data for metal(II) complexes, **8 - 11**.

Complex	$\lambda_{\text{em}}$ (nm)	$\lambda_{\text{abs}}$ (nm), $\epsilon$ (M <sup>-1</sup> cm <sup>-1</sup> )	Assignment
<b>8</b>	361, 377	225 ( $\epsilon = 33840$ ); 273 ( $\epsilon = 32540$ ); 294 ( $\epsilon = 10270$ ) 611	$\pi \rightarrow \pi^*$ (phen) d-d
<b>9</b>	361, 377	225 ( $\epsilon = 36490$ ); 273 ( $\epsilon = 35240$ ); 294 ( $\epsilon = 10940$ ) 611	$\pi \rightarrow \pi^*$ (phen) d-d
<b>10</b>	366, 380	227 ( $\epsilon = 35560$ ); 271 ( $\epsilon = 32550$ ); 292 ( $\epsilon = 10330$ )	$\pi \rightarrow \pi^*$ (phen)
<b>11</b>	366, 380	227 ( $\epsilon = 42530$ ); 271 ( $\epsilon = 38900$ ); 292 ( $\epsilon = 12460$ )	$\pi \rightarrow \pi^*$ (phen)

The UV spectra of complexes **8 - 11** show intense bands at  $\sim 225$  nm,  $\sim 273$  nm and  $\sim 294$  nm (**Table 5.7**) which may be attributed to the second and

higher order internal  $\pi$ - $\pi^*$  transitions of the coordinated phen (Jin et al., 2000). The observations matched well with the results for the known phenanthroline complexes,  $[\text{Cu}(\text{phen})(\text{acac})(\text{NO}_3)] \cdot \text{H}_2\text{O}$ ,  $[\text{Cu}(\text{phen})(\text{L-thr})(\text{H}_2\text{O})]\text{NO}_3 \cdot \text{ClO}_4$ ,  $[\text{Cu}(\text{phen})(\text{L-pro})(\text{H}_2\text{O})]\text{NO}_3$ ,  $[\text{Cu}_2(\text{phen})_2(\text{PDI-Ala})(\text{H}_2\text{O})_2](\text{ClO}_4)_2 \cdot 2\frac{1}{2}\text{H}_2\text{O}$ ,  $[\text{Cu}_4(\text{phen})_6(\text{D,L-PDIAla})(\text{H}_2\text{O})_2](\text{ClO}_4)_6 \cdot 3\text{H}_2\text{O}$  and  $[\text{Cu}_2(\text{phen})_2(\text{D,L-PDIAla})(\text{H}_2\text{O})](\text{ClO}_4)_2 \cdot \frac{1}{2}\text{H}_2\text{O}$  (acac = acetylacetonate; L-thr = L-threonine; L-pro = L-proline; PDI-Ala = N,N'-(p-xylylene)di-alanine; D,L-PDIAla = N,N'-(p-xylylene)di-D,L-alanine) (Paulovicova et al., 2001; Zhang et al., 2004; Rao et al., 2007; Chetana et al., 2009; Jia et al., 2010). The plots of absorbance versus concentration for the three maximum absorption peaks in the UV region for complexes **8** - **11** are shown in **Appendices 5.7 - 5.10**. Regression lines for each plot are drawn as described in previous chapter. The correlation coefficient ( $R^2$ ) values for all the plotted graphs are close to 1.0000 showing that the data obtained fit in the regression line and obeyed the Beer-Lambert Law. The average molar absorptivity values were obtained for all four ternary complexes based on the Beer-Lambert Law and the general linear equation. Thus, absorbance values of unknown solutions of these complexes at these wavelengths can be used to determine their concentrations.

Both Cu(II) and Zn(II) pairs of enantiomeric complexes in water-methanol (1:1 v/v) still retain the FL emission property of the free phen ligand in the same solvent mixture. Threonine has no FL emission. Due to conjugated structure, the free phen gives rise to a greater FL emission intensity in water-methanol (1:1 v/v) compared to Cu(II) pairs of enantiomeric complexes. When

coordinated to the Cu(II) ion center, the highly emissive phen is partially quenched by Cu(II). The quenching mechanism has previously been ascribed to static quenching by Seng and coworkers in 2008. The Zn(II) complexes show an enhancement (>2X) in FL emission intensity. Higher FL emission by Zn(II) complex (compared to Cu(II) complexes) has been attributed to the full  $d^{10}$  electron configuration of the Zn(II) ion (Hu et al., 2010). The enhancement mechanism may be similar to  $ZnX_2(phen)$  complexes ( $X = Cl, Br, I$ ) (Ikeda et al., 1996). The chirality of the threoninato ligand of complexes does not seem to have an influence on the fluorescence emission intensities, as the same intensities were observed in the spectra of the enantiomeric pairs for both Cu(II) and Zn(II) complexes. However, the fluorescence seems to be affected by the type of metal ions, as shown in **Figure 5.6**. The order of compounds in terms of increasing FL emission intensity is  $8 \approx 9 < phen < 10 \approx 11$ .

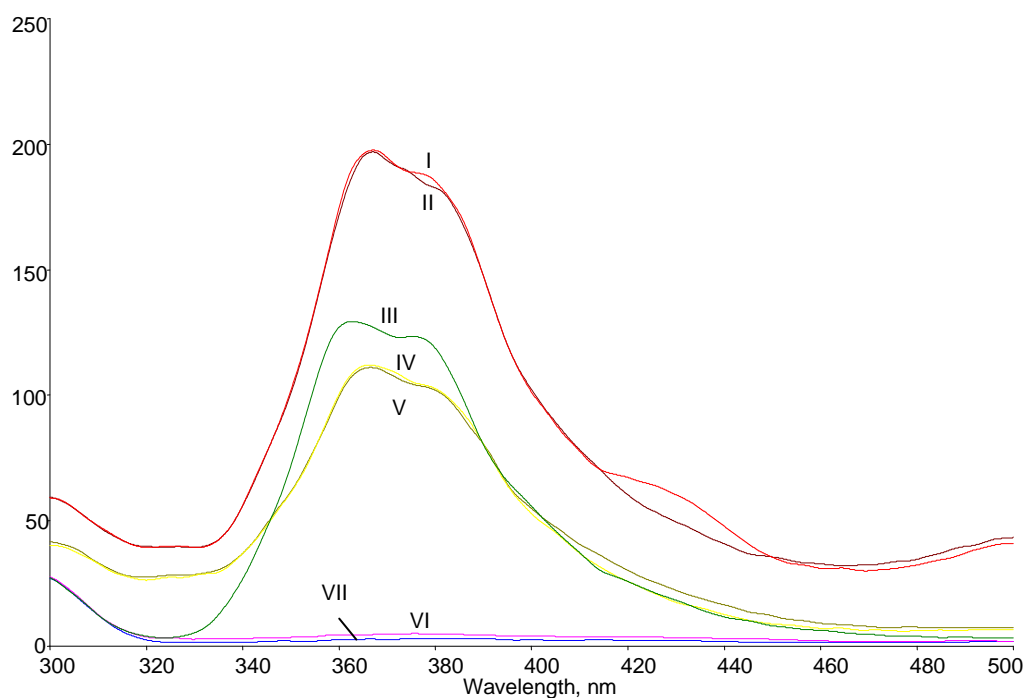


**Figure 5.6:** Fluorescence spectra of **9** (I), **10** (II), phen (III), **7** (IV), **8** (V), L-thr (VI) and D-thr (VII) at 0.5  $\mu$ M.

The circular dichroism (CD) studies are useful in determining the enantiomeric pair of metal(II) complexes. A pair of enantiomers should give rise to a mirror image in CD spectra like those reported by Ivičić and Simeon (1981). The CD spectra of the two Cu(II) complexes (**8** and **9**) are mirror-image of each other, showing that these two species are a pair of enantiomers. Similarly, the CD spectra of the pair of Zn(II) complexes (**10** and **11**) shows that they are also a pair of enantiomers (**Figure 5.7**). Based on the mirror image spectra obtained, it was proven that the enantiomeric pairs for both Cu(II) and Zn(II) complexes were successfully prepared.

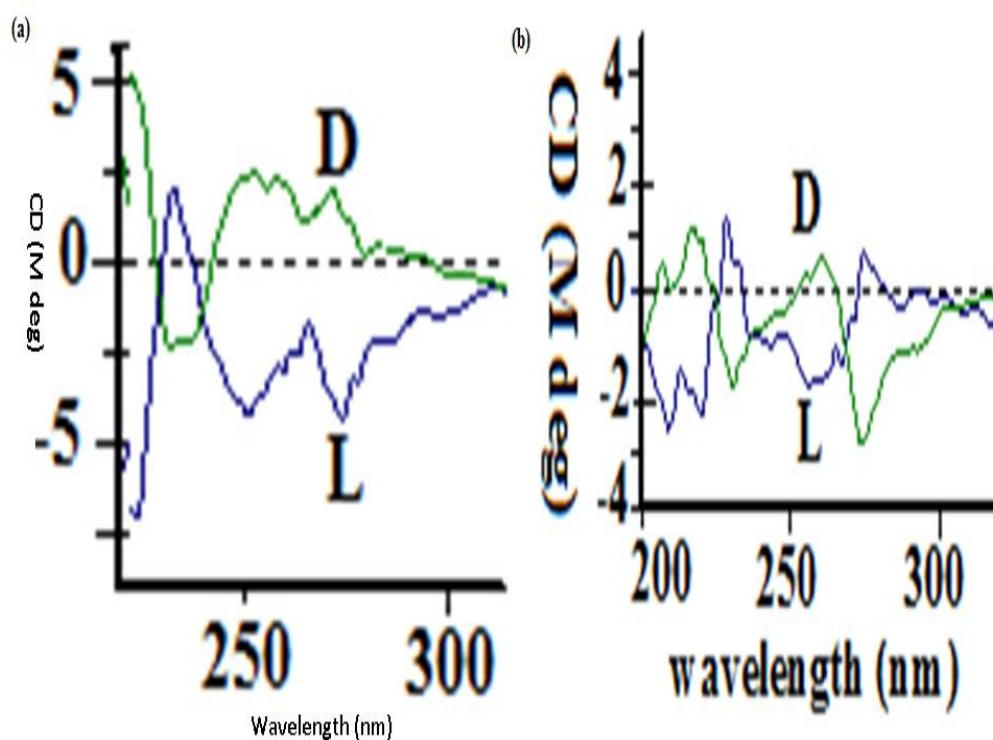


**Figure 5.7:** CD spectra of (a) Cu(II) complexes, **8 - 9** and (b) Zn(II) complexes, **10 - 11**

## 5.4 CONCLUSION

Fourier Transform Infrared Spectroscopy (FTIR), elemental analysis and ESI-MS show that  $[\text{Cu}(\text{phen})(\text{L-thr})(\text{H}_2\text{O})\text{Cl}] \cdot 2\text{H}_2\text{O}$  **8**,  $[\text{Cu}(\text{phen})(\text{D-thr})(\text{H}_2\text{O})\text{Cl}] \cdot 2\text{H}_2\text{O}$  **9**,  $[\text{Zn}(\text{phen})(\text{L-thr})(\text{H}_2\text{O})\text{Cl}] \cdot 2\text{H}_2\text{O}$  **10** and  $[\text{Zn}(\text{phen})(\text{D-thr})(\text{H}_2\text{O})\text{Cl}] \cdot 2\text{H}_2\text{O}$  **11** were successfully synthesized. All threoninate complexes, **8** - **11**, have a similar distorted octahedral coordination environment around the metal(II) (Cu(II) or Zn(II)) atom in the solid state. A Cl<sup>-</sup> atom and an aqua molecule occupy the axial positions. A phen and a threonine ligand occupy the equatorial positions. Both enantiomeric pairs of Cu(II) and Zn(II) complexes have similar thermal degradation steps. Generally, all four metal(II) complexes undergo dehydration at early stages of decomposition and followed by the removal of chloro ligand. In fact, conductivity measurement data shows that these complexes are 1:1 electrolytes. These complexes, **8** - **11**, probably exist as cationic  $[\text{M}(\text{phen})(\text{AA})(\text{H}_2\text{O})]^+$  and anionic Cl<sup>-</sup> species in aqueous solution. The coordinated phen and threoninate ligands in complexes **8** - **11** seem to be stable within the duration of the conductivity measurement. Dissociation of the threoninate ligand would increase the molar conductivity as cationic species with two positive charges would be produced.

UV absorption aroused from the  $\pi \rightarrow \pi^*$  transition of the coordinated phenanthroline ligand. Visible absorption peaks found in the electronic spectra obtained for both Cu(II) complexes spectra are assigned as d-d transition. Differential FL emission intensities are dependent on the type of metal ion.

The chirality of the threoninate ligand of complexes does not seem to have an influence on the fluorescence emission intensities. There are no significant differences observed for each enantiomer pair of complexes. A change in the type of metal(II) ion influences the FL emission intensity but not the  $\lambda_{\text{max}}$  and shape of the FL emission bands. The order of complexes in terms of increasing FL emission intensity is **8**  $\approx$  **9** < phen < **10**  $\approx$  **11**. Circular dichroism (CD) spectroscopy were used to differentiate and confirm the enantiomeric pairs of the metal(II) (Cu(II) and Zn(II)) complexes in solution. The CD spectra of each pair of enantiomeric complexes are mirror-image of each other.

**CHAPTER 6**  
**BIOLOGICAL STUDIES OF COBALT(II) 1,10-PHENANTHROLINE**  
**COMPLEXES WITH *o,o'*-MALTOL,**  
**[Co(phen)(ma)Cl]·4H<sub>2</sub>O and [Co(phen)(ma)<sub>2</sub>]·5H<sub>2</sub>O\***

**CHAPTER 6**  
**BIOLOGICAL STUDIES OF COBALT(II) 1,10-PHENANTHROLINE**  
**COMPLEXES WITH *O,O'*-MALTOL,**  
**[Co(phen)(ma)Cl]·4H<sub>2</sub>O and [Co(phen)(ma)<sub>2</sub>]·5H<sub>2</sub>O\***

**6.1 INTRODUCTION**

DNA or deoxyribonucleic acid is the genetic material in humans and almost all other organisms. This heredity material is stored as a code made up of adenine (A), guanine (G), cytosine (C) and thymine (T). DNA bases pair up with each other, *i.e.* A with T and C with G, to form units called base pairs. There are two types of nucleobases: the purines, A and G, which are fused five- and six-membered heterocyclic compounds, and the pyrimidines, C and T, which are six-membered rings heterocyclic compounds (Berg et al., 2002). DNA is a long polymer made from repeating units called nucleotides. Nucleotide consists of a base, sugar and phosphate molecule (Saenger, 1983; Alberts et al., 2002). DNA (**Figure 6.1**) is a double helix formed by base pairs attached to sugar-phosphate backbone as described by Watson and Crick (1954). The DNA double helix structure is stabilized by the base pairing between complementary strands and stacking between adjacent bases (Yakovchuk, et al., 2006).

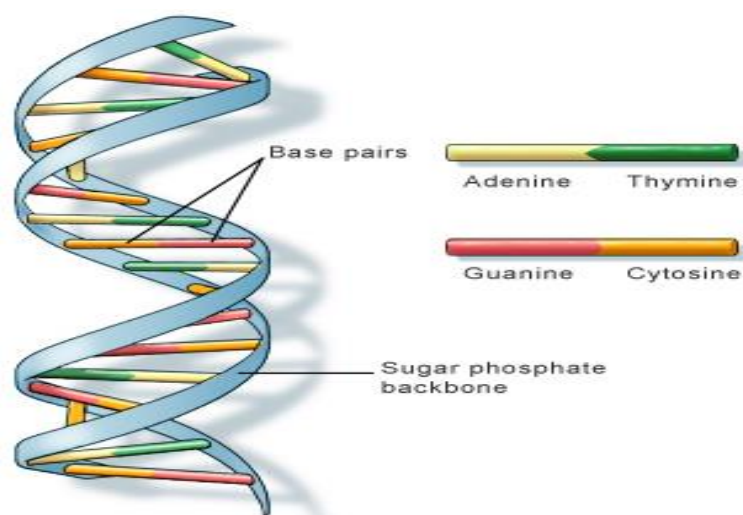


**Figure 6.1:** DNA double helix structure cited from U.S. National Library of Medicine

Metal complexes are known to interact with DNA *via* covalent bonding, hydrogen bonding, intercalation, van der Waals forces and electrostatic interaction (**Figure 6.2**). Basically, metal complexes can bind to DNA in each of three different non-covalent modes which are: (a) groove binding (b) intercalation and (c) insertion.

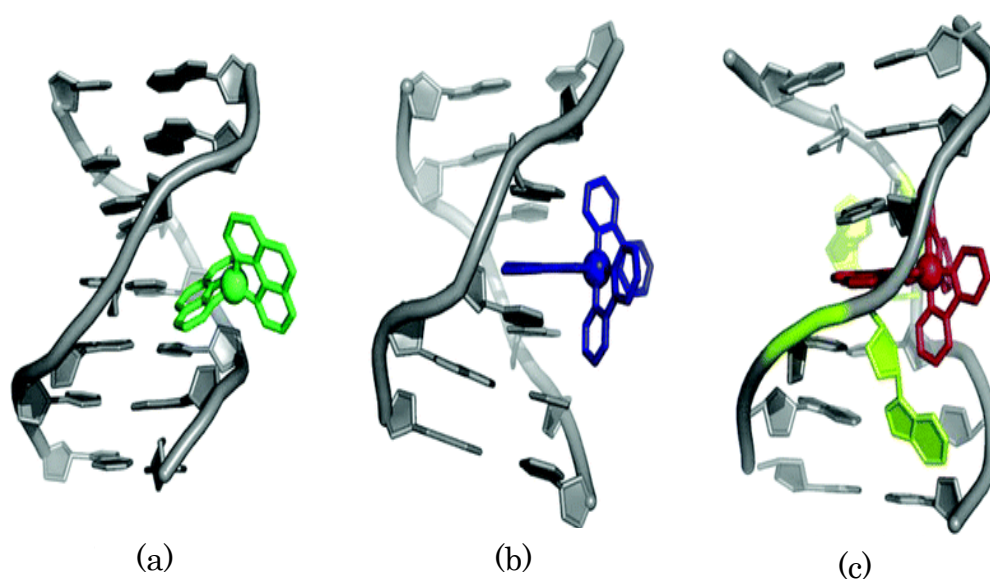


**Figure 6.2:** The three binding modes of metal complexes with DNA: (a) groove binding, (b) intercalation, and (c) insertion. (Taken from Zeglis et al., 2007)

Small organic molecules have been extensively investigated for their use as anticancer, antiviral and antibacterial drugs in addition to their binding specificity for possible modulation and inhibition of DNA replication, transcription and recombination (Du et al., 2010). The DNA specific interactions include abasic, mismatch or bulge site recognition, specific sequence recognition and secondary structure recognition. Similarly, there is also growing research into the DNA recognition by metal complexes or metallomolecules (Boerner and Zaleski, 2005; Richards et al., 2007; Terrón et al., 2007; Zeglis et al., 2007; Keene et al., 2009). However, such DNA recognition ability of metal complexes is not well understood. The type of coordinated ligand is crucial factor in bestowing the binding site specificity and selectivity of a given metal complex. Unlike the inert and more stable Co(III) complexes, Co(II) complexes are less investigated for their interaction with DNA. Recently, preferential binding of (ethylenediamine-*N,N'*-diacetato)(1,10-phenanthroline)metal(II), [M(phen)(edda)], for ds(AT)<sub>6</sub> over ds(CG)<sub>6</sub> and its anticancer property were reported (Ng et al., 2008; Seng et al., 2008). Among these complexes, [Co(phen)(edda)] was the least antiproliferative against breast cancer cell line MCF7 with the IC<sub>50</sub> value of 11.4 μM.

This chapter is an extension of Chapter 3. In this chapter, two cobalt(II) ternary complexes, [Co(phen)(ma)Cl]·4H<sub>2</sub>O **1** and [Co(phen)(ma)<sub>2</sub>]·5H<sub>2</sub>O **4** synthesized in Chapter 3 were tested for their biological properties. Both Co(II) complexes, **1** and **4** were selected to gain an understanding the effect of the

number of coordinated maltolate ligand on the DNA recognition, DNA binding specificity and anticancer properties. The type of biological studies done on these two complexes included DNA binding studies, restriction enzyme inhibition, topoisomerase I inhibition and cell viability assay.

## **6.2 EXPERIMENTAL**

### **6.2.1 Materials and reagents**

Most of the reagents were of analytical grade and were used as supplied. The pBR322, gene ruler 1 kb DNA ladder, 6x loading buffer, and oligonucleotides were bought from BioSyn Tech (Fermentas). Analytical grade agarose powder and 3-[4,5-dimethylthiazol-2-yl]-5-(3-carboxymethoxyphenyl)-2-(4-sulfophenyl)-2H-tetrazolium inner salt (MTS) were purchased from Promega (USA). Calf-thymus DNA, sodium chloride (NaCl), human DNA topoisomerase I, thiazole orange and ethidium bromide were purchased from Sigma Chemical Co. (USA). All solutions for DNA experiments were prepared with ultra-pure water from a Elga PURELAB ULTRA Bioscience water purification system with UV light accessory. The Tris-NaCl (TN) buffer was prepared from the combination of Tris base and NaCl dissolved in aqueous solution in which the pH was adjusted with hydrochloric acid (HCl) solution till pH 7.5. The Tris-NaCl buffer pH 7.5 contains Tris at 5 mM and NaCl at 50 mM. Tris-NaCl buffer were freshly prepared before use.

### 6.2.2 DNA binding studies

Stock solutions of calf thymus DNA (CT-DNA) was prepared by dissolving the DNA in buffer solution at 4 °C, and the resultant homogeneous solutions were used within two days. The purity of the DNA was checked by monitoring the absorbance at 260 and 280 nm. PAGE grade of self-complimentary 12-mer oligonucleotides (CG)<sub>6</sub>, (AT)<sub>6</sub>, CGCGAATTCGCG, CGCGATATCGCG, HPLC grade 22-mer oligonucleotide 5'-AGGGTTAGGGTTAGGGTTAGGG-3' (for annealing G-quadruplex) and 17-mer complementary oligonucleotide pair (5'-CCAGTTCGTAGTAACCC-3' and 3'-GGTCAAGCATCATTGGG-5') were annealed, to give the respective duplexes and G-quadruplex, as specified by the suppliers 1<sup>st</sup> BASE and Eurogentec Ait. Fluorescence (FL) emission spectra in the study of ethidium bromide quenching assay for the duplexes of the various synthetic oligonucleotides were recorded in the wavelength range 550–650 nm by exciting the respectively solutions with light at 545 nm. In the FL emission spectra (thiazole orange quenching assay) for the G-quadruplex and corresponding duplex, the excitation wavelength  $\lambda_{\text{ex}}$  is 504 nm while the emission wavelength  $\lambda_{\text{em}}$  is 527 nm. Excitation and emission slits were set at 10 nm. Solutions of DNA, and the cobalt complexes were prepared in TN buffer (5 mM Tris, 50 mM NaCl) at pH 7.5 unless specifically stated. CD study of the interaction of Co(II) complexes with CT-DNA was carried out with a 1.0 mm quartz cell using a Jasco J-810 spectropolarimeter.

### **6.2.3 Restriction enzyme inhibition assay and human topoisomerase I inhibition assay**

These assays were carried out as described previously (Seng et al., 2010). The apparent binding constants of the  $[\text{Co}(\text{phen})(\text{ma})\text{Cl}]\cdot 4\text{H}_2\text{O}$  **1** and  $[\text{Co}(\text{phen})(\text{ma})_2]\cdot 5\text{H}_2\text{O}$  **4** complexes for the various DNA duplexes and G-quadruplex are tabulated in **Table 6.1**.

### **6.2.4 Anticancer study**

F12 medium, Dulbecco's Modified Eagle's Media (DMEM), fetal bovine serum, MEM non-essential amino acids, horse serum and L-glutamine were purchased from GIBCO®. Hydrocortisone and insulin were purchased from Sigma-Aldrich. Epidermal growth factor was purchased from Invitrogen. MDA-MB-231, MCF7 and MCF10A cells were obtained from American Type Culture Collection. Human breast cancer MDA-MB-231 and MCF7 cells were cultured in Dulbecco's modified Eagle's medium containing 10% fetal calf serum, 100 units/mL of penicillin and 100  $\mu\text{g}/\text{mL}$  of streptomycin. Human breast tissue-derived MCF 10A (immortalized but non-tumorigenic) cells were cultured in 1:1 F12/DMEM media supplemented with 5 % (v/v) horse serum, 1X non essential amino acid, 1X glutamine, insulin, epidermal growth factor, hydrocortisone, 100 units/ml penicillin and 100  $\mu\text{g}/\text{ml}$  streptomycin. All cell lines were maintained at 37°C in a humidified incubator with an atmosphere of 5%  $\text{CO}_2$ .

Cells were seeded in a 96-well plate and were grown to 70–80 % confluence, followed by addition of each compound at the indicated concentrations. After 24 hours of incubation at 37°C, 5% CO<sub>2</sub>, MTS working solution was added for a further 4 hours. Optical density was read using enzyme-linked immunosorbent assay (ELISA) plate reader at a wavelength of 490 nm with background subtraction at 630 nm. The percentage of cell viability was calculated with the formula: Average  $A_{490}$  value for live cell(treated)/average  $A_{490}$  value for live cell (untreated)  $\times$  100. The IC<sub>50</sub> values were obtained from the graphs drawn.

## **6.3 RESULTS AND DISCUSSION**

### **6.3.1 DNA binding studies**

Circular Dichroism (CD) spectroscopy is a useful technique in studying the changes in DNA morphology during drug-DNA interactions, as the band due to base stacking (275 nm) and that due to right-handed helicity (248 nm) are quite sensitive to the mode of DNA interactions with small molecules (Ivanov et al., 1973). The spectra of CT-DNA incubated with and without complexes **1** and **4** have a negative band at ~250 nm due to right-handed DNA helicity and a positive band at ~280 nm due to base stacking, suggesting retention of the B-form DNA upon binding of complexes **1** and **4** (**Figure 6.3**). Both complexes **1** and **4** induced significant intensity enhancement of the positive spectral band at ~280 nm, and this indicated intercalation mode of binding (Li et al., 2006; Sun et al., 2002).

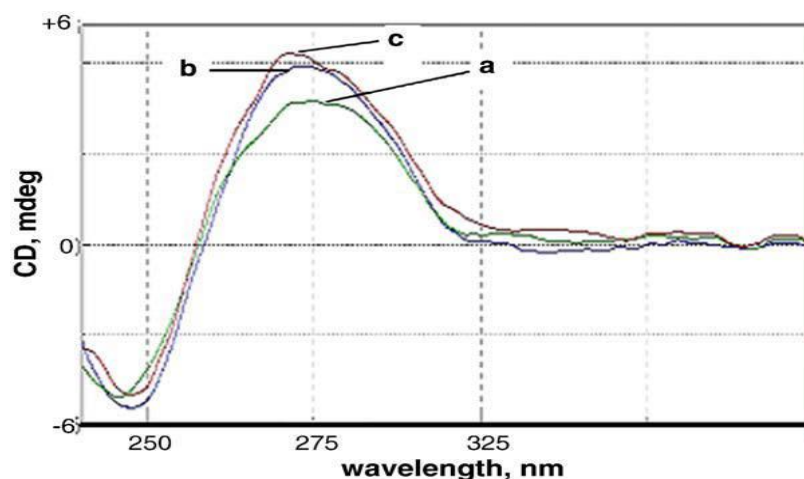


**Figure 6.3:** CD spectra of CT-DNA alone (a) and in the presence of the complexes **1** (b) and **4** (c).

Ethidium bromide (EB) and thiazole orange quenching assays have been successfully used to determine the DNA binding affinity and sequence selectivity of small organic molecules and metal complexes (LePecq and Paoletti, 1967; Boger and Tse, 2001; Rajendra and Nair, 2006; Li et al., 2007; Monchaud et al., 2008; Seng et al., 2010). A complex with a higher binding constant for a given DNA determined by either assay is said to have a higher binding affinity. Likewise, a complex with a higher binding constant for a certain DNA than for another DNA is said to bind more selectively towards the former. It has been concluded in Chapter 3, complex **1** exists as  $[\text{Co}(\text{phen})(\text{ma})]^+$  or its hydrated species and  $\text{Cl}^-$  while complex **4** exists as the neutral  $[\text{Co}(\text{phen})(\text{ma})_2]$  species in aqueous solution. As both Co(II) complexes, **1** and **4**, have higher binding constants for  $\text{ds}(\text{AT})_6$  than for  $\text{ds}(\text{CG})_6$  (**Table 6.1**), hence complexes **1** and **4** have more selectivity towards AT-sequences than CG-sequences. Although the AT:CG binding constant ratio for complex **4** (1.4) is higher than that for complex **1** (1.2), the difference

is not that great. The binding constants for both complexes **1** and **4** suggest their greater binding selectivity for ds(CGCGATATCGCG)<sub>2</sub> over the ds(CGCGAATTCGCG)<sub>2</sub> and this indicated greater binding preference or selectivity for alternate AT-sequence over AATT-sequence. Both complexes **1** and **4** again exhibit greater selectivity for G-quadruplex (G-4) over duplex DNA as they have G-4:duplex binding ratios of 1.4 and 1.5 respectively. Interestingly, the binding constants of complex **4** for CT-DNA, G-4 and duplex are significantly greater than those of complex **1**. For example, the binding constant of complex **4** towards G-4 is nine times more than that of complex **1**.

Since chloride in [Co(phen)(ma)Cl]·4H<sub>2</sub>O **1** is a weak field ligand, it should dissociate easily in aqueous solution to form [Co(phen)(ma)]<sup>+</sup> or its hydrated species. By using the EB quenching assay, it was found that the apparent binding constant decreases from  $5.86 \pm 0.08 \times 10^4 \text{ M}^{-1}$  gradually to  $1.74 \pm 0.10 \times 10^4 \text{ M}^{-1}$  when the NaCl concentration increased from 0 to 40 mM (data not shown). This showed that the interaction of complex **1** with the anionic DNA is electrostatic and that the complex is cationic in aqueous solution. The maltolate ligand has hydrogen-bonding acceptors while the phen moiety can intercalate into adjacent DNA base pairs and thus, non-covalent interactions are envisaged. The binding affinity of cationic complex, [Co(phen)(ma)]<sup>+</sup> towards all the different types of DNA studied above (**Table 6.1**) is not higher than that of neutral complex, [Co(phen)(ma)<sub>2</sub>] towards the corresponding DNA. This may be explained by assuming that the chelated

phen ligand helps to anchor both Co(II) complexes between the adjacent base-pairs, and by doing so fixes the orientation of the other ligands bonded to the cobalt. Looking at it in this way, one may then ascribed the increasing DNA binding strength of complex **4** to the orientation of the maltolate ligands (*viz.* one above and one below the phenanthroline plane) diagonally towards the upper and lower ribose-nucleobases. This then results in stronger attractive interaction of the maltolates with the riboses and nucleobases. The pyrone-oxygen atom in the maltolate can act as H-bond acceptor while the methyl group can have van der Waals interaction. Additionally, stacking interaction can also occur between the pyrone ring with the DNA nucleobase. On the other hand, the maltolate in complex **1** is in the plane of the anchoring intercalated phen and is not positioned nearer to either base pair above or below the plane of intercalation.

**Table 6.1:** Binding constant of Co(II) complexes for various DNA

DNA	[Co(phen)(ma)Cl]·4H <sub>2</sub> O ( <b>1</b> )	[Co(phen)(ma) <sub>2</sub> ]·5H <sub>2</sub> O ( <b>4</b> )	Ratio <b>4/1</b>
CT-DNA	1.162 x 10 <sup>4</sup>	3.559 x 10 <sup>4</sup>	3.1
ds(AT) <sub>6</sub>	2.176 x 10 <sup>4</sup>	2.563 x 10 <sup>4</sup>	1.2
ds(CG) <sub>6</sub>	1.823 x 10 <sup>4</sup>	1.791 x 10 <sup>4</sup>	1.0
ds(CGCGAATTCGCG) <sub>2</sub>	1.217 x 10 <sup>4</sup>	1.474 x 10 <sup>4</sup>	1.2
ds(CGCGATATCGCG) <sub>2</sub>	1.776 x 10 <sup>4</sup>	1.782 x 10 <sup>4</sup>	1.0
G-quadruplex	7.34 x 10 <sup>3</sup>	6.72 x 10 <sup>4</sup>	9.2
G-duplex	5.11 x 10 <sup>3</sup>	4.32 x 10 <sup>4</sup>	8.5

### 6.3.2 Restriction enzyme inhibition

To further investigate the binding specificity of complexes **1** and **4**, twelve restriction enzymes (REs), *viz.* Bst 11071(5'-GTA↓TAC-3'), NdeI (5'-C A↓TATG-3'), EcoR I (5'-↓AATTC-3'), Mun I (5'-C↓AATTG-3'), Ssp I

(5'-A A↓TATT-3'), Ase I (5'—AT↓TAAT-3'), Sca I (5'-AGT↓ACT-3'), Pvu II (5'-CAG↓CTG-3'), Pst I (5'-CTGC A↓G-3'), Sal I (5'-G↓TCGAC-3'), Tsp5091 (5'-↓AATT-3') and Hae III (5'-GC↓GC-3'), were used. The specific sequence recognized by each RE is listed in parenthesis with its cutting site. RE has been used to investigate the binding specificity or selectivity of metal complexes (Gallori et al., 2000; Snow and Sheardy, 2001; Karidi et al., 2005). The choice of these REs is because of the greater preferences of complexes **1** and **4** for AT-sequence or AT-rich duplexes. As comparison, it was observed that EB and thiazole orange (TO) could inhibit all the REs used, suggesting the non-discriminating binding of these intercalator dyes at all the sites, including those at the recognition sites of the twelve REs (data not shown). In contrast, 50 μM of complex **1** can only totally inhibit Ssp I (5'-A A↓TATT-3'), NdeI (5'-CA↓TATG-3') and Bst 11071 (5'-GTA↓TAC-3') (**Appendix 6.1 - 6.2**). This suggests the binding specificity of complex **1**, unlike that of EB or TO. As shown in **Appendix 6.3 – 6.4**, 50 μM of complex **4** can partially inhibit DNA cleavage by Tsp 5091(5'-↓AATT-3'), Hae III (5'-GC↓GC-3') and Pvu II (5'-CAG↓CTG-3') but not the other REs. Like in complex **1**, this selective inhibition of only some REs suggests that complex **4** can bind selectively to DNA. Surprisingly, complex **4** cannot inhibit DNA cleavage by Ssp I, Nde I and Bst 11071 while complex **1** can (**Table 6.2**). Complex **1** has one coordinated phen and one coordinated maltolate while complex **4** has one coordinated phen and two coordinated maltolate. It seems reasonable to ascribe the different binding specificity and recognition of DNA of complexes **1** and **4** to the number of coordinated maltolate ligand.

**Table 6.2:** Restriction enzyme inhibition for Co(II) complexes, **1** and **4**

RE	Sequence	[Co(phen)(ma)Cl] ( <b>1</b> )	[Co(phen)(ma) <sub>2</sub> ] ( <b>4</b> )
Tsp 509I	5'—↓A A T T—3' 3'—T T A A↑—5'		√
Hae III	5'—G C ↓G C—3' 3'—C G ↑C G—5'		√
Sal I	5'—G ↓T C G A C—3' 3'—C A G C T ↑G—5'		
Pst I	5'—C T G C A ↓G—3' 3'—G ↑A C G T C—5'		
Pvu II	5'—C A G ↓C T G—3' 3'—G T C ↑G A C—5'		√
Sca I	5'—A G T ↓A C T—3' 3'—T C A ↑T G A—5'		
Ase I	5'—A T ↓T A A T—3' 3'—T A A T ↑T A—5'		
Ssp I	5'—A A ↓T A T T—3' 3'—T T A T ↑A A—5'	√	
Mun I	5'—C ↓A A T T G—3' 3'—G T T A A ↑C—5'		
EcoR I	5'—G ↓A A T T C—3' 3'—C T T A A ↑G—5'		
NdeI	5'—C A ↓T A T G—3' 3'—G T A T ↑A C—5'	√	
Bst 11071	5'—G T A ↓T A C—3' 3'—C A T ↑A T G—5'	√	

### 6.3.3 Human topoisomerase I inhibition

Topoisomerase I (Topo I) is one of the enzymes that control the topology of the DNA by a single-strand cut, passing the other strand through the cutting site and religating the cut strand (Feng et al., 2009). These topoisomerases are important in DNA replication and transcription. Topo I inhibitors have been reported to be among the most widely used clinical drugs for treatment of cancer (Rothenberg, 1997; Beretta et al., 2008; Teicher, 2008; Pommier, 2008; Sunami et al., 2009). However, there are not many metal complexes that have been reported to inhibit topoisomerases (Chuang et al., 1996). Gel electrophoresis can be used to view the topoisomers which result from relaxation of supercoiled pBR322 by Topo I (Webb and Ebeler, 2008).

More relaxed topoisomers will migrate slower than less relaxed topoisomers while the supercoiled DNA will migrate fastest.

In **Figure 6.4**, 1 unit of Topo I could fully convert the supercoiled pBR322 DNA to fully relaxed topoisomers (**Lane 4**). Incubating the DNA with **1** (5 – 40  $\mu\text{M}$ ) and Topo I resulted in appearance of slower moving bands of more relaxed DNA (**Lane 6 - 9**). The initial inhibitory effect of complex **1** started from 5  $\mu\text{M}$  (**Lane 6**). The inhibitory effect of the Topo I is enhanced by increasing complex concentration (5 – 40  $\mu\text{M}$ ). At 40  $\mu\text{M}$ , complex **1** is still not enough to fully inhibit the function of the Topo I.

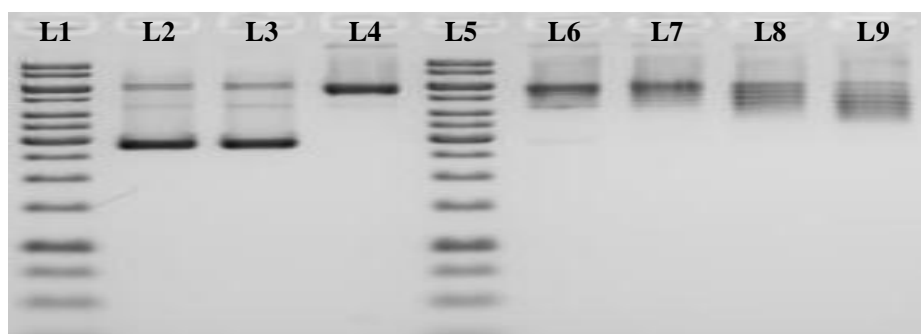


**Figure 6.4:** Human topoisomerase I inhibition assay by gel electrophoresis. Electrophoresis results of incubating human topoisomerase I (1 unit/21 $\mu\text{L}$ ) with pBR322 (0.25  $\mu\text{g}$ ) in the absence or presence of 5-40  $\mu\text{M}$  of complex **1**: Lane 1 & 5, gene ruler 1 Kb DNA ladder; Lane 2, DNA alone; Lane 3, DNA + 40  $\mu\text{M}$  complex **1** (control); Lane 4, DNA + 1 unit Human Topoisomerase I (control). Lanes 6-9, DNA + 1 unit Human Topoisomerase I + varying concentration of complex **1**: Lane 6, 5  $\mu\text{M}$  complex **1**; Lane 7, 10  $\mu\text{M}$  complex **1**; Lane 8, 20  $\mu\text{M}$  complex **1**; Lane 9, 40  $\mu\text{M}$  complex **1**.

**Figure 6.5** showed the inhibition assay results for the corresponding  $[\text{Co}(\text{phen})(\text{ma})_2] \cdot 5\text{H}_2\text{O}$ , **4**. As the banding pattern for DNA incubated with

complex **4** (200  $\mu\text{M}$ ) is the same as that of the DNA alone, it is concluded that complex **4** by itself could not relax or cleave the DNA at this concentration (**Figure 6.5, lane 3**). Done at a different time, one unit of Topo I converted the supercoiled DNA into mostly fully relaxed topoisomers and few bands of very slow moving topoisomers on top of the gel. Complex **4** showed practically no inhibition on the activity of the Topo I in the concentration range 10 – 50  $\mu\text{M}$  as substantial amount of supercoiled DNA was converted to fully relaxed topoisomers (**Figure 6.5, Lanes 7 - 9**). At 100  $\mu\text{M}$ , the Co(II) complex **4** started to inhibit the Topo I as can be seen by the appearance of distinct bands of faster moving topoisomers (**Figure 6.5, lane 10**). On increasing the concentration of complex **4** to 200  $\mu\text{M}$ , faster moving, new bands (less relaxed topoisomers) appeared, indicating greater inhibition of the Topo I by complex **4** (**Figure 6.5, lane 11**).



**Figure 6.5:** Human topoisomerase I inhibition assay by gel electrophoresis. Electrophoresis results of incubating human topoisomerase I (1 unit/21 $\mu\text{L}$ ) with pBR322 (0.25  $\mu\text{g}$ ) in the absence or presence of 10-200  $\mu\text{M}$  of complex **4**: Lanes 1 & 12, gene ruler 1 Kb DNA ladder; Lane 2, DNA alone; Lane 3, DNA + 200  $\mu\text{M}$  complex **4** (control); Lane 4, empty; Lane 5, DNA + 1 unit Human Topoisomerase I (control); Lane 6, empty. Lanes 7-11, DNA + 1 unit Human Topoisomerase I + varying concentration of complex **4**: Lane 7, 10  $\mu\text{M}$  complex **4**; Lane 8, 20  $\mu\text{M}$  complex **4**; Lane 9, 50  $\mu\text{M}$ ; Lane 10, 100  $\mu\text{M}$  complex **4**; Lane 11, 200  $\mu\text{M}$  complex **4**.

The above results showed that the Co(II) complexes **1** and **4** are inhibitors and not topoisomerase poisons. Topoisomerase poisons give rise to permanent DNA cleavage (Palumbo et al., 2002). Topoisomerase poisons block the religation step, thereby enhancing the formation of persistent DNA breaks responsible for cell death. Permanent single-strand (nicked band) or double-strand (linear band) cleavage can be easily observed by gel electrophoresis.

#### **6.3.4 Anticancer study**

3-[4,5-dimethylthiazol-2-yl]-5-(3-carboxymethoxyphenyl)-2-(4-sulfophenyl)-2H-tetrazolium (MTS) assay was used to examine the antiproliferating effect of the Co(II) complexes, **1** and **4**, against two breast cancer cell lines MCF7 and MDA-MB-231, and one corresponding normal breast cell line MCF10A. Estrogen receptor (ER) positive MCF7 and ER negative MDA-MB-231 breast cancer cells have been found to exhibit differential sensitivity to both organic or metal-based anticancer drugs (Shanmugam et al., 2001; Mazzei et al., 2001; Nikitin et al., 2010). Surprisingly, the MDA-MB-231 cancer cells are more resistant than the normal cells towards the two Co(II) complexes as their  $IC_{50}$  values are more than 450  $\mu$ M (**Table 6.3**). The  $IC_{50}$  values for both Co(II) complexes on the MCF10A normal cells are the same, at 160  $\mu$ M. Nevertheless, complexes **1** and **4** are more antiproliferative against the cancer cell line MCF7, with  $IC_{50}$  values of 75 and 55  $\mu$ M respectively. Thus, the antiproliferative activity and the accompanying growth inhibitory

mechanism of these two Co(II) complexes are cell-type dependent. Such cell-type dependent antiproliferative and growth inhibition mechanism (NF $\kappa$ B inhibition) were observed for extracts from medicinal plants against MCF7, MDA-MB-231 and HEK293T embryonal kidney cell lines (Kaileh et al., 2007).

**Table 6.3:** IC<sub>50</sub> values of complexes **1** and **4** for the MDA-MB-231, MCF7 and MCF10A cell lines

Co(II) complex	IC <sub>50</sub> ( $\mu$ M)		
	MDA-MB-231	MCF7	MCF10A
<b>1</b>	>600	75	160
<b>4</b>	495	55	160

#### 6.4 CONCLUSION

The two Co(II) complexes are found to exhibit different binding affinity and selectivity towards different types of duplex DNA. For the G-quadruplex, the binding constant of complex **4** is considerably higher than that of complex **1**. The number of maltolate ligand seems to be important parameter in DNA recognition. This is further exemplified by the RE inhibition experiment results which show that the binding specificity of complexes **1** and **4** are totally different. Although both Co(II) complexes can inhibit Topo I, their inhibitory behavior is again different. The antiproliferative property of both complexes is cell-type dependent, and their potential use as anticancer drug towards MCF7 is indicated. The cytotoxicity of these tested Co(II) complexes may be either due to the binding to DNA to prevent the binding of Topo I or their binding to Topo I to inactivate it. Another mechanism may involve DNA

damage by the cobalt complexes. However, MDA-MB-231 cancer cells are insensitive towards both Co(II) complexes although both have distinctly differential IC<sub>50</sub> values.

**CHAPTER 7**  
**BIOLOGICAL STUDIES OF ZINC(II) 1,10-PHENANTHROLINE**  
**COMPLEXES WITH *O,N,O'*-DIPICOLINIC ACID**  
**OR *N,O*-L-THREONINE**  
**[Zn(phen)(dipico)(H<sub>2</sub>O)]·H<sub>2</sub>O and [Zn(phen)(L-thr)(H<sub>2</sub>O)Cl]·2H<sub>2</sub>O\***

**CHAPTER 7**  
**BIOLOGICAL STUDIES OF ZINC(II) 1,10-PHENANTHROLINE**  
**COMPLEXES WITH *O,N,O'*-DIPICOLINIC ACID**  
**OR *N,O*-L-THREONINE**  
**[Zn(phen)(dipico)(H<sub>2</sub>O)]·H<sub>2</sub>O and [Zn(phen)(L-thr)(H<sub>2</sub>O)Cl]·2H<sub>2</sub>O\***

**7.1 INTRODUCTION**

Zinc is an outstanding micronutrient with diverse biological, clinical, and public health importance (Burdette and Lippard, 2001; Chang and Lippard, 2006; Hambidge et al., 2010). There are over 300 natural zinc metalloenzymes (Stehbens, 2003; Lin et al., 2005). Artificial zinc finger proteins and zinc complexes with simple organic ligands have been shown to have sequence-specific DNA binding recognition (Nagaoka and Sugiura, 2000; Papworth et al., 2006). Some zinc complexes are now beginning to be reported be able to inhibit topoisomerase I and II, which are nuclear enzymes needed for modification of topological state of DNA (Chuang et al., 1996; Kikuta et al., 2000; Seng et al., 2010). An important property of topoisomerase I (Topo I) inhibitors is their anticancer property (Chuang et al., 1996; Rothenberg, 1997; Kikuta et al., 2000; Pommier, 2008; Beretta et al., 2008; Sunami et al., 2009). In fact, numerous clinical, anticancer drugs are Topo I inhibitors. However, none of these clinical drugs are zinc complexes. Actually, not many zinc complexes have been studied for their anticancer property (Liguori et al., 2010; Wen et al., 2011). Simple mixed-ligand metal complexes with

intercalating ligand may have both DNA binding and molecular recognition capabilities (Seng et al., 2010). Unlike cisplatin, such mononuclear metallointercalators can use the intercalating ligand to anchor the metal complex between adjacent DNA bases and consequently orientate the subsidiary ligand(s) to interact with nucleobases in their vicinity.

Among all the Zn(II) complexes ( $[\text{Zn}(\text{phen})(\text{ma})\text{Cl}] \cdot 1\frac{1}{2}\text{H}_2\text{O}$  **3**,  $[\text{Zn}(\text{phen})(\text{dipico})(\text{H}_2\text{O})] \cdot \text{H}_2\text{O}$  **7**,  $[\text{Zn}(\text{phen})(\text{L-thr})(\text{H}_2\text{O})\text{Cl}] \cdot 2\text{H}_2\text{O}$  **10** and  $[\text{Zn}(\text{phen})(\text{D-thr})(\text{H}_2\text{O})\text{Cl}] \cdot 2\text{H}_2\text{O}$  **11**) synthesized in my study, only two Zn(II) complexes **7** and **10** were chosen. One reason for choosing complexes **7** and **10** was their similarities and differences. The dipicolinate and L-threoninate ligands contain carboxylate group(s). The coordinated dipicolinate ligand has two H-acceptor sites whereas threoninate has both H-acceptor and H-donor sites. Complexes **7**, **10** and **11** have a similar octahedral geometry about their Zn atom whereas complex **3** has a square pyramidal geometry. Complex **10** was chosen because L-amino acids have been reported to play an important role in biological process compared to D-amino acids (Shahjee et al., 2002; Conti et al., 2011). In this chapter, the choices of two Zn(II) complexes ( $[\text{Zn}(\text{phen})(\text{dipico})(\text{H}_2\text{O})] \cdot \text{H}_2\text{O}$  **7** and  $[\text{Zn}(\text{phen})(\text{L-thr})(\text{H}_2\text{O})\text{Cl}] \cdot 2\text{H}_2\text{O}$  **10**) allows investigation into the effect of two different and yet related subsidiary ligands (dipicolinate and L-threoninate) on biological properties *viz.* DNA binding studies, restriction enzyme inhibition, topoisomerase inhibition and anticancer studies.

## **7.2 EXPERIMENTAL**

### **7.2.1 Materials and reagents**

Both complexes **7** and **10** were synthesized and characterized in Chapter 4 and Chapter 5, respectively. Most of the reagents were analytical grade and used as supplied. The pBR322, gene ruler 1 kb DNA ladder, 6x loading buffer, and oligonucleotides were bought from BioSyn Tech (Fermentas). Analytical grade agarose powder and 3-[4,5-dimethylthiazol-2-yl]-2,5-diphenyltetrazolium bromide (MTT) were purchased from Promega (USA). Sodium chloride (NaCl), human DNA topoisomerase I, thiazole orange and ethidium bromide were purchased from Sigma Chemical Co. (USA). All solutions for DNA experiments were prepared with ultra-pure water from an Elga PURELAB ULTRA Bioscience water purification system with UV light accessory. The Tris-NaCl (TN) buffer was prepared from the combination of Tris base and NaCl dissolved in aqueous solution in which the pH was adjusted with hydrochloric acid (HCl) solution till pH 7.5. The Tris-NaCl buffer pH 7.5 contains Tris at 5 mM and NaCl at 50 mM. All stock solutions in Tris-NaCl buffer were freshly prepared daily.

### **7.2.2 DNA binding studies**

The studies were carried out as described in Chapter 6, section 6.2.2. The apparent binding constants of complexes **7** and **10** for the various DNA duplexes and G-quadruplex are tabulated in **Table 7.1**.

### **7.2.3 Restriction Enzyme inhibition assay and human topoisomerase I inhibition assay**

The restriction enzyme and human topoisomerase I inhibitory assays were carried out for complexes **7** and **10** as described in Chapter 6, section 6.2.3.

### **7.2.4 Anticancer studies**

NPC cell lines growing at log-phase were used. HONE-1 cell line was a kind gift from Prof. Sam CK (University of Malaya) The cell line was established from a biopsy from a 68-year old Chinese man diagnosed with a poorly differentiated NPC with lymph node metastasis (Sung et al., 2005). The absence of EBV in HONE-1 was rechecked by PCR analysis of genomic DNA. NP69, an immortalized human nasopharyngeal epithelial cell line, and HK1 cell line were obtained from the University of Hong Kong Culture Collection. HONE-1 cells were maintained as a monolayer culture in RPMI medium supplemented with 10 % (v/v) fetal bovine serum (FBS) and kept in incubator with humidified atmosphere containing 5 % CO<sub>2</sub> at 37 °C. HK1 cell line was grown in MEM medium (Invitrogen Corp.) supplemented with 10% FBS. NP69 was maintained in keratinocyte serum-free medium supplemented with 0.1 ng/mL of epidermal growth factor, 50 µg/mL of bovine pituitary extract, and a final Ca<sup>2+</sup> concentration of 0.3 mmol/L.

For MTT assay, approximately  $3.0 - 5.0 \times 10^3$  HONE-1, HK1, NP69, MDCK, or NRK-52E cells were seeded into each of a series of wells in separate 96-well culture plates and allowed to adhere overnight (24 hours). Different concentrations of the complexes tested (0 - 300  $\mu\text{M}$ ; several trials were done to get a suitable range to obtain the concentration causing 50 % inhibition of cell proliferation *i.e.*  $\text{IC}_{50}$  for each compound) were added to the wells, except for control cells, to which only the culture medium was added. The set of cultures without and with increasing concentration of the added compound was done in triplicate. At the end of the incubation period (72 hours), 20  $\mu\text{L}$  of 5.0 mg/mL MTT in phosphate-buffered saline (PBS) was added and incubated in a 5 %  $\text{CO}_2$  humidified incubator for 3 hours. Medium and excess MTT were aspirated and formazan formed was solubilized with 100  $\mu\text{l}$  of dimethyl sulfoxide. Optical density of the resultant formazan solutions, which corresponded to the number of viable cells, was determined by Spectramax plate reader at 570 nm.  $\text{IC}_{50}$  values of tested complexes were estimated from plots of percentage cell viability versus increasing concentration of test complexes ( $\mu\text{M}$ ).

For apoptosis study, HONE-1 cells were treated with  $\text{IC}_{50}$  concentration of each compound for 72 hours. Culture media were collected and cells were washed with cold PBS. Cells were treated with accutase at 37  $^{\circ}\text{C}$  for 5 minutes to completely detached them and the collected cells were centrifuged at 1000 rpm. The cells were resuspended in 1x binding buffer to give a final concentration of  $1.0 \times 10^6$  cells/ml. 100  $\mu\text{L}$

of FITC Annexin V and 5  $\mu$ L PI were added. The cells were mixed gently and incubated for 15 minutes at room temperature in the dark. 400  $\mu$ L of 1x binding buffer was added to each tube and analyzed immediately with a Becton-Dickinson FACS-Calibur flow cytometer.

For cell cycle analysis, different sets of HONE-1 cells ( $0.45 \times 10^6$ ) were incubated with or without  $IC_{50}$  concentration of each zinc(II) complexes (**7** and **10**) in 60 mm dishes for 24 hours. Washing, trypsination, centrifugation and resuspension in PBS were carried out as in apoptosis study. Cell count was performed with Countess® Automated Cell Counter. Cell concentration was adjusted to  $0.5-1.0 \times 10^6$  cells/mL, and then centrifuged at 1000 rpm for 5 minutes. The supernatant was discarded and mixed well with 300  $\mu$ L of hypotonic DNA staining buffer (0.25 g sodium citrate, 0.75 mL Triton-X 100, 0.025 g propidium iodide, 0.005 g ribonuclease A and 250 mL distilled water). Filtered samples, with minimum of 20,000 cells per sample, were kept at 4 °C in the dark for at least 10 minutes before analysis with Beckton-Dickinson FACS-Calibur Fluorescence Activated Cell Sorter with a Cell Quest Pro software. The percentages of cells in cell cycle phases  $G_0/G_1$  (resting), S (DNA synthesis) and  $G_2/M$  (mitotic cells) obtained and recorded using ModFit LT™ software (Verity Software House, Inc. ME).

## 7.3 RESULTS AND DISCUSSION

### 7.3.1 DNA binding studies

As in Chapter 6, ethidium bromide and thiazole-orange quenching assays were used to find the DNA binding affinity and sequence selectivity of  $[\text{Zn}(\text{phen})(\text{dipico})(\text{H}_2\text{O})]\cdot\text{H}_2\text{O}$  **7** and  $[\text{Zn}(\text{phen})(\text{L-thr})(\text{H}_2\text{O})\text{Cl}]\cdot 2\text{H}_2\text{O}$  **10**. Using these assays, the apparent binding constants of complexes **7** and **10** for different duplex oligonucleotides and G-quadruplex (G-4) were determined and calculated (**Table 7.1**). A higher value for the binding constant indicates the metal complexes have a greater binding affinity and preference for the given duplex. Only complex **7** has distinctly higher binding constant for  $\text{ds}(\text{AT})_6$  than for  $\text{ds}(\text{CG})_6$  (1.7x), indicating greater affinity for  $\text{ds}(\text{AT})_6$  than  $\text{ds}(\text{CG})_6$  (**Table 7.1**). Other metal complexes which bind preferentially to AT-sequence are also known (Eriksson et al., 1994; Franklin et al., 1996; Wheate and Collins, 2000; Kikuta et al., 1999; Patra et al., 2007; Rajendiran et al., 2008). There does not seem to be any easily recognisable common feature(s) among these metal complexes, as can be seen from examples such as  $[\text{Cu}(\text{L-arg})_2]\text{NO}_3$ ,  $[\text{Cu}(\text{L-arg})(\text{phen})\text{Cl}]\text{Cl}$ ,  $[\text{Pt}(\text{en})_2]^{2+}$ ,  $[\text{Ru}(\text{phen})_3]^{2+}$  and  $[\text{Zn}(\text{cyclen-derivatives})]^{2+}$ . As mentioned earlier in section 7.1, dipicolinate ligand has two H-acceptor sites whereas L-threoninate has both H-acceptor and H-donor sites. Hence, both complexes **7** and **10** are expected to have different DNA binding ability. However, there seems to be very minor effect of changing the subsidiary ligand on the DNA binding affinity of the ternary Zinc(II)-phen complexes as both complexes **7** and **10** have similar binding constants for

ds(AT)<sub>6</sub>, ds(CG)<sub>6</sub>, ds(CGCGAATTCGCG)<sub>2</sub>, ds(CGCGATATCGCG)<sub>2</sub>, G-4 and the corresponding duplex of G-4.

**Table 7.1:** Binding constants for various duplexes and G-4 (with standard deviations < ±0.1)

	<b>7</b> (10 <sup>4</sup> M <sup>-1</sup> )	<b>10</b> (10 <sup>4</sup> M <sup>-1</sup> )
ds(AT) <sub>6</sub>	3.0	2.2
ds(CG) <sub>6</sub>	1.8	1.8
ds(CGCGAATTCGCG) <sub>2</sub>	1.6	1.2
ds(CGCGATATCGCG) <sub>2</sub>	2.0	1.8
G-4 (5'-AGGGTTAGGGTTAGGGTTAGGG-3')	2.5	2.1
duplex mimic of G-4 (5'-CCAGTTCGTAGTAACCC-3') (3'-GGTCAAGCATCATTGGG-5')	2.0	1.7

### 7.3.2 Restriction Enzyme (RE) inhibition

In the previous chapter, restriction enzyme (RE) inhibition assay was used to investigate the effect of number of chelated maltolate in Co(II) complexes, **1** and **4**, on their binding specificity. Restriction enzyme inhibition results showed that the binding specificity of complexes **1** and **4** are totally different. As in chapter 6, restriction enzyme inhibition was used to investigate the binding specificity difference between complexes **7** and **10**. Restriction enzyme inhibition assay has been successfully used to show sequence selective binding of Pt(II) and Ru(II) complexes by other researchers (Gallori et al., 2000; Nakabayashi et al., 2001; Snow and Sheardy, 2001; Rahman et al., 2007). The same twelve restriction enzymes as listed in chapter 6, section 6.3.2 were used. ZnCl<sub>2</sub> and phen could not inhibit any of the REs (**Appendices 7.1-7.2**). However, all the REs can be inhibited by thiazole orange, an intercalator fluorescent dye and a random site binder (**Appendix 7.3**),

suggesting the non-discriminating binding of these intercalator dyes at all the sites.

Unlike intercalator dye, complex **7** could only inhibit Ssp I and Nde I (**Appendix 7.4**). In contrast, complex **10** could inhibit only Ase I, Ssp I, Nde I and Bst 11071, suggesting binding of at least one molecule of complex **10** to the six base pair recognition sequence of each of these REs, and its binding selectivity for the sequences recognised by these four REs (**Appendix 7.5**) (Gallori et al., 2000; Snow and Sheardy, 2001; Nakabayashi et al., 2006; Rahman et al., 2007). By changing the subsidiary ligand from L-threoninate to dipicolinate, the binding selectivity of the ternary zinc-phen complex (**Table 7.2**) is greatly enhanced. Both complexes **7** and **10** could inhibit Ssp I and Nde I, hence, it is reasonable to ascribe this ability to the coordinated phen ligand which confers recognition of nucleotide binding sequences of these REs to complexes **7** and **10**. Interestingly, complex **10** is able to discriminate the palindromic sequences 5'-CATATG-3' (Nde I) and 5'-GTATAC-3' (Bst 11071), which are dissimilar in terms of their orientation. In order to find out whether binding of Zn(II) complexes to the RE could result in enzymatic inhibition, two tests were carried out. The circular dichroism spectrum of the RE remained unchanged when incubated with Zn(II) complexes, suggesting no binding of complex or no effect on conformation of RE. In addition, changing the sequence of mixing to RE with Zn(II) complexes first before adding the DNA produced the same inhibition result. Gallori et al. (2000) had also previously demonstrated that Ru(II) complex bound to DNA, not free Ru(II)

complex, was responsible for RE inhibition.

**Table 7.2:** Restriction enzyme inhibition for Zn(II) complexes

RE	Sequence	7	10
Tsp 509I	5'—↓AATT—3' 3'—TTAA↑—5'		
Hae III	5'—G C ↓G C —3' 3'—C G ↑C G —5'		
Sal I	5'—G ↓T C G A C—3' 3'—C A G C T ↑G—5'		
Pst I	5'—C T G C A ↓G—3' 3'—G ↑A C G T C—5'		
Pvu II	5'—C A G ↓C T G—3' 3'—G T C ↑G A C—5'		
Sca I	5'—A G T ↓A C T—3' 3'—T C A ↑T G A—5'		
Ase I	5'—A T ↓T A A T—3' 3'—T A A T ↑T A—5'	√	√
Ssp I	5'—A A ↓T A T T—3' 3'—T T A T ↑A A—5'		√
Mun I	5'—C ↓A A T T G—3' 3'—G T T A A ↑C—5'		
EcoR I	5'—G ↓A A T T C—3' 3'—C T T A A ↑G—5'		
NdeI	5'—C A ↓T A T G—3' 3'—G T A T ↑A C—5'	√	√
Bst 11071	5'—G T A ↓T A C—3' 3'—C A T ↑A T G—5'		√

### 7.3.3 Human topoisomerase I inhibition

Topoisomerase I (Topo I) and Topoisomerase II (Topo II) inhibitors have been reported to be among the most widely used clinical drugs for treatment of cancer and their inhibition can lead to apoptosis (Rothenberg, 1997; Beretta et al., 2008; Teicher, 2008; Pommier, 2008; Sunami et al., 2009; Arjmand et al., 2010; Chashoo et al., 2011). These topoisomerases play an important role in biological processes, such as DNA replication during mitosis, by respectively introducing single or double transient breaks in the DNA strands (Wang et al., 1998). Topo I unwinds duplex DNA by repeated single-

strand cut, passing the other strand through the cutting site and finally religating the cut strand. In the Topo I inhibition assay, 1 unit of human Topo I can convert all the plasmid pBR322 into fully relaxed DNA topoisomers which appear as the usual slowest moving nicked DNA band (**Appendix 7.6: A and B, lane 5**) (Seng et al, 2010). At 80  $\mu\text{M}$ , both complexes **7** and **10** partially inhibited Topo I as a smear of faster moving, overlapping bands of less relaxed topoisomers can be seen (**Appendix 7.6, lane 8**). When the concentration of complexes was increased to 120  $\mu\text{M}$ , both complexes could almost totally inhibit the Topo I as the DNA pattern now appears as mainly closed circular, supercoiled DNA band and a thin nicked open circular DNA band, as is observed for the untreated DNA (**Appendix 7.6, A and B lane 9**). This inhibition of Topo I and the preceding discovery of possible sequence-selective binding of complexes **7** and **10** to DNA is akin to the recent realisation that topoisomerase inhibitor of organic origin also has sequence-selective activity as evidenced by stabilization of topoisomerase-DNA cleavage complexes at specific sites (Capranico et al., 1997; Arimondo et al., 2006; Rao et al., 2007).

#### **7.3.4 Anticancer studies**

According to American Cancer Society, nasopharyngeal cancer (NPC) is a cancer that starts in the nasopharynx. Nasopharynx (**Figure 7.1**) is the upper part of the throat behind the nose and near the base of the skull. It is a common cancer in southern China, Malaysia and other Southeast Asian

countries (Sung et al., 2005). Almost all cases of NPC worldwide are associated with Epstein-Barr virus (EBV) (American Cancer Society, 2012). The link between EBV infection and NPC is complicated and not yet completely understood. NPC has high invasive-cum-metastatic tendency and intense inflammatory tumour microenvironment (Wong et al., 2010). Recurrence and distant metastasis are still the main causes of NPC deaths despite aggressive treatment involving concurrent chemo-radiotherapy (Wong et al., 2010). Two NPC cell lines were screened, *viz.* HK1 which is highly differentiated squamous cell carcinoma from a Chinese male patient, and HONE-1 which is poorly differentiated squamous cell carcinoma (Glaser et al., 1989; Wong et al., 2010). HONE-1 cell line was previously used to confirm relationship of NPC metastasis and antiapoptotic B cell lymphoma-2 (bcl-2) protein expression, which is a biomarker of poor prognosis with current therapy and whose over expression in NPC confers chemoresistance (Gulley et al., 1998; Dolcetti and Menezes, 2003). Bcl-2 was also previously found to be highly over expressed in HK1 cells (Gulley et al., 1998). Both HK1 and HONE-1 are EBV-negative cell lines (Glaser et al., 1989; Wong et al., 2010). Interestingly, there exists a strong link between infection with EBV and undifferentiated nasopharyngeal carcinoma (Schobert et al., 2011). Cancers from Hong Kong tended to be less differentiated and more frequently associated with EBV (To et al., 2009).

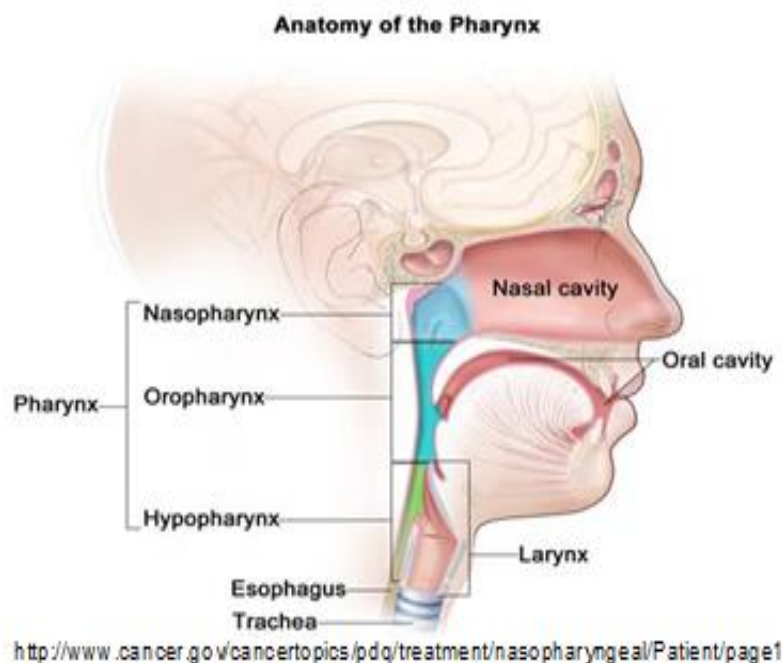


**Figure 7.1:** Anatomy of the pharynx (taken from National Cancer Institute)

Both Zn(II) complexes **7** and **10**, and cisplatin were tested against the above two cancer cell lines and one non-cancer cell line, NP69 by using MTT antiproliferative assay. From the results obtained, both complexes **7** and **10** were more efficient than cisplatin, by a factor of ~2-4, in inhibiting the proliferation of HONE-1 and HK1 cancer cells. Interestingly, both complexes **7** and **10** were more antiproliferative towards HK1 cells than HONE-1 cells (by 2x or 4x). To quantitatively compare the selectivity of these complexes for cancer cells over normal cells and to show practical clinical applicability, their therapeutic indices (TI) [ $TI = IC_{50}(NP69)/IC_{50}(HK1 \text{ or } HONE-1)$ ] were calculated and these are partially shown for HK1 in **Table 7.3** (Wang et al., 2006).

A tested drug with TI value greater than 1 shows selectivity. Higher TI value shows higher selectivity and better safety. TI values of complexes **7** and **10** against HONE-1 are less than 1 (values not shown), showing their non-selectivity. Cisplatin, a clinical anticancer drug with some harmful side effects, is cytotoxic and not selective against both cancer cell lines over corresponding normal cell line. In fact, cisplatin has been previously reported to be highly cytotoxic to normal nasopharyngeal cell lines (SUNE1, CNE2, C666-1, NP69) than cancer nasopharyngeal cell lines (CCD19Lu, PBMC) (Cao et al., 2010; Ghosh et al., 2011). However, complexes **7** and **10** are selective against HK1 over NP69. As HK1 cells and most human epithelial carcinomas have very high expression of epithelial growth factor receptor (EGFR) and there is correlation between high EGFR level with more aggressive phenotype, resistance to treatment and poor prognosis, these two Zn(II) complexes are good candidates for further development into NPC anticancer drugs (Sung et al., 2005).

When MTT assay was performed for treatment of NPC HONE-1 cells with complexes **7** ( $IC_{50}$ , 4.5  $\mu$ M), **10** ( $IC_{50}$ , 5.6  $\mu$ M), and cisplatin ( $IC_{50}$ , 12  $\mu$ M) for 72 h, phen and  $[Zn(phen)Cl_2]$  were included in the study. A similar  $IC_{50}$  value (8.10  $\mu$ M) for cisplatin was previously obtained (Heffeter et al., 2006). The  $IC_{50}$  values of phen and  $[Zn(phen)Cl_2]$  are 10.3 and 4.0  $\mu$ M. Chelating the phen to Zn(II) in the three Zn(II) complexes clearly enhanced its antiproliferative property. Both complexes **7** and **10** are more antiproliferative towards HONE-1 than cisplatin.

**Table 7.3:** IC<sub>50</sub> values of incubating cancer and non cancer nasopharyngeal cells with compounds for 72 hours

	<b>HONE-1</b>	<b>HK1</b>	<b>NP69</b>	<b>NP69/HK1</b>
<b>7</b>	4.5	2.3	4.5	1.9
<b>10</b>	5.6	1.3	5.1	3.9
cisplatin	12	4.9	4.9	1

Recently, Liguori et al. (2010) synthesised a series of ternary Zn(II) complexes with *N,N*-chelating ligand (4,4'-dinonyl-2,2'-bipyridine) as main ligand and different diketonate (tropoloid) as subsidiary ligand, and found that they were antiproliferative against various human prostate cancer cell lines with IC<sub>50</sub> (3 to >100 μM) values which were dependent on the subsidiary ligand. Here, apoptosis and cell cycle arrest were not investigated. However, a recently synthesised Zn(II) complex of N-(2-hydroxyacetophenone)glycinate was found to have poor antiproliferative property against various T-lymphoblastic leukemia cell lines (IC<sub>50</sub> > 500 μM, 72 hours incubation) (Stanojkovic et al., 2010). Obviously, the choice of ligand(s) is crucial for the efficacy of Zn(II) complexes as anticancer agents.

In cytotoxic drug treatment, most of the cell death is due to apoptosis (Stanojkovic et al., 2010). Hence, flow cytometry was used to find out the cause(s) of decrease in HONE-1 cell viability by complexes **7** and **10**, phen, [Zn(phen)Cl<sub>2</sub>] and cisplatin at IC<sub>50</sub> concentrations for 72 hours incubation.

Percentage of necrotic cells found for cancer cells treated with all these compounds is less than 4% which is comparable to that found in untreated cells (Figures 7.2 and 7.3). The % apoptotic cells induced by complexes 7, 10, phen, [Zn(phen)Cl<sub>2</sub>] and cisplatin are 31, 55, 38, 54 and 69 respectively. Thus, these compounds kill the cancer cells by inducing apoptosis. Based on % apoptotic cells induced, complex 10 and [Zn(phen)Cl<sub>2</sub>] are equally cytotoxic, and they are both more cytotoxic than complex 7.

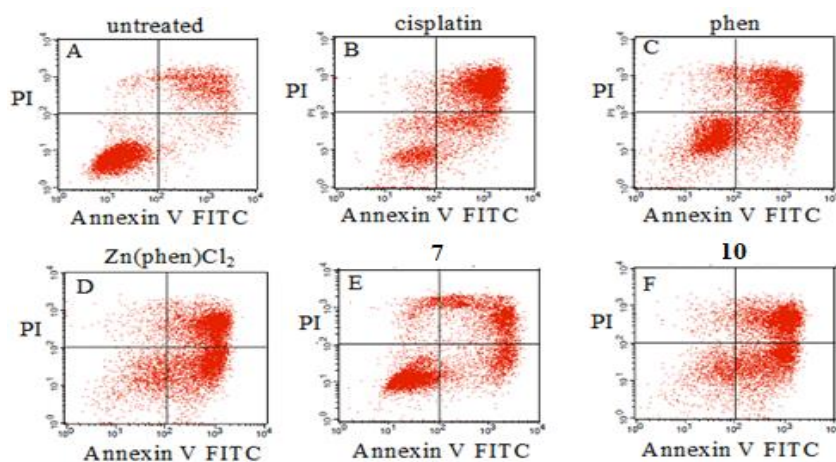


**Figure 7.2:** Apoptosis analysis of HONE-1 cells untreated (A) or treated for 72 hours with IC<sub>50</sub> concentration of cisplatin (B), phen (C), [Zn(phen)Cl<sub>2</sub>] (D), 7 (E) and 10 (F).

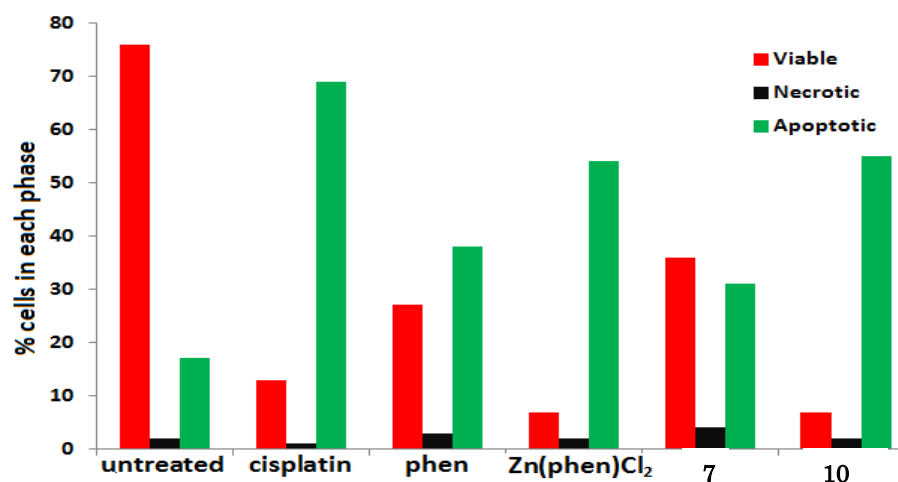


**Figure 7.3:** % viable cells, necrotic cells and apoptotic cells for HONE-1 treated with test compounds.

Since inhibition of cancer cell proliferation could result from induction of apoptosis and/or cell cycle arrest, cell cycle analysis was carried out for HONE-1 cells treated with IC<sub>50</sub> concentration of complexes **7** and **10**. Compared to untreated cells, cells treated with complex **7** for 24 hours resulted in an increase in S phase population from 46.9% to 65.6% while the G<sub>2</sub>/M phase population decreased significantly. In the presence of complex **10**, G<sub>0</sub>/G<sub>1</sub> population increased from 37.7% to 72.8% while the S phase population decreased significantly. Therefore, complexes **7** and **10** could induce cell cycle arrest in HONE-1 cells at S and G<sub>0</sub>/G<sub>1</sub> phases respectively (**Figure 7.4**).

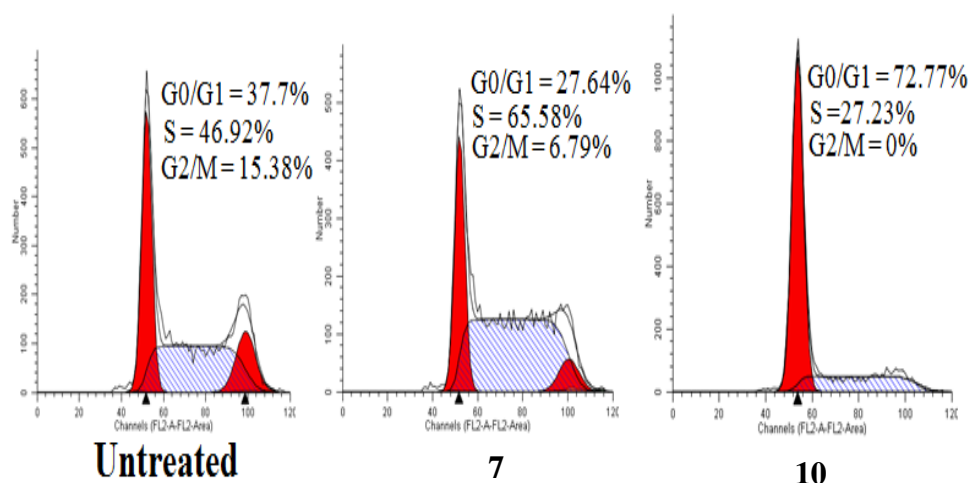


**Figure 7.4:** Cell cycle analysis of HONE-1 cells untreated and treated with **7** and **10** for 24 hours.

Von and colleagues (2012) have treated KB-3-1 cancer cells (cervix) with 5  $\mu$ M [*Tris*(1,10-phenanthroline)lanthanum(III)] trithiocyanate for 8 hours, it underwent a massive block in G<sub>0</sub>/G<sub>1</sub> phase while corresponding cells treated with 5  $\mu$ M 1,10-phenanthroline for 24

hours underwent a modest arrest in S phase. Cell cycle arrest at S phase implies inhibition of DNA synthesis by complex **7** whereas cell cycle arrest at G<sub>0</sub>/G<sub>1</sub> is often the result of respective cell cycle checkpoint activation due to DNA damage (Von et al., 2012). In contrast to the present Zn(II) complexes **7** and **10**, two previously reported Zn(II) complexes containing the same 2-acetyl pyridine 1-(4-fluorophenyl)piperazinyl thiosemicarbazone induced cell cycle arrest at S phase for K562, HeLa and MDA-MB-453 cancer cell lines while they caused MDA-MB-361 cancer cells to arrest at G<sub>0</sub>/G<sub>1</sub> (Von et al., 2012). However, the change in subsidiary ligand in ternary Zn(II)-phen complexes (*i.e.* complexes **7** and **10**) is responsible for alteration in cell cycle arrest in the same cancer cell line.

#### **7.4 CONCLUSION**

By changing the subsidiary ligand from dipicolinate to L-threoninate ligand, binding affinity of both Zn(II) complexes for ds(AT)<sub>6</sub> and ds(CG)<sub>6</sub> is moderated. Apparently, complex **7** bind preferentially to AT-sequence. However, both Zn(II) complexes have insignificant effect for other DNA duplexes and G-quadruplex tested. Although both complexes show DNA binding selectivity by inhibiting some REs, complex **7** bind more selectively than complex **10**. The degree of antiproliferation, percentage induced apoptosis and the phase at which cell cycle arrest occurs in HONE-1 cancer cells are also affected by the nature of the subsidiary ligand. However, no distinct difference in topoisomerase I inhibition is observed.

**CHAPTER 8**

**GENERAL CONCLUSION**

**SYNTHESIS, CHARACTERISATION AND BIOLOGICAL  
PROPERTIES OF METAL(II) POLYPYRIDYL COMPLEXES WITH  
*OO'*-, *ONO'*- OR *NO*-CHELATING COLIGANDS**

## CHAPTER 8

### GENERAL CONCLUSION

This project has two parts, *viz.* the synthesis and characterization of three series of ternary metal(II) complexes and the biological study of some of these metal(II) complexes. The complexes are (i) maltolato complexes ( $[M(\text{phen})(\text{ma})\text{Cl}] \cdot x\text{H}_2\text{O}$  ( $M = \text{Co}, \text{Cu}$  or  $\text{Zn}$ ) and  $[\text{Co}(\text{phen})(\text{ma})_2] \cdot 5\text{H}_2\text{O}$ ), (ii) dipicolinato complexes ( $[M(\text{phen})(\text{dipico})(\text{H}_2\text{O})] \cdot x\text{H}_2\text{O}$  ( $\text{Co}$  or  $\text{Zn}$ ) and  $\{[\text{Cu}_2(\text{phen})_3(\text{dipico})(\text{H}_2\text{O})][\text{Cu}(\text{dipico})_2] \cdot [(11\text{H}_2\text{O})(\text{CH}_3\text{OH})]\}$ ) and (iii) threoninato complexes ( $[M(\text{phen})(\text{AA})(\text{H}_2\text{O})\text{Cl}] \cdot x\text{H}_2\text{O}$  ( $M = \text{Cu}$  or  $\text{Zn}$ ;  $\text{AA} = \text{L-thr}$  or  $\text{D-thr}$ ). There are two parts in the characterization studies (**Table 1.1**), *viz.* the characterization of the solids of complexes (solid state) and the characterization of aqueous solutions of complexes. Analysis of the data (FT-IR, CHN elemental analysis and X-ray (if any)) of the solid complexes suggests that the three series of ternary metal(II) complexes were successfully prepared. Based on the elemental analyses, molecular formulae of the synthesised metal(II) complexes are  $[\text{Co}(\text{phen})(\text{ma})\text{Cl}] \cdot 4\text{H}_2\text{O}$  **(1)**,  $[\text{Cu}(\text{phen})(\text{ma})\text{Cl}] \cdot \frac{1}{2}\text{H}_2\text{O}$  **(2)**,  $[\text{Zn}(\text{phen})(\text{ma})\text{Cl}] \cdot 1\frac{1}{2}\text{H}_2\text{O}$  **(3)**,  $[\text{Co}(\text{phen})(\text{ma})_2] \cdot 5\text{H}_2\text{O}$  **(4)**,  $[\text{Co}(\text{phen})(\text{dipico})(\text{H}_2\text{O})] \cdot 2\text{H}_2\text{O}$  **(5)**,  $\{[\text{Cu}_2(\text{phen})_3(\text{dipico})(\text{H}_2\text{O})][\text{Cu}(\text{dipico})_2] \cdot [(11\text{H}_2\text{O})(\text{CH}_3\text{OH})]\}$  **(6)**,  $[\text{Zn}(\text{phen})(\text{dipico})(\text{H}_2\text{O})] \cdot \text{H}_2\text{O}$  **(7)**,  $[\text{Cu}(\text{phen})(\text{AA})(\text{H}_2\text{O})\text{Cl}] \cdot 2\text{H}_2\text{O}$  **(8 - 9)** and  $[\text{Zn}(\text{phen})(\text{AA})(\text{H}_2\text{O})\text{Cl}] \cdot 2\text{H}_2\text{O}$  **(10 - 11)** (where  $\text{AA} = \text{L-thr}$  or  $\text{D-thr}$ ). Analysis of FTIR spectra also helped to established the presence of chelated 1,10-phenanthroline and coligands (maltolate, dipicolinate, L-threoninate and

D-threoninate).

This study has gathered some important information regarding the effect of number of chelated maltolato ligands, changing coligand and changing metal(II) ion of the ternary metal(II) complexes on the solid and solution properties. As discussed in Chapter 3, the number of chelated maltolato ligands influence the geometrical structure of the metal(II) complexes. With one coordinated maltolato ligand,  $[\text{Co}(\text{phen})(\text{ma})\text{Cl}] \cdot 4\text{H}_2\text{O}$  **1** has a square pyramidal geometry. However,  $[\text{Co}(\text{phen})(\text{ma})_2] \cdot 5\text{H}_2\text{O}$  **4**, with two coordinated maltolato ligands, has an octahedral geometry. Apparently, the number of chelated maltolato ligands not only affected the structural geometry but also the electrolytic nature of complex **1** (1:1 electrolyte) and complex **4** (non-electrolyte). The intensities of FL emission of complex **1** is slightly higher than complex **4**. Thus, the structural geometry and number of coordinated maltolato ligands affected the FL emission intensity. In addition, changing the type of metal(II) ion also influence the FL emission intensity but not the  $\lambda_{\text{max}}$  and shape of the FL emission bands. It was found that Co(II) and Cu(II) have quenching ability while Zn(II) ion enhanced the FL emission intensity of the coordinated phen. Hence, FL emission studies of complexes **1** - **4** revealed that FL emission intensity is affected by structural geometry, number of coordinated maltolato ligands and type of metal(II) ion.

The effect of changing the type of metal(II) ion on the solution properties of the set of metal(II)-phen-dipicolinate complexes was discussed in Chapter 4. Both  $[\text{Co}(\text{phen})(\text{dipico})(\text{H}_2\text{O})]\cdot 2\text{H}_2\text{O}$  **5** and  $[\text{Zn}(\text{phen})(\text{dipico})(\text{H}_2\text{O})]\cdot \text{H}_2\text{O}$  **7** are mononuclear complexes. Aqua, phen and dipico ligands are coordinated to the metal(II) center (Co(II) or Zn(II)), forming distorted octahedral complexes. The structure of both phen and dipico (planarity, rigidity and denticity) and limited span width of both carboxylate ligating atoms (O(1) and O(3)) of dipico causes complex **7** to be highly distorted.  $[\text{Cu}_2(\text{phen})_3(\text{dipico})(\text{H}_2\text{O})][\text{Cu}(\text{dipico})_2]\cdot[(11\text{H}_2\text{O})(\text{CH}_3\text{OH})]$  **6** is a trinuclear ionic compound consisting of a  $[\text{Cu}_2(\text{phen})_3(\text{dipico})(\text{H}_2\text{O})]^{2+}$  cation and a  $[\text{Cu}(\text{dipico})_2]^{2-}$  anion. The dicopper(II) cation  $[\text{Cu}_2(\text{phen})_3(\text{dipico})(\text{H}_2\text{O})]^{2+}$  has a distorted square pyramidal geometry about each copper, and the counter anion  $[\text{Cu}(\text{dipico})_2]^{2-}$  has a distorted octahedral geometry about the copper atom. Both complexes **5** and **7** exist as neutral complex species in aqueous solution and complex **6** is a 1:1 electrolyte. The low molar conductivity ( $37 - 43 \Omega^{-1} \text{ cm}^2 \text{ mol}^{-1}$ ) of complex **6** compared to theoretical values ( $75 - 95 \Omega^{-1} \text{ cm}^2 \text{ mol}^{-1}$ ) is due to the low mobility of bulky cations and anions of an ionic compound in the solution. Similar to other phen based complexes in this chapter, the UV absorption peak is due to  $\pi \rightarrow \pi^*$  transition of the coordinated phenanthroline ligand. FL emission intensities of the coordinated phen increases in the following order: **6** < **5** < phen < **7**. Zn(II) enhances the FL of the coordinated phen while Co(II) and Cu(II) partially quenches the FL of the coordinated phen. Once again, it shows that the type of metal(II) ion influences the FL emission intensities of ternary metal(II) complexes of phen.

However, in changing the coligand in  $[M(\text{phen})(\text{AA})(\text{H}_2\text{O})\text{Cl}]\cdot 2\text{H}_2\text{O}$  ( $M = \text{Cu}$  or  $\text{Zn}$ ) **8 - 11** from L-threonine to D-threonine, there are no significant differences observed for each enantiomer pair of complexes in their FTIR spectra, CHN data, UV-Visible absorption, FL emission, molar conductivity, ESI-MS and TGA except for 3D supramolecular framework and circular dichroism spectrum. In the solid state, complexes **8 - 11** have a similar distorted octahedral geometry. The crystal packing of non-chiral molecules are superimposable at the same axis. Interestingly, the crystal packing of both pairs of Cu(II) and Zn(II) enantiomers show a mirror image in the direction of  $a$ -axis. This suggests that the chirality of each of complexes **8 - 11** is controlled by the chirality of the coligand (L-threoninato and D-threoninato). The CD spectra of each pair of Cu(II) and Zn(II) enantiomers are mirror-image of each other and this proves that the enantiomeric pairs for both Cu(II) and Zn(II) complexes were successfully prepared. It is important to highlight that a change in the type of metal(II) ion (Co(II), Cu(II) or Zn(II)) influence the FL emission intensity but not the  $\lambda_{\text{max}}$  and the shape of the bands. Among all three types of metal ion mentioned earlier, it is found that Zn(II) ion enhanced the FL emission intensity of phen whereas Co(II) and Cu(II) ions have different quenching of the FL intensity of phen. The chirality of the threoninate coligand of  $[M(\text{phen})(\text{AA})(\text{H}_2\text{O})\text{Cl}]\cdot 2\text{H}_2\text{O}$  ( $M = \text{Cu}$  or  $\text{Zn}$ ) **8 - 11** does not seem to have an influence on the FL emission intensities. Each enantiomer pair of Cu(II) and Zn(II) complexes is found to undergo dehydration at an early stage of its thermal degradation.

Two sets of metal(II) complexes, viz. Co(II) ([Co(phen)(ma)Cl]·4H<sub>2</sub>O **1** and [Co(phen)(ma)<sub>2</sub>]·5H<sub>2</sub>O **4**), and Zn(II) ([Zn(phen)(dipico)(H<sub>2</sub>O)]·H<sub>2</sub>O **7** and [Zn(phen)(L-thr)(H<sub>2</sub>O)Cl]·2H<sub>2</sub>O **10**), have been studied for their biological properties. The results have been presented and discussed in Chapters Six and Seven. As both Co(II) complexes, **1** and **4** have higher binding affinity for ds(AT)<sub>6</sub> (**1**: 2.176 × 10<sup>4</sup> M<sup>-1</sup>; **4**: 2.563 × 10<sup>4</sup> M<sup>-1</sup>) than for ds(CG)<sub>6</sub> (**1**: 1.823 × 10<sup>4</sup> M<sup>-1</sup>; **4**: 1.791 × 10<sup>4</sup> M<sup>-1</sup>), they are said to have more binding selectivity towards AT-sequences than CG-sequences. The greater binding constants for both complexes **1** and **4** towards ds(CGCGATATCGCG)<sub>2</sub> (**1**: 1.776 × 10<sup>4</sup> M<sup>-1</sup>; **4**: 1.782 × 10<sup>4</sup> M<sup>-1</sup>) over the ds(CGCGAATTCGCG)<sub>2</sub> (**1**: 1.217 × 10<sup>4</sup> M<sup>-1</sup>; **4**: 1.474 × 10<sup>4</sup> M<sup>-1</sup>), suggest greater binding preference or selectivity for ATAT-sequence over AATT-sequence. Interestingly, the binding constant of complex **4** towards G-4 is nine times greater than complex **1**. It is important to highlight that both Co(II) complexes, **1** and **4** are found to exhibit different binding affinity and selectivity towards different types of duplex DNA. Restriction enzyme inhibition and topoisomerase I inhibitory behavior of both complexes **1** and **4** are also found to be different. The different binding specificity and recognition of DNA of complexes **1** and **4** can be ascribed to the number of coordinated maltolate ligand. Both Co(II) complexes, **1** and **4** shows antiproliferative activity towards cancer cell line MCF7, with IC<sub>50</sub> values of 75 and 55 μM respectively. The antiproliferative property of both complexes is cell-type dependent. The number of chelated maltolate ligands of Co(II) complexes seems to influence their binding specificity, recognition and antiproliferative property.

Changing the type of coligand from dipicolinato (two H-acceptor sites) to L-threoninato (H-acceptor and H-donor sites) in the Zn(II) complexes, *i.e.* [Zn(phen)(dipico)(H<sub>2</sub>O)]·H<sub>2</sub>O **7** and [Zn(phen)(L-thr)(H<sub>2</sub>O)Cl]·2H<sub>2</sub>O **10**, are expected to have different binding affinity. However, the results disprove the proposed hypotheses as no significant difference is found in their binding affinity towards ds(AT)<sub>6</sub>, ds(CG)<sub>6</sub>, ds(CGCGAATTCGCG)<sub>2</sub>, ds(CGCGATATCGCG)<sub>2</sub>, G-4 and the corresponding duplex of G-4. Surprisingly, both complexes **7** and **10** shows DNA binding selectivity by inhibiting some REs. Complex **7** is found to bind more selectively than complex **10** as complex **10** can inhibit Ase I, Ssp I, Nde I and Bst 11071 while complex **7** can only inhibit Ssp I and Nde I. A change of coligand from L-threoninato to dipicolinato, seems to enhance their binding specificity.

Both zinc(II) complexes, **7** and **10** are found to be able to inhibit topoisomerase I. However, there is no significant difference in their topoisomerase I inhibition.

For both Zn(II) complexes, **7** and **10**, it is found that both have better anticancer activity than cisplatin against HK1 (**7**: 4.5 μM; **10**: 5.6 μM; cisplatin: 12 μM) and HONE-1 cancer cell lines (**7**: 2.3 μM; **10**: 1.3 μM; cisplatin: 4.9 μM). Both complexes **7** and **10** were 2x or 4x more antiproliferative towards HK1 cells than HONE-1 cells. The % apoptotic cells induced by complexes **7** and **10** are 31 and 55 respectively. These two Zn(II)

complexes killed the cancer cells by inducing apoptosis. The % apoptotic cells indicate that complex **10** is more cytotoxic than complex **7**. Cell cycle analysis suggested that complex **7** could induce cell cycle arrest in HONE-1 cells at S phase. However, the other Zn(II) complex, **10** induced cell cycle arrest in HONE-1 cells at G<sub>0</sub>/G<sub>1</sub> phase. A change of coligand in ternary Zn(II) complexes seems to alter the cell cycle arrest in the same cancer cell line. In conclusion, a change of type of coligand of Zn(II) complexes is found to be a factor in influencing their DNA recognition and antiproliferative properties.

Overall analysis of all the metal(II) complexes in this study shows retention of some properties of the phen although the type of coligand (*OO'*-maltolate, *ONO'*-dipicolinate, *NO*-L-threoninate or *NO*-D-threoninate) changed. The UV peaks (~ 226 nm and ~ 269 nm) of all the metal(II) complexes, **1** - **11**, arose from  $\pi \rightarrow \pi^*$  transition of the coordinated phenanthroline ligand. Besides, a change of the type of coligand did not affect the  $\lambda_{\text{max}}$  and the shape of the FL peaks of complexes **1** - **11**. However, changing the type of metal(II) ion was found to change the FL emission intensity. This study revealed that Co(II) and Cu(II) quenched the FL emission intensity of phen but Zn(II) ion enhanced it. The quenching mechanism is ascribed to static quenching and the enhancement is attributed to the full d<sup>10</sup> electron configuration of the Zn(II) ion. In general, FL emission intensities of metal(II) complexes in terms of increasing order as follow: Cu(II) complexes < Co(II) complexes < phen < Zn(II) complexes. Additionally, a change of coligand was found to influence the DNA binding, molecular recognition

capability and antiproliferative property of “metal-phen-coligand complexes” as mentioned in Chapters 6 and 7.

In conclusion, the type of metal(II) ion, coligand and the number of coordinated ligands were found to affect only some of the physical properties of the synthesized metal complexes. Similar effects are also found in the biological properties of the studied metal(II) complexes. This work has provided some information on the structure activity relationship (SAR) of transition metal complexes from a biological/biomedical science perspective. These results will be useful in the future exploration of the potential use of transition metal complexes in life science.

For future study, other *OO'*-, *ONO'*- and *NO*-coligands can be assembled to study their solid and solution properties. In the present work, enantiomeric pair of metal(II) complexes were synthesized and characterized in their solid and solution states but it does not cover their biological studies. The biological studies of enantiomeric pair of metal(II) complexes are limited, hence, future work should include it. The interaction of metal(II) complex with proteins is an interesting research topic as its mechanisms is not clearly understood. Recently, molecular docking plays an important role in rational design of drugs. Molecular docking is a computational simulation to monitor the molecular recognition process. There are several molecular docking programs such as GOLD suite, DOCK, FlexX, GLIDE, ICM, PhDOCK, and

Surflex which are available in the market. It is useful to determine the interaction of metal(II) complexes with proteins and to predict their strength of binding affinity and the detailed interactions between metal complexes and proteins. Besides, nuclear magnetic resonance spectroscopy (NMR) can also be used to study the interaction between metal(II) complex and proteins. Hence, in future studies, molecular docking and NMR spectroscopy methods can be use to find out the interaction between metal(II) complexes and proteins. Complexes **7** and **10** under this study are recommended for further investigation for treatment of cancers with high expression of topoisomerase I, antiapoptotic Bcl-2 protein and those diagnosed with high EGFR level. This will be a potential direction for future work since Zn(II) complexes that have anticancer properties are rare.

## REFERENCES

- Abdel-Rahman, L.H., Battaglia, L.P. and Mahmoud, M.R., 1996. Synthesis, characterization and stability constant determination of L-phenylalanine ternary complexes of cobalt(II), nickel(II), copper(II) with N-heterocyclic aromatic bases and X-ray crystal structure of aqua-1,10-phenanthroline-L-phenylalaninatocopper(II) perchlorate complex. *Polyhedron*, 15 (2), pp. 327 - 334.
- Aboul-Gheit, A.K. et al., 2011. Platinum 1,10-phenanthroline: Photosensitizer for photocatalytic degradation of 4-chlorophenol. *European Journal of Chemistry*, 2 (1), pp. 104 - 108.
- Abreum F.R. et al., 2003. New metal catalysts for soybean oil transesterification. *Journal of American Oil Chemists Society*, 80 (6), pp. 601 - 604.
- Accorsi, G. et al., 2009. 1,10-phenanthrolines: versatile building blocks for luminescent molecules, materials and metal complexes. *Chemical Society Reviews*, 38, pp. 1690 - 1700.
- Adachi, Y. and Sakurai, H., 2004. Comparative study of insulin-mimetic activity of vanadium and zinc complexes. *Biomedical Research on Trace Elements*, 15 (4), pp. 351 - 354.
- Adman, E.T., 1991. Copper protein structures. *Advance Protein Chemistry*, 42, pp. 145 - 197.
- Agwara, M.O. et al., 2010. Synthesis, characterization and antimicrobial activities of cobalt(II), copper(II) and zinc(II) mixed-ligand complexes containing 1,10-phenanthroline and 2,2'-bipyridine. *Bulletin of Chemical Society of Ethiopia*, 24 (3), pp. 383 - 389.
- Ahmed, S.I. et al., 2000. The structures of bis-maltolato-zinc(II) and of bis-3-hydroxy-1,2-dimethyl-4-pyridinonato-zinc(II) and lead(II). *Polyhedron*, 19, pp. 129 - 135.

- Ahmet, M.T., Frampton, C.S. and Silver, J., 1988. A potential iron pharmaceutical composition for the treatment of iron-deficiency anaemia. The crystal and molecular structure of *mer-tris*-(3-hydroxy-2-methyl-4*H*-4-onato)iron(III). *Journal of Chemical Society, Dalton Transaction*, 5, pp. 1159 - 1163.
- Alberts, B., Johnson, A., Lewis, J., Raff, M., Roberts, K. and Walter, P., 2002. Molecular Biology of the cell. In: *Chapter 4. DNA and Chromosomes*. 4<sup>th</sup> edition, New York: Garland Science.
- Allan, J.R. et al., 1989. Thermal analysis studies on pyridine carboxylic acid complexes of Zinc(II). *Thermochimica Acta*, 153, pp. 249 – 256.
- American Cancer Society, *What is nasopharyngeal cancer* [Online]. Available at:<http://www.cancer.org/cancer/nasopharyngealcancer/detailedguide/nasopharyngeal-cancer-what-is-nasopharyngeal-cancer> [Accessed: 20 march 2013].
- An, Y. et al., 2006. Double-strand DNA cleavage by copper complexes of 2,2'-dipyridyl with electropositive pendants, *Dalton Transactions*, 17, pp. 2066 - 2071.
- Anderegg, G., 1963. Pyridinderivate als Komplexbildner V. Die Metallkomplexe von 1,10-phenanthrolin und  $\alpha$ ,  $\alpha'$ -Dipyridyl. *Helvetica Chimica Acta*, 46, pp. 2397 - 2410.
- Andreev, G. et al., 2010. Novel mixed valance U(VI)/U(IV) dipicolinate. *Inorganic Chemistry Communications*, 13, pp. 577 – 579.
- Apelblat, A., 2011. Representation of electrical conductances for polyvalent electrolytes by the Quint-Viallard conductivity equation. Part 4. Symmetrical 2:2, 3:3 and unsymmetrical 2:1, 3:1 and 1:3 type electrolytes in pure organic solvents, *Journal of Solution Chemistry*, 40 (7), pp. 1234 - 1257.
- APEX2 and SAINT software reference manuals, 2002. Bruker AXS Inc., Madison.
- Araya, J. et al., 2002. Inhibition of proteasome activity is involved in cobalt-induced apoptosis of human alveolar macrophages. *Journal of the American Physiological Society*, 283 (4), pp. 849 - 858.

- Archer, C.M., Dilworth, J.R. and Jobanputra, P., 1991. The preparation and characterization of some imido- and diazenido-rhenium complexes of maltol. The X-ray crystal structure of  $[\text{Re}(\text{maltol})_2(\text{NPh})(\text{PPh}_3)][\text{BPh}_4]$ . *Polyhedron*, 10, pp. 1539 – 1543.
- Arimondo, P.B. et al., 2006. Exploring the cellular activity of camptothecin-triple-helix-forming oligonucleotide conjugates. *Molecular and Cellular Biology*, 26 (1), pp. 324 - 333.
- Arjmand, F. and Muddassir, M., 2010. Design and synthesis of heterobimetallic topoisomerase I and II inhibitor complexes: *In Vitro* DNA binding, interaction with 5'-GMP and 5'-TMP and cleavage studies. *Journal of Photochemistry and Photobiology B: Biology*, 101 (1), pp. 37 - 46.
- Arjmand, F., Muddassir, M. and Khan, R.H., 2010. Chiral preference of L-tryptophan derived metal-based antitumor agent of late 3d-metal ions (Co(II), Cu(II) and Zn(II)) in comparison to D- and DL-tryptophan analogues: Their *in vitro* reactivity towards CT DNA, 5'-GMP and 5'-TMP. *European Journal of Medical Chemistry*, 45 (9), pp. 3549 - 3557.
- Amaroli, N., 2001. Photoactive mono- and polynuclear Cu(I)-phenanthroline. A viable alternative to Ru(II)-polypyridines. *Chemical Society Review*, 30, pp. 113 - 124.
- Asadi, M. et al., 2010. Synthesis, characterization, *ab initio* calculations, thermal behaviour and thermodynamics of some oxovanadium(IV) complexes involving O,O- and N,N-donor moieties. *Journal of Chemical Sciences*, 122 (4), pp. 539-548.
- Balzani, V., Credi, A. and Venturi, M., 2008. Molecular Devices and Machines. In: *Concepts and Perspectives for the Nanoworld*, 2nd ed., Germany: Wiley-VCH, Weinheim.
- Barnes, L.S. et al., 2011. Effects of terbium chelate structure on dipicolinate ligation and the detection of *Bacillus* spore. *Journal of Inorganic Biochemistry*, 105, pp. 1580 - 1588.
- Barton J.K., 1986, Metals and DNA: molecular left-handed complements. *Science*, 233, pp. 727 – 734.

- Barton, J.K. and Raphael, A.L., 1985. Site-specific cleavage of left-handed DNA in pBR322 by  $\Lambda$ -tris(4,7-diphenyl-1,10-phenanthroline)cobalt(III). *Proceedings of the National Academy of Sciences USA*, 82, pp. 6460 - 6464.
- Becco, L. et al., 2012. New achievements on biological aspects of copper complexes Casiopeínas®: Interaction with DNA and proteins and anti-Trypanosoma cruzi activity. *Journal of Inorganic Biochemistry*, 109, pp. 49 - 56.
- Belousoff, M.J. et al., 2006. Synthesis, X-ray crystal structures, magnetism, and phosphate ester cleavage properties of copper(II) complexes of N-substituted derivatives of 1,4,7-triazacyclononane. *Inorganic Chemistry*, 45 (9), pp. 3746 - 3755.
- Belousoff, M.J. et al., 2008a. Synthesis, X-ray Crystal structures, and phosphate ester cleavage properties of bis(2-pyridylmethyl)amine copper(II) complexes with guanidinium pendant groups. *Inorganic Chemistry*, 47 (19), pp. 8641 - 8651.
- Belousoff, M.J., Graham, B. and Spiccia, L., 2008b. Copper(II) complexes of N-methylated derivatives of ortho- and meta-xylyl-bridged bis(1,4,7-triazacyclononane) ligands: Synthesis, X-ray structure and reactivity as artificial nucleases. *European Journal of Inorganic Chemistry*, 26, pp. 4133 - 4139.
- Bencini, A. and Lippolis, V., 2010. 1,10-Phenanthroline: A versatile building block for the construction of ligands for various purposes. *Coordination Chemistry Reviews*, 254, pp. 2096 - 2180.
- Beretta, G.L., Perego, P. and Zunino, F., 2008. Targeting topoisomerase I: molecular mechanisms and cellular determinants of response to topoisomerase I inhibitors. *Expert Opinion on Therapeutic Targets*, 12 (10), pp. 1243 - 1256.
- Berg, J.M., Tymoczko, J.L. and Stryer, L., 2002. *Biochemistry*. 5th edition. New York: Freeman, W. H.
- Bernhardt, P.V., Flanagan, B.M. and Riley, M.J., 1999. Metal-centred versus ligand-centre luminescence quenching of a macrocyclic copper(II) complex. *Journal of the Chemical Society, Dalton Transactions*, 20, pp. 3579 - 3584.

- Bernstein, L.R. et al., 2000. Chemistry and pharmacokinetics of gallium maltolate, a compound with high oral gallium bioavailability. *Metal-based Drug*, 7 (1), pp. 33 - 47.
- Bernstein, L.R., 2012. Successful treatment of refractory postherpetic neuralgia with topical gallium maltolate: case report. *Pain Medicine*, 13, pp. 915 - 918.
- Bharti, S.K. and Singh, S.K., 2009. Recent developments in the field of anticancer metallopharmaceuticals. *International Journal of PharmTech Research*, 1 (4), pp. 1406 - 1420.
- Bhattacharya, P.K., 2005. Metal ions in Biochemistry. *Chapter 1 - Structure of Cells and Introduction to Bioinorganic Chemistry*. United Kingdom: Alpha Science International Ltd., pp. 13 - 15.
- Bodoki, A. et al., 2009. Oxidative DNA cleavage by copper ternary complexes of 1,10-phenanthroline and ethylenediamine-sulfonamide derivatives. *Polyhedron*, 28, pp. 2537 - 2544.
- Boerner, L.J.K. and Zaleski, J., 2005. Metal complex-DNA interactions: from transcription inhibition to photoactivated cleavage. *Current Opinion in Chemical Biology*, 9, pp. 135 - 144.
- Boger, D.L. and Tse, W.C., 2001. Thiazole orange as the fluorescent intercalator in a high resolution FID assay for determining DNA binding affinity and sequence selectivity of small molecules. *Bioorganic and Medicinal Chemistry*, 9, pp. 2511 - 2518.
- Boger, D.L. et al., 2007. A simple, high-resolution method for establishing DNA binding affinity and sequence selectivity. *Journal of the American Chemical Society*, 123 (25), pp. 5878 - 5891.
- Boghaei, D.M. and Gharagozlou, M., 2007. Spectral characterization of novel ternary zinc(II) complexes containing 1,10-phenanthroline and schiff bases derived from amino acids and salicylaldehyde-5-sulfonates. *Spectrochimica Acta*, A67, pp. 944 - 949.

- Bolletta, F. et al., 1999. A  $[\text{Ru}^{\text{II}}(\text{bipy})_3]$ -[1,9-diamino-3,7-diazanonane-4,6-dione] two-component system, as an efficient ON-OFF luminescent chemosensor for  $\text{Ni}^{2+}$  and  $\text{Cu}^{2+}$  in water, based on an ET (energy transfer) mechanism. *Journal of the Chemical Society, Dalton Transactions*, 9, pp. 1381 - 1386.
- Bordbar, A-K. et al., 2009. Calorimetric studies of the interaction between the insulin-enhancing drug candidate bis(maltolato)oxovanadium(IV) (BMOV) and human serum apo-transferrin. *Journal of Inorganic Biochemistry*, 103, pp. 643 - 647.
- Bossert, J. and Daniel, C., 2008. Electronic absorption spectroscopy of  $[\text{Ru}(\text{phen})_2(\text{bpy})]^{2+}$ ,  $[\text{Ru}(\text{phen})_2(\text{dmbp})]^{2+}$ ,  $[\text{Ru}(\text{tpy})(\text{phen})(\text{CH}_3\text{CN})]^{2+}$  and  $[\text{Ru}(\text{tpy})(\text{dmp})(\text{CH}_3\text{CN})]^{2+}$  A theoretical study. *Coordination Chemistry Review*, 252, pp. 2493 - 2503.
- Brahma, S. et al., 2008. Adducts of bis(acetylacetonato)zinc(II) with 1,10-phenanthroline and 2,2'-bipyridine. *Acta crystallographica*, C64, m 140 - 143.
- Brandt, W.W., Dwyer, F.P. and Gyarfás, E.D., 1954. Chelate complexes of 1,10-phenanthroline and related compounds. *Chemical Reviews*, 54 (6), pp. 959 - 1017.
- Brito, Y.C. et al., 2008. Fatty acid methyl esters preparation in the presence of maltolate and *n*-butoxide Ti(IV) and Zr(IV) complexes. *Applied Catalysis A: General*, 351, pp. 24 - 28.
- Bruker (2002). APEX2 and SAINT, Bruker AXS Inc., Madison.
- Brunner, H., Valério, C. and Zabel, M., 2000. Optically active transition metal complexes. Part 123: new chiral half-sandwich ruthenium complexes, in which the arene ligand is tethered to a PN ligand. *New Journal of Chemistry*, 24, pp. 275 - 279.
- Bryan, P.S. and Dabrowiak, J.C., 1975. Transition metal complexes containing an optically active macrocyclic ligand. Manganese(III), nickel(II) and copper(II). *Inorganic Chemistry*, 14 (2), pp. 299 - 302.
- Bulut, İ., Uçar, I. and Kazak, C., 2009. Spectroscopic and structural study of Ni(II) dipicolinate complex with 2-Amino-4-methylpyrimidine. *TüBiTAK*, 33, pp. 347 - 357.

- Burdette, S.C. and Lippard, S.J., 2001. ICC34 - golden edition of coordination chemistry reviews. Coordination chemistry for the neurosciences. *Coordination Chemistry Review*, 216-217, pp. 333 - 361.
- Cable, M.L. et al., 2009. Detection of bacterial spores with Lanthanide-macrocyclic binary complexes. *Journal of the American Chemistry Society*, 131 (27), pp. 9562 - 9570.
- Cai, M., Chen, J. and Taha, M., 2010. Synthesis, structures and antibacterial activities of two complexes of yttrium(III) with 2,6-pyridinedicarboxylate. *Inorganic Chemistry Communication*, 13, pp. 199 - 202.
- Cameron, B.R. et al., 2003. Ruthenium(III) triazacyclononane dithiocarbamate, pyridinecarboxylate, or aminocarboxylate complexes as scavengers of nitric oxide. *Inorganic Chemistry*, 42 (13), pp. 4102 - 4108.
- Cao, J.Y. et al., 2010. Prognostic significance and therapeutic implications of centromere protein F expression in human nasopharyngeal carcinoma. *Molecular Cancer*, 9, pp. 237 - 249.
- Capranico, G. et al., 1997. A protein-mediated mechanism for the DNA sequence-specific action of topoisomerase II poisons. *Trends in Pharmacological Sciences*, 18 (4), pp. 323 - 329.
- Caravan, P. et al., 1995. Reaction chemistry of BMOV, bis(maltolato)oxovanadium(IV), a potent insulin mimetic agent. *Journal of the American Chemical Society*, 117 (51), pp. 12759 - 12770.
- Carey, F.A., 2000. Organic Chemistry. *Chapter 7 - Stereochemistry*, 4<sup>th</sup> edition, McGraw-Hill, pp. 259 - 300.
- Carland, M., Tan, K.J., White, J.M., Stephenson, J., Murray, V., Denny, W.A. and McFadyen, W.D., 2005. Syntheses, crystal structure and cytotoxicity of diamine platinum(II) complexes containing maltol. *Journal of Inorganic Biochemistry*, 99, pp. 1738 - 1743.

- Castiñeiras, A. et al., 2002. Intramolecular "Aryl-Metal chelate ring"  $\pi$ ,  $\pi$ -interactions as structural evidence for metalloaromaticity in (Aromatic  $\alpha$ - $\alpha'$ -Diimine)-Copper(II) chelates: Molecular and crystal structure of aqua(1,10-phenanthroline)(2-benzylmalonato)copper(II) three hydrate. *Inorganic Chemistry Communication*, 41, pp. 6956 - 6958.
- Chandra, S. and Kumar, U., 2005. Spectral and magnetic studies on manganese(II), cobalt(II) and nickel(II) complexes with schiff bases. *Spectrochimica Acta Part A*, 61, pp. 219-224.
- Chandraleka, S. et al., 2011. Antifungal activity of amino acid schiff base Copper(II) complexes with phenanthroline and bipyridyl. *International Journal of Chemical and Analytical Science*, 2 (10), pp. 1235 - 1240.
- Chang, C.J. and Lippard, S.J., 2006. Metal ions in life sciences. In: Sigel, A., Sigel, H., Sigel, R.K.O. (eds.). *Neurodegenerative diseases and metal ions*. Wiley, Chichester, pp. 321 - 370.
- Chang, J.H., Choi, Y.M. and Shin, Y.K., 2001. Significant fluorescence quenching of anthrylaminobenzocrown ethers by paramagnetic metal cations. *Bulletin Korean Chemical Society*, 22 (5), pp. 527 - 530.
- Chashoo, G. et al., 2011. A propionyloxy derivative of 11-keto- $\beta$ -boswellic acid induces apoptosis in HL-60 cells mediated through topoisomerase I & II inhibition. *Chemico-Biological Interactions*, 189 (1-2), pp. 60 - 71.
- Chatterjee, M. et al., 1998. Studies of V(III) complexes with selected  $\alpha$ -N-heterocyclic carboxylato NO donor ligands structure of a new seven coordinated pentagonal bipyramidal complex containing picolinato ligands. *Journal of the Chemical Society, Dalton Transactions*, pp. 3641 - 3645.
- Chem Spider, Royal Society of Chemistry, *Advancing the Chemical Sciences* [Online]. Available at: <http://www.chemspider.com/Chemical-Structure.6051.html> [Accessed: 5 Jan 2013].
- Chem Spider, Royal Society of Chemistry, *Advancing the Chemical Sciences* [Online]. Available at: <http://www.chemspider.com/Chemical-Structure.62643.html?rid=731a489d-81dc-4022-9554-ea63da6f49e6> [Accessed: 5 Jan 2013].

- Chen, C.B., Gorin, M.B. and Sigman, D.S., 1993. Sequence-specific scission of DNA by the chemical nuclease activity of 1,10-phenanthroline-copper(I) targeted by RNA. *Proceeding of the National Academy of Sciences of the United States of America*, 90 (9), pp. 4260 - 4210.
- Chen, D. et al., 2009. Metal complexes, their cellular targets and potential for cancer therapy. *Current Pharmaceutical Design*, 19 (42), pp. 777 - 791.
- Chen, H.L. et al., 2010. The ligand- structure-selective binding of oligonucleotide by cobalt complexes. *Inorganic Chemistry Communication*, 13 (2), pp. 310 - 313.
- Chen, L., 2012. *Catena*-Poly[[1,10-phenanthroline]zinc]- $\mu$ -3-[3-(carboxylatomethoxy)phenyl]-acrylate]. *Acta Crystallographica*, E68, m882.
- Chen, Z.N., Fan, Y. and Ni, J., 2008. Luminescent heteropolynuclear or multicomponent complexes with polypyridyl-functionalized alkynyl ligands. *Dalton Transaction*, 5, p. 573 - 581.
- Cheng, C.C., Luo, C.F. and Wang, W.J., 1999. A new Co<sup>II</sup> complex as a bulge-specific probe for DNA. *Angewandte Chemie International Edition*, 38 (9), pp. 1255 - 1257.
- Chetana, P.R. et al., 2009. New ternary copper(II) of L-alanine and heterocyclic bases: DNA binding and oxidative DNA cleavage activity. *Inorganic Chimica Acta*, 362, pp. 4692 - 4698.
- Chin, L.F. et al., 2011. Synthesis, characterization and biological properties of cobalt(II) complexes of 1,10-phenanthroline and maltol. *Journal of Inorganic Biochemistry*, 105, pp. 221 - 229.
- Chitambar, C.R. et al., 2007. Development of gallium compounds for treatment of lymphoma: gallium maltolate, a novel hydroxypyron gallium compound, induces apoptosis and circumvents lymphoma cell resistance to gallium nitrate. *Journal of Pharmacology and Experimental Therapeutics*, 322 (3), pp. 1228 - 1236.
- Chow, C.S. and Barton, J.K., 1992. Transition metal complexes as probes of nucleic acids. *Methods in Enzymology*, 212, pp. 219 - 242.

- Chris, J.J., 2002. d- and f- block chemistry. *Chapter 4 - Coordination compounds*. New York: The Royal Society of Chemistry, pp. 55 - 70.
- Chua, M-S. et al., 2006. Gallium maltolate is a promising chemotherapeutic agent for the treatment of hepatocellular carcinoma. *Anticancer Research*, 26, pp. 1739 - 1344.
- Chuang, N.N., Lin, C.L. and Chen, H.K., 1996. Modification of DNA topoisomerase I enzymatic activity with phosphotyrosyl protein phosphatase and alkaline phosphatase from the hepatopancreases of the shrimp *Penaeus japonicus* (Crustacea: Decapoda). *Comparative Biochemistry and Physiology - Part B: Biochemistry & Molecular Biology*, 114B (2), pp. 145 - 151.
- Clarke, M.J., Zhu, F. and Frasca, D.R., 1999. Non-platinum chemotherapeutic metallopharmaceuticals. *Chemical Review*, 99, pp. 2511 - 2553.
- Clou, K. et al., 2003. Influence of hydrogen bonding on the thermal behaviour of some amides and thioamides. *Thermochimica Acta*, 398, pp. 47 - 58.
- Çolak, A.T. et al., 2010. Synthesis, spectroscopic, thermal, crystal characterization and biological activity of  $\{[\text{Ni}(\text{phen})_3][\text{Ni}(\text{dipic})_2]\}_2 \cdot 17\text{H}_2\text{O}$  (H<sub>2</sub>dipic: pyrdine-2,6-dicarboxylic acid, phen:1,10-phenanthroline). *Journal of the Iranian Chemical Society*, 7 (2), pp. 384 - 393.
- Conti, P. et al., 2011. Drug discovery targeting amino acid racemases. *Chemical Reviews*, pp. 1 - 28.
- Coury, L., 1999. Conductance measurements. Part 1: Theory. *Current separation*, 18 (3), pp. 91- 96.
- Coyle, B. et al., 2004. Induction of apoptosis in yeast and mamalian cells by exposure to 1,10-phenanthroline metal complexes. *Toxicology*, 18 (1), pp. 63 - 70.
- DeLeon, K. et al., 2009. Gallium maltolate treatment eradicates *Pseudomonas aeruginosa* infection in thermally injured mice. *Antimicrobial Agents and Chemotherapy*, 53 (4), pp. 1331 - 1337.

- Devereux, M. et al., 2002. Synthesis and catalytic activity of manganese(II) complexes of heterocyclic carboxylic acids: X-ray crystal structures of  $[\text{Mn}(\text{pyr})_2]_n$ ,  $[\text{Mn}(\text{dipic})(\text{bipy})_2] \cdot 4.5\text{H}_2\text{O}$  and  $[\text{Mn}(\text{chedam})(\text{bipy})] \cdot \text{H}_2\text{O}$  (pyr = 2-pyrazinecarboxylic acid; dipic = pyridine-2,6-dicarboxylic acid; chedam = chelidamic acid (4-hydroxypyridine-2,6-dicarboxylic acid); bipy = 2,2'-bipyridine). *Polyhedron*, 21, pp. 1063 - 1071.
- Dolcetti, R. and Menezes, J., 2003. Epstein-Barr virus and undifferentiated nasopharyngeal carcinoma: New immunobiological and molecular insights on a long-standing etiopathogenic association. *Advances in Cancer Research*, 87, pp. 127 - 157.
- Douglas, B.E. and Saito, Y., 1980. Stereochemistry of optically active transition metal compounds, *Journal of the American Chemical Society*, 119, pp. 1 - 12.
- Du, Y.H. et al., 2010. Specific recognition of DNA by small molecules. *Current Medicinal Chemistry*, 17 (2), pp. 173 - 189.
- Ducommun, Y. et al., 1989. Variable pressure spectrophotometric equilibrium and  $^{139}\text{La}$  NMR kinetic studies of lanthanum(III) ion complex formation with 2,6-dicarboxy-4-hydroxypyridine in aqueous solution. *Inorganica Chimica Acta*, 158, pp. 3 - 4.
- Dutta, N.K. and Sarma, U.U.M., 1975. Chemistry of lanthanons - XLI. Isolation and characterization of tris chelates of lanthanides with maltol, kojic acid and chloro-kojic acid. *Journal of Inorganic Nuclear Chemistry*, 37, pp. 1801 - 1802.
- Dutta, R. L. and Ray, T., 1981. Cr(III) chelates. *Journal of Inorganic Nuclear Chemistry*, 43, pp. 1985 - 1987.
- Dutta, R.L. and Satapathi, S.K., 1980. Phenylmercury(II) compounds-III. Pyridine and quinoline carboxylic acid compounds. *Journal of Inorganic Nuclear Chemistry*, 42, pp. 1647 - 1648.
- Eastman, A., 1999. Cisplatin. In: Lippert, B. (ed.). *Chemistry and Biochemistry of a Leading Anticancer Drug*. Wiley-VCH: Weinheim, pp. 111.

- Efthimiadou, E.K., Karaliota, A. and Psomas, G., 2008. Structure, antimicrobial activity and DNA-binding properties of the cobalt(II)-sparfloxacin complex. *Bioorganic & Medicinal Chemistry Letters*, 18 (14), pp. 4033 - 4037.
- Enyedy, E.A. et al., 2006. An in vitro study of interactions between insulin-mimetic zinc(II) complexes and selected plasma components. *Journal of Inorganic Biochemistry*, 100, pp. 1936 - 1945.
- Erikson, T.E., Grenthe, L., Puigdomenech, L., 1987. A kinetic investigation of lanthanide(III) complex formation with picolinic acid. *Inorganic Chimica Acta*, 126, pp. 131 - 135.
- Eriksson, M. et al., 1994. Binding of delta- and lamda-[Ru(phen)<sub>3</sub>]<sup>2+</sup> to [d(CGCGATCGCG)<sub>2</sub>] studied by NMR. *Biochemistry*, 33 (17), pp. 5031 - 5040.
- Erkkila, K.E., Odom, D.T. and Barton, J.K., 1999. Recognition and reaction of metallointercalators with DNA. *Chemical Review*, 99, pp. 2777-2796.
- Ettinger, M.J., 1984. In: Lontie, R. (Ed.), Copper proteins and copper enzymes, vol. 3, CRC Press, Boca Raton, FL., pp. 175 - 229.
- Failes, T.W. and Hambley, T.W., 2006. Models of hypoxia activated prodrugs: Co(III) complexes of hydroxamic acids. *Dalton Transaction*, 15, pp. 1895 - 1901.
- Farrar, G., Morton, A.P. and Blair, J.A., 1988. Tissue distribution of gallium following administration of the gallium-maltol complex in the rat: a model for an aluminium-maltol complex of neurotoxicological interest. *Food and Chemical Toxicology*, 26 (6), pp. 523 - 525.
- Farrell, N., 2003. Comprehensive Coordination Chemistry II. In: *Chapter 9.18 - Metal Complexes as Drugs and Chemotherapeutic Agents*. vol. 9, UK : Elsevier, pp. 809 - 840.
- Feng, W. et al., 2009. Novel topoisomerase I-targeting antitumor agents synthesized from the *N,N,N*-trimethylammonium derivatives of ARC-111, 5*H*-2,3-dimethoxy-8,9-methylenedioxy-5-[(2-*N,N,N*-trimethylammonium)ethyl]dibenzo[*c,h*][1,6]-naphthyridin-6-one iodide. *European Journal of Medicinal Chemistry*, 44, p. 3433 - 3438.

- Fenton, D.E., 1995. *Biocoordination Chemistry*, 1st ed., Oxford University Press, Oxford, pp. 1 - 80.
- Fernandes, A. et al., 2001. Study of new lanthanide complexes of 2,6-pyridinedicarboxylate: synthesis, crystal structure of Ln(Hdipic)(dipic) with Ln = Eu, Gd, Tb, Dy, Ho, Er, Yb, luminescence properties of Eu(Hdipic)(dipic). *Polyhedron*, 20, pp. 2385 - 2391.
- Fernandes, A.G. de A. et al., 2008. Rhenium chelate complexes with maltolate or kojate. *Polyhedron*, 27, pp. 2983 – 2989.
- Finnegan, M.M., Rettig, S.J. and Orvig, C., 1986. Neutral water-soluble aluminium complex of neurological interest. *Journal of American Society Chemistry*, 108 (16), pp. 5033 - 5035.
- Florea, A-M. and Büsselberg, D., 2011. Cisplatin as an anti-tumor drug: Cellular mechanisms of activity, drug resistance and induced side effects. *Cancer*, 3, pp. 1351 - 1371.
- Fouad, D.M. et al., 2010. Synthesis and thermal studies of mixed ligand complexes of Cu(II), Co(II), Ni(II) and Cd(II) with mercaptotriazoles and dehydroacetic acid. *Natural Science*, 2 (8), pp. 817 - 827.
- Franklin, C.A., Fry, J.V. and Collins, J.G., 1996. NMR evidence for sequence-specific DNA minor groove binding by bis(ethylenediamine)platinum(II). *Inorganic Chemistry*, 35 (26), pp. 7541 - 7545.
- Fry, F.H. et al., 2005. Kinetics and mechanism of hydrolysis of a model phosphate diester by  $[\text{Cu}(\text{Me}_3\text{-tacn})(\text{OH}_2)_2]^{2+}$  ( $\text{Me}_3\text{tacn} = 1,4,7\text{-triazacyclononane}$ ). *Inorganic Chemistry*, 44 (4), pp. 941 - 950.
- Fugono, J. et al., 2002. Metallokinetic study of zinc in the blood of normal rats given insulinomimetic zinc(II) complexes and improvement of diabetes mellitus in type 2 diabetic GK rats by their oral administration. *Drug Metabolism and Pharmacokinetics*, 17 (4), pp. 340 - 347.
- Gahan, L.R. et al., 2009. Phosphate ester hydrolysis: Metal complexes as purple acid phosphatase and phosphotriesterase analogues. *European Journal of Inorganic Chemistry*, 19, pp. 2745 - 2758.

- Gallori, E. et al., 2000. DNA as a possible target for antitumor ruthenium(III) complexes: A spectroscopic and molecular biology study of the interactions of two representative antineoplastic ruthenium(III) complexes with DNA. *Archives of Biochemistry and Biophysics*, 376 (1), pp. 156 - 162.
- García-Raso, A. et al., 2003. Synthesis, structure and nuclease properties of several ternary copper(II) peptide complexes with 1,10-phenanthroline. *Journal of Inorganic Biochemistry*, 95, pp. 77 - 86.
- Geary, W.J., 1971. The use of conductivity measurements in organic solvents for the characterisation of coordination compounds. *Coordination Chemistry Reviews*, 7, pp. 81-122.
- Ghosh, R.D. et al., 2011. An *in vitro* and *in vivo* study of a novel zinc complex, zinc *N*-(2-hydroxyacetophenone)glycinate to overcome multidrug resistance in cancer. *Dalton Transactions*, 40 (41), pp. 10873 - 10884.
- Glaser, R. et al., 1989. Two epithelial tumor cell lines (HNE-1 and HONE-1) latently infected with Epstein-Barr virus that were derived from nasopharyngeal carcinomas. *Proceedings of the National Academy of Sciences of the United States of America*, 86 (23), pp. 9524 - 9528.
- Golchoubian, H. and Fazilati, H., 2012. Synthesis and spectral studies on heteroleptic chelated copper(II) complexes of diamine and acetylacetonate, *Iranica Journal of Energy & Environment*, 3 (3), pp. 264 - 269.
- Goličnik, M., 2010. Metallic fluoride complexes as phosphate analogues for structural and mechanistic studies of phosphoryl group transfer enzymes. *Acta Chimica Slovenica*, 57 (2), pp. 272 - 287.
- Gonzalez, V.M. et al., 2001. Is cisplatin-induced cell death always produced by apoptosis? *Molecular Pharmacology*, 59, pp. 657 - 663.
- Gonzalez-Baró, A.C. et al., 2005. Synthesis, crystal structure and spectroscopic characterization of a novel bis (oxo-bridged) dinuclear vanadium(V)-dipicolinic acid complex. *Polyhedron*, 24, pp. 49 - 55.
- Greaves, S.J. and Griffith, W.P., 1988. Surface-enhanced Raman spectroscopy (SERS) of ligands and their complexes on silver sols – I. Maltol, Tropolone and their complexes with group VIII and Group VI metals. *Polyhedron*, 7, pp. 1973 – 1979.

- Griffith, D. et al., 2007. Novel platinum pyridinehydroxamic acid complexes: Synthesis, characterisation, X-ray crystallographic study and nitric oxide related properties. *Polyhedron*, 26, pp. 4697 - 4706.
- Groves, J.T. and Kady, I.O., 1993. Sequence-specific cleavage of DNA by oligonucleotide-bound metal complexes. *Inorganic Chemistry*, 32 (18), pp. 3868 - 3872.
- Gulley, M.L. et al., 1998. Epstein-Barr virus infection is associated with p53 accumulation in nasopharyngeal carcinoma. *Human Pathology*, 29 (3), pp. 252 - 259.
- Gültekin, A. et al., 2010. Nanosensors having dipicolinic acid imprinted nanoshell for *Bacillus cereus* spores detection. *Journal of Nanoparticle Research*, 12 (6), pp. 2069 - 2079.
- Gust, R. et al., 2004. Development of Cobalt(3,4-diarylsalen) complexes as tumor therapeutics. *Journal of Medicinal Chemistry*, 47 (24), pp. 5837 - 5846.
- Hadadzadeh, H. et al., 2010. Pyridine-2,6-dicarboxylic acid (Dipic): Crystal structure from Co-crystal to a mixed ligand nickel(II) complex. *Journal of Chemical Crystallography*, 40, pp. 48 - 57.
- Hakansson, K. et al., 1993. The structure of two solid zinc dipicolinate complexes. *Acta Chemica Scandinavica*, 47, pp. 449 - 455.
- Hall, J.P. et al., 2011. Structure determination of an intercalating ruthenium dipyridophenanzine complex which kinks DNA by semiintercalation of a tetraazaphenanthrene ligand. *Proceedings of the National Academy of Sciences*, early edition, pp. 1 - 5.
- Hambidge, K.M. et al., 2010. Zinc bioavailability and homeostasis. *The American Journal of Clinical Nutrition*, 91 (5), pp. 1478 - 1483.
- Hanauer, M., Neshat, A. and Bigioni, T.P., 2008. Tris(1,10-phenanthroline- $\kappa^2$ N,N')-cobalt(III) tris(trifluoromethane-sulfonate) dihydrate. *Acta Crystallographica*, C64, m111 - 113.

- Hanson, G.R., Sun, Y. and Orvig, C., 1996. Characterization of the potent insulin mimetic agent *bis(maltolato)oxovanadium(IV)* (BMOV) in solution by EPR spectroscopy. *Inorganic Chemistry*, 35 (22), pp. 6507-6512.
- Harding, D.J., Harding, P. and Adams, H., 2008. Tris(phenanthroline- $\kappa^2N,N'$ )Cobalt(II) tetrafluoroborate acetonitrile solvate. *Acta Crystallographica*, E64, m1538.
- Harrison, W.T.A., Ramadevi, P. And Kumaresan, S., 2006. Aqua(dipicolinato- $\kappa^3O,N,O'$ )(1,10-phenanthroline- $\kappa^2N,N'$ )zinc(II) monohydrate. *Acta crystallographica*, E62, m513 - 515.
- He, L. et al., 2012. Control of intramolecular  $\pi$ - $\pi$  stacking interaction in cationic Iridium complexes via fluorination of pendant phenyl rings. *Inorganic Chemistry*, 51 (8), pp. 4502 - 4510.
- He, Y.T. et al., 2007. A new two-dimensional supramolecule composed of  $\mu$ -2,6-dimethylpyridine-3,5-dicarboxylato- $\kappa^4O^3,O^{3'},O^5,O^{5'}$ -bis[chloro(1,10-phenanthroline- $\kappa^2N,N'$ ) zinc(II)]. *Acta Crystallographica*, C63, m161 - 162.
- Heffeter, P. et al., 2006. Anticancer activity of the lanthanum compound [tris(1,10-phenanthroline)lanthanum(III)]trithiocyanate (KP772; FFC24). *Biochemical pharmacology*, 71, pp. 426 - 440.
- Hegg, E.L. and Burstyn, J.N., 1996. Copper(II) macrocycles cleave single-stranded and double-stranded DNA under both aerobic and anaerobic conditions. *Inorganic Chemistry*, 35 (26), pp. 7474 - 7481.
- Hegg, E.L. et al., 1997. Hydrolysis of double-stranded and single-stranded RNA in hairpin structures by the copper(II) macrocycle Cu([9]aneN<sub>3</sub>)Cl<sub>2</sub>. *Inorganic Chemistry*, 36 (8), pp. 1715 - 1718.
- Hegg, E.L. and Burstyn, J.N., 1998. Toward the development of metal-based synthetic nucleases and peptidases: a rationale and progress report in applying the principles of coordination chemistry. *Coordination Chemistry Reviews*, 173 (1), pp. 133 - 165.
- Hernández, R. et al., 2008. Structure-activity studies of Ti(IV) complexes: aqueous stability and cytotoxic properties in colon cancer HT-29 cells. *Journal of Biological Inorganic Chemistry*, 13 (5), pp. 685 - 692.

- Hernández, R. et al., 2010. Titanium(IV) complexes: cytotoxicity and cellular uptake of titanium(IV) complexes on caco-2 cell line. *Toxicology in Vitro*, 24, pp. 178 - 183.
- Hindle, A.A. and Hall, E.A.H., 1999. Dipicolinic acid (DPA) assay revisited and appraised for spore detection. *Analyst*, 124 (11), pp. 1599 - 1604.
- Hironishi, M. et al., 1996. Maltol (3-hydroxy-2-methyl-4-pyrone) Toxicity in neuroblastoma cell lines and primary murine fetal hippocampal neuronal cultures. *Neurodegeneration*, 5, pp. 325 - 329.
- Hsieh, W.Y. et al., 2006. Mn(II) complexes of monoanionic bidentate chelators: X-ray crystal structures of Mn(dha)<sub>2</sub>(CH<sub>3</sub>OH)<sub>2</sub> (Hdha = dehydroacetic acid) and [Mn(ema)<sub>2</sub>(H<sub>2</sub>O)]<sub>2</sub>.2H<sub>2</sub>O (Hema = 2-ethyl-3-hydroxy-4-pyrone). *Inorganica Chimica Acta*, 359, pp. 228 - 236.
- Hu, B. et al., 2010. Alteration of molecular conformations and spectral properties for nickel(II), zinc(II) and copper(II) complexes having 3,8-di(thiophen-2',2'-yl)-1,10-phenanthroline ligands. *Inorganica Chimica Acta*, 363 (7), pp. 1348 - 1354.
- Huang, R., Wallqvist, A. and Covell, D.G., 2005. Anticancer metal compounds in NCI's tumor-screening database: putative mode of action. *Biochemical Pharmacology*, 69, pp. 1009 - 1039.
- Ikeda, S., Kimachi, S. and Azumi, T., 1996. Spectroscopic study on fluorescing processes of (nd)<sup>10</sup> Transition-metal complexes. 1. ZnX<sub>2</sub>(phen) (X = Cl, Br, I; phen = 1,10-phenanthroline monohydrate). *Journal of Physical Chemistry*, 100 (25), pp. 10528-10530.
- Ivanov, V.I. et al., 1973. Different conformations of double-stranded nucleic acid in solution as revealed by circular dichroism. *Biopolymers*, 12 (1), pp. 89 - 110.
- Ivičić N. and Simeon VI., 1981. Stability and C.D. spectra of Co<sup>2+</sup> and Cu<sup>2+</sup> complexes with epimeric threonines and isoleucines. *Journal of Inorganic and Nuclear Chemistry*, 43 (10), pp. 2581-2584.
- Janiak, C., 2000. A critical account on  $\pi$ - $\pi$  stacking in metal complexes with aromatic nitrogen-containing ligands. *Journal of the Chemical Society Dalton Transactions*, 21, pp. 3885-3896.

- Jayaraju, D., Vashisht Gopal, Y.N. and Kondapi, A.K., 1999. Topoisomerase II is a cellular target for antiproliferative cobalt salicylaldehyde complex. *Archives of Biochemistry and Biophysics*, 369 (1), pp. 68 - 77.
- Jia, L. et al., 2010. Synthesis, crystal structures, DNA-binding properties, cytotoxic and antioxidation activities of several new ternary copper(II) complexes of N,N'-(p-xylene)di-alanine acid and 1,10-phenanthroline. *Inorganica Chimica Acta*, 363, pp. 855-865.
- Jiao, K. et al., 2005. Synthesis, characterization and DNA-binding properties of a new cobalt(II) complex:  $\text{Co}(\text{bbt})_2\text{Cl}_2$ , *Journal of Inorganic Chemistry*, 99 (6), pp. 1369 - 1375.
- Jin, V.X. and Ranford, J.D., 2000. Complexes of platinum(II) with 1,10-phenanthroline and amino acids. *Inorganica Chimica Acta*, 304, pp. 38-44.
- Kaileh, M., Berghe, W.V., Boone, E., Essawi, T. and Haegeman, G., 2007. Screening of indigenous Palestinian medicinal plants for potential anti-inflammatory and cytotoxic activity. *Journal of Ethnopharmacology*, 113, pp. 510 - 516.
- Kalia, S.B. et al., 2009. Antimicrobial and toxicological studies of some metal complexes of 4-methylpiperazine-1-carbodithioate and phenanthroline mixed ligands. *Brazilian Journal of Microbiology*, 40 (4), pp. 916 - 922.
- Karidi, K. et al., 2005. Synthesis, characterization, in vitro antitumor activity, DNA-binding properties and electronic structure (DFT) of the new complex  $\text{cis}(\text{Cl},\text{Cl})[\text{Ru}^{\text{II}}\text{Cl}_2(\text{NO}^+)(\text{terpy})]\text{Cl}$ . *Dalton Transaction*, 7, pp. 1176 - 1187.
- Karlin, K.D. and Tyeklar, Z., 1993. *Bioinorganic Chemistry of Copper*, Chapman & Hall, New York, London.
- Karlin, K.D. and Zubieta, J., 1996. In: *Biological and Inorganic Copper Chemistry*, Academic Press, New York.
- Kato, M. and Muto, Y., 1988. Factors affecting the magnetic properties of dimeric copper(II) complexes. *Coordination Chemistry Reviews*, 92, pp. 45 - 83.
- Kato, Y., 2003. Chemical and sensory changes in flavor of roux prepared from wheat flour and butter by heating to various temperatures. *Journal of Food Science and Technology Research*, 9 (3), pp. 264 - 270.

- Katsetos, C.D. et al., 1990. Neuronal cytoskeletal lesions induced in the CNS by intraventricular and intravenous aluminium maltol in rabbits. *Neuropathology and Applied Neurobiology*, 16, pp. 511 - 528.
- Kawase, M. et al., 2004. Liver protection by bis(maltolato)zinc(II) complex. *Journal of Experimental Animal Science*, 53 (1), pp. 1 - 9.
- Keene, F.R., Smith, J.A. and Collins, J.G., 2009. Metal complexes as structure-selective binding agents for nucleic acids. *Coordination Chemistry Reviews*, 253 (15 - 16), pp. 2021 - 2035.
- Kennedy, D.C. et al., 2005. *Tris*(pyronato)- and *tris*(pyridonato)-ruthenium(III) complexes and solution NMR studies. *Inorganic Chemistry*, 44 (19), pp. 6529 - 6535.
- Kennedy, D.C. et al., 2006. Ruthenium(III)-maltolato-nitroimidazole complexes: Synthesis and biological activity. *Journal of Inorganic Biochemistry*, 100, pp. 1974 - 1982.
- Keppler, B.K. et al., 1991. Tumor-inhibiting Bis(b-diketonato)metal complexes. Butotitane, cis-diethoxybis(1-phenylbutane-1,3-dionato) titanium(IV). *Structure and Bonding*, 78, pp. 97 - 127.
- Kikuta, E. et al., 1999. Novel recognition of thymine base in double-stranded DNA by zinc(II)-macrocyclic tetraamine complexes appended with aromatic groups. *Journal of the American Chemical Society*, 121 (23), pp. 5426 - 5436.
- Kikuta, E., Koike, T. and Kimura, E., 2000. Controlling gene expression by zinc(II)-macrocyclic tetraamine complexes. *Journal of Inorganic Biochemistry*, 79 (1-4), pp. 253 - 259.
- Kirillova, M.V. et al., 2007. 3D hydrogen bonded heteronuclear  $\text{Co}^{\text{II}}$ ,  $\text{Ni}^{\text{II}}$ ,  $\text{Cu}^{\text{II}}$  and  $\text{Zn}^{\text{II}}$  aqua complexes derived from dipicolinic acid. *Inorganic Chimica Acta*, 360, pp. 506 - 512.
- Kiss, T. et al., 1998. The formation of ternary complexes between  $\text{VO}(\text{maltolate})_2$  and small bioligands. *Inorganic Chimica Acta*, 283, pp. 202 - 210.

- Klanicová, A. et al., 2006. Synthesis, characterization and in vitro cytotoxicity of Co(II) complexes with N6-substituted adenine derivatives: X-ray structures of 6-(4-chlorobenzylamino)purin-di-ium diperchlorate dihydrate and  $[\text{Co}_6(\mu\text{-L}_6)_4\text{Cl}_8(\text{DMSO})_{10}]\cdot 4\text{DMSO}$ . *Polyhedron*, 25, pp. 1421 - 1432.
- Koman, M., Meink, M. and Moncol. J., 2000. Crystal and molecular structure of copper(II) (pyridine-2,6-dicarboxylato)(2,6-dimethanolpyridine). *Inorganic Chemistry Communications*, 3 (5), pp. 262 - 266.
- Kong, D.Y. and Xie, Y.Y., 2000. Synthesis, structural characterization and potentiometric studies of divalent metal complexes with an octadentate tetraazamacrocyclic ligand and their DNA cleavage ability. *Polyhedron*, 19 (12), pp. 1527 - 1537.
- Kort, R. et al., 2005. Assessment of heat resistance of bacterial spores from food product isolates by fluorescence monitoring or dipicolinic acid release. *Applied and Environmental Microbiology*, 71 (7), pp. 3556 - 3564.
- Kostova, I., 2006. Platinum complexes as anticancer agents. *Recent Patents on Anti-Cancer Drug Discovery*, 1, pp. 1 - 22.
- Krzysztof, Z., Grybos, R. and Proniewicz, L.M., 2005. Molecular structures of oxovanadium(IV) complexes with maltol and kojic acid: a quantum mechanical study. *Inorganic Chemistry Communications*, 8, pp. 76 - 78.
- Krzysztof, Z., Grybos, R. and Proniewicz, L.M., 2007. Structure modification of maltol (3-hydroxy-2-methyl-4H-pyran-4-one) upon cation and anion formation studied by vibrational spectroscopy and quantum-mechanical calculations. *Vibrational Spectroscopy*, 43, pp. 34 - 350.
- Kumar, K.A., Dayalan, A. and SethuSankar, K., 2009. *Cis-Aquachloridobis(1,10-phenanthroline- $\kappa^2N,N'$ )Cobalt(II) chloride 2.5-hydrate*. *Acta Crystallographica*, E65, m1300 – m1301.
- Laine, P., Gourdon, A. and Launay, J.P., 1995. Chemistry of iron with dipicolinic acid. 2. Bridging role of carboxylate groups in solid state structures. *Inorganic Chemistry*, 34 (21), pp. 5138 - 5149.

- Lambooy, J.L. et al., 2007. Synthesis, solution and solid state structure of Titanium-maltol complex. *Inorganic Chimica Acta*, 360, pp. 2115 – 2120.
- Lamour, E. et al., 1999. Oxidation of Cu II to Cu III, free radical production and DNA cleavage by hydroxysalen copper complexes. *Journal of the American Chemical Society*, 121, pp. 1862 - 1869.
- Lamture, J.B. et al., 1995. Luminescence properties of Terbium(III) complexes with 4-substituted dipicolinic acid analogs. *Inorganic Chemistry*, 34 (4), pp. 864 – 869.
- Latva, M. et al., 1997. Correlation between the lowest triplet state energy level of the ligand and the lanthanide(III) luminescence quantum yield. *Journal of Luminescence*, 75, pp. 149 - 169.
- Lavie-Cambot, A. et al., 2008. Improving the photophysical properties of copper(I) bis(phenanthroline) complexes. *Coordination Chemistry Review*, 252, pp. 2572 - 2584.
- LeBlanc, D.T. and Akers, H.A., 1989. Maltol and ethyl maltol: from the larch tree to successful food additives. *Food Technology*, 43 (4), pp. 78 – 84.
- LePecq, J.B. and Paoletti, C., 1967. A fluorescent complex between ethidium bromide and nucleic acids. *Journal of Molecular Biology*, 27, pp. 87-106.
- Lever, A.B.P., 2003. *Comprehensive Coordination Chemistry II*, vol. 1, Oxford, UK: Elsevier.
- Li, F.H. et al., 2006. Synthesis, characterization and biological activity of lanthanum(III) complexes containing 2-methylene-1,10-phenanthroline units bridge by aliphatic diamines. *Journal of Inorganic Biochemistry*, 100 (1), pp. 36 - 43.
- Li, M. et al., 2008. Inhibition of protein tyrosine phosphate 1B and alkaline phosphate by bis(maltolato)oxovanadium (IV). *Journal of Inorganic Biochemistry*, 102, pp. 1846 - 1853.

- Li, Q. et al., 2012. Anticancer activity of novel ruthenium complex with 1,10-phenanthroline-selenazole as potent telomeric G-quadruplex inhibitor. *Inorganic Chemistry Communications*, 20, pp. 142 - 146.
- Li, X.F., Zhao, H.J. and Zeng, Q.H., 2013. Chirality and absolute helicity in a pair of enantiomeric amino acid derivatives and their complexes: Structure, chiroptical, and photoluminescent properties. *Cryst. Eng., Commun.*, Accepted Manuscript.
- Li, Y-H., Wang, B-D. and Yang, Z-Y., 2007. Infrared and DNA- binding on ultraviolet and fluorescence spectra of new copper and zinc complexes with a naringenin Schiff-base ligand. *Spectrochimica Acta Part A*, 67, pp. 395 – 401.
- Liang, H.C., Zhang, Y. and Hetu, M.M., 2007. Phosphate diester hydrolysis promoted by new Cu(II) alkoxide complexes, *Inorganic Chemistry Communications*, 10 (2), pp. 204 - 208.
- Liguori, P.F. et al., 2010. Non-classical anticancer agents: synthesis and biological evaluation of zinc(II) heteroleptic complexes. *Dalton Transactions*, 39 (17), pp. 4205 - 4212.
- Lin, J.G., Qiu, L. and Xu, Y.Y., 2009. A two-dimensional supramolecular network built through unique  $\pi$ - $\pi$  stacking: Synthesis and characterization of  $[\text{Cu}(\text{phen})_2(\mu\text{-IDA})\text{Cu}(\text{phen})\cdot(\text{NO}_3)](\text{NO}_3)\cdot 4(\text{H}_2\text{O})$ . *Bulletin of the Korean Chemical Society*, 30 (5), pp. 1021 - 1025.
- Lin, L. et al., 2005. Topors, a p53 and topoisomerase I-binding RING finger protein, is a coactivator of p53 in growth suppression induced by DNA damage. *Oncogene*, 24 (21), pp. 3385 - 3396.
- Linder, M.C., 1991. *Biochemistry of Copper*, Plenum, New York.
- Liu, Y. et al., 2009. Triaquachlorido(1,10-phenanthroline- $\kappa^2N,N'$ )Cobalt(II) chloride monohydrate. *Acta Crystallographica*, E65, m114.
- Liu, Y.N. et al., 2010. DNA binding and photocleavage properties and apoptosis-inducing activities of a ruthenium porphyrin complex  $[(\text{Py-3}')\text{TPP-Ru}(\text{phen})_2\text{Cl}]\text{Cl}$  and its heterometallic derivatives. *Chemico-Biological Interactions*, 183, pp. 349 - 356.

- Liu, Z. et al., 2011. Organometallic half-sandwich Iridium anticancer complexes. *Journal of Medicinal Chemistry*, 54, pp. 3011 - 3026.
- Liu, Z.P. et al., 2005. Selective and controlled synthesis of  $\alpha$ - and  $\beta$ -cobalt hydroxides in highly developed hexagonal platelets. *Journal of the American Chemical Society*, 127 (40), pp. 13869 - 13874.
- Lo, Y.C. et al., 2009. Terpyridine-platinum(II) complexes are effective inhibitors of mammalian topoisomerases and human thioredoxin reductase. *Journal of Inorganic Biochemistry*, 103 (7), pp. 1082 - 1092.
- Loganathan, R. et al., 2012. Mixed ligand copper(II) complexes of *N,N*-bis(benzimidazol-2-ylmethyl)amine (BBA) with diimine Co-ligands: Efficient chemical nuclease and protease activities and cytotoxicity. *Inorganic Chemistry*, 51 (10), pp. 5512 - 5532.
- Lubes, G., Rodriguez, M. and Lubes, V., 2010. Ternary complex formation between Vanadium(III), dipicolinic acid and picolinic acid in aqueous solution. *Journal of Solution Chemistry*, 39, pp. 1134 – 1141.
- Luman, C.R. and Castellano, F.N., 2004. In: McCleverty, J.A., Meyer, T.J. and Lever, A.B.P. (eds.). *Comprehensive Coordination Chemistry*, vol. 1. Oxford, UK: Elsevier, pp. 25.
- Ma, C. et al., 2003. The first structurally characterized trinuclear dipicolinato manganese complex and its conversion into a mononuclear species by ligand substitution. *European Journal of Inorganic Chemistry*, 2003 (6), pp. 1227 - 1231.
- Ma, C.B. et al., 2002. Aqua(dipicolinato- $\kappa^3\text{O}^2, \text{N}, \text{O}^6$ )(1,10-phenanthroline- $\kappa^2\text{N}, \text{N}'$ )manganese(II) monohydrate. *Acta Crystallographica*, C58 m553 - m555.
- Magnus, K.A., Ton-That, H. and Carpenter, J.E., 1994. Recent structural work on the oxygen transport protein hemocyanin. *Chemical Reviews*, 94 (3), pp. 727 -735.
- Maheswari, P.U. et al., 2008. Structure, cytotoxicity, DNA-cleavage properties of the complex  $[\text{Cu}^{\text{II}}(\text{pbt})\text{Br}_2]$ . *Inorganic Chemistry*, 47 (9), pp. 3719 - 3727.

- Manikandamathavan, V.M. et al., 2011. Cytotoxic copper(II) mixed ligand complexes: Crystal structure and DNA cleavage activity. *European Journal of Medicinal Chemistry*, 46, pp. 4537 - 4547.
- Mao, L. et al., 2004. A novel three-dimensional supramolecular framework with one-dimensional channels: synthesis and crystal structure of [Cu(DPC)(H<sub>2</sub>O)<sub>3</sub>] (H<sub>2</sub>DPC = pyridine-2,6-dicarboxylic acid). *Journal of Molecular Structure*, 688, pp. 197 - 201.
- Marcu, A. et al., 2008. Structural investigations of some metallic complexes with threonine as ligand. *Journal of optoelectronics and advanced materials*, 10 (4), pp. 830 - 833.
- Marwaha, S.S., Kaur, J. and Sodhi, G.S., 1994. Organomercury(II) complexes of kojic acid and maltol: Synthesis, characterization, and biological studies. *Journal of Inorganic Chemistry*, 54, pp. 67 - 74.
- Maurya, R. C. et al., 2011. Oxoperoxomolybdenum(VI) complexes of catalytic and biomedical relevance: Synthesis, characterization, antibacterial activity and 3D-Molecular modeling of some oxoperoxomolybdenum(VI) chelates in mixed (O,O) coordination environment involving maltol and  $\beta$ -diketoenolates. *Arabian Journal of Chemistry*, accepted manuscript.
- Maurya, R.C., Sahu, S. and Bohre, P., 2008. Synthesis, characterization, antibacterial activity and 3D-molecular modeling of some oxoperoxomolybdenum(VI) chelates in mixed (O,O) coordination environment involving 2-hydroxy-1-naphthaldehyde and  $\beta$ -diketoenolates. *Indian Journal of Chemistry*, 47A, pp. 1333 - 1342.
- Mazzei, M. et al., 2001. Unsymmetrical methylene derivatives of indoles as antiproliferative agents. *European Journal of Medicinal Chemistry*, 36, pp. 915 - 923.
- McKenzie, E.D., 1971. The steric effect in bis(2,2'-bipyridyl) and bis(1,10-phenanthroline) metal compounds. *Coordination Chemistry Reviews*, 6, pp. 187-216.
- McNeill, J.H. et al., 1992. Bis(maltolato)oxovanadium(IV) is a potent insulin mimetic. *Journal of Medicinal Chemistry*, 35 (8), pp. 1489 - 1491.

- Mesquita, M.E. et al., 2002. Synthesis, spectroscopic studies and structure prediction of the new  $Tb(3-NH_2PIC)_3 \cdot 3H_2O$  complex. *Inorganic Chemistry Communication*, 5, pp. 292 – 295.
- Mesquita, M.E. et al., 2009. Highly luminescent di-ureasil hybrid doped with a Eu(III) complex including dipicolinate ligands. *Journal of Photochemistry and Photobiology A: Chemistry*, 205, pp. 156 - 160.
- Milacic, V. et al., 2008. Pyrrolidine dithiocarbamate-zinc(II) and copper(II) complexes induce apoptosis in tumor cells by inhibiting the proteasomal activity. *Toxicology and Applied Pharmacology*, 231 (1), pp. 24 - 33.
- Mishra, A.P., Tiwari, A., and Jain, R.K., 2012. Microwave induced synthesis and characterization of semiconducting 2-thiophenecarboxaldehyde metal complexes. *Advanced Materials Letters*, 3 (3), pp. 213-219.
- Miyake, H. et al., 2004. Dynamic helicity inversion by achiral anion stimulus in synthetic labile Cobalt(II) complex. *Journal of the American Chemical Society*, 126 (21), pp. 6524 - 6525.
- Monchaud, D. et al., 2008. Ligands playing musical chairs with G-quadruplex DNA: A rapid and simple displacement assay for identifying selective G-quadruplex binders. *Biochimie*, 90, pp. 1207 - 1223.
- Monzon, L.M.A., 2010. Electrochemical characterisation of bis(1,10-phenanthroline) gadolinium (III) trichloride formed *in situ*. *Journal of Electroanalytical Chemistry*, 648, pp. 47 - 53.
- Murakami, K. and Yoshino, M., 1998. Dipicolinic acid as an antioxidant: Protection of glutathione reductase from the inactivation by copper. *Biomedical Research*, 20, pp. 321 - 326.
- Murakami, K. et al., 1998. Antioxidant effect of dipicolinic acid on the metal-catalyzed peroxidation and enzyme inactivation. *Biomedical Research*, 19, 205 - 208.
- Murakami, K. et al., 2006. Maltol/iron-mediated apoptosis in HL60 cells: Participation of reactive oxygen species. *Toxicology Letters*, 161, pp. 102 - 107.

- Murakami, K., Tanemura, Y. and Yoshino, M., 2003. Dipicolinic acid prevents the copper-dependent oxidation of low density lipoprotein. *The Journal of Nutritional Biochemistry*, 14, pp. 99 - 103.
- Na'aliya, J., 2010. The stability constants of nickel(II) complexes of amino acids with polar uncharged R-groups. *Bayero Journal of Pure and Applied Sciences*, 3 (1), pp. 241 - 244.
- Nagababu, P. et al., 2008. DNA binding and photocleavage studies of Cobalt(III) ethylenediamine pyridine complexes:  $[\text{Co}(\text{en})_2(\text{py})_2]^{3+}$  and  $[\text{Co}(\text{en})_2(\text{mepy})_2]^{3+}$ . *Metal-Based Drugs*, 2008, pp. 1 - 8.
- Nagane, R., Koshigoe, T. and Chikira, M., 2003. Interaction of Cu(II)-Arg-Gly-His-Xaa metallopeptides with DNA: effect of C-terminal residues, Leu and Glu. *Journal of Inorganic Biochemistry*, 93 (3 - 4), pp. 204 - 212.
- Nagaoka, M. and Sugiura, Y., 2000. Artificial zinc finger peptides: creation, DNA recognition, and gene regulation. *Journal of Inorganic Biochemistry*, 82 (1-4), pp. 57 - 63.
- Nakabayashi, Y. et al., 2004. Interactions of mixed ligand ruthenium(II) complexes containing an amino acid and 1,10-phenanthroline with DNA. *Inorganic Chimica Acta*, 357, pp. 2553 - 2560.
- Nakabayashi, Y. et al., 2006. DNA-binding properties of flexible diamine bridged dinuclear ruthenium(II)-2,2'-bipyridine complexes. *Inorganic Chemistry Communications*, 9 (10), pp. 1033 - 1036.
- Nakamoto, K., 1977. Infrared and Raman Spectra of Inorganic and Coordination Compounds. Wiley-interscience publication, pp. 226 - 317.
- Nelson, W.O. et al., 1988. Aluminium and gallium compounds of 3-hydroxy-4-pyridinones: synthesis, characterization, and crystallography of biologically active complexes with unusual hydrogen bonding. *Inorganic Chemistry*, 27 (6), pp. 1045 - 1051.

- Ng, C.H. et al., 2002. Reactions of *Bis*( $\beta$ -alaninato)metal(II) complexes with formaldehyde and benzamide: The crystal structure of *Bis*[*N*-methyl-*N*-(*N'*-methyl-benzamido)- $\beta$ -alaninato]copper(II) monohydrate and characterization of *Bis*[*N,N*-Di(*N'*-methylbenzamido)- $\beta$ -alaninato]metal(II) complexes. *Journal of Coordination Chemistry*, 55 (8), pp. 909 - 916.
- Ng, C.H. et al., 2003. Effect of different  $\alpha$ - on the Mannich reaction of copper(II) chelated  $\alpha$ -amino acids with formaldehyde and acetamide: X-ray structure of aquabis(3-methylacetamido-5-methyl-oxazolidine-4-carboxylato)-copper(II). *Polyhedron*, 22, pp. 521 - 528.
- Ng, C.H. et al., 2006. Mono- and di-*N*-acetamidomethylated derivatives of *Bis*(*L*-alaninato)copper(II): Characterization and nucleolytic property crystal structure of *Bis*[*N,N*-di-(*N'*-methylacetamido)-*L*-alaninato]copper(II). *Polyhedron*, 25, pp. 1287 - 1291.
- Ng, C.H. et al., 2007. Synthesis, characterization, DNA-binding study and anticancer properties of ternary metal(II) complexes of edda and an intercalating ligand. *Dalton Transaction*, 4, pp. 447 - 454.
- Ng, C.H. et al., 2008. Synthesis, characterization, DNA-binding study and anticancer properties of ternary metal(II) complexes of edda and an intercalating ligand. *Dalton Transaction*, 4, pp. 447 - 454.
- Ni, Y., Zhang, G. and Kokot, S., 2005. Simultaneous spectrophotometric determination of maltol, ethyl maltol, vanillin and ethyl vanillin in foods by multivariate calibration and artificial neural networks. *Food Chemistry*, 89, pp. 465-473.
- Nikitin, K. et al., 2010. Organometallic SERMS (selective estrogen receptor modulators): Cobaltifens, the (cyclobutadiene)cobalt analogues of hydroxytamoxifen. *Journal of Organometallic Chemistry*, 695, pp. 595 - 608.
- Nishizawa, S. et al., 1999. Fluorescence ratio sensing of alkali metal ions based on control of the intramolecular exciplex formation. *Journal of the Chemical Society, Perkin Transactions 2*, 2, pp. 141-144.
- Norden, B. and Tjerneld, F., 1976. Binding of inert metal complexes to deoxyribonucleic acid detected by linear dichroism. *FEBS Letters*, 67 (3), pp. 368 - 370.

- Novitchi, G. et al., 2004. Richness of isomerism in labile octahedral Werner-type cobalt(II) complexes demonstrated by  $^{19}\text{F}$  NMR spectroscopy: structure and stability. *Magnetic Resonance in Chemistry*, 42 (9), pp. 801 - 806.
- Obulesu, M., Dowlathabad, M.R. and Shama Sundar, N.M., 2009. Studies on genomic DNA stability in aluminium-maltolate treated aged New Zealand rabbit: relevance to the Alzheimer's animal model. *Journal of Clinical Medical Research*, 1 (4), pp. 212 - 218.
- O'Connor, M. et al., 2012. Copper(II) complexes of salicylic acid combining superoxide dismutase mimetic properties with DNA binding and cleaving capabilities display promising chemotherapeutic potential with fast acting in vitro cytotoxicity against cisplatin sensitive and resistant cancer cell lines. *Journal of Medicinal Chemistry*, 55 (5), pp. 1957 - 1968.
- Okabe, N. and Oya, N., 2000. Copper(II) and zinc(II) complexes of pyridine-2,6-dicarboxylic acid. *Acta Crystallographica*, C56, pp. 305 - 307.
- Oliveira, M.C.B. et al., 2009. Mononuclear  $\text{Cu}^{\text{II}}$ -phenolate bioinspired complex is catalytically promiscuous: Phosphodiester and peptide amide bond cleavage. *Inorganic Chemistry*, 48 (7), pp. 2711 - 2713.
- Palumbo, M. et al., 2002. Sequence-specific interactions of drugs interfering with the topoisomerase-DNA cleavage complex. *Biochimica et Biophysica Acta*, 1587, pp. 145 - 154.
- Papadopoulos, C.D. et al., 2007. Substitution effect on new Co(II) addition compounds with salicylaldehydes and the nitrogenous bases phen or neoc: Crystal and molecular structures of  $[\text{Co}^{\text{II}}(5\text{-NO}_2\text{-salicylaldehyde})_2(\text{phen})]$ ,  $[\text{Co}^{\text{II}}(5\text{-CH}_3\text{-salicylaldehyde})_2(\text{neoc})]$  and  $[\text{Co}^{\text{II}}(5\text{-Cl-salicylaldehyde})_2(\text{neoc})]$ . *Inorganic Chimica Acta*, 360, pp. 3581 - 3589.
- Papworth, M., Kolasinska, P. and Minczuk, M., 2006. Designer zinc-finger proteins and their applications. *Gene*, 366 (1), pp. 27 - 38.
- Parajón-Costa, B. and Baran, E.J., 2011. Vibrational spectra of bis(maltolato)oxovanadium(IV): A potent insulin mimetic agent. *Spectrochimica Acta Part A: Molecular and Biomolecular Spectroscopy*, 78, pp. 133 - 135.

- Patra, A.K. et al., 2007. Metal-based netropsin mimics showing AT-selective DNA binding and DNA cleavage activity at red light. *Inorganic Chemistry*, 46 (22), pp. 9030 - 9032.
- Paulovicova, A., El-Ayaan, U. and Fukuda, Y., 2001. Synthesis, characterization and X-ray crystal structures of two five-coordinate ternary copper(II) complexes containing acetylacetonate with 1,10-phenanthroline and 2,9-dimethylphenanthroline. *Inorganic Chimica Acta*, 321, pp. 56 – 62.
- Peters, K.G. et al., 2003. Mechanism of insulin sensitization by BMOV (bis maltolato oxo vanadium); unliganded vanadium ( $\text{VO}_4$ ) as the active component. *Journal of Inorganic Biochemistry*, 96, pp. 321 - 330.
- Piulats, J.M. et al., 2009. Molecular mechanisms behind the resistance of cisplatin in germ cell tumours. *Clinical Translational Oncology*, 12, pp. 780 - 786.
- Pommier, Y., 2006. Topoisomerase I inhibitors: camptothecins and beyond. *Nature Reviews Cancer*, 6 (10), pp. 789 - 802.
- Qi, Y. et al., 2004. Structure characterization and physical properties of a complex with supramolecular architectures  $\text{Co}_2(2,6\text{-DPC})_2\text{Co}(\text{H}_2\text{O})_5 \cdot 2\text{H}_2\text{O}$  (DPC = 2,6-pyridinedicarboxylate). *Journal of Molecular Structure*, 694, pp. 73 - 78.
- Qin, C. et al., 2005. A series of three-dimensional Lanthanide coordination polymers with Rutile and unprecedented Rutile-Related topologies. *Inorganic Chemistry*, 44 (20), pp. 7122 – 7129.
- Qu, X.G. et al., 2000. Allosteric, chiral-selective drug binding to DNA. *Proceedings of the National Academy of Sciences*, 97 (22), pp. 12032 - 12037.
- Radanović, D.D. et al., 2003. Simple synthetic method and structural characteristics of (1,3-propanediaminetetraacetato)cobalt(II) complexes: uniform crystal packing in a series of metal(II) complexes with 1,3-propanediaminetetraacetate ligand. *Polyhedron*, 22, pp. 2745 - 2753.

- Rafique, S. et al., 2010. Transition metal complexes as potential therapeutic agents. *Biotechnology and Molecular Biology Review*, 5 (2), pp. 38 - 45.
- Rahman, Md.M. et al., 2007. Inhibition of endonuclease cleavage and DNA replication of *E. coli* plasmid by antitumor rhodium(II) complex. *Archives of Biochemistry and Biophysics*, 464 (1), pp. 28 - 35.
- Rajendiran, V. et al., 2008. Non-covalent DNA binding and cytotoxicity of certain mixed-ligand ruthenium(II) complexes of 2,2'-dipyridylamine and diimines. *Dalton Transactions*, 16, pp. 2157 - 2170.
- Rajendran, A. and Nair, B.U., 2006. Unprecedented dual binding behaviour of acridine group of dye: A combined experimental and theoretical investigation for the development of anticancer chemotherapeutic agents. *Biochimica et Biophysica Acta*, 1760, pp. 1794 - 1801.
- Raman, N. and Sobha, S., 2010. Synthesis, characterization, DNA interaction and antimicrobial screening of isatin-based polypyridyl mixed-ligand Cu(II) and Zn(II) complexes. *Journal of the Serbian Chemical Society*, 75 (0), pp. 1 - 16.
- Raman, N. et al., 2010. New insights into the antibacterial and antifungal activity study of mixed-ligand metal complexes containing tridentate schiff base. *Journal for Bloomers of Research*, 3 (1), pp. 6 - 12.
- Rana, V.B., Sahni, S.K. and Sangal, S.K., 1979. Oxovanadium(IV) complexes of potential pentadentate ligands. *Journal of Inorganic Nuclear Chemistry*, 41, pp. 1498 - 1500.
- Ranjbar, M., Aghabozorg, H. and Moghimi, A., 2002. A seven-coordinate pyridine-2,6-dicarboxylate-bridged cadmium(II) complex, at 110 K. *Acta Crystallographica*, E58, m304 - m306.
- Rao, R., Patra, A. K. and Chetana, P. R., 2008. Synthesis, structure, DNA binding and oxidative cleavage activity of ternary (L-leucine/isoleucine) copper(II) complexes of heterocyclic bases. *Polyhedron*, 27 (5), pp. 5331 - 5338.
- Rao, R., Patra, A.K. and Chetana, P.R., 2007. DNA binding and oxidative cleavage activity of ternary (L-proline)copper(II) complexes of heterocyclic bases. *Polyhedron*, 26 (18), pp. 5331 - 5338.

- Rao, V.A. et al., 2007. Batracylin (NSC 320846), a dual inhibitor of DNA topoisomerase I and II induces histone  $\gamma$ -H2AX as a biomarker of DNA damage. *Cancer Research*, 67 (20), pp. 9971 - 9979.
- Reddy, P.M. et al., 2007. Synthesis, spectral studies and antibacterial activity of novel macrocyclic Co(II) compounds. *Spectrochimica Acta Part A*, 68, pp. 1000 – 1006.
- Reddy, P.R., Rao, K.S. and Satyanarayana, B., 2006. Synthesis and DNA cleavage properties of ternary Cu(II) complexes containing histamine and amino acids. *Tetrahedron Letters*, 47, pp. 7311-7315.
- Reinhammer, B., 1984. Copper proteins and copper enzymes, vol. 3, CRC Press, Boca Raton, FL, pp. 1 - 35.
- Richards, A.D. and Rodger, A., 2007. Synthetic metallomolecules as agents for the control of DNA structure. *Chemical Society Reviews*, 36 (3), pp. 471 - 483.
- Rizzi, A.C. et al., 2000. Structure and single crystal EPR study of Cu(II) (L-threonine)<sub>2</sub>.H<sub>2</sub>O. *Inorganic Chimica Acta*, 305, pp. 19 - 25.
- Rothenberg, M.L., 1997. Topoisomerase I inhibitors: Review and update. *Annals of Oncology*, 8 (9), pp. 837 - 855.
- Roy, N. et al., 2009. Polynuclear complexes containing the redox noninnocent schiff base ligand 2-[(E)-2-Mercaptophenylimino]methyl-4,6-di-*tert*-butylphenolate(2-). *European Journal of Inorganic Chemistry*, 2009 (18), pp. 2655 - 2663.
- Rubin-Preminger, J.M., Kozlov, L. and Goldberg, I., 2008. Hydrogen-bonding and  $\pi$ - $\pi$  stacking interactions in aquachloridobis(1,10-phenanthroline)cobalt(II) chloride dichloridobis(1,10-phenanthroline)-cobalt(II) hexahydrate. *Acta Crystallographica*, C64, m83 - 86.
- Saatchi, K. et al., 2005. Coordination chemistry and insulin-enhancing behavior of vanadium complexes with maltol C<sub>6</sub>H<sub>6</sub>O<sub>3</sub> structural isomers. *Inorganic Chemistry*, 44 (8), pp. 2689 - 2697.

- Saenger, W., 1983. *Principles of Nucleic acid structure*. 1st edition. New York: Springer-Verlag.
- Sahni, S.K. et al, 1977. Some 5-coordinate nickel(II) complexes of dipicolinic acid hydrazide. *Journal of Inorganic Nuclear Chemistry*, 39, pp. 1098 – 1100.
- Sakurai, H. et al., 2002. Antidiabetic vanadium(IV) and zinc(II) complexes. *Coordination Chemistry Review*, 226, pp. 187 - 198.
- Sakurai, H., 2010. Overview and frontier for the development of metallopharmaceutics. *Journal of Health Science*, 56 (2), pp. 129 - 143.
- Sakurai, H., Yasui, H. and Adachi, Y., 2003. The therapeutic potential of insulin-mimetic vanadium complexes. *Expert Opinion On Investigation Drugs*, 12, pp. 1189 - 1203.
- Sammes, P.G. and Yahioğlu, G., 1994. 1,10-phenanthroline: a versatile ligand. *Chemical Society Reviews*, 23, pp. 327 - 334.
- Savory, J. et al., 1993. Quantitative studies on aluminium deposition and its effects on neurofilament protein expression and phosphorylation, following the intraventricular administration of aluminium maltolate to adult rabbits. *Neurotoxicology*, 14, pp. 9 - 12.
- Scaltrito, D.V. et al., 2000. MLCT excited states of cuprous bis-phenanthroline coordination compounds. *Coordination Chemistry Reviews*, 208, pp. 243 - 266.
- Schenck, J.R. and Speilmen, M.A.J., 1945. The formation of maltol by the degradation of streptomycin, *Journal of the American Chemical Society*, 67 (12), pp. 2276 – 2277.
- Schilling, T. et al., 1996. Clinical phase I and pharmacokinetic trial of the new titanium complex budotitane. *Investigational New Drugs*, 13, pp. 322-327.
- Schilt, A.A. and Taylor, R.C., 1958. Infra-Red spectra of 1,10-phenanthroline metal complexes in the rock salt region below 2000  $\text{cm}^{-1}$ . *Journal of Inorganic Nuclear Chemistry*, 9, pp. 211 – 221.
- Schobert, R. et al., 2011. Cancer selective metallocenedicarboxylates of the fungal cytotoxin iludin M. *Journal of Medicinal Chemistry*, 54 (18), pp. 6177 - 6182.

- Seng, H.L. et al., 2008. Factors affecting nucleolytic efficiency of some ternary metal complexes with DNA binding and recognition domains. Crystal and molecular structure of Zn(phen)(edda). *Journal of Inorganic Biochemistry*, 102, pp. 1997 - 2011.
- Seng, H.L. et al., 2010. Crystal structure, DNA binding studies, nucleolytic property and topoisomerase I inhibition of zinc complex with 1,10-phenanthroline and 3-methyl-picolinic acid. *Biometals*, 23 (1), pp. 99 - 118.
- Shahjee, MD. H., Banerjee, K. and Ahmad, F., 2002. Comparative analysis of naturally occurring L-amino acid osmolytes and their D-isomers on protection of *Escherichia coli* against environmental stresses. *Journal of Biosciences*, 27 (5), pp. 515 - 520.
- Shanmugam, M. et al., 2001. A role for protein kinase C  $\delta$  in the differential sensitivity of MCF-7 and MDA-MB 231 human breast cancer cells to phorbol ester-induced growth arrest and p21<sup>WAF1/CIP1</sup> induction. *Cancer Letters*, 172, pp. 43 - 53.
- Shebl, M., Khalil, S.M.E. and Al-Gohani, F.S., 2010. Preparation, spectral characterization and antimicrobial activity of binary and ternary Fe(III), Co(II), Ni(II), Cu(II), Zn(II), Ce(III) and UO<sub>2</sub>(VI) complexes of a thiocarbohydrazone ligand. *Journal of Molecular Structure*, 980, pp. 78 - 87.
- Sheldrick, G.M. 1997. SADABS, A software for Empirical Absorption Correction, *University of Göttingen*, Germany.
- Sheldrick, G.M., 1996. SADABS, *University of Göttingen*, Germany.
- Sheldrick, G.M., 2001. SADABS: A software for Empirical Absorption Correction, *University of Göttingen*, Germany.
- Sheldrick, G.M., 2008. A short history of SHELX, *Acta Cryst. A* 64, pp. 112 - 122.
- SHELXTL Reference Manual, 2000. version 6.10, Bruker AXS GmbH, Karlsruhe, Germany.

- Shi, H. et al., 2007. Oxidation of L-serine and L-threonine by bis(hydrogen periodato)argentate(III) complex anion: A mechanistic study. *Journal of Inorganic Biochemistry*, 101, pp. 165 - 172.
- Shiu, K.B. et al., 2004. Hexaaquacobalt(II) *trans*-bis( $\eta^3$ -pyridine-2,6-dicarboxylato- $\kappa^3 O,N,O'$ )cobaltate(II) dihydrate. *Acta Crystallographica*, E60, m35 - 37.
- Sigel, A., Sigel, H. and Sigel, R.K.O. (eds), 2006. In: Zinc Metalloneurochemistry: Physiology, Pathology, and Probes, in Metal ions in life sciences. Wiley, Chichester.
- Sigman, D.S. et al., 1979. Oxygen-dependent cleavage of DNA by the 1,10-phenanthroline. cuprous complex. *The Journal of Biological Chemistry*, 254, pp. 12269 - 12272.
- Sigman, D.S. et al., 1996. Metal Ions in Biological Systems. In: Sigel, A. and Sigel, H. (eds.). *Probing of Nucleic Acids by Metal Ion Complexes of Small Molecules*, vol. 33, Marcel Dekker, New York: USA, pp. 485.
- Sigman, D.S. et al., 1993a. Targeted chemical nucleases. *Accounts of Chemical Research*, 26 (3), pp. 98 - 104.
- Sigman, D.S., Mazumder, A. and Perrin, D.M., 1993b. Chemical nucleases. *Chemical Reviews*, 93 (6), pp. 2295 - 2316.
- Sileo, E. E. et al., 1997. Kinetic study of the thermal dehydration of copper(II) dipicolinates: crystal and molecular structure of Cu(II) (pyridine 2,6-dicarboxylato) Di- and Trihydrated. *Journal of Physics and Chemistry of Solids*, 58 (7), pp. 1127 - 1135.
- Silva, P.P. et al., 2011. Two new ternary complexes of copper(II) with tetracycline or doxycycline and 1,10-phenanthroline and their potential as antitumoral: Cytotoxicity and DNA cleavage. *Inorganic Chemistry*, 50 (14), pp. 6414 - 6424.
- Sitlani, A. et al., 1992. DNA photocleavage by phenanthrenequinone diimine complexes of rhodium(III): shape-selective recognition and reaction. *Journal of the American Chemical Society*, 114 (7), pp. 2303 - 2312.

- Skoog, D.A., Holler, F.J., Crouch, S.R., 2007. *Principles of Instrumental Analysis*. Sixth Edition, Thomson Brooks/Cole, USA.
- SMART (Version 5.631) & SAINT (Version 6.63) Software Reference Manuals, 2000. Bruker AXS GmbH, Karlsruhe, Germany.
- Snow, A.M. and Sheardy, R.D., 2001. Locating cobalt-binding sites on DNA using restriction endonucleases. *Methods Enzymol.*, 340, pp. 519 - 528.
- Snyder, A.P., 1996. *Biochemical and Biotechnological Applications of Electrospray Ionization Mass Spectrometry*. American Chemical Society, Washington, DC.
- Solomon, E.I. and Hadt, R.G., 2011. Recent advances in understanding blue copper proteins. *Coordination Chemistry Review*, 255 (7-8), pp. 774 - 789.
- Solomon, E.I. et al., 2001. Oxygen binding, activation, and reduction to water by copper proteins. *Angewandte Chemie International Edition*, 40 (24), pp. 4570 - 4590.
- Solomon, E.I., Sundaram, U.M. and Machonkin, T.E., 1996. Multicopper oxidases and oxygenases. *Chemical Reviews*, 96 (7), pp. 2563 - 2606.
- Song, C. et al., 2011. Chlorobis(1,10-phenanthroline)zinc(II) tetrachloro(1,10-phenanthroline)-bismuthate(III) monohydrate. *Acta Crystallographica*, E67, m109 - 110.
- Sorenson, J.R., 1989. Copper complexes offer a physiological approach to treatment of chronic diseases. *Progress Medicinal Chemistry*, 26, pp. 437 - 568.
- Sreedaran, S. et al., 2008. Novel unsymmetrical macrocyclic dicompartmental binuclear copper(II) complexes bearing 4- and 6-coordination sites: Electrochemical, magnetic, catalytic and antimicrobial studies. *Polyhedron*, 27 (13), pp. 2931 - 2938.
- Stanojkovic, T.P. et al., 2010. Zinc(II) complexes of 2-acetyl pyridine 1-(4-fluorophenyl)-piperazinyl thiosemicarbazone: Synthesis, spectroscopic study and crystal structures - Potential anticancer drugs. *Journal of Inorganic Biochemistry*, 104 (4), pp. 467 - 476.

- Stehbens, W.E., 2003. Oxidative stress, toxic hepatitis, and antioxidants with particular emphasis on zinc. *Experimental and Molecular Pathology*, 75 (3), pp. 265 - 276.
- Su, C.C. et al., 1993. Bonding properties of copper(II)-N chromophores: molecular and electronic structures of copper(II) complexes containing ethylenediamine and heterocyclic diimine ligands. *Polyhedron*, 12 (22), pp. 2687 - 2696.
- Sukanya, D. Prabhakaran, R. and Natarajan, K., 2006. Ruthenium(III) complexes of dipicolinic acid with PPh<sub>3</sub>/AsPh<sub>3</sub> as co-ligand: Synthesis and structural characterization. *Polyhedron*, 25, pp. 2223 – 2228.
- Summers, L.A., 1978. The Phenanthrolines. *Advances in Heterocyclic Chemistry*, 22, pp. 1 - 69.
- Sun, X.G. et al., 2002. The divalent cation-induced DNA condensation studied by atomic force microscopy and spectra analysis. *Inorganic Chemistry Communication*, 5 (3), pp. 181 - 186.
- Sun, Y. et al., 1996. Oxidation kinetics of the potent insulin mimetic agent bis(maltolato)oxovanadium(IV) (BMOV) in water and in methanol. *Inorganic Chemistry*, 35 (6), p. 1667 - 1673.
- Sunami, S. et al., 2009. Synthesis and biological activities of topoisomerase I inhibitors, 6-arylmethylamino analogues of edotecarin. *Journal of Medicinal Chemistry*, 52 (10), pp. 3225 - 3237.
- Sung, F.L. et al., 2005. Antitumor effect and enhancement of cytotoxic drug activity by Cetuximab in Nasopharyngeal Carcinoma Cells. *In Vivo*, 19 (6), pp. 237 - 246.
- Svensson, F.R. et al., 2011. Ruthenium(II) complex enantiomers as cellular probes for diastereomeric interactions in confocal and fluorescence lifetime imaging microscopy. *Journal of Physical Chemistry Letters*, 2 (5), pp. 397 - 401.
- Tan, K.W. et al., 2008. Chlorido(2-methyl-4-oxo-4H-pyran-3-olato- $\kappa^2 O^3, O^4$ )(1,10-phenanthroline- $\kappa^2 N, N'$ )copper(II). *Acta Crystallographica*, E64, m1104.

- Teicher, B.A., 2008. Next generation topoisomerase I inhibitors: Rationale and biomarker strategies. *Biochemical Pharmacology*, 75, pp. 1262 - 1271.
- Teoh, S.G. et al., 2008. Oxovanadium(IV) dipicolinate: structure nucleolytic and anticancer property. *Modern Applied Science*, 2 (2), pp. 117 - 126.
- Terrón, A. et al., 2007. Biological recognition patterns implicated by the formation and stability of ternary metal ion complexes of low-molecular-weight formed with amino acid/peptides and nucleobases/nucleosides. *Coordination Chemistry Reviews*, 251 (15 – 16), pp. 1973 - 1986.
- Theдераhn, T.B. et al., 1989. Nuclease activity of 1,10-phenanthroline-copper: kinetic mechanism. *Journal of the American Chemical Society*, 111 (13), pp. 4941 - 4946.
- Thompson, K.H. et al., 2003. Preparation and characterization of vanadyl complexes with bidentate maltol-type ligands; in vivo comparisons of anti-diabetic therapeutic potential. *Journal of Biological Inorganic Chemistry*, 8 (1 - 2), pp. 66 - 74.
- Thompson, K.H. et al., 2004. Comparison of anti-hyperglycemic effect amongst vanadium, molybdenum and other metal maltol complexes. *Journal of Inorganic Biochemistry*, 98, pp. 683 – 690.
- To, Y.F. et al., 2009. Gold(III) porphyrin complex is more potent than cisplatin in inhibiting growth of nasopharyngeal carcinoma *in vitro* and *in vivo*. *International Journal of Cancer*, 124 (8), pp. 1971 - 1979.
- Tolman, W.B., 1997. Making and breaking the dioxygen O-O bond: New insights from studies of synthetic copper complexes. *Accounts of Chemical Research*, 30 (6), pp. 227 - 237.
- Trivedi, M. et al., 2010. A new single pot synthesis of  $\mu$ -bis(oxido)bis{oxidovanadium(v)}dipicolinato complex with 2-aminopyridinium as counter cation: Spectroscopic, structural, catalytic and theoretical studies. *Journal of Organometallic Chemistry*, 695, pp. 1722 – 1728.

- Tsaryuk, V.T. et al., 2010. Structural regularities and luminescence properties of dimeric europium and terbium carboxylates with 1,10-phenanthroline (C.N. = 9). *Journal of Photochemistry and Photobiology A: Chemistry*, 211, pp. 7 - 19.
- Tunçel, M. and Serin, S., 2006. Synthesis and characterization of new azo-linked schiff bases and their cobalt(II), copper(II) and nickel(II) complexes. *Transition Metal Chemistry*, 31 (6), pp. 805 - 812.
- Uma, V. et al., 2005. Oxidative DNA cleavage mediated by a new copper(II) terpyridine complex: Crystal structure and DNA binding studies. *Journal of Inorganic Chemistry*, 99, pp. 2299 - 2307.
- Uma, V., Elango, M. and Nair, B.U., 2007. Copper(II) terpyridine complexes: Effect of substituent on DNA binding and nuclease activity. *European Journal of Inorganic Chemistry*, 2007 (22), pp. 3484 - 3490.
- Uçar, I., Bulut, A. and Büyükgüngör, O., 2007. Synthesis, crystal structure, EPR and electrochemical studies of copper(II) dipicolinate complex with 2,2'-dipyridylamine ligand. *Journal of Physics and Chemistry of Solids*, 68, pp. 2271 - 2277.
- Vargová, Z. et al., 2004. Correlation of thermal and spectral properties of zinc(II) complexes of pyridinecarboxylic acids with their crystal structures. *Thermochimica Acta*, 423, pp. 149 - 157.
- Versiane, O. et al., 2006. Synthesis, molecular structure and vibrational spectra of a dimeric complex formed by cobalt and glycine. *Spectrochimica Acta Part A*, 65, pp. 1112 - 1119.
- Von, S.T. et al., 2012. DNA molecular recognition and cellular selectivity of anticancer metal(II) complexes of ethylenediaminediacetate and phenanthroline: multiple targets. *Journal of Biological Inorganic Chemistry*, 17 (1), pp. 57 - 69.
- Wang, L. et al., 2004a. Novel hydrogen-bonded three-dimensional network complexes containing cobalt-pyridine-2,6-dicarboxylic acid. *Transition Metal Chemistry*, 29 (2), pp. 212-215.
- Wang, L. et al., 2004b. Synthesis of novel copper compounds containing isonicotinic acid and/or 2,6-pyridinedicarboxylic acid: third-order nonlinear optical properties. *Journal of Coordination Chemistry*, 57 (13), pp. 1079 - 1087.

- Wang, X. et al., 1998. Differential effects of camptothecin derivatives on topoisomerase I-mediated DNA structure modification. *Biochemistry*, 37 (26), pp. 9399 - 9408.
- Wang, Y. et al., 2006. Proteomic characterization of the cytotoxic mechanism of gold(III) porphyrin 1a, a potential anticancer drug. *Proteomics*, 6 (1), pp. 131 - 142.
- Wang, Z.M. et al., 2000. *Cis*-Bis(dicyanamido)bis(1,10-phenanthroline)-manganese(II) and *cis*-bis-(dicyanamido)bis(1,10-phenanthroline)zinc(II). *Acta Crystallographica*, C56, e242 - 244.
- Warra, A.A., 2011. Transition Metal Complexes and their application in drugs and cosmetics - A Review. *Journal of Chemical and Pharmaceutical Research*. 3 (4), pp. 951 - 958.
- Watson, J.D. and Crick, F.H.C., 1953. A structure for deoxyribonucleic acid. *Nature*, 171 (4356), pp. 737 - 738.
- Webb, M.R. et al., 2008. Anthocyanin interactions with DNA: Intercalation, topoisomerase I inhibition and oxidative reactions. *Journal of Food Biochemistry*, 32 (5), pp. 576- 596.
- Weder, J.E. et al., 2002. Copper complexes of non-steroidal anti-inflammatory drugs: an opportunity yet to be realized. *Coordination Chemistry Reviews*, 232, pp. 95 - 126.
- Wen, J.H. et al., 2011. A potent antitumor  $Zn^{2+}$  tetraazamacrocyclic complex targeting DNA: the fluorescent recognition, interaction and apoptosis studies. *Chemical Communications*, 47 (40), pp. 11330 - 11332.
- Wen, Y. H. et al., 2002. Pentaqua( $\mu$ -pyridine-2,6-dicarboxylato-*N,O,O',O''*)(pyridine-2,6-dicarboxylato-*N,O,O''*)dinickel(II) dihydrate. *Acta Crystallographica*, E58, m762 - 764.
- Wheate, N.J. and Collins, J.G., 2000. A  $^1H$  NMR study of the oligonucleotide binding of  $[(en)Pt(\mu-dpzm)_2Pt(en)]Cl_4$ . *Journal of Inorganic Biochemistry*, 78 (4), pp. 313 - 320.

Wikipedia®, 2012. *Threonine* [Online]. Available at: <http://en.wikipedia.org/wiki/Threonine> [Accessed: 5 Jan 2013].

Willsky, G.R. et al., 2011. Anti-diabetic effects of a series of vanadium dipicolinate complexes in rats with streptozotocin-induced diabetes. *Coordination Chemistry Reviews*, 255, pp. 2258 - 2269.

Wong, J.H.T. et al., 2010. A small molecule inhibitor of NF- $\kappa$ B, dehydroxymethylepoxyquinomicin (DHMEQ), suppresses growth and invasion of nasopharyngeal carcinoma (NPC) cells. *Cancer Letters*, 287 (1), pp. 23 - 32.

Xiao, H.P., Li, X.H. and Ng, S.W., 2005. *catena*-Poly[bis[aqua(1,10-phenanthroline- $\kappa^2$ N,N')-cobalt(II)-di- $\mu$ -4,4'-oxydibenzoato-1:2 $\kappa^4$ O:O']]. *Acta Crystallographica*, E61, m344 - 345.

Xie, J.R.H, Jr. Smith, V.H. and Allen, R.E., 2006. Spectroscopic properties of dipicolinic acid and its dianion. *Chemical Physics*, 322, pp. 254 - 268.

Xie, L. et al., 2004. 2D and 3D binuclear cobalt supramolecular complexes: synthesis and crystal structures. *Journal of Molecular Structure*, 692, pp. 201 - 207.

Yakovchuk, P., Protozanova, E. and Frank-Kamenetskii, M., 2006. Base-stacking and base-pairing contributions into thermal stability of the DNA double helix. *Nucleic Acids Research*, 34 (2), pp. 564 - 574.

Yanagimoto, K. et al., 2004. Antioxidative activities of fractions obtained from brewed coffee. *Journal of Agricultural and Food Chemistry*, 52 (3), pp. 592 - 596.

Yang, C.T. et al., 2003. Synthesis, characterization and properties of ternary copper(II) complexes containing reduced schiff base *N*-(2-hydroxybenzyl)- $\alpha$ -amino acids and 1,10-phenanthroline. *Dalton Transaction*, 5, pp. 880-889.

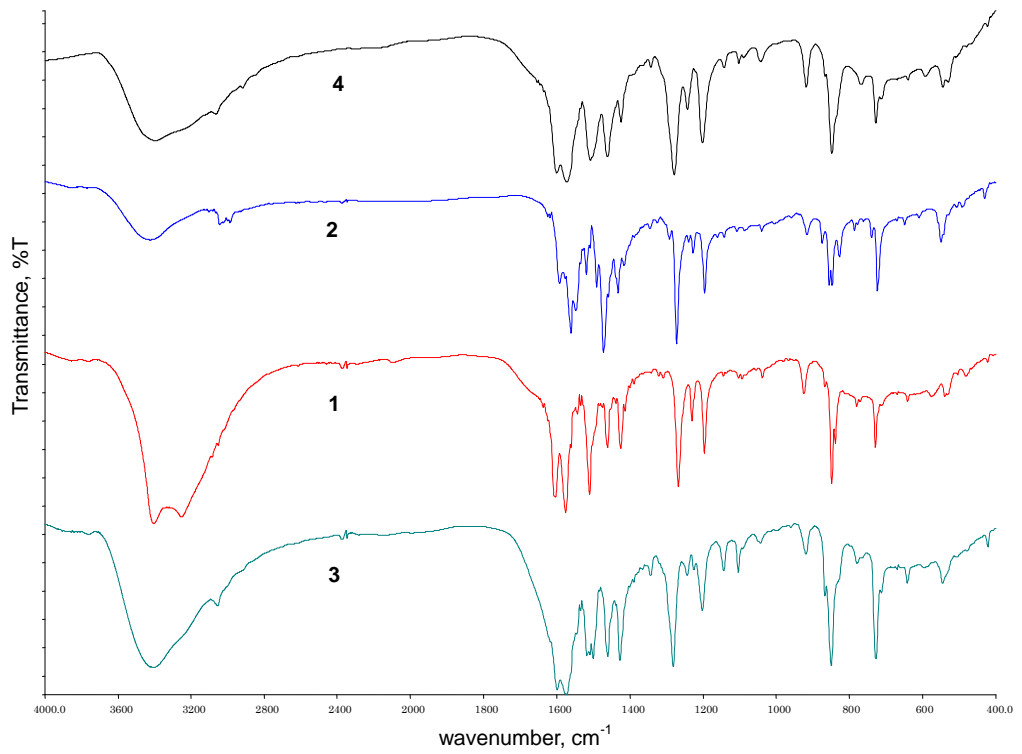
Yang, L. et al., 2002. Cobalt(II) and Cobalt(III) dipicolinate complexes: solid state, solution, and in vivo insulin-like properties. *Inorganic Chemistry*, 41 (19), pp. 4859 - 4871.

- Yang, W. and Du, D.M., 2011. Highly enantioselective Henry reaction catalyzed by  $C_2$ -symmetric modular BINOL-Oxazoline schiff base copper(II) complexes generated *In Situ*. *European Journal of Organic Chemistry*, 2011 (8), pp. 1552 - 1556.
- Yang, Y. et al., 2006. Maltol inhibits apoptosis of human neuroblastoma cells induced by hydrogen peroxide. *Journal of Biochemistry and Molecular Biology*, 39 (2), pp. 145 - 149.
- Yasumoto, E. et al., 2004. Cytotoxic activity of deferiprone, maltol and related hydroxyketones against human tumor cell lines. *Anticancer Research*, 24, pp. 755 – 762.
- Yenikaya, C. et al., 2009. Synthesis, characterization and biological evaluation of a novel Cu(II) complex with the mixed ligands 2,6-pyridinedicarboxylic acid and 2-aminopyridine. *Polyhedron*, 28, pp. 3526 - 3532.
- Yodoshi, M., Odoko, M. and Okabe, N., 2007. Structures and DNA-binding and cleavage properties of ternary copper(II) complexes of glycine with phenanthroline, bipyridine, and bipyridylamine. *Chemical and Pharmaceutical Bulletin*, 55 (6), pp. 853 - 860.
- Yoshikawa, Y. et al., 2001. Insulinomimetic bis(maltolato)zinc(II) complex: blood glucose normalizing effect in KK-A(y) mice with type 2 diabetes mellitus. *Biochemical and Biophysical Research Communications*, 281 (5), pp. 1190 - 1193.
- Yoshikawa, Y. et al., 2001. New insulinomimetic zinc(II) complexes of  $\alpha$ -amino acids and their derivatives with  $Zn(N_2O_2)$  coordination mode. *Chemical and Pharmaceutical Bulletin*, 49 (5), pp. 652 - 654.
- Yu, P. et al., 2002. Rates of solvent exchange in aqueous aluminium(III)-maltolate complexes. *Journal of the Chemical Society, Dalton Transactions*, pp. 2119 - 2125.
- Zborowski, K., Grybos, R. and Proniewicz, L.M., 2007. Structure modification of maltol (3-hydroxy-2-methyl-4H-pyran-4-one) upon cation and anion formation studies by vibrational spectroscopy and quantum-mechanical calculations. *Vibrational Spectroscopy*, 43, pp. 344 – 350.

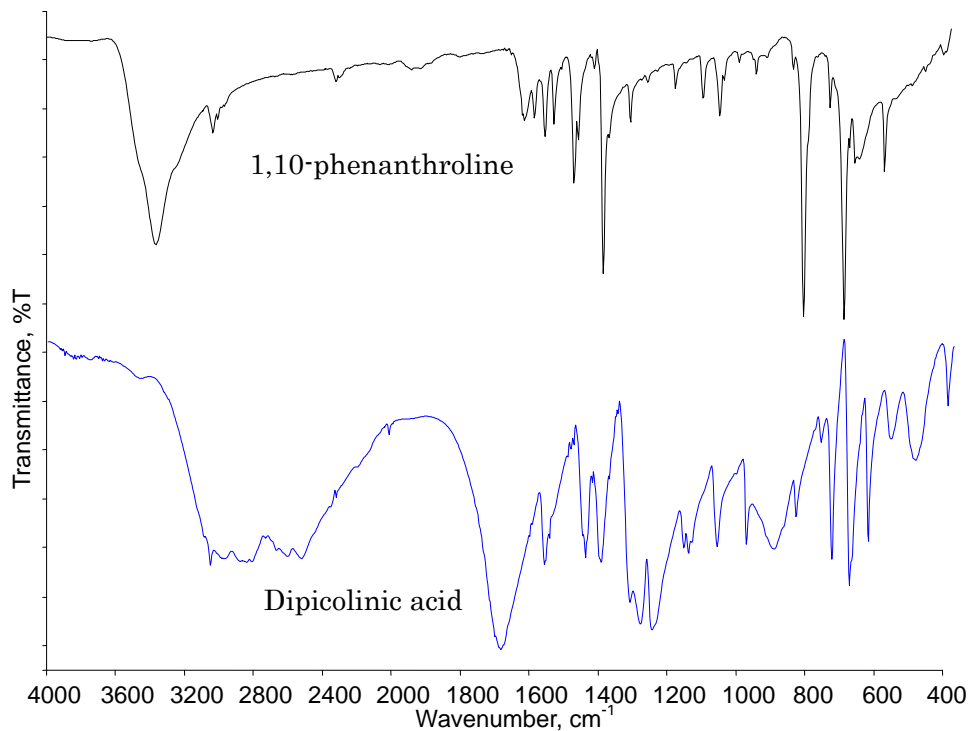
- Zeglis, B.M., Pierre, V.C. and Barton, J.K., 2007. Metallo-intercalators and metallo-insertors. *Chemical Communication*, 44, pp. 4565 - 4579.
- Zelder, F.H., Mokhir, A.A. and Kramer, R., 2003. Sequence selective hydrolysis of linear DNA using conjugates of Zr(IV) complexes and peptide nucleic acids. *Inorganic Chemistry*, 42 (26), pp. 8618 - 8620.
- Zelenko, O. et al., 1998. Chemical nuclease activity of 1,10-phenanthroline-copper. Isotopic probes of mechanism. *Inorganic Chemistry*, 37 (9), pp. 2198 - 2204.
- Zhang, G.F. et al., 2007. Synthesis, structural characterization and catalytic activities of dicopper(II) complexes derived from tridentate pyrazole-based N<sub>2</sub>O ligands. *Applied Organometallic Chemistry*, 21 (12), pp. 1059 - 1065.
- Zhang, H.J. et al., 1997. The photophysical properties of binary and ternary complexes of rare earths with conjugated carboxylic acids and 1,10-phenanthroline. *Journal of Photochemistry and Photobiology A: Chemistry*, 109, pp. 223 - 228.
- Zhang, L. et al., 2007. Chiral separation of L,D-tyrosine and L,D-tryptophan by CT-DNA. *Separation and Purification Technology*, 55, pp. 388 - 391.
- Zhang, L. et al., 2009. Enantioselective binding of L,D-phenylalanine to CT-DNA. *Spectrochimica Acta Part A: Molecular and Biomolecular Spectroscopy*, 74, pp. 835 - 838.
- Zhang, L.M. et al., 2008. Facile synthesis of leaf-like Cu(OH)<sub>2</sub> and its conversion into CuO with nanospores. *Acta Physica Sinica*, 24 (12), pp. 2257 - 2262.
- Zhang, R. et al., 2012. Developing red-emissive ruthenium(II) complex-based luminescent probes for cellular imaging. *Bioconjugate Chemistry*, 23 (4), pp. 725 - 733.
- Zhang, S.C. et al., 2004. A novel cytotoxic ternary copper(II) complex with 1,10-phenanthroline and L-threonine with DNA nuclease activity. *Journal of Inorganic Biochemistry*, 98 (12), pp. 2099 - 2106.

- Zhang, Y. et al., 2006. The permeability and cytotoxicity of insulin-mimetic vanadium (III, IV, V)-dipicolinate complexes. *Journal of Inorganic Biochemistry*, 100, pp. 80 - 87.
- Zhong, W.Y. et al., 2005. Synthesis, structure characterization and anti-tumor activity of lanthanide complex  $\text{Ln}[(\text{Phen})_2(5\text{-Fu})_3(\text{NO}_3)](\text{NO}_3)_2$ . *PubMed*, 40 (11), pp. 997 - 1000.
- Zhou, J.J. et al., 2011. Synthesis, crystal structure and magnetic properties of novel copper compound  $\text{Cu}(\text{phen})(\text{m-CBA})_2$ , *Transaction of Nonferrous Metals Society of China*, 21, pp. 2660 - 2664.
- Zhou, Y., Yue, L. and Liu, J., 2009. Hydrothermal synthesis, crystal structure and spectroscopic properties of a novel 3D chromium(III) complex. *Inorganic Chemistry Communications*, 12, pp. 1085 - 1087.

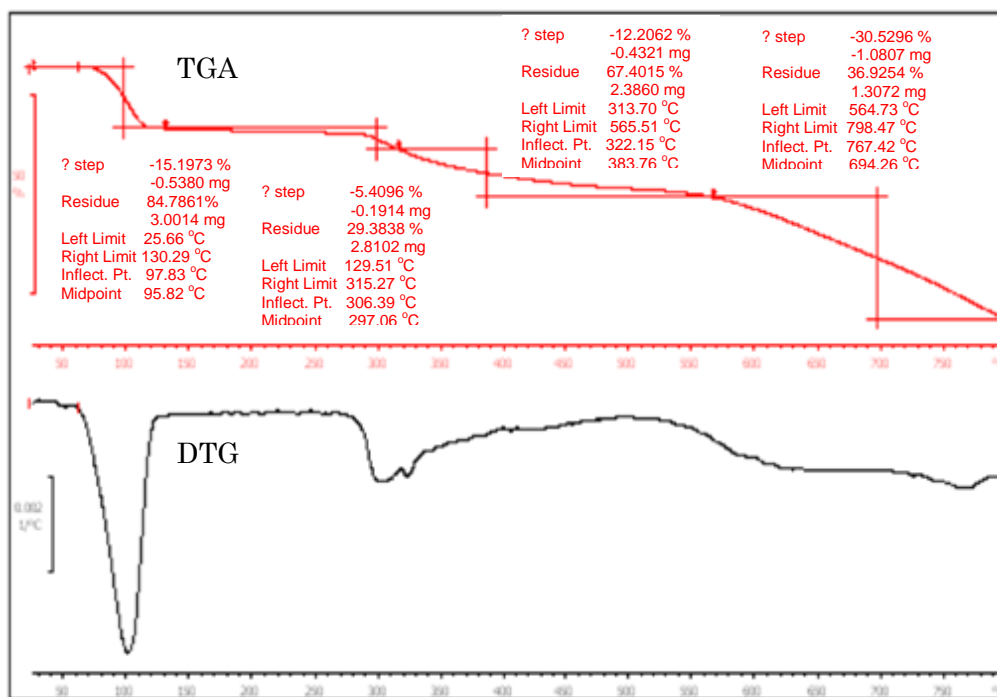
**Appendices:**



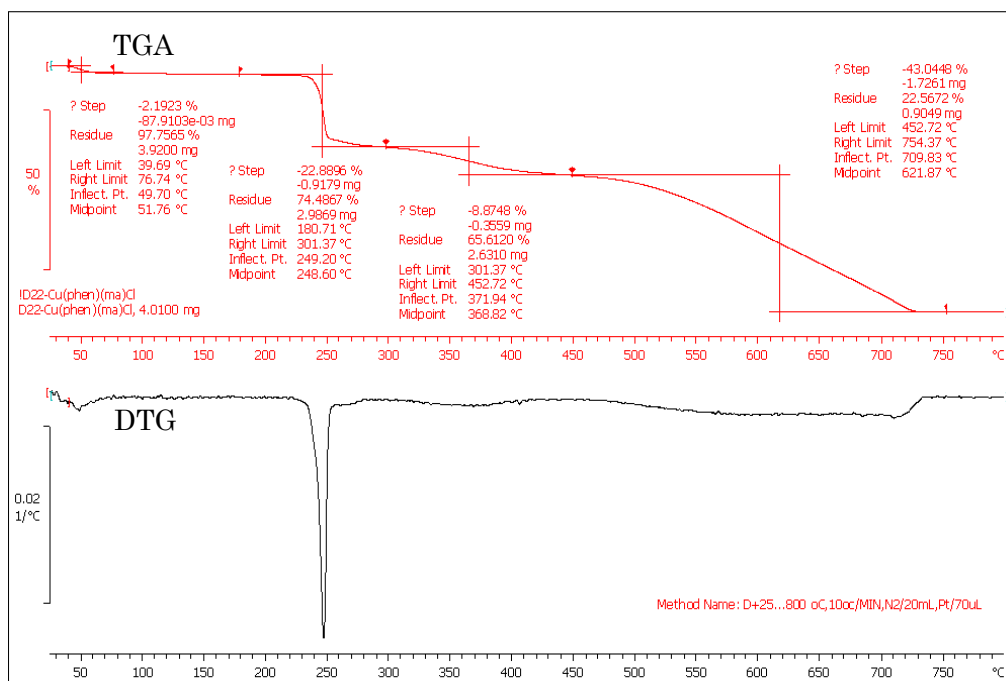
**Appendix 3.1:** FTIR spectra of metal complexes, 1 - 4.



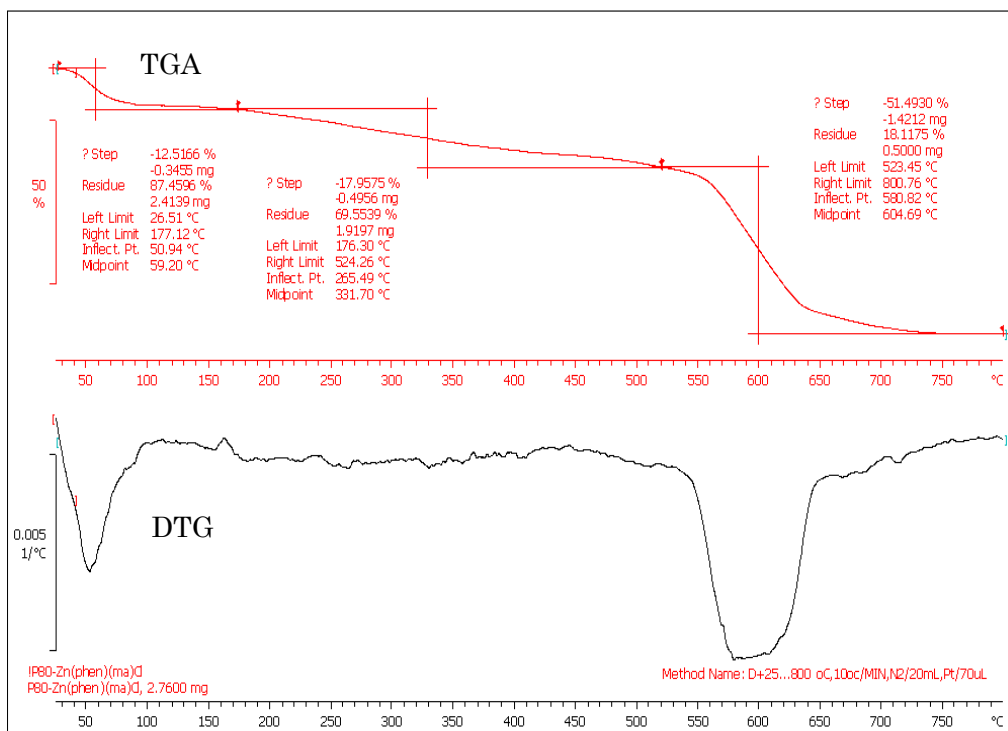
**Appendix 3.2:** FTIR spectra of 1,10-phenanthroline and dipicolinic acid



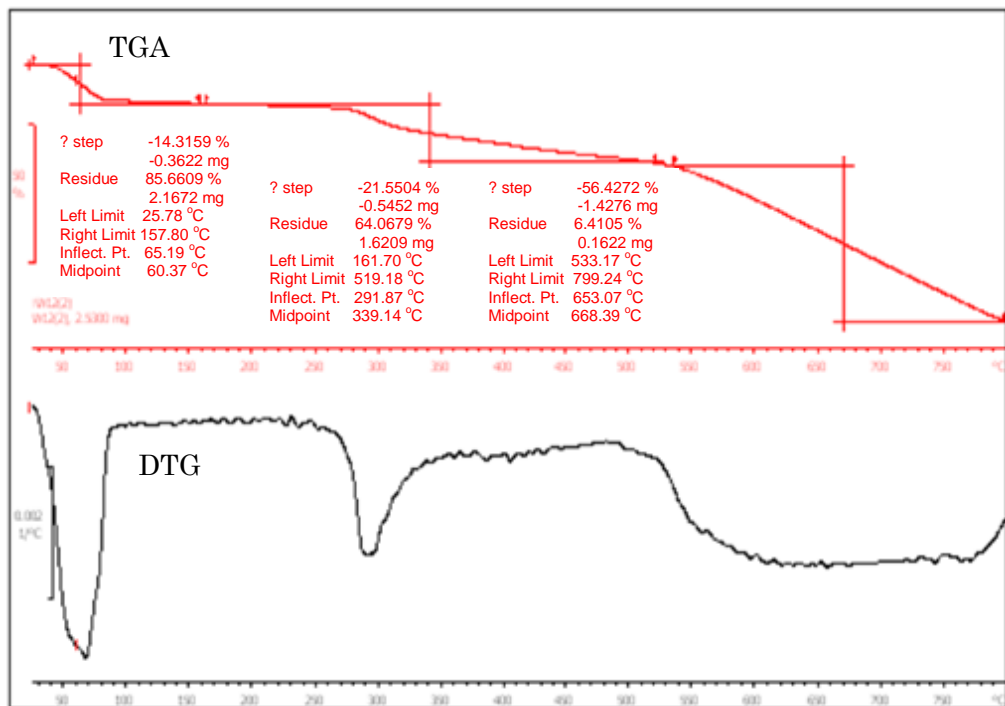
**Appendix 3.3: TGA (top) and DTG (bottom) curves of complex 1**



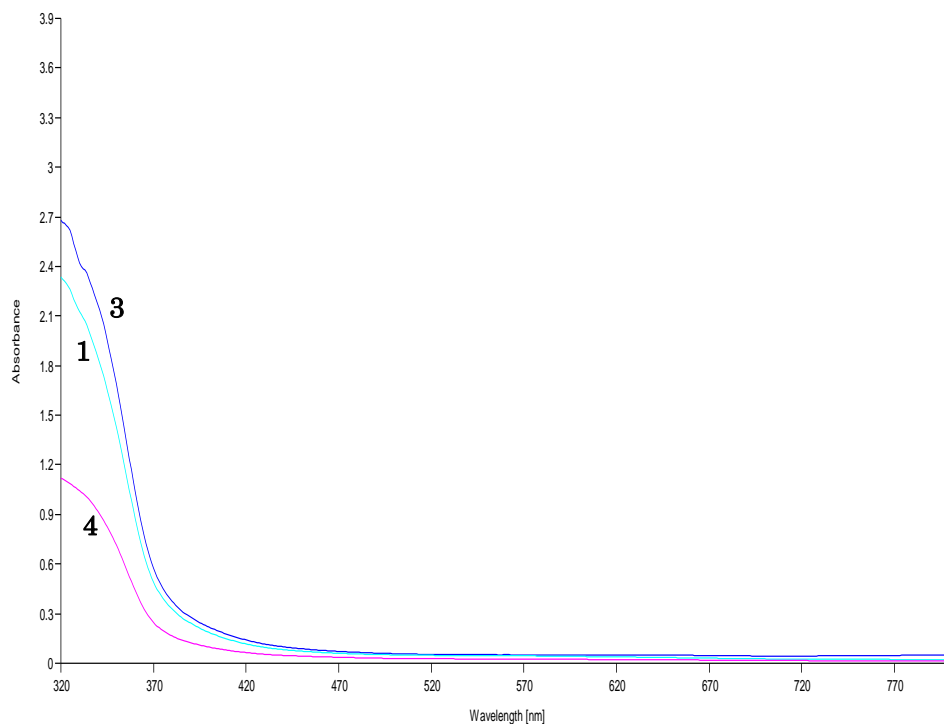
**Appendix 3.4: TGA (top) and DTG (bottom) curves of complex 2**



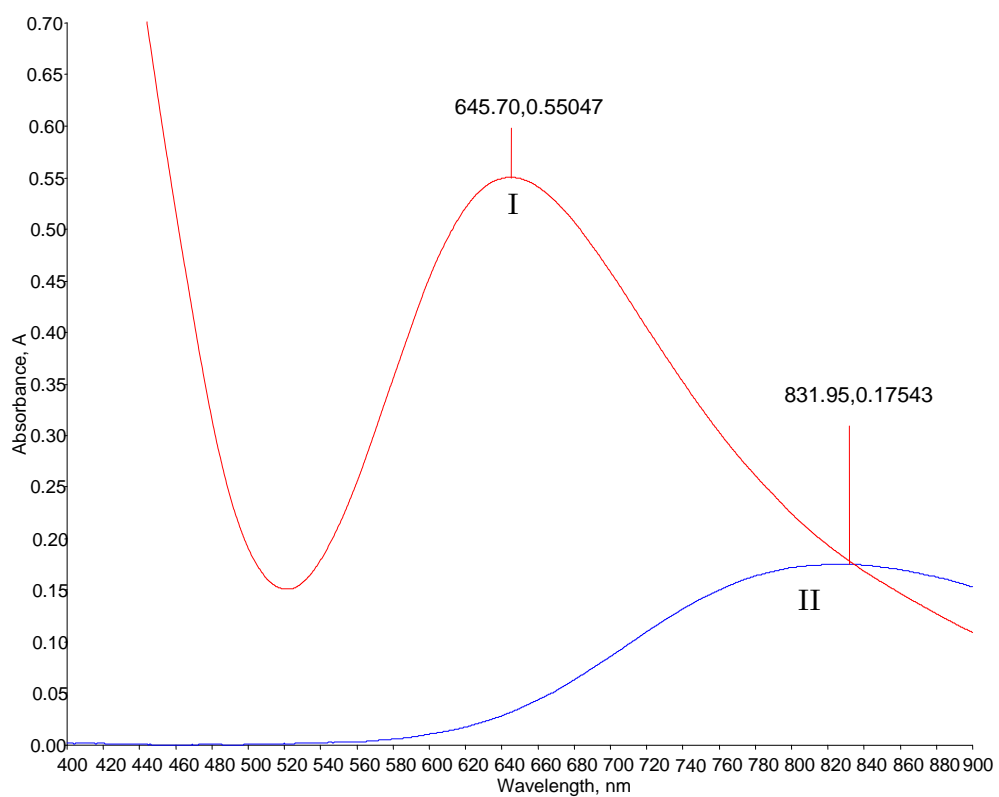
**Appendix 3.5: TGA (top) and DTG (bottom) curves of complex 3**



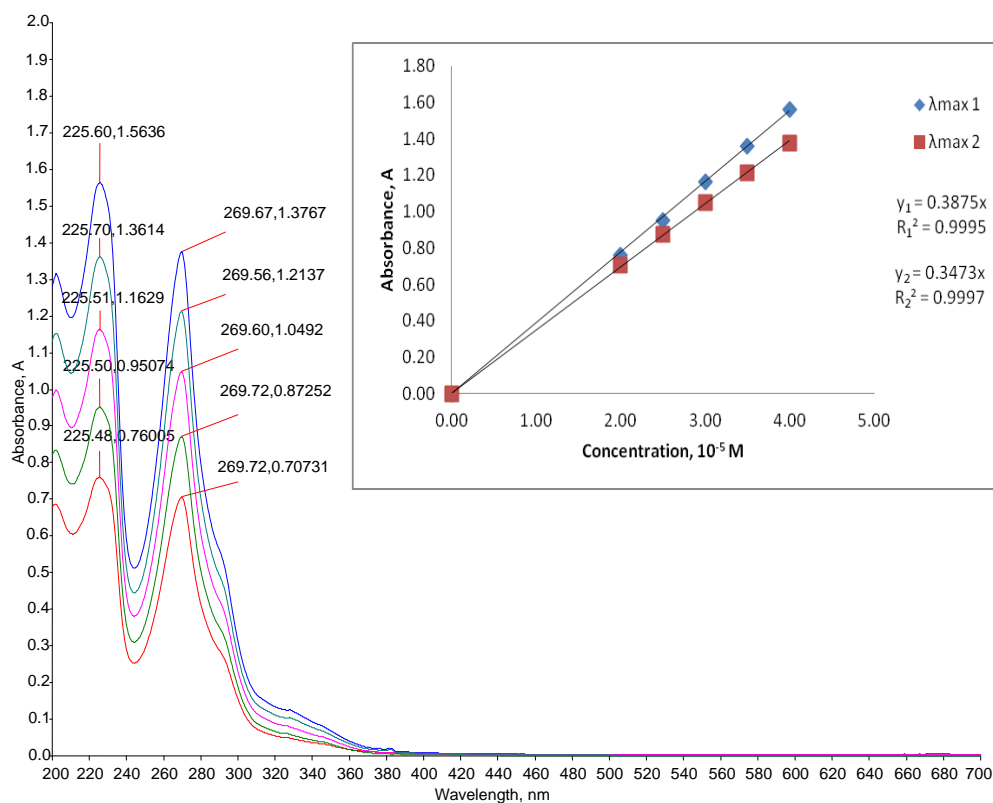
**Appendix 3.6: TGA (top) and DTG (bottom) curves of complex 4**



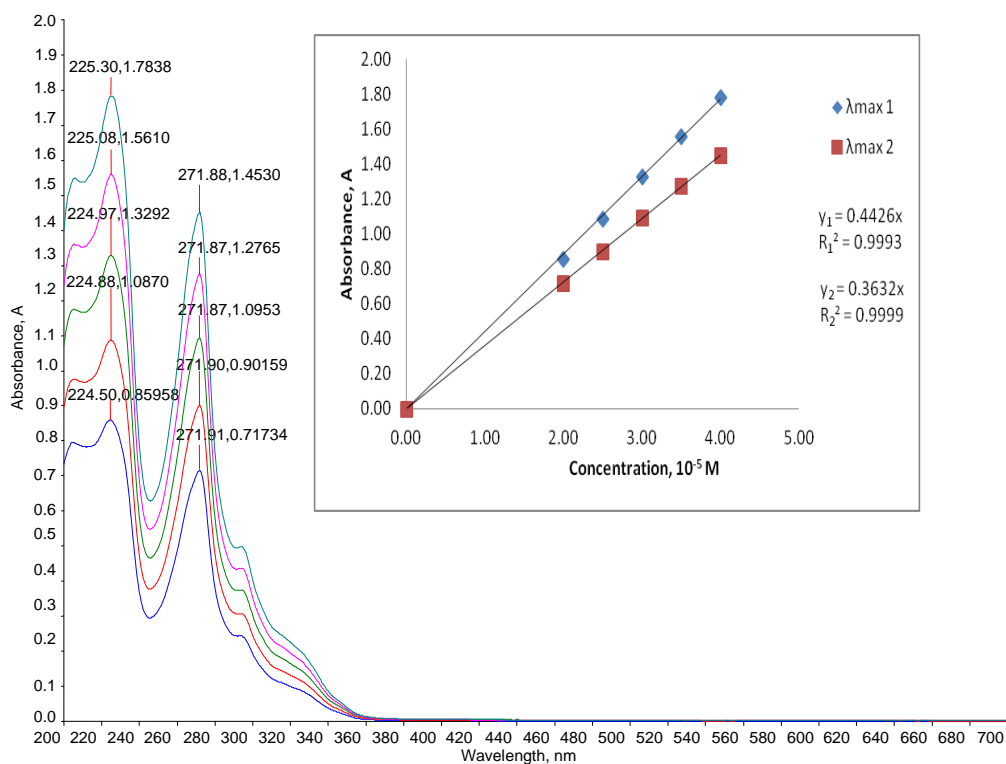
**Appendix 3.7:** Visible spectra of  $[\text{Co}(\text{phen})(\text{ma})\text{Cl}]\cdot 4\text{H}_2\text{O}$  (**1**),  $[\text{Zn}(\text{phen})(\text{ma})\text{Cl}]\cdot 1\frac{1}{2}\text{H}_2\text{O}$  (**3**) and  $[\text{Co}(\text{phen})(\text{ma})_2]\cdot 5\text{H}_2\text{O}$  (**4**) at 2 mM.



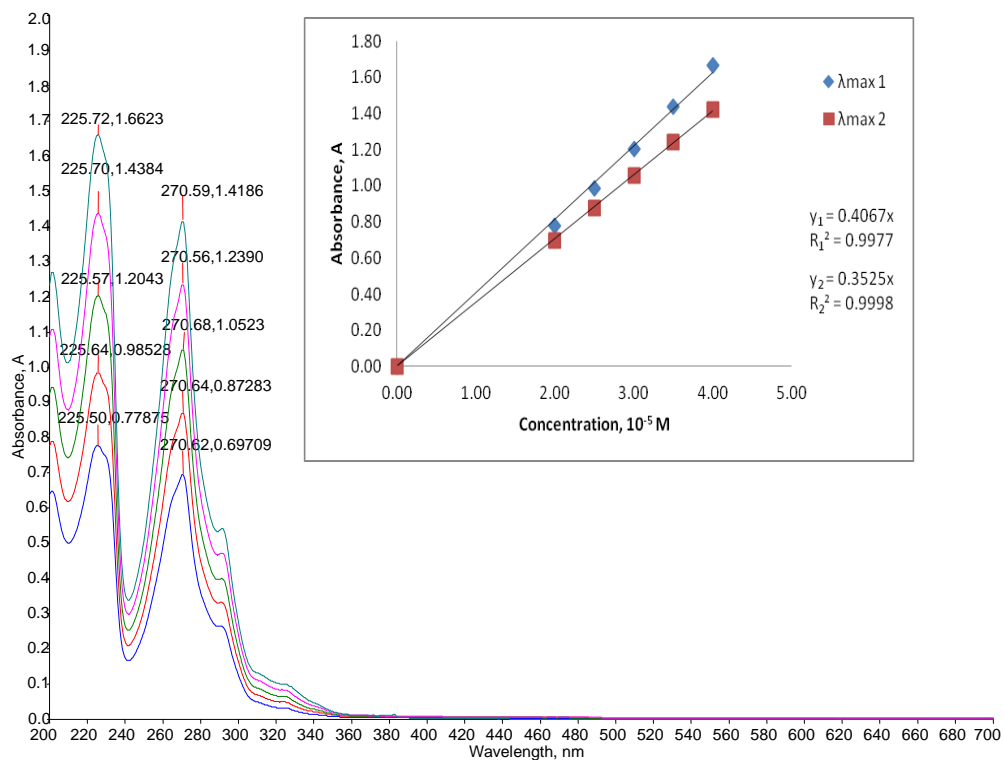
**Appendix 3.8:** Visible spectra of 0.01 M of complex **2** (I) and  $\text{CuCl}_2$  (II)



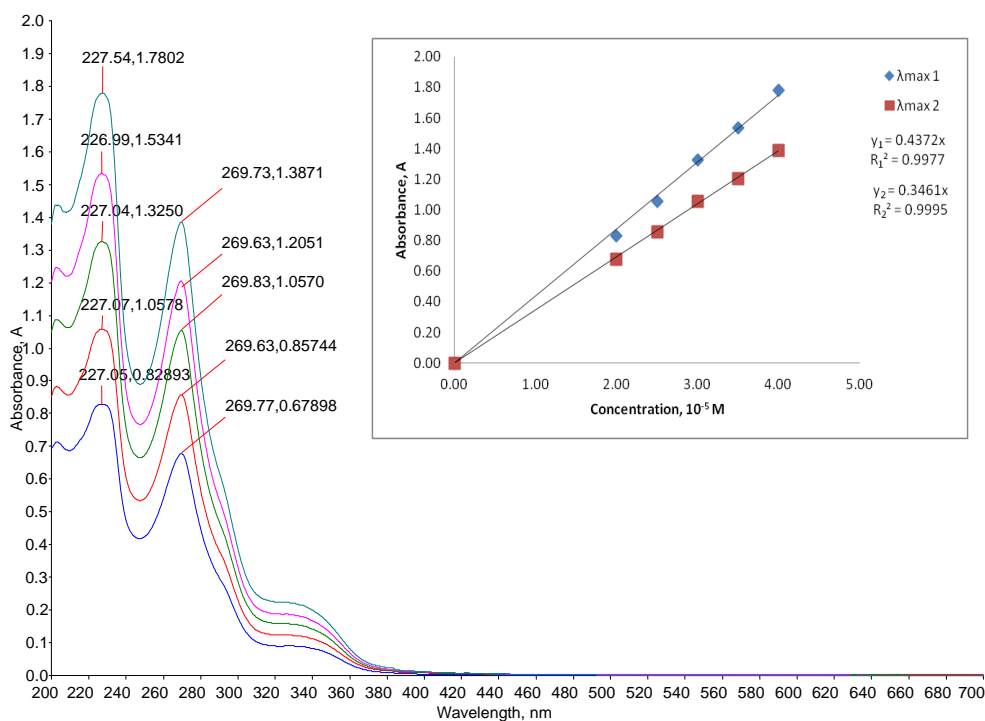
**Appendix 3.9:** UV spectra and plot of absorbance against concentration of complex 1.



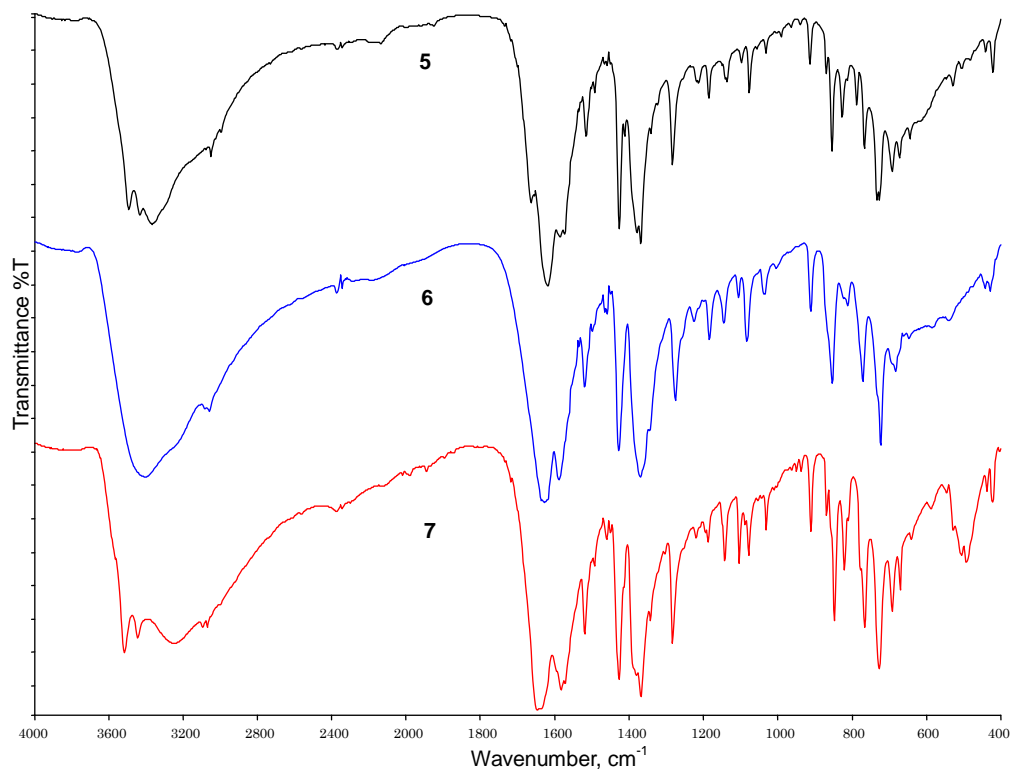
**Appendix 3.10:** UV spectra and plot of absorbance against concentration of complex 2.



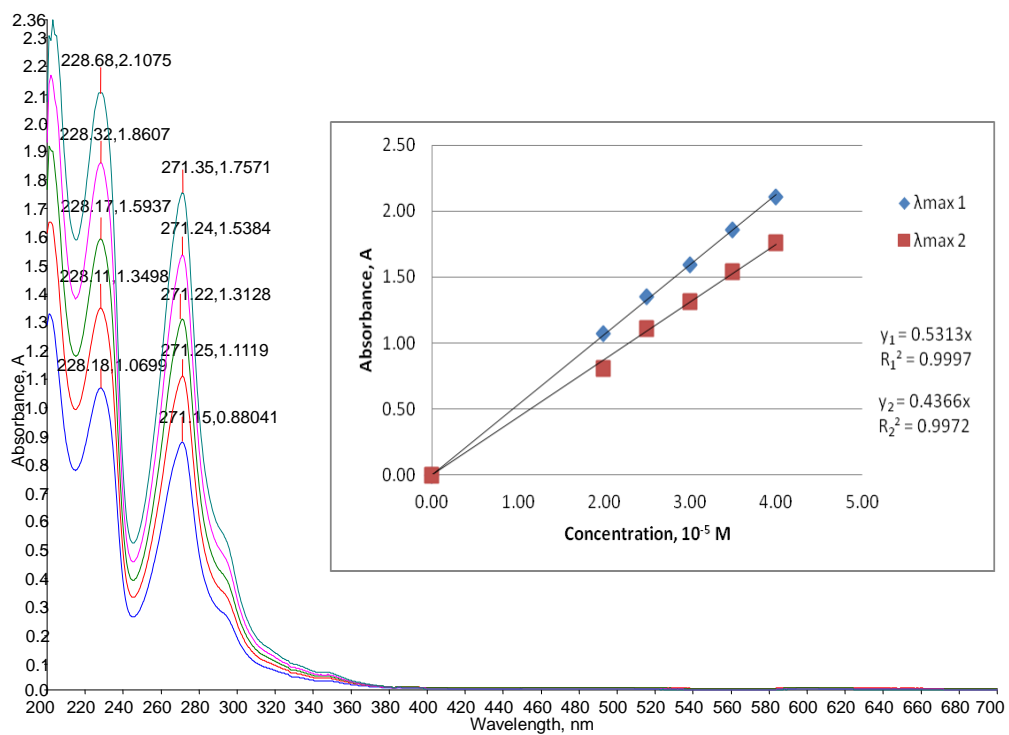
**Appendix 3.11:** UV spectra and plot of absorbance against concentration of complex 3.



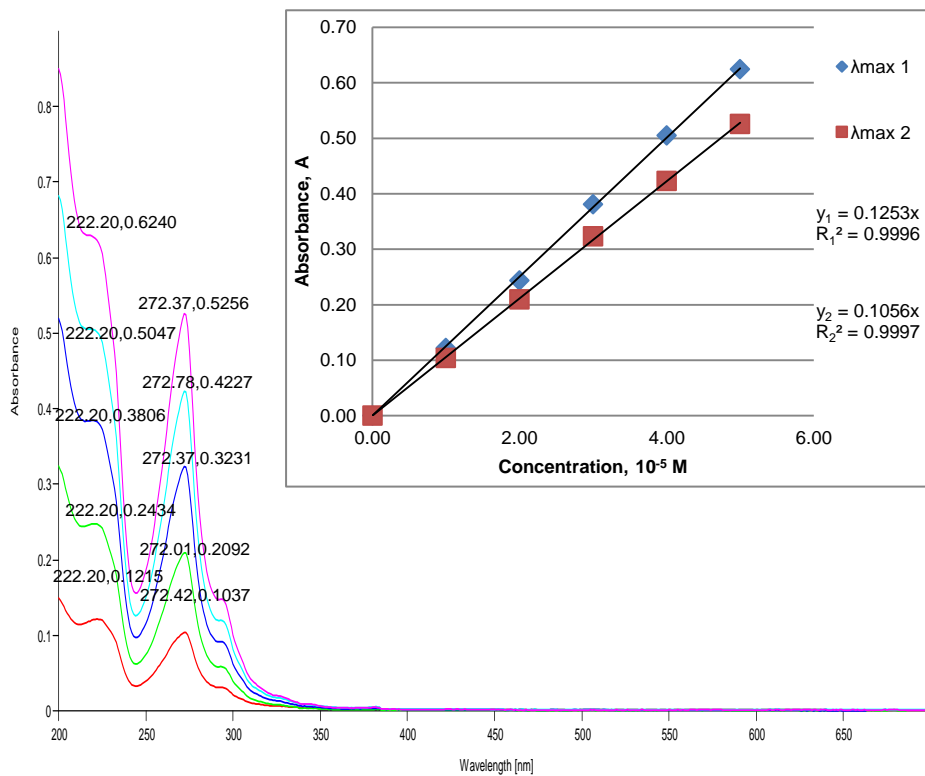
**Appendix 3.12:** UV spectra and plot of absorbance against concentration of complex 4.



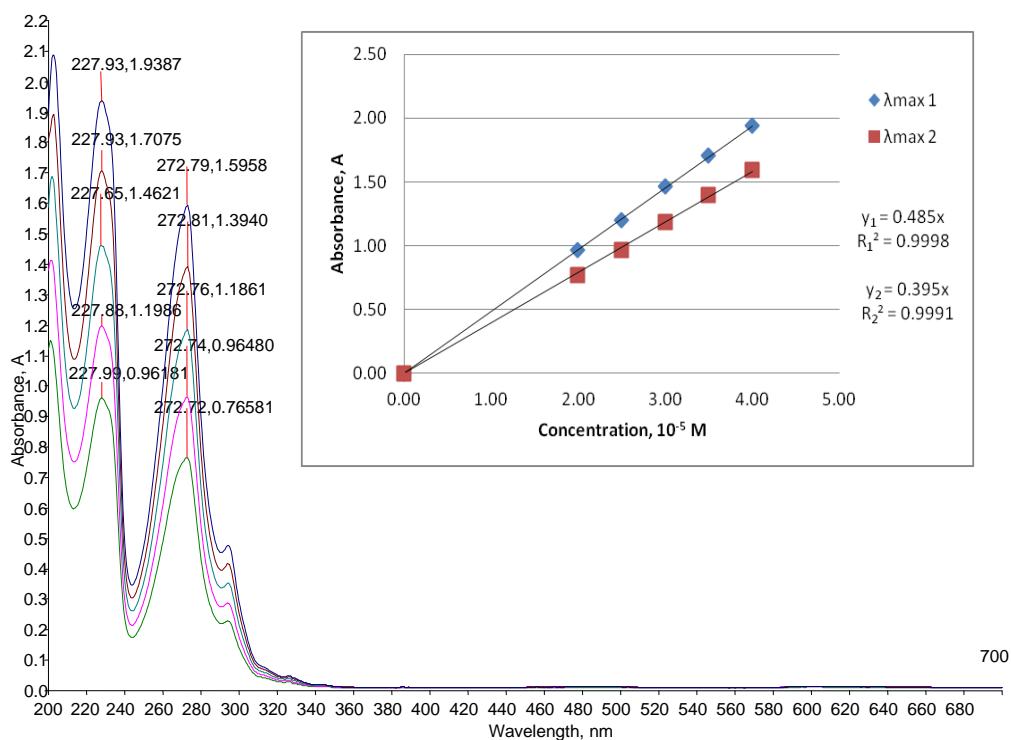
**Appendix 4.1:** FTIR spectra of metal(II) complexes, 5 - 7.



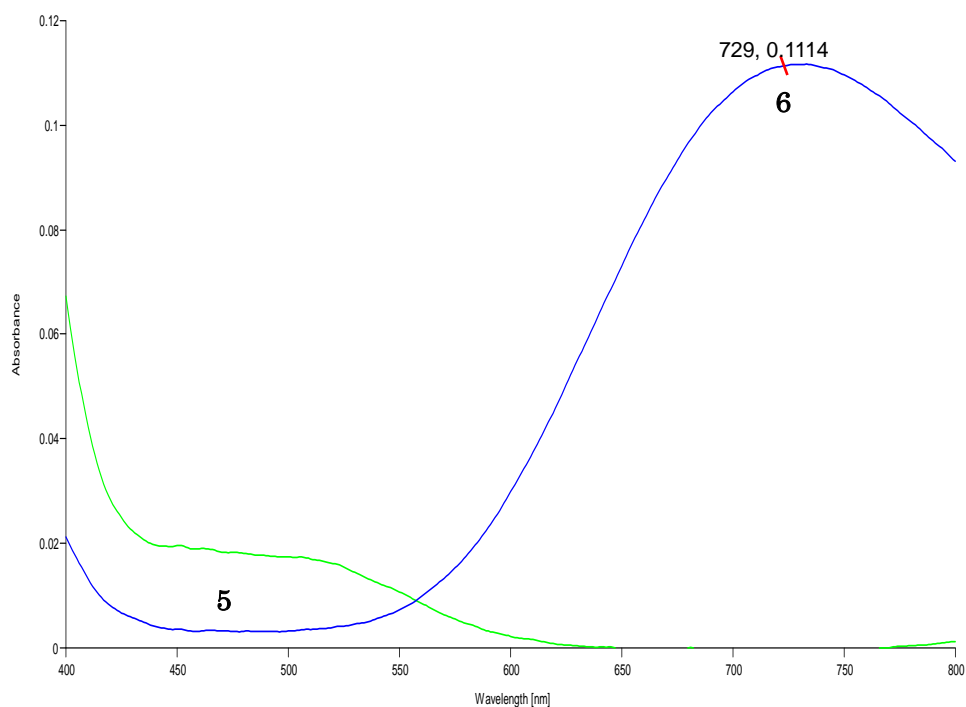
**Appendix 4.2:** UV spectra and plot of absorbance against concentration of complex 5.



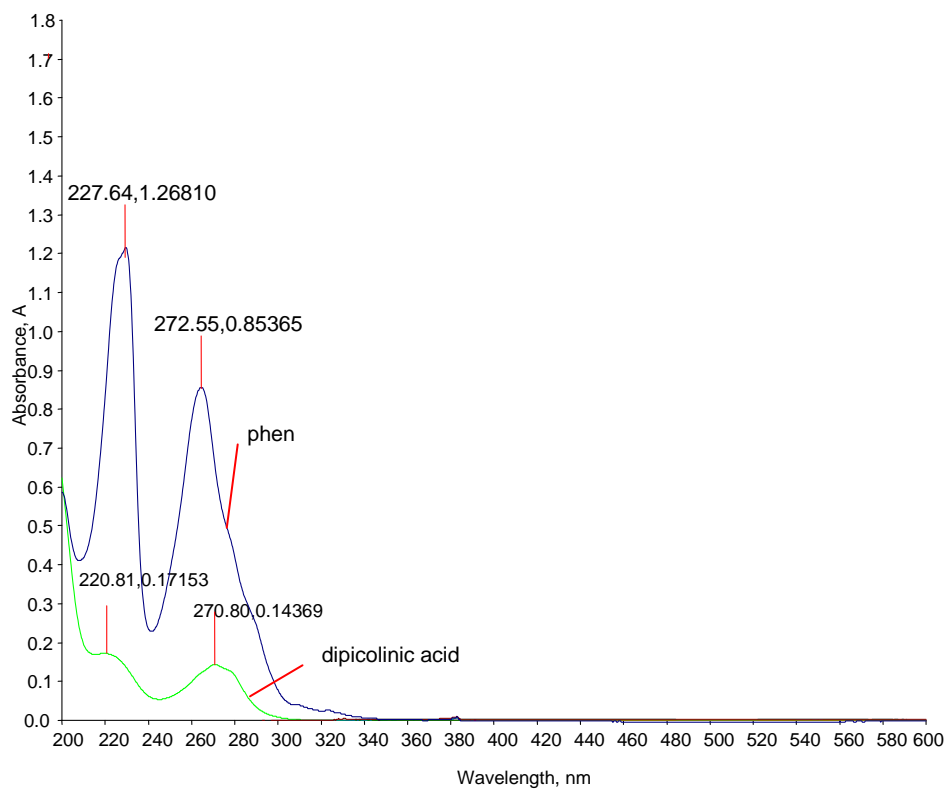
**Appendix 4.3:** UV spectra and plot of absorbance against concentration of complex 6.



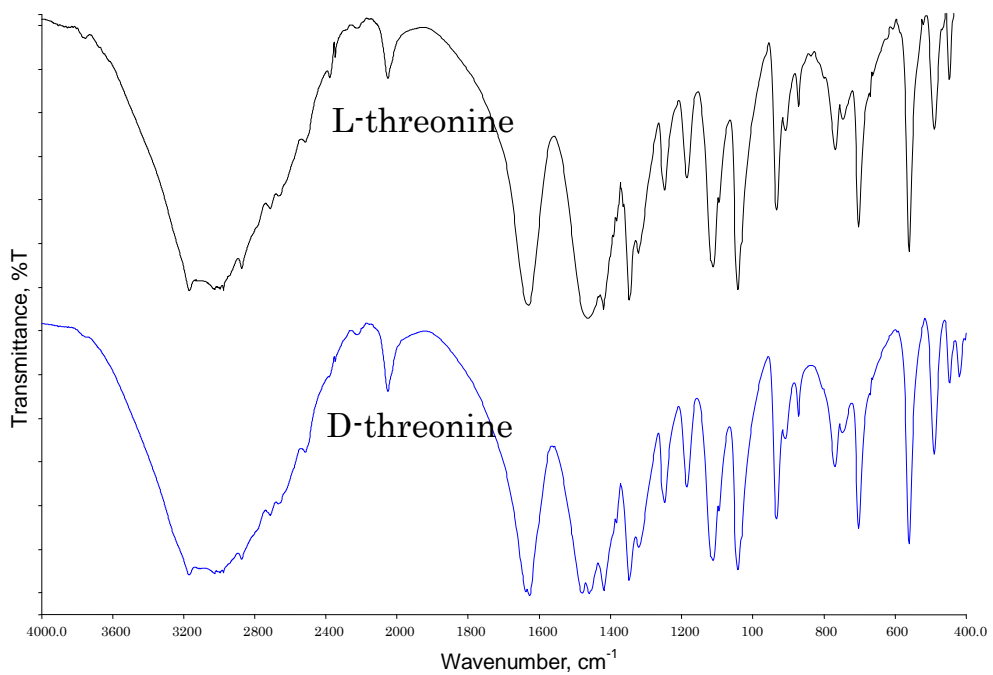
**Appendix 4.4:** UV spectra and plot of absorbance against concentration of complex 7.



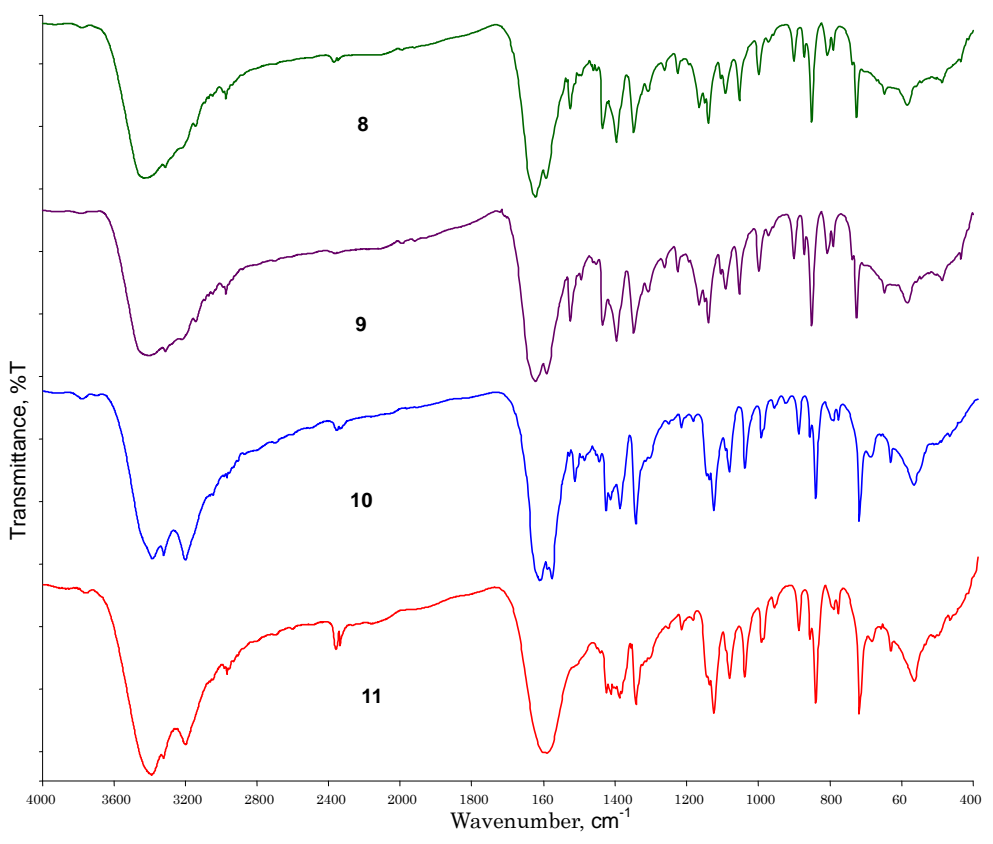
**Appendix 4.5:** Visible spectra of complexes **5** and **6** at 0.01 M.



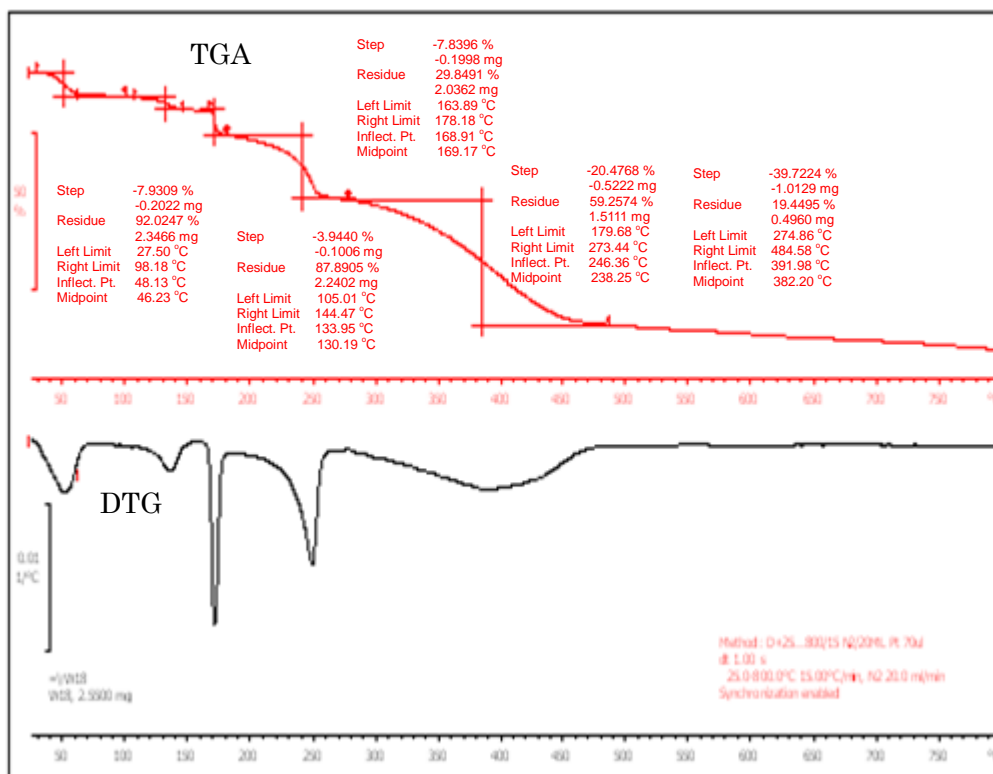
**Appendix 4.6:** UV spectra of phen and dipicolinic acid at  $1.0 \times 10^{-5}$  M



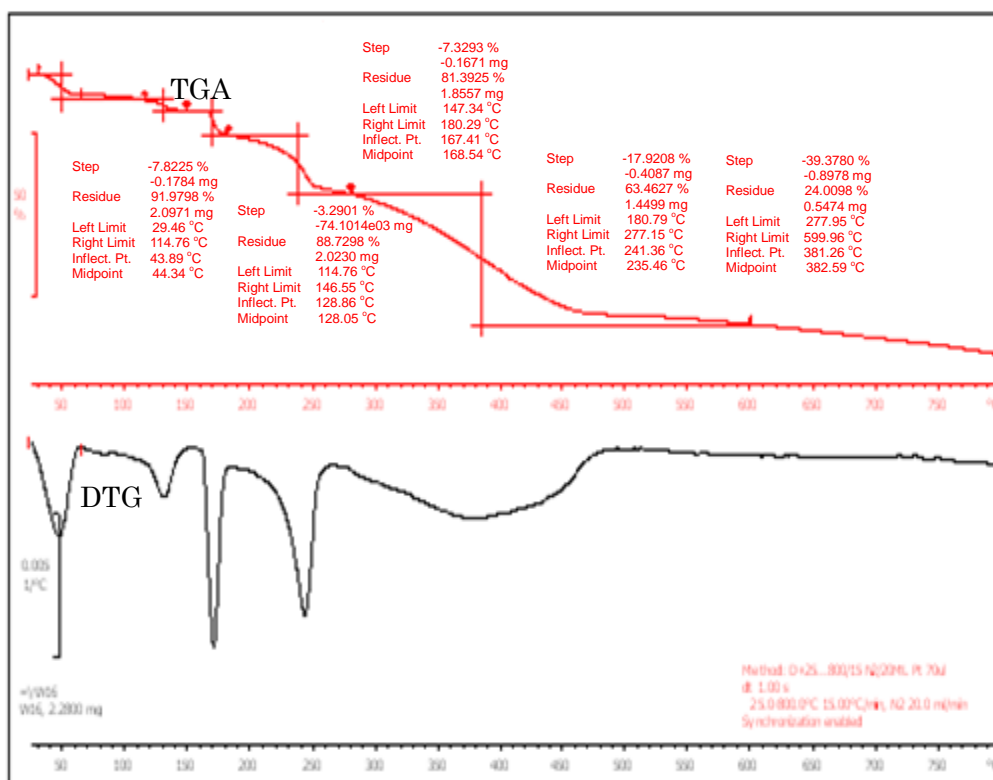
**Appendix 5.1: FTIR spectra of L-threonine and D-threonine**



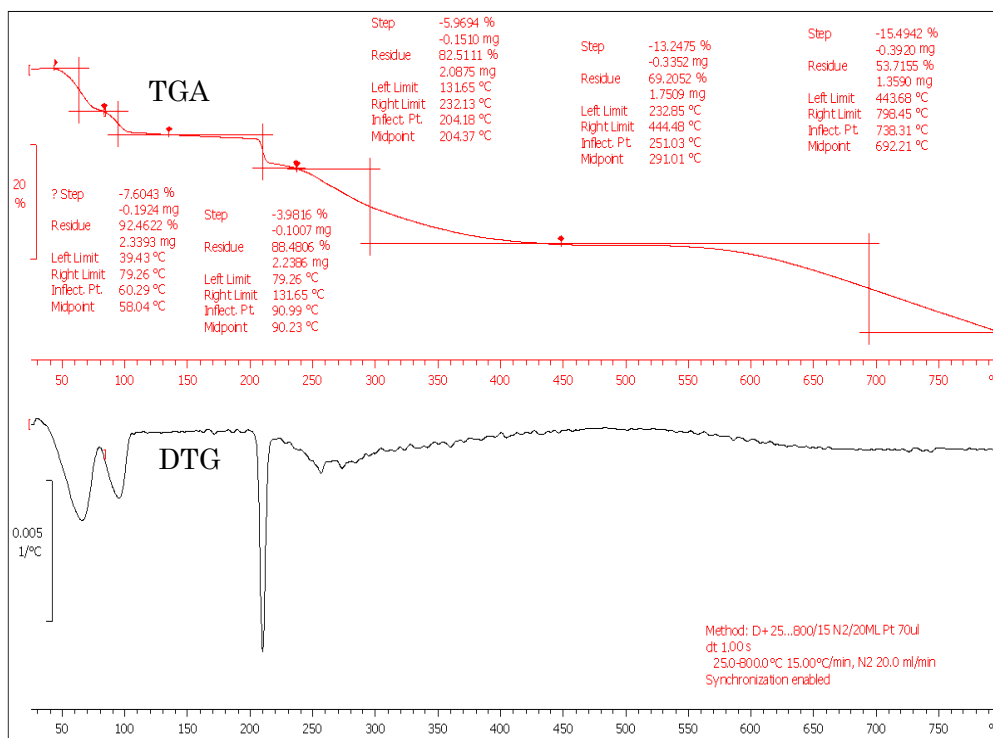
**Appendix 5.2: FTIR spectra of metal(II) complexes 8 – 11**



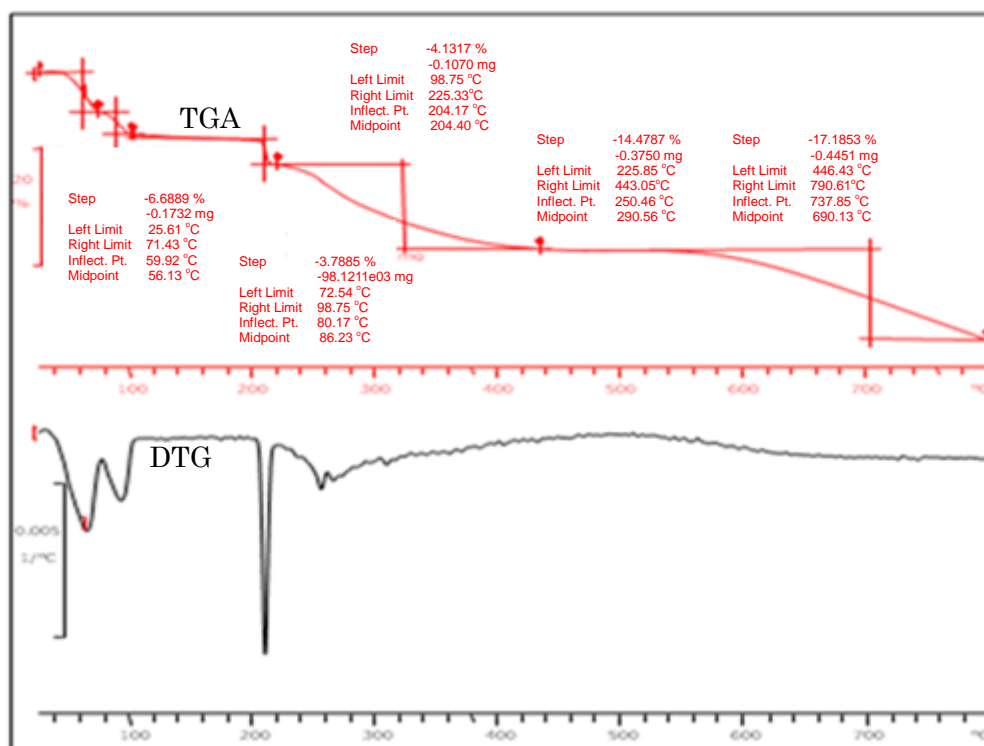
**Appendix 5.3:** TGA (top) and DTG (bottom) curves of complex 8



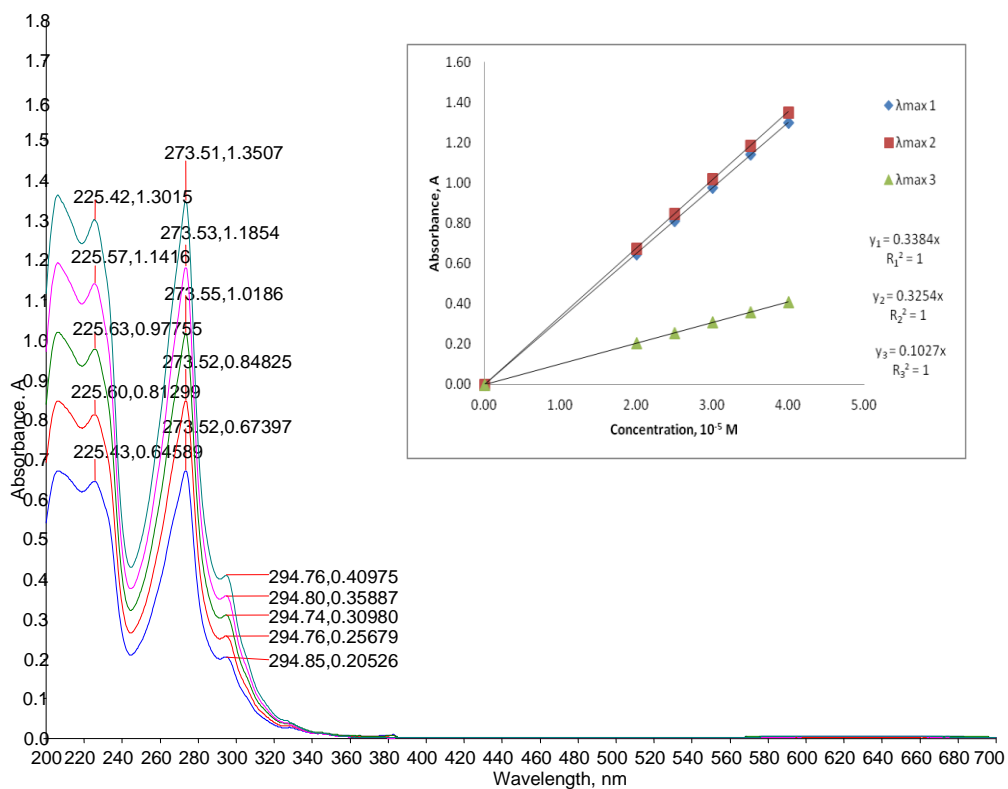
**Appendix 5.4:** TGA (top) and DTG (bottom) curves of complex 9



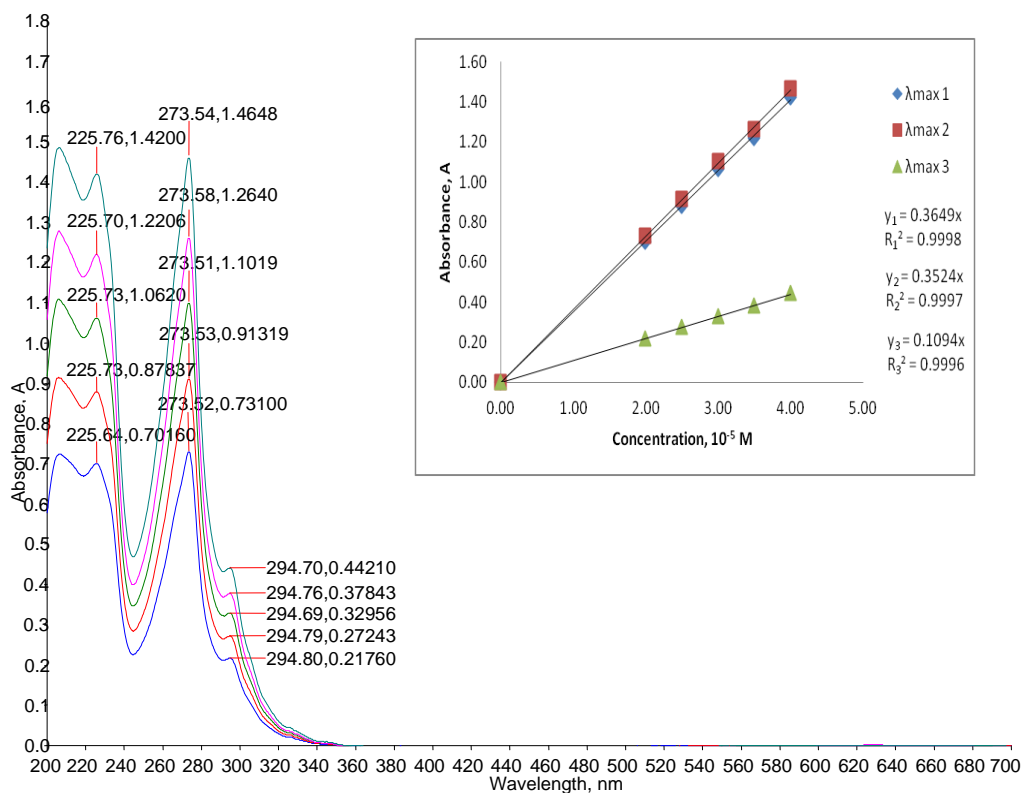
**Appendix 5.5: TGA (top) and DTG (bottom) curves of complex 10**



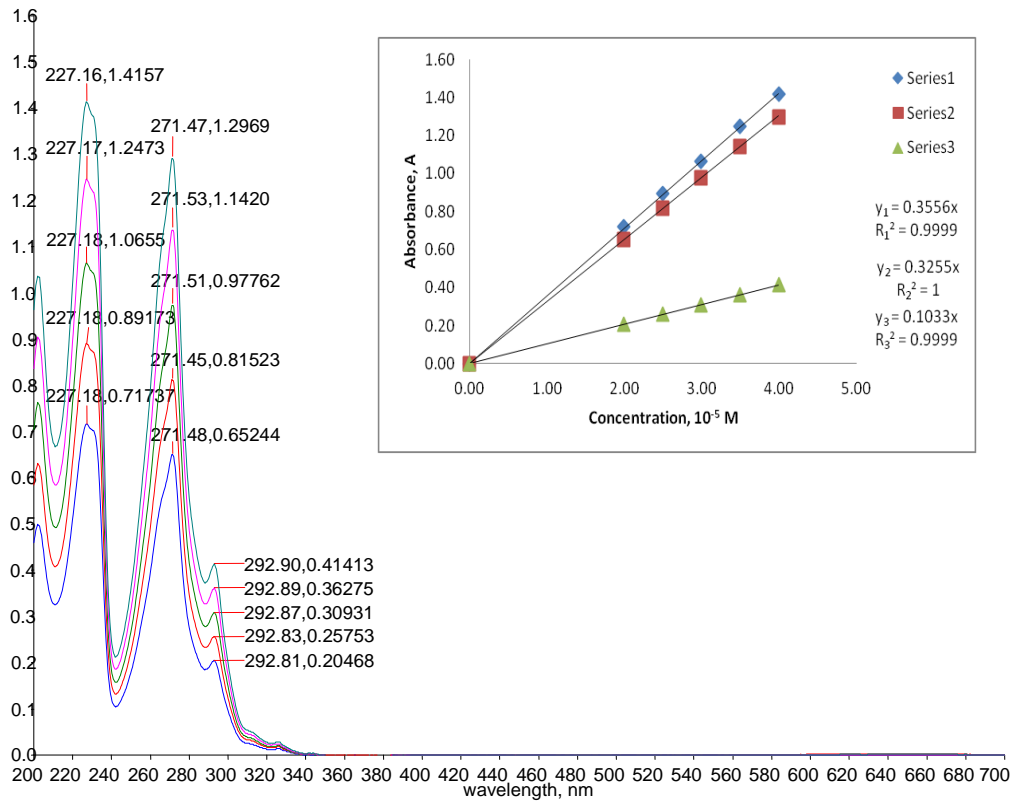
**Appendix 5.6: TGA (top) and DTG (bottom) curves of complex 11**



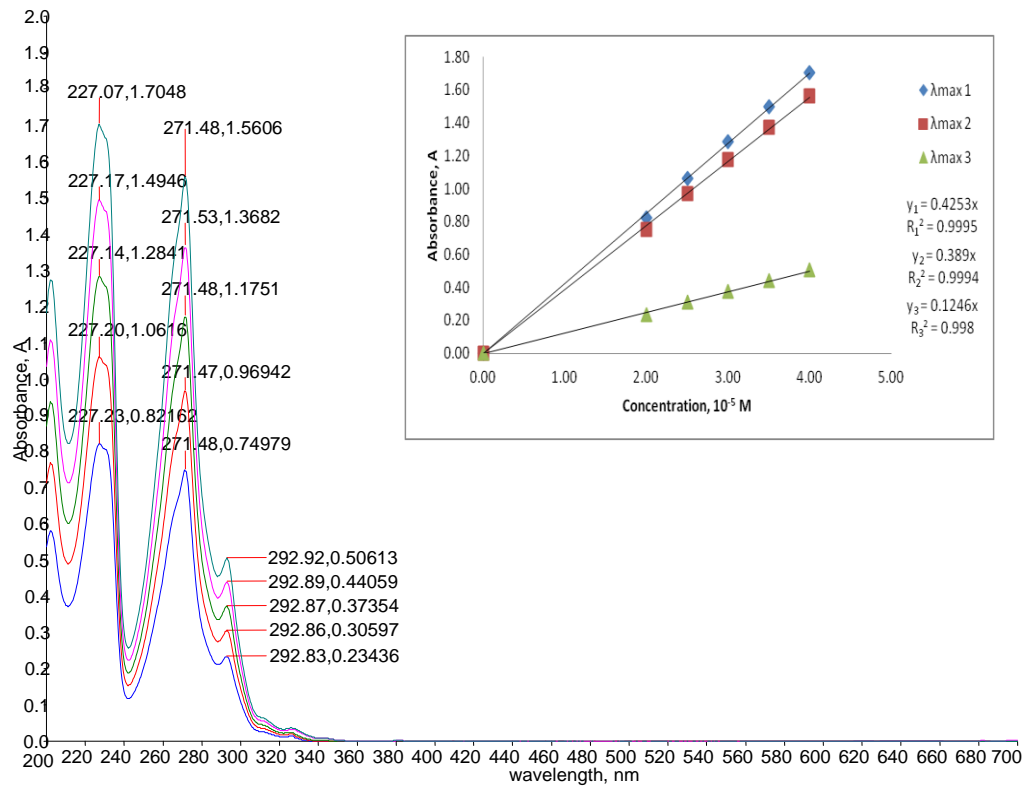
**Appendix 5.7: UV dilution for complex 8 at different concentration**



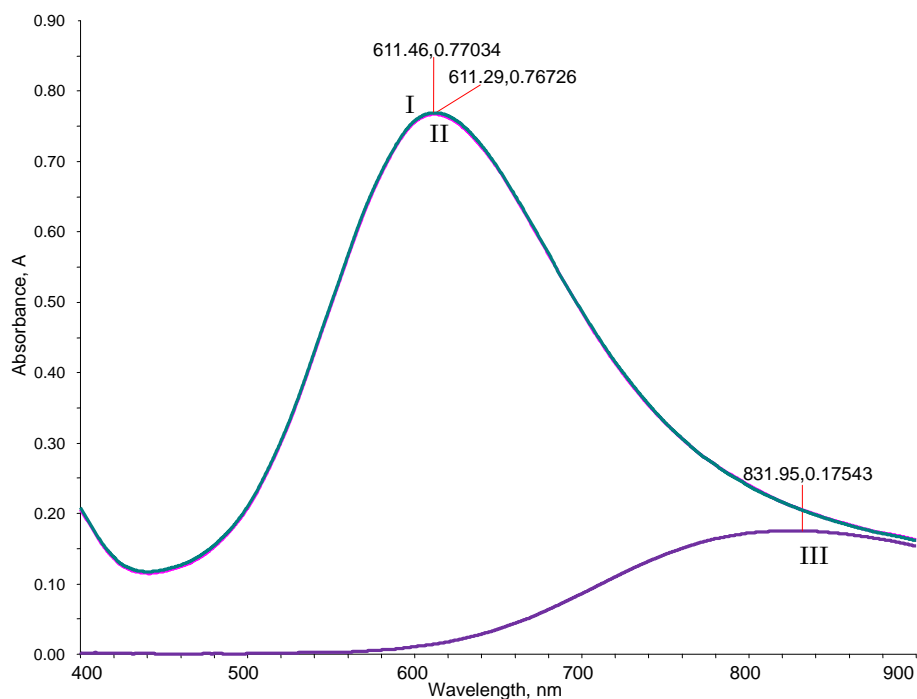
**Appendix 5.8: UV dilution for complex 9 at different concentration**



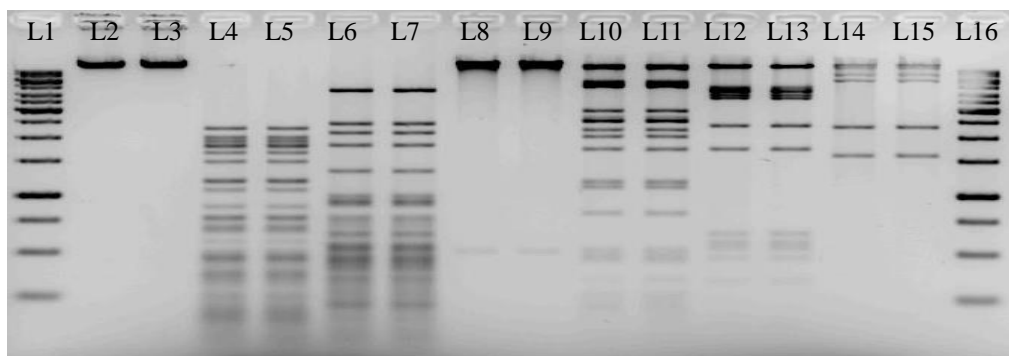
**Appendix 5.9:** UV dilution for complex 10 at different concentration



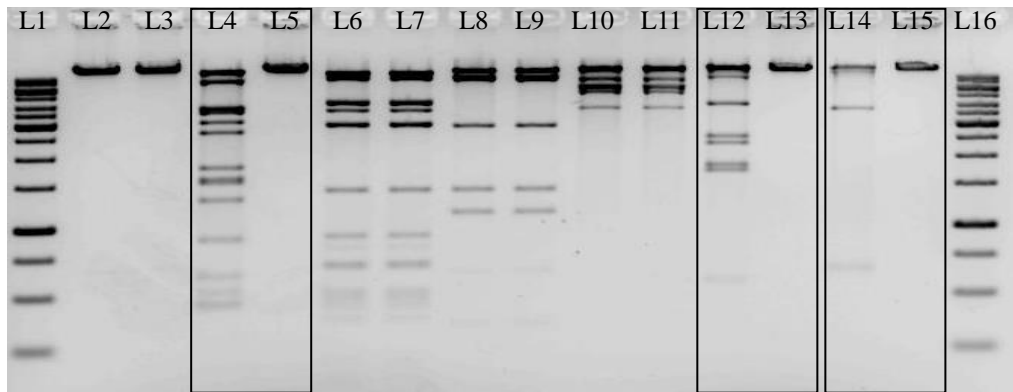
**Appendix 5.10:** UV dilution for complex 11 at different concentration



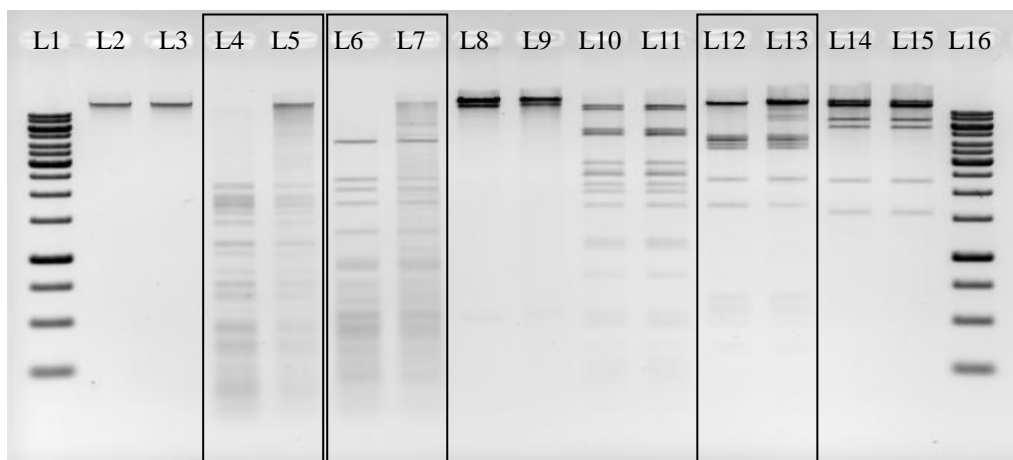
**Appendix 5.11:** Visible spectra of  $[\text{Cu}(\text{phen})(\text{L-thr})(\text{H}_2\text{O})\text{Cl}]\cdot 2\text{H}_2\text{O}$  **8** (I),  $[\text{Cu}(\text{phen})(\text{D-thr})(\text{H}_2\text{O})\text{Cl}]\cdot 2\text{H}_2\text{O}$  **9** (II) and  $\text{CuCl}_2$  (III).



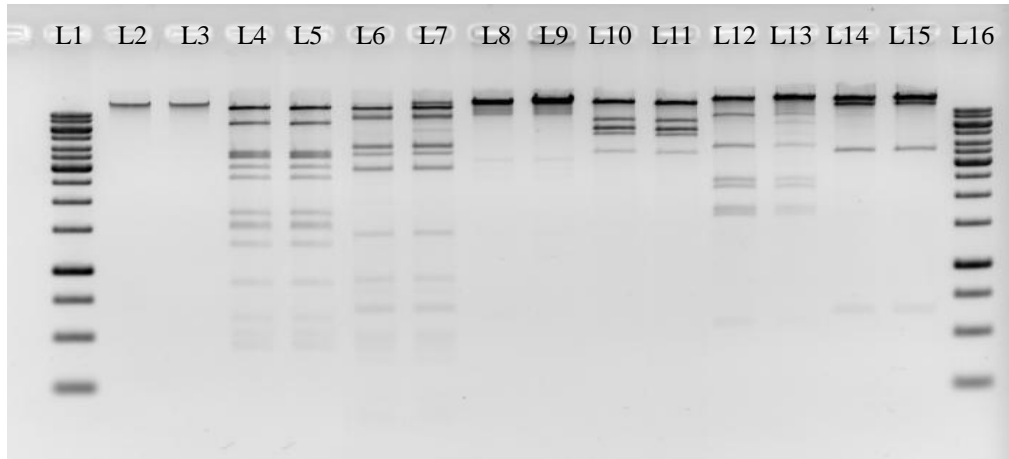
**Appendix 6.1:** Electrophoresis results of incubating  $\lambda$  DNA ( $0.5 \mu\text{g}/\mu\text{L}$ ) with 5 unit of restriction enzyme in the presence or absence of  $50 \mu\text{M}$  complex **1** for 2 hours at  $37^\circ\text{C}$ . Lane 1, 1kb DNA ladder; Lane 2,  $\lambda$  DNA alone ( $0.5 \mu\text{g}$ ); Lane 3,  $\lambda$  DNA +  $50 \mu\text{M}$  complex **1**; Lane 4,  $\lambda$  DNA + 5 unit Tsp 509I (control); Lane 5,  $\lambda$  DNA + 5 unit Tsp 509I +  $50 \mu\text{M}$  complex **1**; Lane 6,  $\lambda$  DNA + 5 unit Hae III (control); Lane 7,  $\lambda$  DNA + 5 unit Hae III +  $50 \mu\text{M}$  complex **1**; Lane 8,  $\lambda$  DNA + 5 unit Sal I (control); Lane 9,  $\lambda$  DNA + 5 unit Sal I +  $50 \mu\text{M}$  complex **1**; Lane 10,  $\lambda$  DNA + 5 unit Pst I (control); Lane 11,  $\lambda$  DNA + 5 unit Pst I +  $50 \mu\text{M}$  complex **1**; Lane 12,  $\lambda$  DNA + 5 unit Pvu II (control); Lane 13,  $\lambda$  DNA + 5 unit Pvu II +  $50 \mu\text{M}$  complex **1**; Lane 14,  $\lambda$  DNA + 5 unit Sca I (control); Lane 15,  $\lambda$  DNA + 5 unit Sca I +  $50 \mu\text{M}$  complex **1**; Lane 16, 1kb DNA ladder



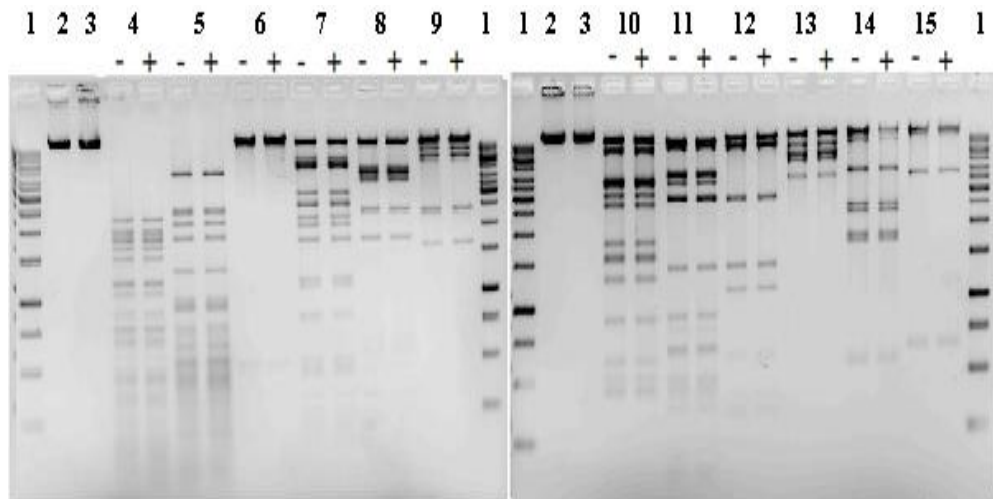
**Appendix 6.2:** Electrophoresis results of incubating  $\lambda$  DNA (0.5  $\mu\text{g}/\mu\text{L}$ ) with 5 unit of restriction enzyme in the presence or absence of 50  $\mu\text{M}$  complex **1** for 2 hours at 37°C. Lane 1, 1kb DNA ladder; Lane 2,  $\lambda$  DNA alone (0.5  $\mu\text{g}$ ); Lane 3,  $\lambda$  DNA + 50  $\mu\text{M}$  complex **1**; Lane 4,  $\lambda$  DNA + 5 unit Ssp I (control); Lane 5,  $\lambda$  DNA + 5 unit Ssp I + 50  $\mu\text{M}$  complex **1**; Lane 6,  $\lambda$  DNA + 5 unit Ase I (control); Lane 7,  $\lambda$  DNA + 5 unit Ase I + 50  $\mu\text{M}$  complex **1**; Lane 8,  $\lambda$  DNA + 5 unit Mun I (control); Lane 9,  $\lambda$  DNA + 5 unit Mun I + 50  $\mu\text{M}$  complex **1**; Lane 10,  $\lambda$  DNA + 5 unit EcoR I (control); Lane 11,  $\lambda$  DNA + 5 unit EcoR I + 50  $\mu\text{M}$  complex **1**; Lane 12,  $\lambda$  DNA + 5 unit NdeI (control); Lane 13,  $\lambda$  DNA + 5 unit NdeI + 50  $\mu\text{M}$  complex **1**; Lane 14,  $\lambda$  DNA + 5 unit Bst 11071 (control); Lane 15,  $\lambda$  DNA + 5 unit Bst 11071 + 50  $\mu\text{M}$  complex **1**; Lane 16, 1kb DNA ladder



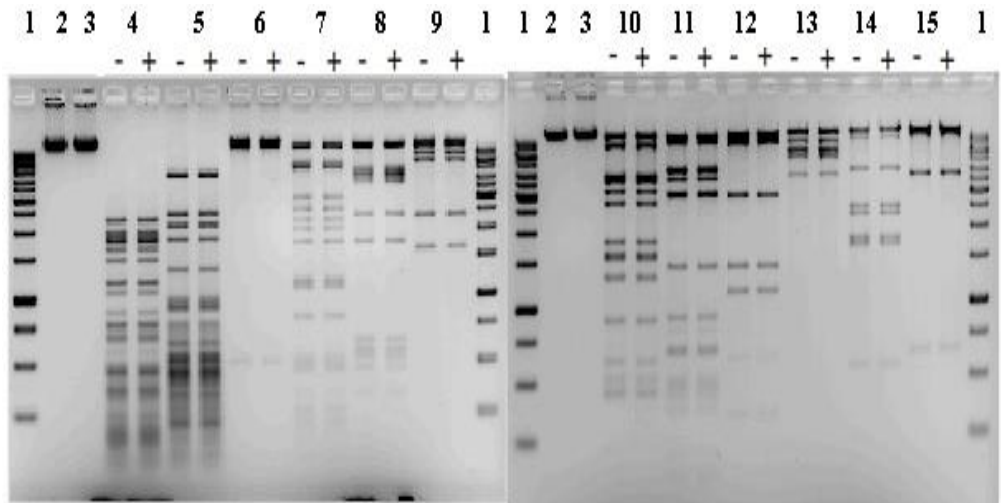
**Appendix 6.3:** Electrophoresis results of incubating  $\lambda$  DNA (0.5  $\mu\text{g}/\mu\text{L}$ ) with 5 unit of restriction enzyme in the presence or absence of 50  $\mu\text{M}$  complex **4** for 2 hours at 37°C. Lane 1, DNA Ladder; Lane 2, DNA Alone; Lane 3, DNA + 50  $\mu\text{M}$  complex **4**; Lane 4, DNA + TSP5091; Lane 5, DNA + complex **4** + TSP5091; Lane 6, DNA + Hae III; Lane 7, DNA + complex **4** + Hae III; Lane 8, DNA + Sal I; Lane 9, DNA + complex **4** + Sal I; Lane 10, DNA + Pst I; Lane 11, DNA + complex **4** + Pst I; Lane 12, DNA + Pvu II; Lane 13, DNA + complex **4** + Pvu II; Lane 14, DNA + Sca I; Lane 15, DNA + complex **4** + Sca I; Lane 16, DNA Ladder



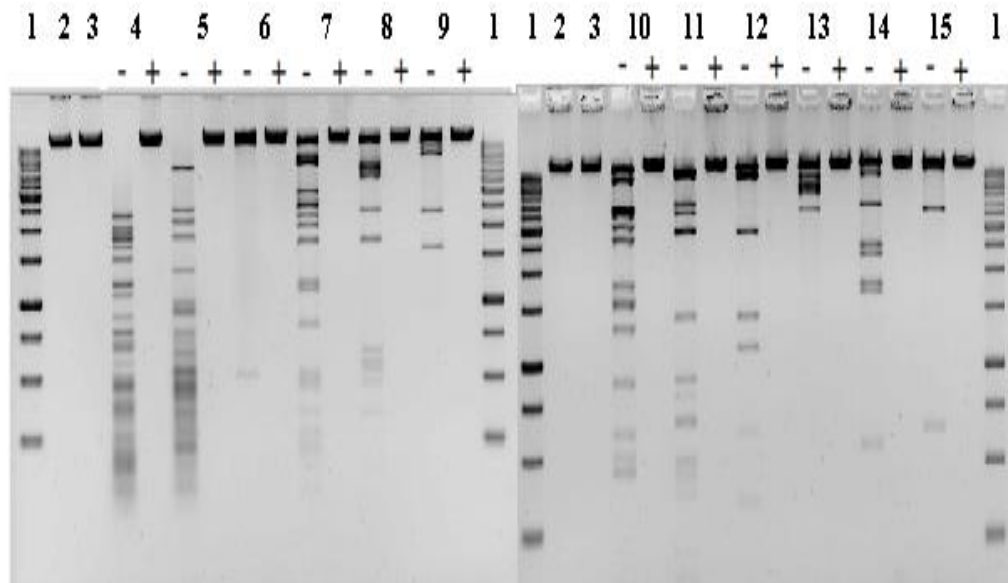
**Appendix 6.4:** Electrophoresis results of incubating  $\lambda$  DNA ( $0.5 \mu\text{g}/\mu\text{L}$ ) with 5 unit of restriction enzyme in the presence or absence of  $50 \mu\text{M}$  complex **4** for 2 hours at  $37^\circ\text{C}$ . Lane 1, DNA Ladder; Lane 2, DNA Alone; Lane 3, DNA +  $50 \mu\text{M}$  complex **4**; Lane 4, DNA + Ase I; Lane 5, DNA + complex **4** + Ase I; Lane 6, DNA + SSp I; Lane 7, DNA + complex **4** + SSp I; Lane 8, DNA + Mun I; Lane 9, DNA + complex **4** + Mun I; Lane 10, DNA + EcoR I; Lane 11, DNA + complex **4** + EcoR I; Lane 12, DNA + Nde I; Lane 13, DNA + complex **4** + Nde I; Lane 14, DNA + Bst11071; Lane 15, DNA + complex **4** + Bst11071; Lane 16, DNA Ladder



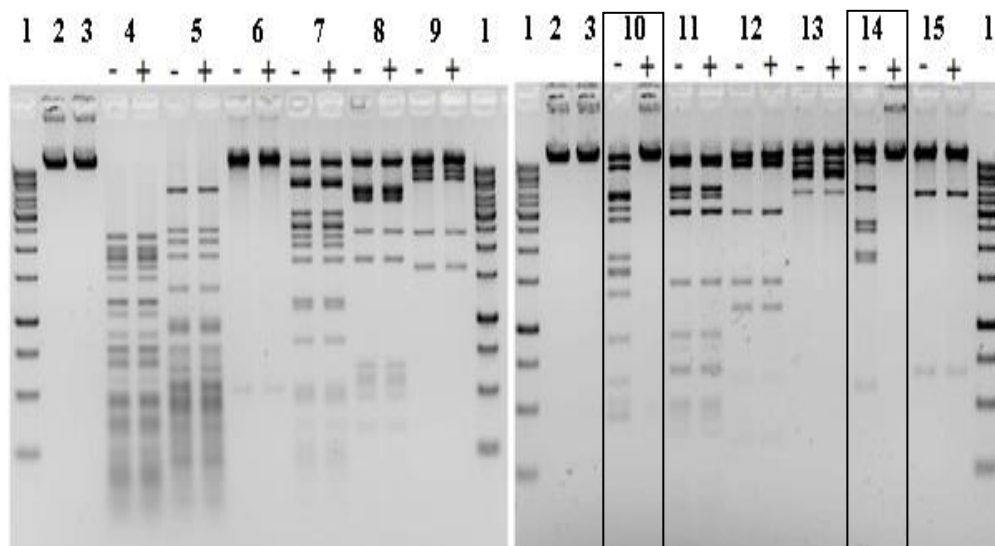
**Appendix 7.1:** Electrophoresis results of incubating  $\lambda$  DNA ( $0.5 \mu\text{g}/\mu\text{L}$ ) with 5 unit of restriction enzyme in the absence (-) or presence (+) of  $50 \mu\text{M}$   $\text{ZnCl}_2$  for 2 hours at  $37^\circ\text{C}$ . Lane 1, 1 kb  $\lambda$  DNA; 2,  $\lambda$  DNA alone; 3,  $\lambda$  DNA +  $\text{ZnCl}_2$  alone. Restriction enzymes, Lanes 4 – 15: 4, Tsp 509I; 5, Hae III; 6, Sal I; 7, Pst I; 8, Pvu II; 9, Sca I; 10, Ssp I; 11, Ase I; 12, Mun I; 13, EcoR I; 14, Nde I; 15, Bst 11071.



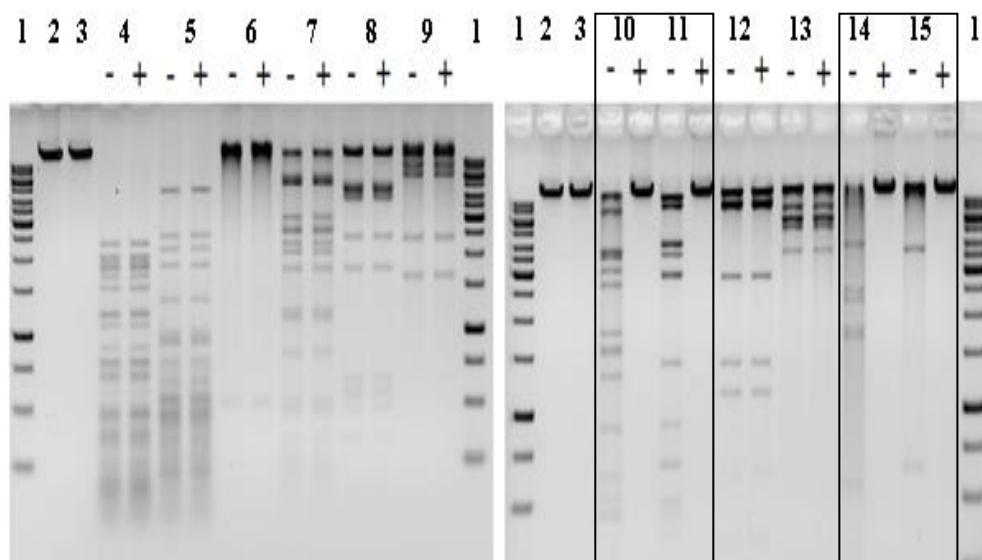
**Appendix 7.2:** Electrophoresis results of incubating  $\lambda$  DNA ( $0.5 \mu\text{g}/\mu\text{L}$ ) with 5 unit of restriction enzyme in the absence (-) or presence (+) of  $50 \mu\text{M}$  phenol for 2 hours at  $37^\circ\text{C}$ . Lane 1, 1 kb  $\lambda$  DNA; 2,  $\lambda$  DNA alone; 3,  $\lambda$  DNA + phenol alone. Restriction enzymes, Lanes 4 – 15: 4, Tsp 509I; 5, Hae III; 6, Sal I; 7, Pst I; 8, Pvu II; 9, Sca I; 10, Ssp I; 11, Ase I; 12, Mun I; 13, EcoR I; 14, NdeI; 15, Bst 11071.



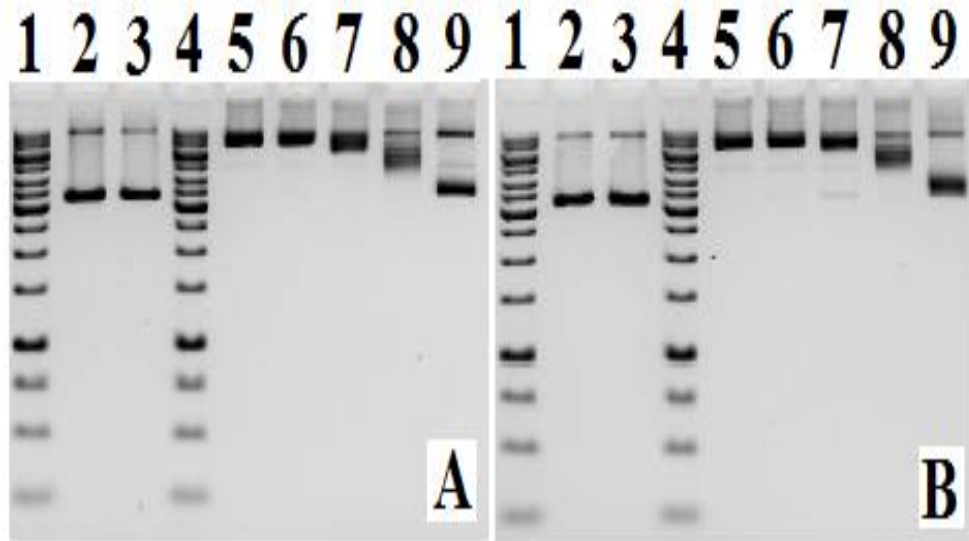
**Appendix 7.3:** Electrophoresis results of incubating  $\lambda$  DNA ( $0.5 \mu\text{g}/\mu\text{L}$ ) with 5 unit of restriction enzyme in the absence (-) or presence (+) of  $50 \mu\text{M}$  thiazole orange for 2 hours at  $37^\circ\text{C}$ . Lane 1, 1 kb  $\lambda$  DNA; 2,  $\lambda$  DNA alone; 3,  $\lambda$  DNA + thiazole orange alone. Restriction enzymes, Lanes 4 – 15: 4, Tsp 509I; 5, Hae III; 6, Sal I; 7, Pst I; 8, Pvu II; 9, Sca I; 10, Ssp I; 11, Ase I; 12, Mun I; 13, EcoR I; 14, NdeI; 15, Bst 11071.



**Appendix 7.4:** Electrophoresis results of incubating  $\lambda$  DNA ( $0.5 \mu\text{g}/\mu\text{L}$ ) with 5 unit of restriction enzyme in the absence (-) or presence (+) of  $50 \mu\text{M}$   $[\text{Zn}(\text{phen})(\text{dipico})(\text{H}_2\text{O})] \cdot \text{H}_2\text{O}$  **7** for 2 hours at  $37^\circ\text{C}$ . Lane 1, 1 kb  $\lambda$  DNA; 2,  $\lambda$  DNA alone; 3,  $\lambda$  DNA + **7** alone. Restriction enzymes, Lanes 4 – 15: 4, Tsp 509I; 5, Hae III; 6, Sal I; 7, Pst I; 8, Pvu II; 9, Sca I; 10, Ssp I; 11, Ase I; 12, Mun I; 13, EcoR I; 14, NdeI; 15, Bst 11071.



**Appendix 7.5:** Electrophoresis results of incubating  $\lambda$  DNA ( $0.5 \mu\text{g}/\mu\text{L}$ ) with 5 unit of restriction enzyme in the absence (-) or presence (+) of  $50 \mu\text{M}$   $[\text{Zn}(\text{phen})(\text{L-Thr})(\text{H}_2\text{O})\text{Cl}] \cdot 2\text{H}_2\text{O}$  **10** for 2 hours at  $37^\circ\text{C}$ . Lane 1, 1 kb  $\lambda$  DNA; 2,  $\lambda$  DNA alone; 3,  $\lambda$  DNA + **10** alone. Restriction enzymes, Lanes 4 – 15: 4, Tsp 509I; 5, Hae III; 6, Sal I; 7, Pst I; 8, Pvu II; 9, Sca I; 10, Ssp I; 11, Ase I; 12, Mun I; 13, EcoR I; 14, NdeI; 15, Bst 11071.



**Appendix 7.6:** Human topo I inhibition assay by gel electrophoresis. Electrophoresis results of incubating human topoisomerase I (1 unit/21 $\mu$ L) with pBR322 (0.25  $\mu$ g) in the absence or presence of 40  $\mu$ M of Zn(II) complexes **7** (A) and **10** (B): Lane 1 & 4, gene ruler 1 Kb DNA ladder; Lane 2, DNA alone; Lane 3, DNA + 40  $\mu$ M complex (control); Lane 5, DNA + 1unit Topo I (control); Lane 6, DNA + 10  $\mu$ M complex + 1unit Topo I; Lane 7, DNA + 20  $\mu$ M complex + 1unit Topo I; Lane 8, DNA + 80  $\mu$ M complex + 1unit Topo I; Lane 9, DNA + 120  $\mu$ M complex + 1unit Topo I.

## LIST OF PUBLICATIONS / CONFERENCE PRESENTATIONS

### PUBLICATIONS

1. Chin, L.F., Kong, S.M., Seng, H.L., Khoo, K.S., Vikneswaran, R., Teoh, S.G., Munirah, A., Alan Khoo, S.B., Mohd Jamil Maah and Ng, C.H., 2011. Synthesis, characterization and biological properties of cobalt(II) complexes of 1,10-phenanthroline and maltol. *Journal of Inorganic Biochemistry*, 105 (2011), pp. 221 - 229.
2. Chin, L.F., Kong, S.M., Seng, H.L., Tiong, Y.L., Neo, K.E., Munirah, A., Alan Khoo, S.B., Mohd Jamil Maah, Andy Hor, T.S., Lee, H.B., San, S.L., Chye, S.M. and Ng, C.H., 2012. [Zn(phen)(O,N,O)(H<sub>2</sub>O)] and [Zn(phen)(O,N)(H<sub>2</sub>O)] with O,N,O is 2,6-dipicolinate and N,O is L-threoninate: synthesis, characterization, and biomedical properties. *Journal of Biological Inorganic Chemistry*, 17, pp. 1093 - 1105.

### CONFERENCE PRESENTATIONS

1. Chin, L.F., Kong, S.M., Seng, H.L., Khoo, K.S., Vikneswaran, R., Teoh, S.G., Munirah, A., Alan Khoo, S.B., Mohd Jamil Maah and Ng, C.H., 2011. Synthesis, characterization and biological properties of cobalt(II) complexes of 1,10-phenanthroline and maltol. *AsBIC V*, 1 Nov - 5 Nov 2010, Kaohsiung, Taiwan. (Poster)

2. Chin, L.F., Kong, S.M., Seng, H.L., Tiong, Y.L., Neo, K.E., Munirah, A., Alan Khoo, S.B., Mohd Jamil Maah, Andy Hor, T.S., Lee, H.B., San, S.L., Chye, S.M. and Ng, C.H., 2012. New anticancer zinc compounds for nasopharyngeal cancer. 5<sup>th</sup> International Symposium on Nasopharyngeal Carcinoma (NPC 2011), 22 June - 24 June 2011, Penang, Malaysia. (Poster)